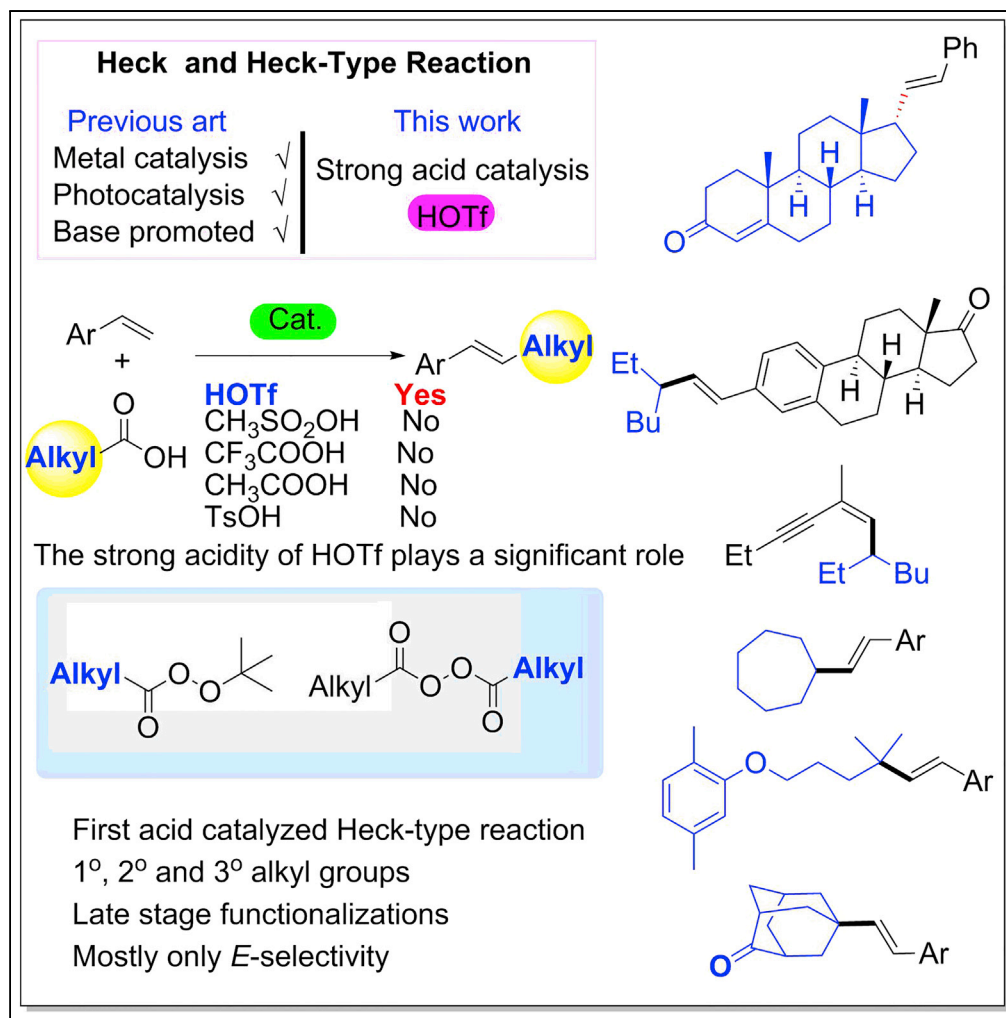


Article

HOTf-Catalyzed Alkyl-Heck-type Reaction



Huan Zhou, Liang Ge, Jinshuai Song, Wujun Jian, Yajun Li, Chunsen Li, Hongli Bao

chunsen.li@fjirsm.ac.cn (C.L.)
hlybao@fjirsm.ac.cn (H.B.)

HIGHLIGHTS

First acid-catalyzed Heck-type reaction

Aliphatic acids are utilized as the sources of alkyl functionalities

E-alkenes exclusively in most cases

Strong acid effect

Article

HOTf-Catalyzed Alkyl-Heck-type Reaction

Huan Zhou,^{1,3,4} Liang Ge,^{1,3,4} Jinshuai Song,¹ Wujun Jian,¹ Yajun Li,¹ Chunsen Li,^{1,*} and Hongli Bao^{1,2,5,*}

SUMMARY

The Heck reaction, along with other cross-coupling reactions, led to a revolution in organic chemistry. In the last 50 years, metal-catalyzed, photo-induced, or base-mediated Heck and Heck-type reactions have been elegantly developed. Brønsted acid-catalyzed Heck (or Heck-type) reactions are still unknown, however. By introducing alkyl peroxides as the key intermediates, primary, secondary, and tertiary aliphatic carboxylic acids are therefore applied here in a one-pot Brønsted acid-catalyzed Heck-type reaction, to deliver *E*-alkenes exclusively in most cases. The use of HOTf is vital to the reaction, whose mechanism is supported by both experimental and computational results. This method can be expanded to the direct alkylation of complex natural products.

INTRODUCTION

The Heck reaction, pioneered by Heck and Mizoroki in the late 1960s and the early 1970s (Heck, 1968; Mizoroki et al., 1971; Heck and Nolley, 1972), along with other cross-coupling reactions, led to a revolution in organic chemistry (Johansson Seechurn et al., 2012). In the last 50 years, many types of Heck and Heck-type reactions, including metal-catalyzed (Heck, 1968; Mizoroki et al., 1971; Heck and Nolley, 1972; Littke and Fu, 2001; Farrington et al., 2002; Na et al., 2004; Loska et al., 2008; Delcamp et al., 2013; Nishikata et al., 2013; Standley and Jamison, 2013), photo-induced (Iqbal et al., 2012; Liu et al., 2013; Paria et al., 2014; Yu et al., 2014), or base-mediated (Rueping et al., 2011; Shirakawa et al., 2011; Sun et al., 2011) reactions, have been elegantly developed (Beletskaya and Cheprakov, 2000; Dounay and Overman, 2003; Wu et al., 2010; Le Bras and Muzart, 2011; Mc Cartney and Guiry, 2011; Tang et al., 2015). Notwithstanding these classical reaction modes, there is no precedent of Brønsted acid-catalyzed or Brønsted acid-promoted Heck (or type) reaction being realized. Moreover, compared with aryl Heck reactions, the alkyl-Heck (type) reaction has been developed less. This is due mainly to the potential accompanying side reactions. Significant breakthroughs in alkyl-Heck-type reactions have, however, been made (Ikeda et al., 2002; Liu et al., 2012, 2015; Nishikata et al., 2013; McMahan and Alexanian, 2014; Zou and Zhou, 2014; Kurandina et al., 2018; Wang et al., 2018) (Scheme 1A), and in this article, we report a Brønsted acid-catalyzed alkyl-Heck-type reaction.

As is well known, alkyl halides are one of the most frequently used alkyl functionalities for alkyl-Heck-type reactions (Kambe et al., 2011; Weix, 2015; Tellis et al., 2016; Choi and Fu, 2017). However, their shortcomings, such as limited availability and perceived instability might prevent more extensive applications (Qin et al., 2016). Furthermore, there are still significant challenges remaining for alkyl-Heck-type reactions such as *E/Z* selectivity, use of metal catalysis, and diversity of alkyl sources (Scheme 1A). Carboxylic acids are inexpensive, stable, non-toxic, and structurally diverse feedstock chemicals that have been widely used in numerous reactions. For example, they have been utilized in cross-coupling with prefunctionalized alkenes such as vinyl halides or their derivatives to generate alkenes (Mai et al., 2013; Noble et al., 2015; Toriyama et al., 2016; Wang et al., 2016; Edwards et al., 2017; Xu et al., 2017; Zhang et al., 2017) (Scheme 1B). However, the decarboxylative cross-couplings of aliphatic acids or their derivatives with alkenes (X = H) are very rare (Wang et al., 2018). As part of our ongoing interest in the application of aliphatic acids as the alkyl source (Li et al., 2016; Ge et al., 2017; Jian et al., 2017; Qian et al., 2017; Ye et al., 2017; Zhu et al., 2017) and our interests in the discovery of different reaction models of alkyl peroxides, we have developed the first Brønsted acid-catalyzed alkyl-Heck-type reaction of alkenes with aliphatic acids via alkyl peroxide intermediates (Scheme 1C).

RESULTS AND DISCUSSION

Optimization Study

We commenced our studies by screening a variety of Brønsted acids for the alkyl-Heck-type reaction of styrene with aliphatic acid. The aliphatic acid was converted into alkyl peresters in the presence of trifluoroacetic anhydride (TFAA) and tert-butyl hydroperoxide (TBHP) and used *in situ* for the subsequent step

¹State Key Laboratory of Structural Chemistry, Fujian Institute of Research on the Structure of Matter, Chinese Academy of Sciences, 155 Yangqiao Road West, Fuzhou, Fujian 350002, People's Republic of China

²Key Laboratory of Coal to Ethylene Glycol and Its Related Technology, Center for Excellence in Molecular Synthesis, Fujian Institute of Research on the Structure of Matter, Chinese Academy of Sciences, 155 Yangqiao Road West, Fuzhou, Fujian 350002, People's Republic of China

³University of Chinese Academy of Sciences, Beijing 100049, People's Republic of China

⁴These authors contributed equally

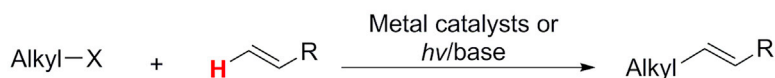
⁵Lead Contact

*Correspondence: chunsen.li@fjirm.ac.cn (C.L.), hlbao@fjirm.ac.cn (H.B.)

<https://doi.org/10.1016/j.isci.2018.04.020>

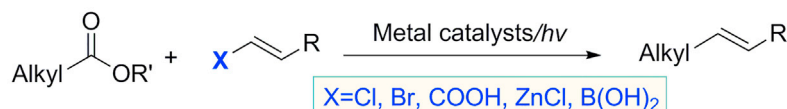


A



Challenges: Aliphatic acids as alkyl sources; *E/Z* ratio; Acid catalyzed reaction

B



C

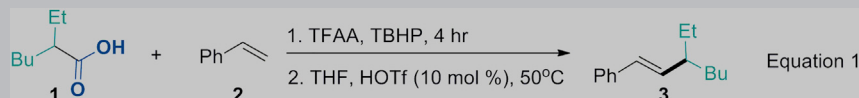


- 📌 First acid catalyzed Heck-type reaction
- 📌 Mostly only *E*-selectivity
- 📌 1°, 2° and 3° alkyl groups
- 📌 Late stage functionalizations

Scheme 1. Intermolecular Alkyl-Heck-Type Reaction of General Alkyl Groups and Decarboxylative Vinylic Alkylation of Aliphatic Acids

- (A) Previous alkyl-Heck-type reactions by Oshima, Alexanian, Zhou, Li, Fu, Lei, and Nishikata.
 (B) Previous decarboxylative vinylic alkylation with aliphatic acid derivatives.
 (C) This work: Brønsted acid-catalyzed alkyl-Heck-type reaction.

(Donchak et al., 2006). The best Brønsted acid was found to be HOTf, which offered the desired alkylated alkene **3** exclusively as a single *E*-isomer in 88% yield, determined by ¹H nuclear magnetic resonance (NMR) analysis (Equation 1 and Table 1, entry 1). Studies of acids showed that Tf₂O had a lower efficiency (Table 1,



Entry	Variation from the Standard Conditions	Yield(%) ^{a,b}
1	None	88(75 ^c)
2	Tf ₂ O instead of HOTf	78
3	TsOH·H ₂ O instead of HOTf	Trace
4	CF ₃ COOH instead of HOTf	Trace
5	HOAc instead of HOTf	Trace
6	MeSO ₃ H instead of HOTf	Trace
7	Room temperature instead of 50°C	70
8	Fresh distilled HOTf	88
9	In dark	90
10	Without HOTf	Trace

Table 1. Optimizations of Reaction Condition

^aReaction conditions: First, 2-ethylhexanoic acid **1** (1.5 mmol), TBHP (1.5 mmol), and TFAA (1.5 mmol) at 0°C–rt for 4 hr, and then THF (2 mL), styrene **2** (0.5 mmol), and HOTf (0.05 mmol) were added. The mixture was stirred at 50°C for 8 hr.

^b¹H NMR yield.

^cYield of the isolated product.

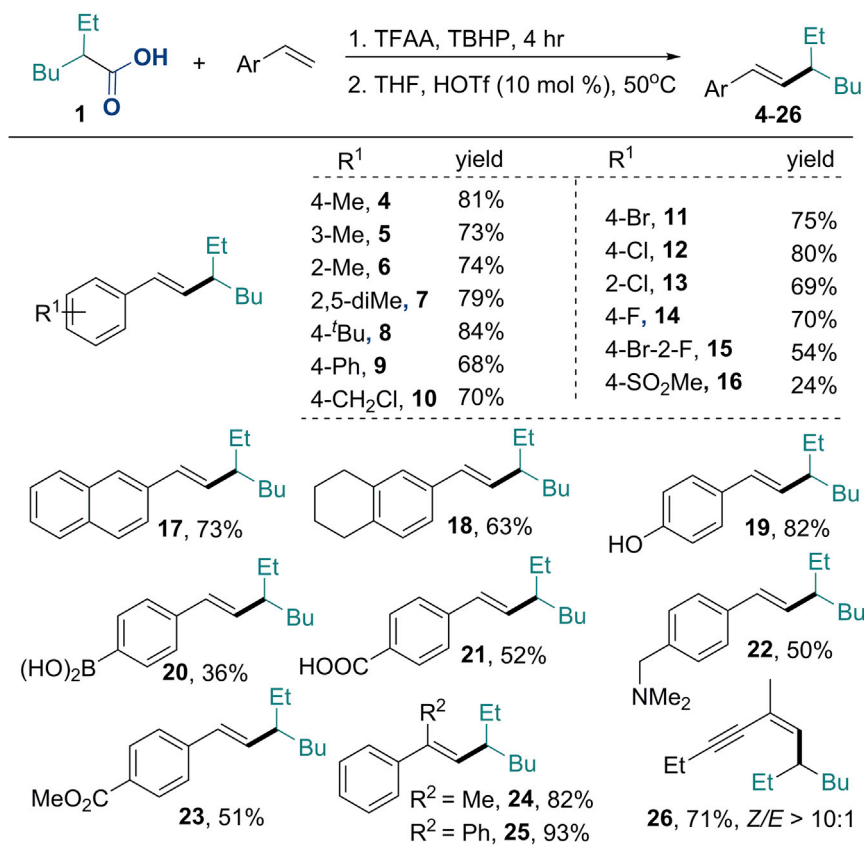


Figure 1. Alkyl-Heck-Type Reaction of Alkenes

Top: One-pot process from aliphatic acid: First, 2-ethylhexanoic acid **1** (1.5 mmol), TBHP (1.5 mmol), and TFAA (2.0 mmol) at 0°C–rt for 4 hr, and then THF (2 mL), alkene (0.5 mmol), and HOTf (0.05 mmol) were added. The mixture was stirred at 50°C for 8 hr; yields of isolated products.

Bottom: HOTf (0.35 mmol) was added for **16**, **18**, **19**, and **21**.

The acetyl group on oxygen atom was removed under the reaction conditions for **19**.

HOTf (0.75 mmol) was added for **22**.

See also Figures S45–S94.

entry 2) and other Brønsted acids such as TsOH·H₂O, CF₃COOH, HOAc, and MeSO₃H were ineffective in this reaction (Table 1, entries 3–6). When performed at room temperature (rt), the reaction afforded the desired product in 70% yield (Table 1, entry 7). To exclude the possibility of interference of trace amount of metal in HOTf, the HOTf was used after redistillation and the product was obtained in the same yield (Table 1, entry 8). The role of light was investigated by conducting the reaction in the dark, but no difference in the yield was observed (Table 1, entry 9). In the absence of HOTf, the alkyl peroxide decomposed completely and the styrene remained unchanged (Table 1, entry 10).

Scope of the Investigation

With the identified conditions in hand, we studied the scope of alkenes for this one-pot process (Figure 1). In most of the cases, the products were obtained as a single *E*-isomer. Reactions of vinyl arenes containing carbon substituents at the *o*-, *m*-, and *p*-positions afforded the corresponding products (**4**–**10**) in good yield (68–84%). Vinyl arenes containing halides reacted with 2-ethylhexanoic acid to give the desired products (**11**–**15**) in moderate to good yield (54%–80%). Functional groups, such as dimethylaminomethyl, and even free carboxylic acid and boronic acid were compatible with the reaction conditions (**20**–**23**). α -Methylstyrene and α -phenylstyrene participated in the reaction smoothly, providing the products (**24**, **25**) in 82% and 93% yields, respectively. Furthermore, an enyne was a suitable substrate for this reaction, and the corresponding terminal-cross-coupled product (**26**) was obtained in good yield (71%). 1-Octene, an unactivated alkene, examined under the standard reaction conditions was not reactive to this reaction.

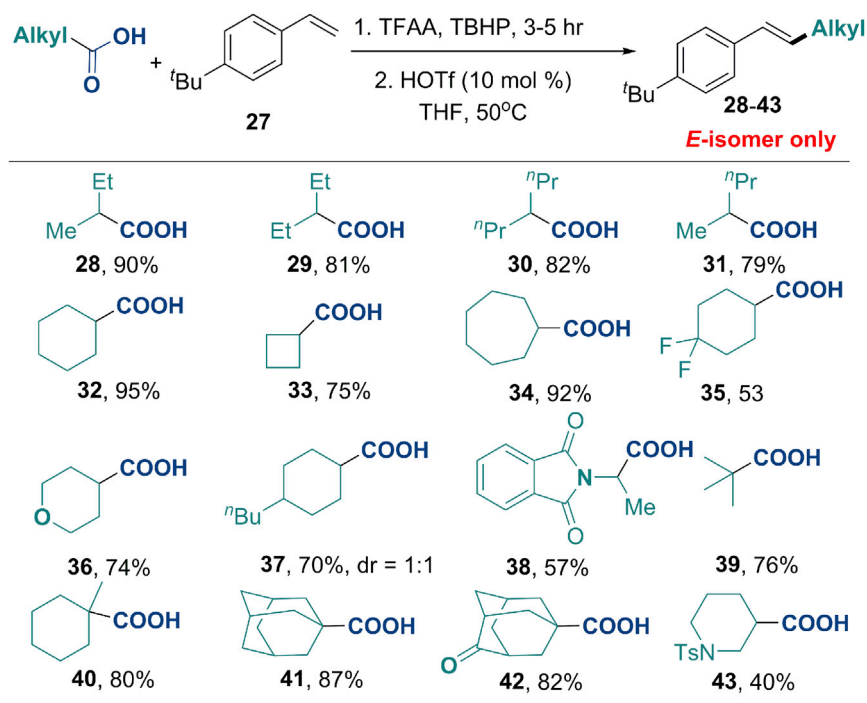


Figure 2. Alkyl-Heck-Type Reaction of Secondary and Tertiary Aliphatic Acids

Top: One-pot process from aliphatic acid: First, acid (1.5 mmol), TBHP (1.5 mmol), and TFAA (2.0 mmol) at 0°C–rt for 3–5 hr, and then THF (2 mL), styrene **27** (0.5 mmol), and HOTf (0.05 mmol) were added. The mixture was stirred at 50°C for 8 hr; yields of isolated products.

Bottom: Styrene **27** (0.5 mmol), perester (1.25 mmol), and HOTf (0.1 mmol) at 80°C for 8 hr for **35**, **36**, **38**, **42**, and **43**. See also [Figures S95–S127](#).

Next, we proceeded to study the scope of the reaction with respect to secondary and tertiary aliphatic carboxylic acids ([Figure 2](#)). The desired products (**28–43**) were obtained in moderate to high yields, using acyclic or cyclic aliphatic acids. The compatibility of various functional groups was good, and many functional groups, such as carbonyl (**42**), imide (**38**), amine (**43**), and ether (**36**), were tolerated. Most importantly, the *E/Z* selectivity of this reaction was excellent and only *E*-alkenes were observed. We then tried to expand this reaction to primary aliphatic acids, but the desired products were obtained in low yields as the methylated vinylic products were observed as by-products ([Zhu et al., 2017](#)). To overcome this problem, primary aliphatic acids were converted into alkyl diacyl peroxides and then subjected to the reaction ([Figure 3](#)). With the similar reaction conditions (please see [Table S4](#) for details), generic primary aliphatic acids afforded the corresponding products (**44–48**) in good yields (60–77%). Primary aliphatic acids with functionalities, e.g., the bromide (**49**), chloride (**50**), ketones (**51** and **52**), ester (**53**), or the alkene (**54**) were well tolerated in the protocol, delivering the corresponding products in moderate to good yields. In every case, the *E*-alkene was obtained exclusively.

Synthetic Applications

To highlight the synthetic utility of this methodology ([Scheme 2](#)), the perester (**55**), which is readily derived from the corresponding steroidal carboxylic acid, was coupled with styrene in the presence of HOTf. The decarboxylative Heck-type coupling product (**56**) was obtained in 48% yield as a single isomer. The configuration of the product (**56**) was reversed, and this was confirmed by X-ray crystallographic analysis (please see [Tables S5](#) and [S6](#) for details). The reaction of **57** afforded the desired product (**58**) in 65% yield with *E*-selectivity. Gemfibrozil **59**, an oral drug used to lower lipid levels, could also be converted into the vinylated product (**60**). These examples demonstrated that this reaction is potentially useful for the functionalization of complex molecules in the late stage.

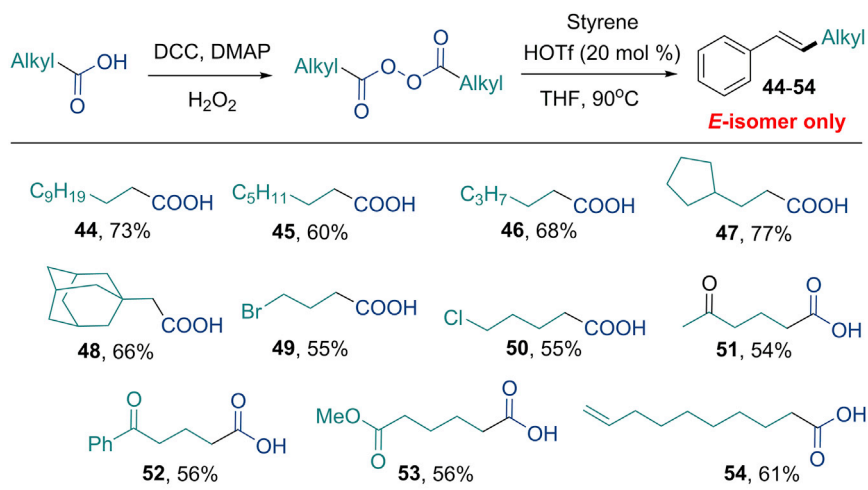


Figure 3. Alkyl-Heck-Type Reaction of Primary Aliphatic Acids

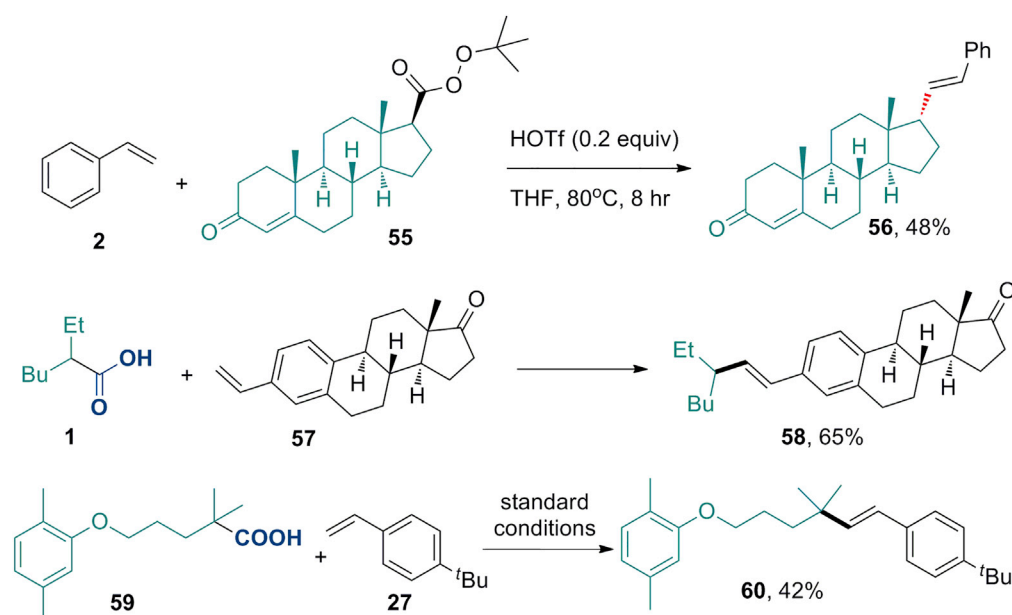
Top: Reaction conditions: alkyl diacyl peroxide (synthesized from acid, 1.0 mmol), styrene **2** (0.5 mmol), and HOTf (0.1 mmol) in THF (1 mL); yields of isolated products.

Bottom: Alkyl diacyl peroxide (synthesized from acid, 1.0 mmol), styrene **2** (0.5 mmol), and HOTf (0.25 mmol) in THF (2 mL) for **49** and **50**.

See also Figures S128–S149.

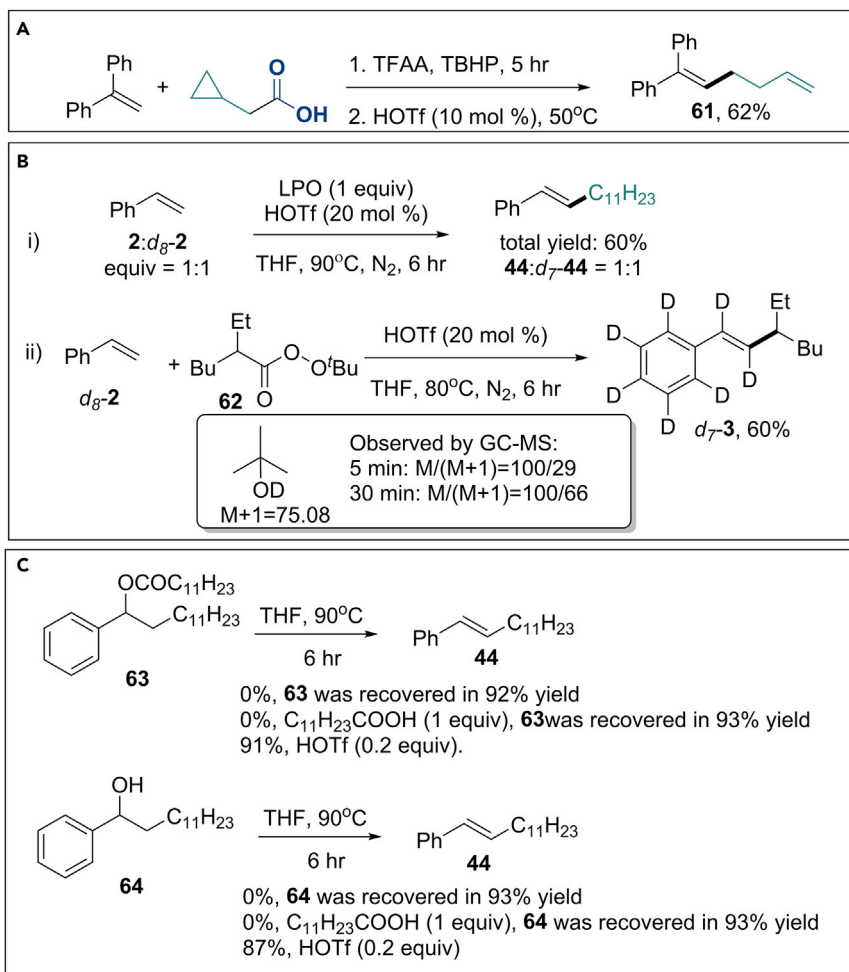
Mechanistic Study

To probe the mechanism of the reaction, a series of control experiments were performed. The reaction of α -phenylstyrene with 2-cyclopropylacetic acid under the standard conditions afforded the ring-opening product (**61**) in 62% yield (Scheme 3A), supporting the assumption of the involvement of radical species in the reaction. The competitive reaction of styrene and d_8 -styrene used in 1:1 ratio in the presence of HOTf and lauroyl peroxide (LPO) offered an identical yield of the corresponding products (Scheme 3B). When the reaction of d_8 -styrene with perester **62** was performed in tetrahydrofuran (THF), the desired



Scheme 2. Synthetic Applications

See also Figures S150–S155.



Scheme 3. Mechanism Studies

(A) Radical clock reaction.

(B) Deuterium labeling experiment.

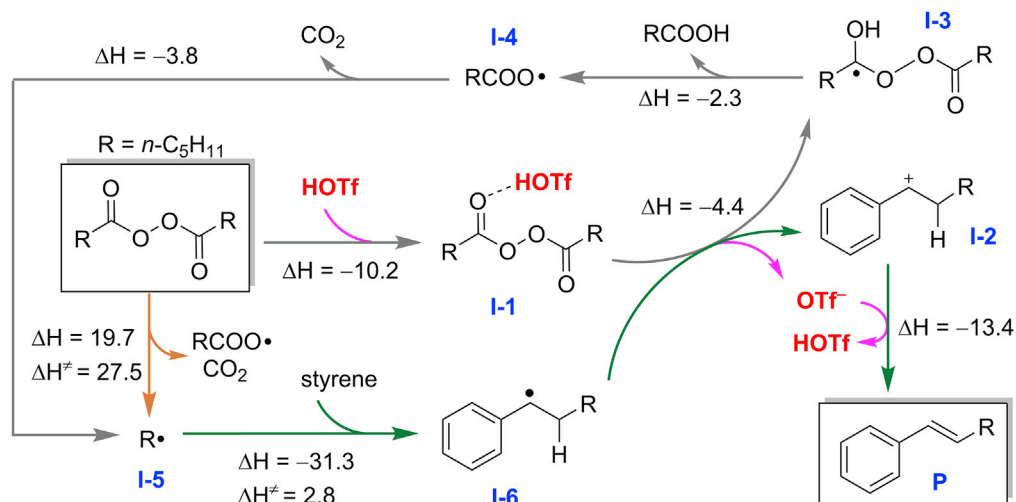
(C) Exclusion of possible intermediates.

See also [Figures S156–S164](#).

product (d_7-3) was isolated (Scheme 3B). Interestingly, the deuterated side products $d(\text{OD})$ -butanol were detected by gas chromatography-mass spectrometry (GC-MS). To further explore the mechanism, possible intermediates **63** and **64** were synthesized and tested with or without HOTf (Scheme 3C). Compounds **63** and **64** are thermally stable in the absence or presence of one equivalent of C₁₁H₂₃COOH. Even though compounds **63** and **64** can be converted to the desired alkene products in the presence of 0.2 equivalent of HOTf, it is unlikely that they are competent intermediates because the formation of **63** or **64** was not observed using GC-MS when the corresponding Heck reaction was conducted no matter with or without HOTf (Ge et al., 2017).

Plausible Reaction Mechanism

As the result shown in entry 10 of Table 1, no desired product was observed in the absence of HOTf, implying that HOTf must play a vital role in the reaction. Density functional theory (DFT) calculations were carried out to gain further insight into the reaction mechanism. As can be seen from Scheme 4, before the catalytic cycle R• radical I-5 can be formed by homolytic dissociation of the alkyl diacyl peroxide, which is a very slow step with a high barrier of 27.5 kcal/mol. However, this is considered as the trigger to invoke the following catalytic cycle. Attack on the styrene substrate by the active species R• radical to form a benzyl radical (I-6) leads to energies lower by 31.3 kcal/mol with a small barrier of 2.8 kcal/mol, indicating



Scheme 4. Plausible Reaction Mechanism

that such a reaction is both thermodynamically and kinetically favorable. In the beginning of the catalytic cycle, LPO binding a molecule of HOTf forms a complex I-1 with a strong hydrogen bonding of 10.2 kcal/mol. This complex oxidizes benzyl radical (I-6) to yield a benzyl cation species (I-2), a radical (I-3), and an OTf⁻ anion, which is exothermic by 4.4 kcal/mol. Meanwhile, the generated OTf⁻ deprotonates I-2 to yield the product and regenerate the acid HOTf with a reaction energy of -13.4 kcal/mol. Thus, from the reactions of LPO and I-6 with the product and I-3, a proton-coupled electron transfer process is promoted by HOTf, which serves as the driving force and proton source for the reaction. Thereby, homolytic dissociation of I-3 leads to RCOO• radical (I-4) and RCOOH, which is exothermic by 2.3 kcal/mol without any barrier. Subsequently, C-C cleavage of I-4 is exothermic by 3.8 kcal/mol, which releases the active species R• radical (I-5) and CO₂ to close the catalytic cycle. Alternatively, in the absence of HOTf formation of this radical I-4 with carboxylic acid RCOOH requires high energies (>27 kcal/mol, See Scheme S1), indicating that the strong acidity of HOTf plays a significant role in the formation of I-4. A similar mechanism of reaction starting from perester was also calculated and presented in Scheme S2.

Conclusion

We have developed a Brønsted acid-catalyzed radical alkyl-Heck-type reaction of alkenes with aliphatic acids. This HOTf-catalyzed process has been shown to be an efficient method to deliver only *E*-alkenes in most cases. Relatively simple and available starting materials are used, and wide substrate scope and good functional group tolerance are observed. Preliminary mechanistic studies illustrated the vital role of HOTf in the reaction, whose proposed mechanism is supported by both the experimental and computational results.

METHODS

All methods can be found in the accompanying [Transparent Methods supplemental file](#).

DATA AND SOFTWARE AVAILABILITY

The data for the X-ray crystallographic structure of **55** and **56** have been deposited in the Cambridge Crystallographic Data Center under accession number CCDC: 1477011 and CCDC: 1476738 (also see [Data S2](#) and [Data S3](#) in [Supplemental Information](#)).

SUPPLEMENTAL INFORMATION

Supplemental Information includes Transparent Methods, 164 figures, 2 schemes, 6 tables, and 3 data files and can be found with this article online at <https://doi.org/10.1016/j.isci.2018.04.020>.

ACKNOWLEDGMENTS

We thank NSFC (Grant Nos. 21502191, 21672213, 21232001, 21603227, 21573237), Strategic Priority Research Program of the Chinese Academy of Sciences (Grant No. XDB20000000), and Haixi Institute of CAS (CXZX-2017-P01) for financial support, and Hundred-Talent Program of the Chinese Academy of Sciences.

AUTHOR CONTRIBUTIONS

Performed synthetic experiments and analyzed the experimental data: H.Z., L.G., W.J., and Y.L.; theoretical calculations: J.S. and C.L.; performed investigations and prepared the manuscript, H.B.

DECLARATION OF INTERESTS

The authors declare no competing interests.

Received: February 16, 2018

Revised: April 12, 2018

Accepted: April 24, 2018

Published: May 25, 2018

REFERENCES

- Beletskaya, I.P., and Cheprakov, A.V. (2000). The heck reaction as a sharpening stone of palladium catalysis. *Chem. Rev.* *100*, 3009–3066.
- Choi, J., and Fu, G.C. (2017). Transition metal-catalyzed alkyl-alkyl bond formation: another dimension in cross-coupling chemistry. *Science* *356*, <https://doi.org/10.1126/science.aaf7230>.
- Delcamp, J.H., Gormisky, P.E., and White, M.C. (2013). Oxidative heck vinylation for the synthesis of complex dienes and polyenes. *J. Am. Chem. Soc.* *135*, 8460–8463.
- Donchak, V.A., Voronov, S.A., and Yur'ev, R.S. (2006). New synthesis of tert-butyl peroxy-carboxylates. *Russ. J. Org. Chem.* *42*, 487–490.
- Dounay, A.B., and Overman, L.E. (2003). The asymmetric intramolecular heck reaction in natural product total synthesis. *Chem. Rev.* *103*, 2945–2963.
- Edwards, J.T., Merchant, R.R., Mcclymont, K.S., Knouse, K.W., Qin, T., Malins, L.R., Vokits, B., Shaw, S.A., Bao, D.H., Wei, F.L., et al. (2017). Decarboxylative alkenylation. *Nature* *545*, 213–218.
- Farrington, E.J., Brown, J.M., Barnard, C.F.J., and Rowsell, E. (2002). Ruthenium-catalyzed oxidative heck reactions. *Angew. Chem. Int. Ed.* *41*, 169–171.
- Ge, L., Li, Y., Jian, W., and Bao, H. (2017). Alkyl esterification of vinylarenes enabled by visible-light-induced decarboxylation. *Chem. Eur. J.* *23*, 11767–11770.
- Heck, R.F. (1968). Acylation, methylation, and carboxyalkylation of olefins by Group VIII metal derivatives. *J. Am. Chem. Soc.* *90*, 5518–5526.
- Heck, R.F., and Nolley, J.P. (1972). Palladium-catalyzed vinylic hydrogen substitution reactions with aryl, benzyl, and styryl halides. *J. Org. Chem.* *37*, 2320–2322.
- Ikeda, Y., Nakamura, T., Yorimitsu, H., and Oshima, K. (2002). Cobalt-catalyzed heck-type reaction of alkyl halides with styrenes. *J. Am. Chem. Soc.* *124*, 6514–6515.
- Iqbal, N., Choi, S., Kim, E., and Cho, E.J. (2012). Trifluoromethylation of alkenes by visible light photoredox catalysis. *J. Org. Chem.* *77*, 11383–11387.
- Jian, W., Ge, L., Jiao, Y., Qian, B., and Bao, H. (2017). Iron-catalyzed decarboxylative alkyl etherification of vinylarenes with aliphatic acids as the alkyl source. *Angew. Chem. Int. Ed.* *56*, 3650–3654.
- Johansson Seechurn, C.C., Kitching, M.O., Colacot, T.J., and Snieckus, V. (2012). Palladium-catalyzed cross-coupling: a historical contextual perspective to the 2010 Nobel Prize. *Angew. Chem. Int. Ed.* *51*, 5062–5085.
- Kambe, N., Iwasaki, T., and Terao, J. (2011). Pd-catalyzed cross-coupling reactions of alkyl halides. *Chem. Soc. Rev.* *40*, 4937–4947.
- Kurandina, D., Rivas, M., Radzhabov, M., and Gevorgyan, V. (2018). Heck reaction of electronically diverse tertiary alkyl halides. *Org. Lett.* *20*, 357–360.
- Le Bras, J., and Muzart, J. (2011). Intermolecular dehydrogenative heck reactions. *Chem. Rev.* *111*, 1170–1214.
- Li, Y., Han, Y., Xiong, H., Zhu, N., Qian, B., Ye, C., Kantchev, E.A., and Bao, H. (2016). Copper-catalyzed regioselective 1,2-alkylesterification of dienes to allylic esters. *Org. Lett.* *18*, 392–395.
- Littke, A.F., and Fu, G.C. (2001). A versatile catalyst for heck reactions of aryl chlorides and aryl bromides under mild conditions. *J. Am. Chem. Soc.* *123*, 6989–7000.
- Liu, C., Tang, S., Liu, D., Yuan, J., Zheng, L., Meng, L., and Lei, A. (2012). Nickel-catalyzed Heck-type alkenylation of secondary and tertiary alpha-carbonyl alkyl bromides. *Angew. Chem. Int. Ed.* *51*, 3638–3641.
- Liu, Q., Yi, H., Liu, J., Yang, Y., Zhang, X., Zeng, Z., and Lei, A. (2013). Visible-light photocatalytic radical alkenylation of alpha-carbonyl alkyl bromides and benzyl bromides. *Chem. Eur. J.* *19*, 5120–5126.
- Liu, W., Li, L., Chen, Z., and Li, C.J. (2015). A transition-metal-free Heck-type reaction between alkenes and alkyl iodides enabled by light in water. *Org. Biomol. Chem.* *13*, 6170–6174.
- Loska, R., Volla, C.M.R., and Vogel, P. (2008). Iron-catalyzed Mizoroki-Heck cross-coupling reaction with styrenes. *Adv. Synth. Catal.* *350*, 2859–2864.
- Mai, W.-P., Song, G., Sun, G.-C., Yang, L.-R., Yuan, J.-W., Xiao, Y.-M., Mao, P., and Qu, L.-B. (2013). Cu/Ag-catalyzed double decarboxylative cross-coupling reaction between cinnamic acids and aliphatic acids in aqueous solution. *RSC Adv.* *3*, 19264.
- Mc Cartney, D., and Guiry, P.J. (2011). The asymmetric Heck and related reactions. *Chem. Soc. Rev.* *40*, 5122–5150.
- Mcmahon, C.M., and Alexanian, E.J. (2014). Palladium-catalyzed Heck-type cross-couplings of unactivated alkyl iodides. *Angew. Chem. Int. Ed.* *53*, 5974–5977.
- Mizoroki, T., Mori, K., and Ozaki, A. (1971). Arylation of olefin with aryl iodide catalyzed by palladium. *Bull. Chem. Soc. Jpn.* *44*, 581.
- Na, Y., Park, S., Han, S.B., Han, H., Ko, S., and Chang, S. (2004). Ruthenium-catalyzed Heck-type olefination and Suzuki coupling reactions: studies on the nature of catalytic species. *J. Am. Chem. Soc.* *126*, 250–258.
- Nishikata, T., Noda, Y., Fujimoto, R., and Sakashita, T. (2013). An efficient generation of a functionalized tertiary-alkyl radical for copper-catalyzed tertiary-alkylative Mizoroki-Heck-type reaction. *J. Am. Chem. Soc.* *135*, 16372–16375.
- Noble, A., Mccarver, S.J., and Macmillan, D.W. (2015). Merging photoredox and nickel catalysis: decarboxylative cross-coupling of carboxylic

- acids with vinyl halides. *J. Am. Chem. Soc.* **137**, 624–627.
- Paria, S., Kais, V., and Reiser, O. (2014). Visible light-mediated coupling of α -bromoaldehydes with alkenes. *Adv. Synth. Catal.* **356**, 2853–2858.
- Qian, B., Chen, S., Wang, T., Zhang, X., and Bao, H. (2017). Iron-catalyzed carboamination of olefins: synthesis of amines and disubstituted beta-amino acids. *J. Am. Chem. Soc.* **139**, 13076–13082.
- Qin, T., Cornella, J., Li, C., Malins, L.R., Edwards, J.T., Kawamura, S., Maxwell, B.D., Eastgate, M.D., and Baran, P.S. (2016). A general alkyl-alkyl cross-coupling enabled by redox-active esters and alkylzinc reagents. *Science* **352**, 801–805.
- Rueping, M., Leiendecker, M., Das, A., Poisson, T., and Bui, L. (2011). Potassium tert-butoxide mediated Heck-type cyclization/isomerization-benzofurans from organocatalytic radical cross-coupling reactions. *Chem. Commun.* **47**, 10629–10631.
- Shirakawa, E., Zhang, X., and Hayashi, T. (2011). Mizoroki-heck-type reaction mediated by potassium tert-butoxide. *Angew. Chem. Int. Ed.* **50**, 4671–4674.
- Standley, E.A., and Jamison, T.F. (2013). Simplifying nickel(0) catalysis: an air-stable nickel precatalyst for the internally selective benzylation of terminal alkenes. *J. Am. Chem. Soc.* **135**, 1585–1592.
- Sun, C.L., Gu, Y.F., Wang, B., and Shi, Z.J. (2011). Direct arylation of alkenes with aryl iodides/bromides through an organocatalytic radical process. *Chem. Eur. J.* **17**, 10844–10847.
- Tang, S., Liu, K., Liu, C., and Lei, A. (2015). Olefinic C-H functionalization through radical alkenylation. *Chem. Soc. Rev.* **44**, 1070–1082.
- Tellis, J.C., Kelly, C.B., Primer, D.N., Jouffroy, M., Patel, N.R., and Molander, G.A. (2016). Single-electron transmetalation via photoredox/nickel dual catalysis: unlocking a new paradigm for sp(3)-sp(2) cross-coupling. *Acc. Chem. Res.* **49**, 1429–1439.
- Toriyama, F., Cornella, J., Wimmer, L., Chen, T.G., Dixon, D.D., Creech, G., and Baran, P.S. (2016). Redox-active esters in Fe-catalyzed C-C coupling. *J. Am. Chem. Soc.* **138**, 11132–11135.
- Wang, G.Z., Shang, R., and Fu, Y. (2018). Irradiation-induced palladium-catalyzed decarboxylative heck reaction of aliphatic N-(acyloxy)phthalimides at room temperature. *Org. Lett.* **20**, 888–891.
- Wang, J., Qin, T., Chen, T.G., Wimmer, L., Edwards, J.T., Cornella, J., Vokits, B., Shaw, S.A., and Baran, P.S. (2016). Nickel-catalyzed cross-coupling of redox-active esters with boronic acids. *Angew. Chem. Int. Ed.* **55**, 9676–9679.
- Weix, D.J. (2015). Methods and mechanisms for cross-electrophile coupling of Csp(2) halides with alkyl electrophiles. *Acc. Chem. Res.* **48**, 1767–1775.
- Wu, X.-F., Anbarasan, P., Neumann, H., and Beller, M. (2010). From noble metal to Nobel Prize: palladium-catalyzed coupling reactions as key methods in organic synthesis. *Angew. Chem. Int. Ed.* **49**, 9047–9050.
- Xu, K., Tan, Z., Zhang, H., Liu, J., Zhang, S., and Wang, Z. (2017). Photoredox catalysis enabled alkylation of alkenyl carboxylic acids with N-(acyloxy)phthalimide via dual decarboxylation. *Chem. Commun.* **53**, 10719–10722.
- Ye, C., Li, Y., and Bao, H. (2017). Copper-catalyzed decarboxylative alkylation of terminal alkynes. *Adv. Synth. Catal.* **359**, 3720–3724.
- Yu, C., Iqbal, N., Park, S., and Cho, E.J. (2014). Selective difluoroalkylation of alkenes by using visible light photoredox catalysis. *Chem. Commun.* **50**, 12884–12887.
- Zhang, J.J., Yang, J.C., Guo, L.N., and Duan, X.H. (2017). Visible-light-mediated dual decarboxylative coupling of redox-active esters with alpha,beta-unsaturated carboxylic acids. *Chem. Eur. J.* **23**, 10259–10263.
- Zhu, N., Zhao, J., and Bao, H. (2017). Iron catalyzed methylation and ethylation of vinyl arenes. *Chem. Sci.* **8**, 2081–2085.
- Zou, Y., and Zhou, J.S. (2014). Palladium-catalyzed intermolecular Heck reaction of alkyl halides. *Chem. Commun.* **50**, 3725–3728.

ISCI, Volume 3

Supplemental Information

HOTf-Catalyzed Alkyl-Heck-type Reaction

Huan Zhou, Liang Ge, Jinshuai Song, Wujun Jian, Yajun Li, Chunsen Li, and Hongli Bao

Supplemental Figures for ^1H NMR, ^{13}C NMR, and ^{19}F NMR Spectra

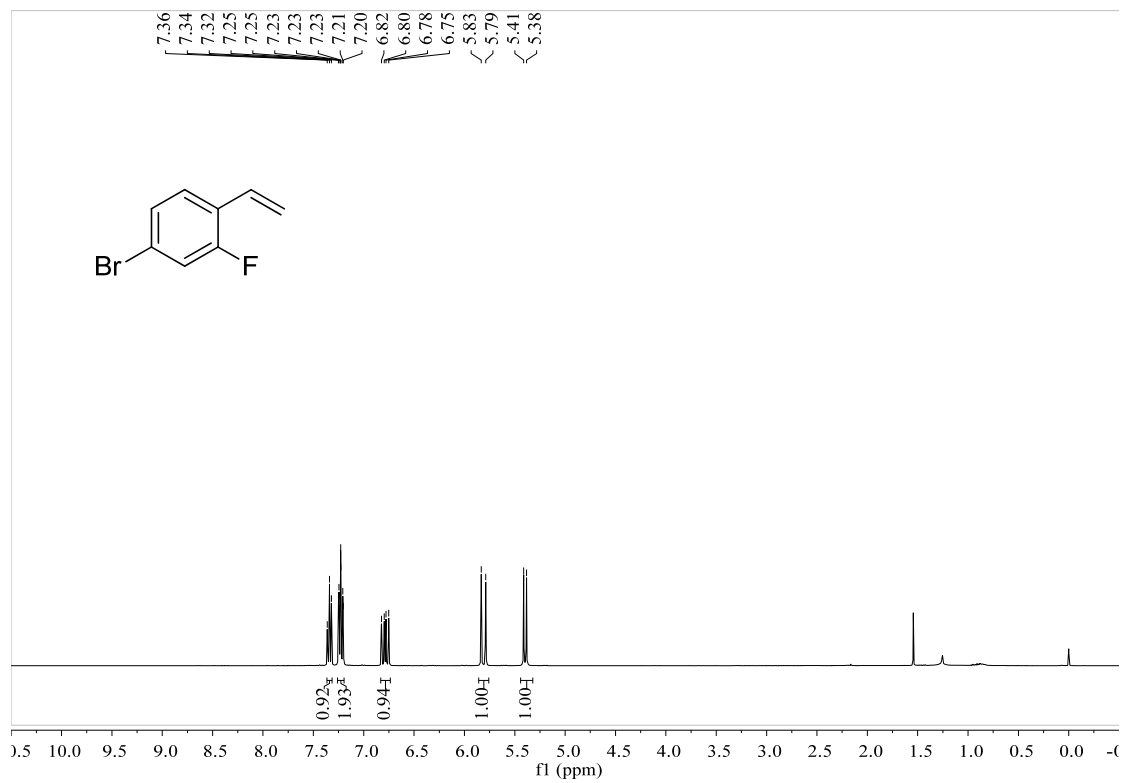


Figure S1. ^1H NMR spectrum of 4-bromo-2-fluoro-1-vinylbenzene, Related to **Figure 1**.

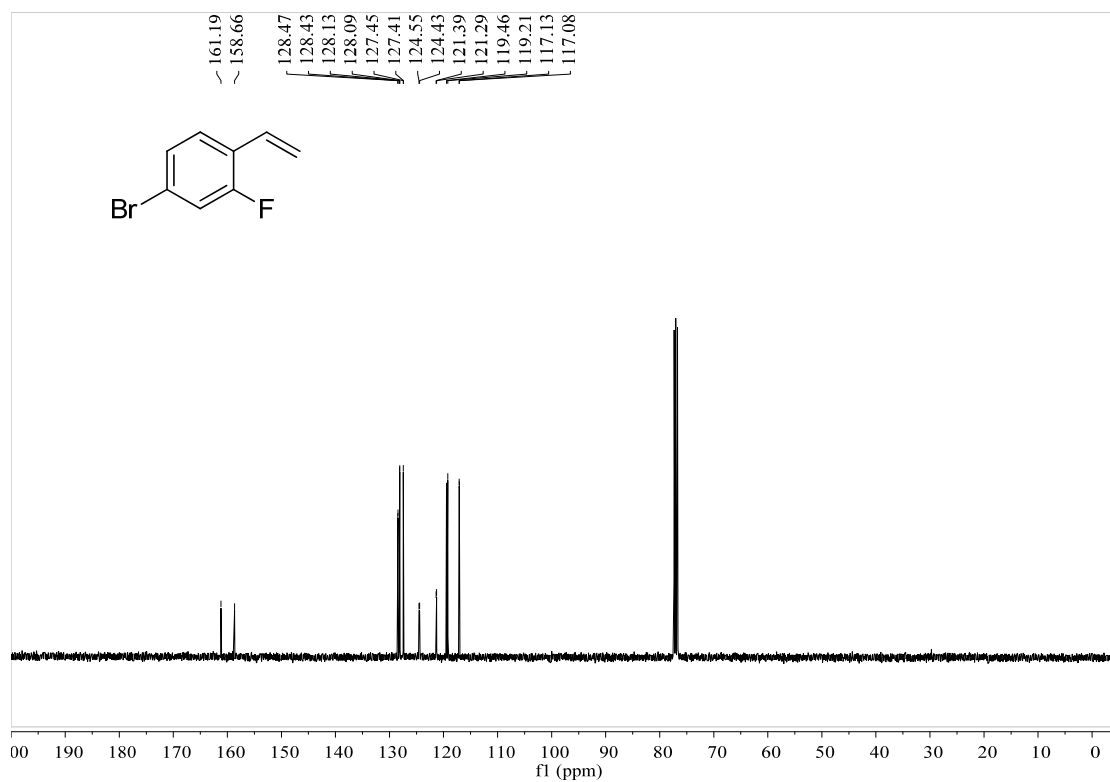


Figure S2. ^{13}C NMR spectrum of 4-bromo-2-fluoro-1-vinylbenzene, Related to **Figure 1**.

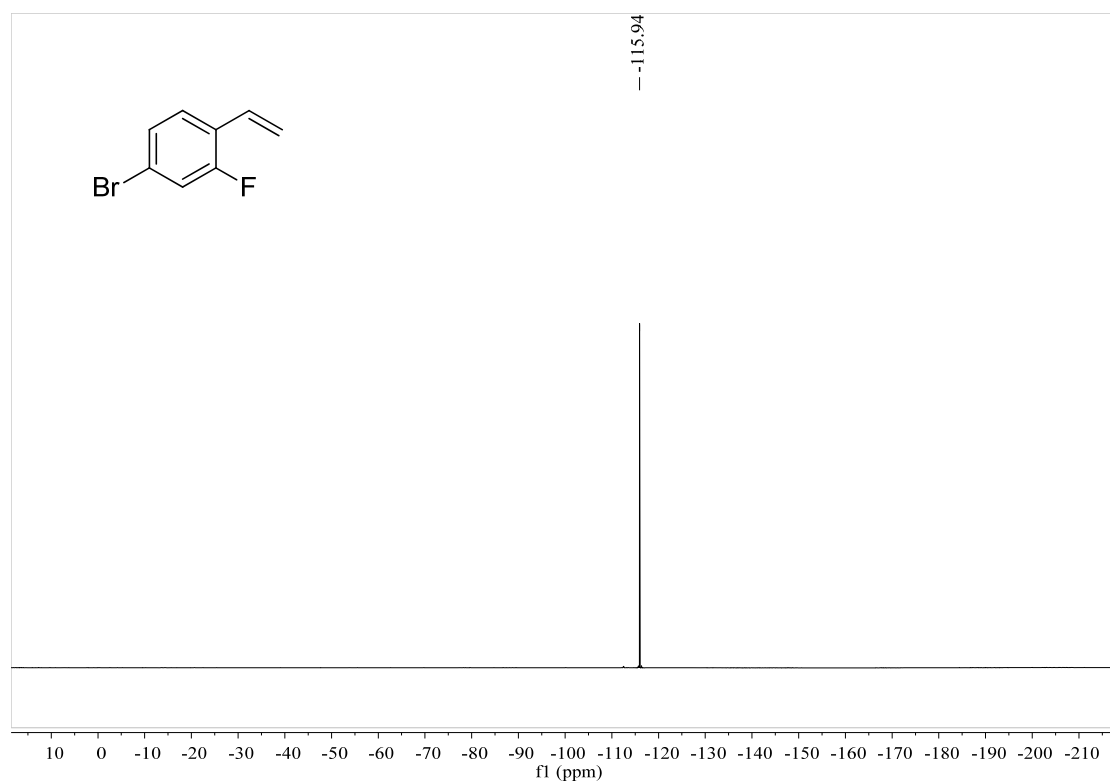


Figure S3. ^{19}F NMR spectrum of 4-bromo-2-fluoro-1-vinylbenzene, Related to **Figure 1**.

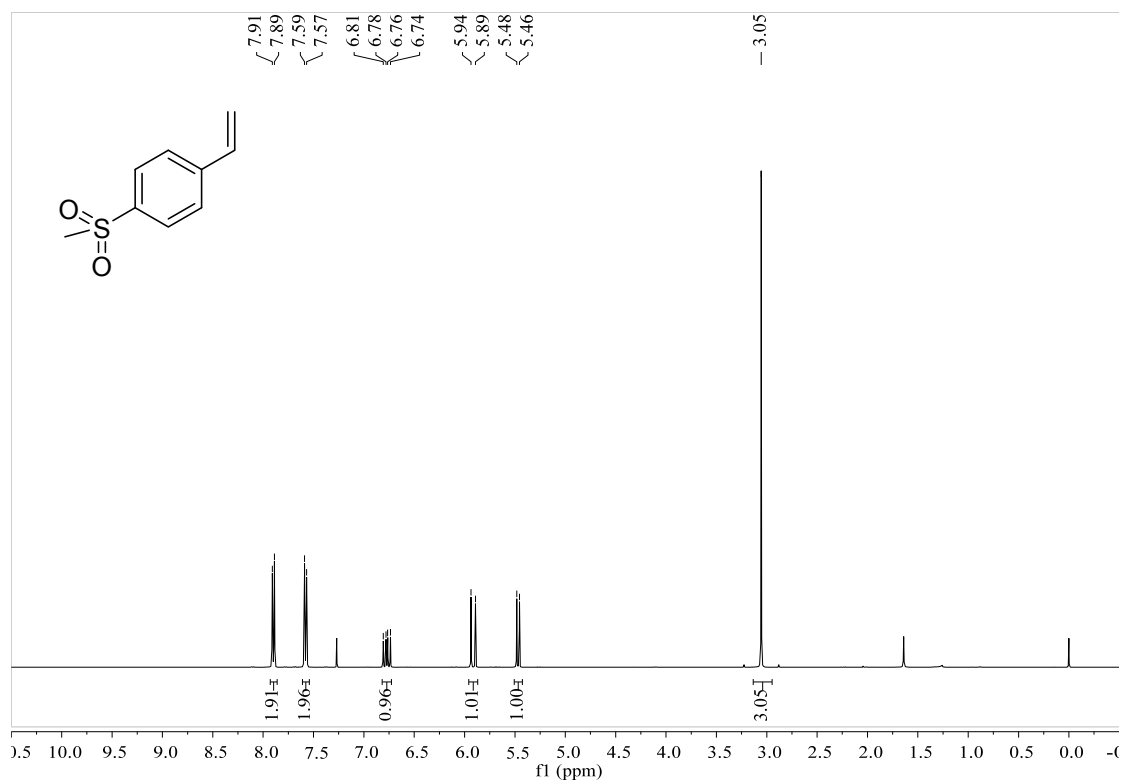


Figure S4. ^1H NMR spectrum of 1-(methylsulfonyl)-4-vinylbenzene, Related to **Figure 1**.

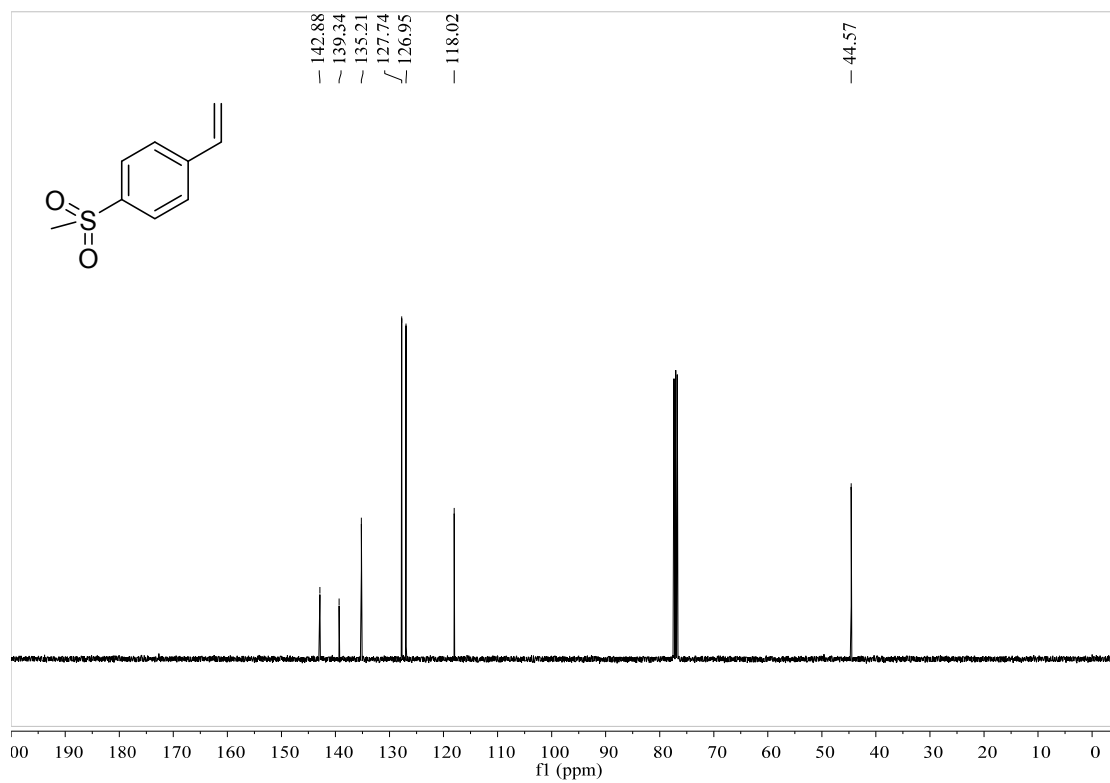


Figure S5. ^{13}C NMR spectrum of 1-(methylsulfonyl)-4-vinylbenzene, Related to **Figure 1**.

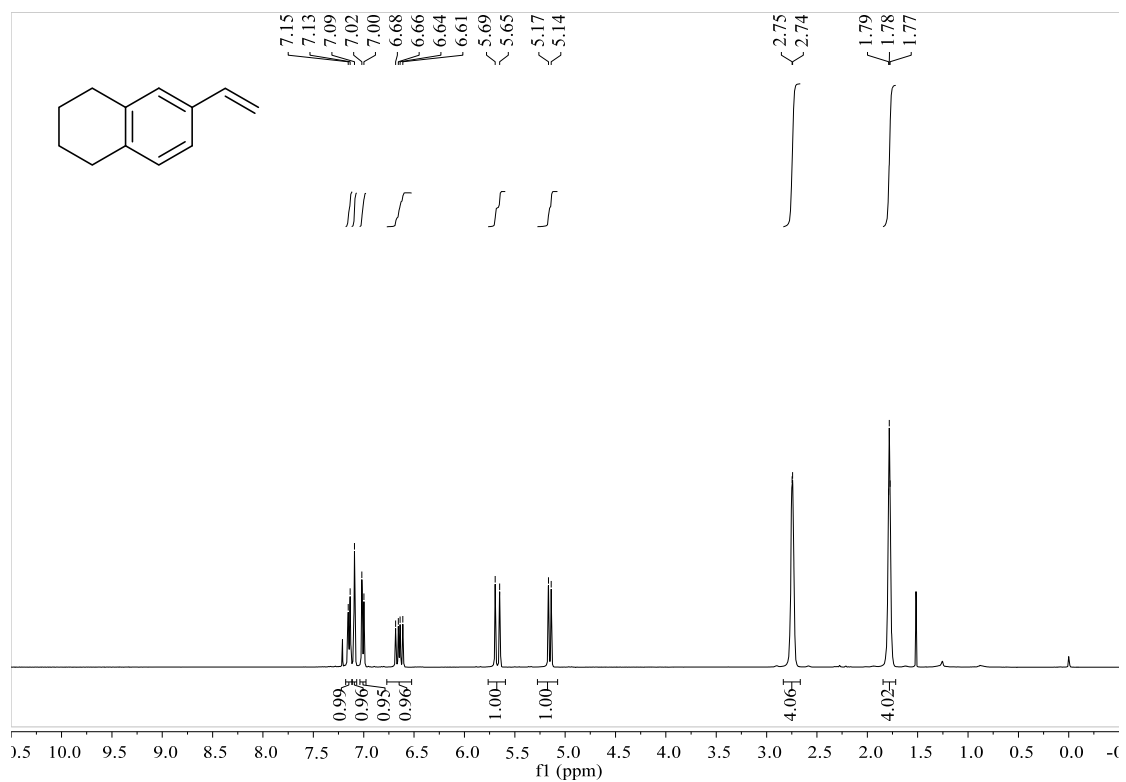


Figure S6. ¹H NMR spectrum of 6-vinyl-1,2,3,4-tetrahydronaphthalene, Related to **Figure 1**.

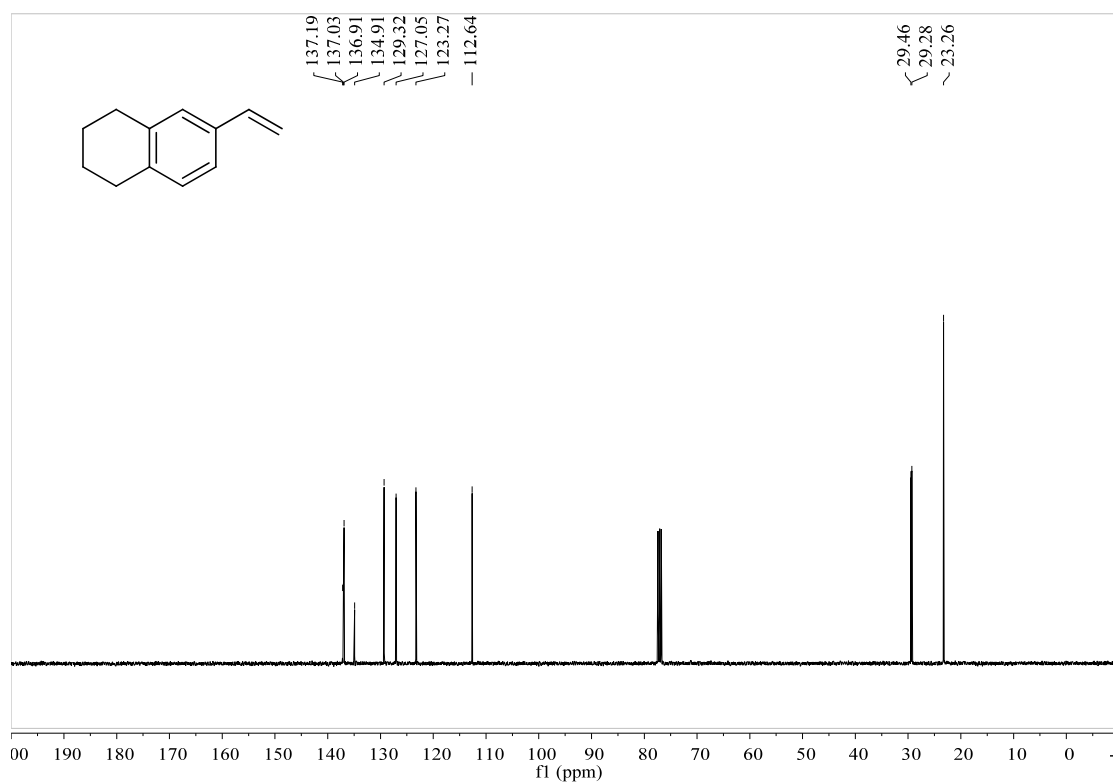


Figure S7. ¹³C NMR spectrum of 6-vinyl-1,2,3,4-tetrahydronaphthalene, Related to **Figure 1**.

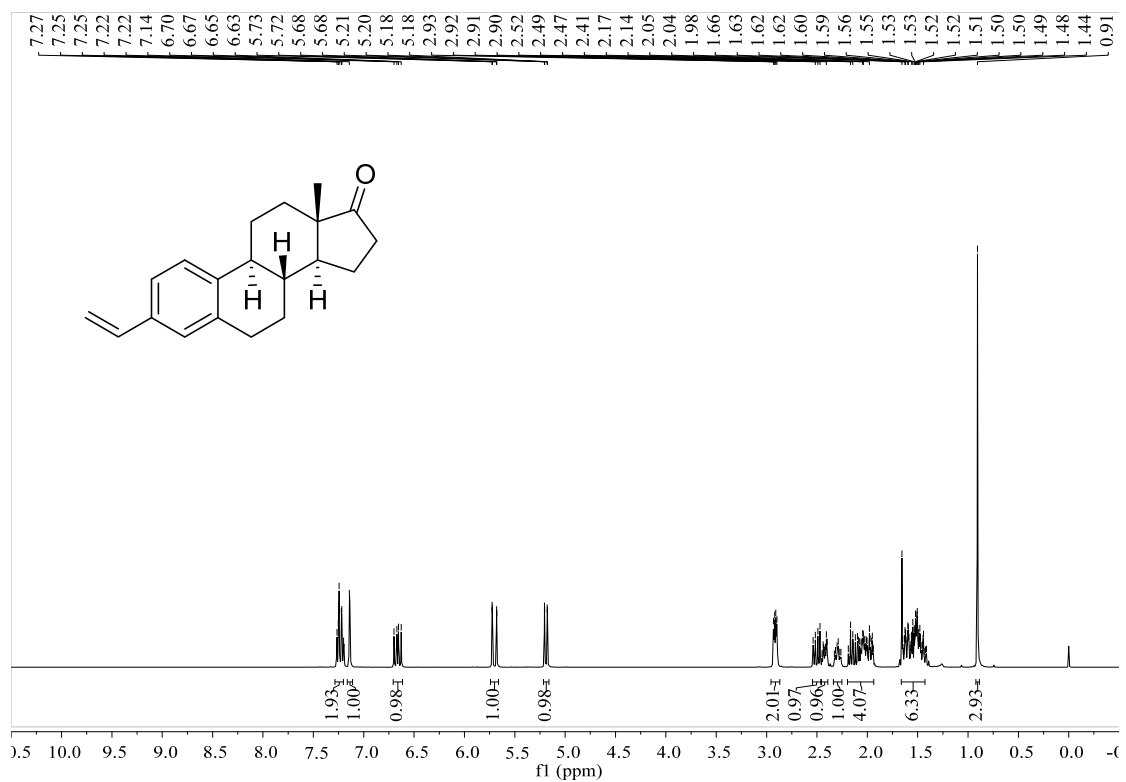


Figure S8. ¹H NMR spectrum of compound 57, related to **scheme 2**.

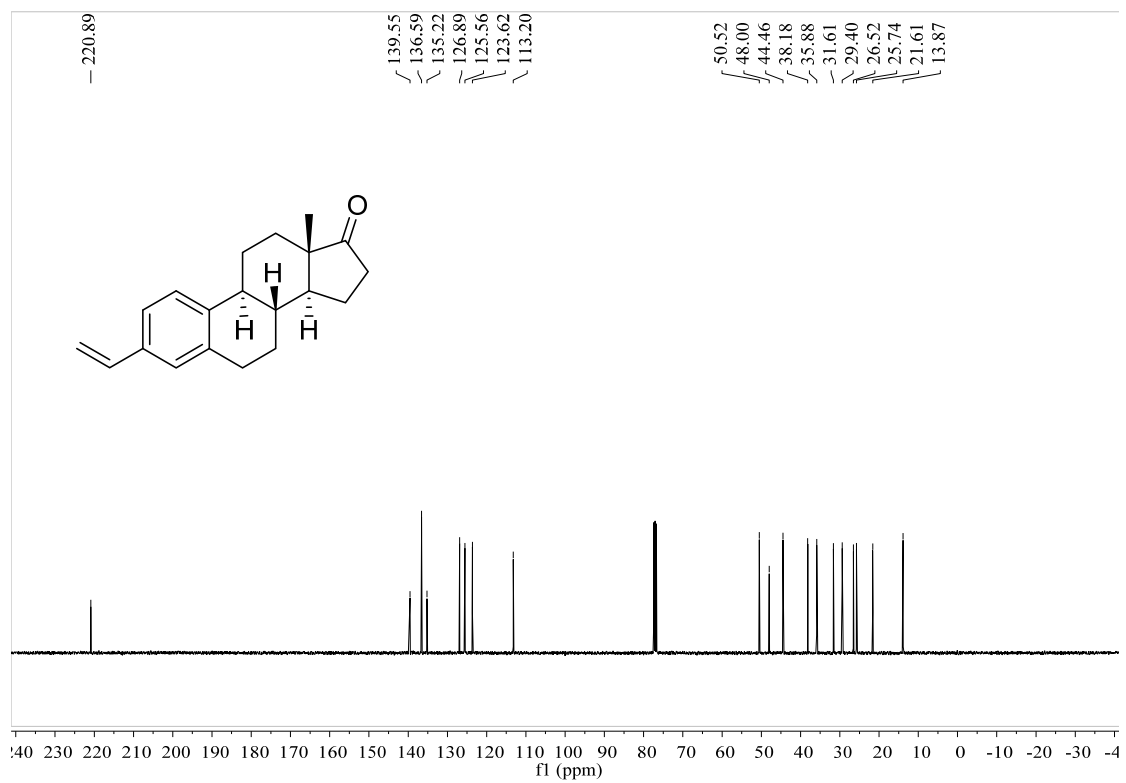


Figure S9. ¹³C NMR spectrum of compound 57, related to **Scheme 2**.

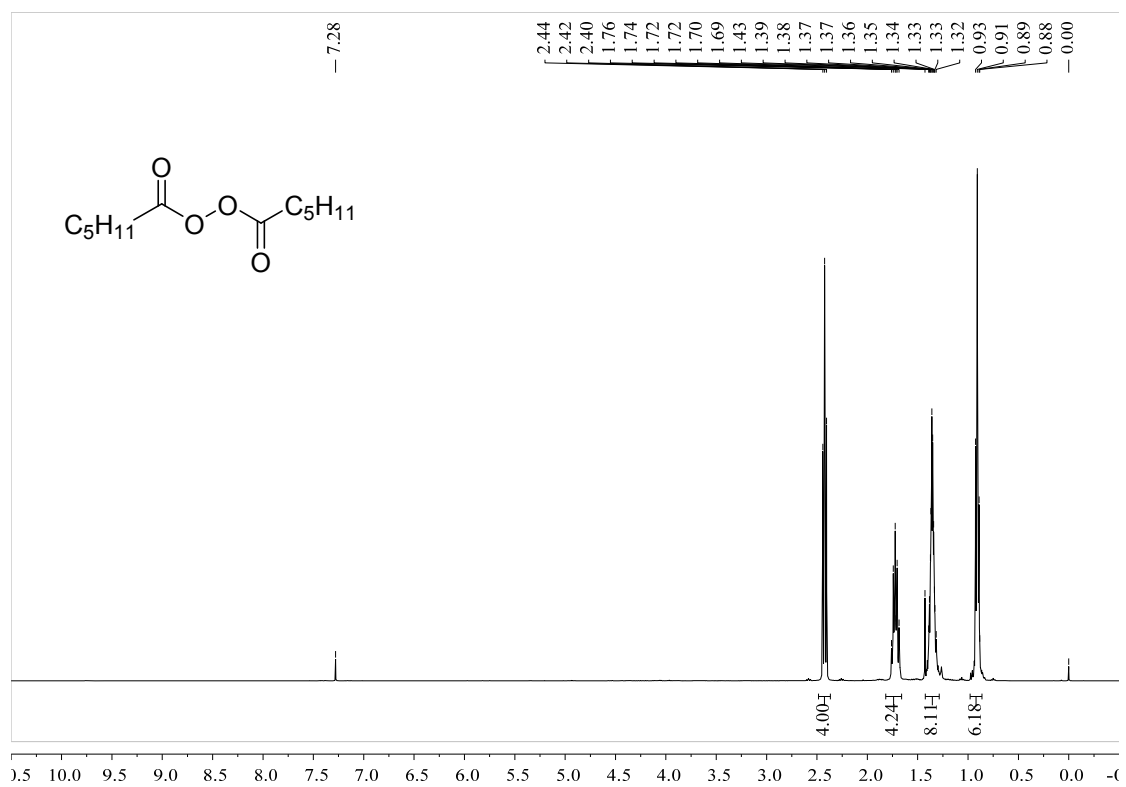


Figure S10. ¹H NMR spectrum of hexanoic peroxyanhydride, related to **Figure 3**.

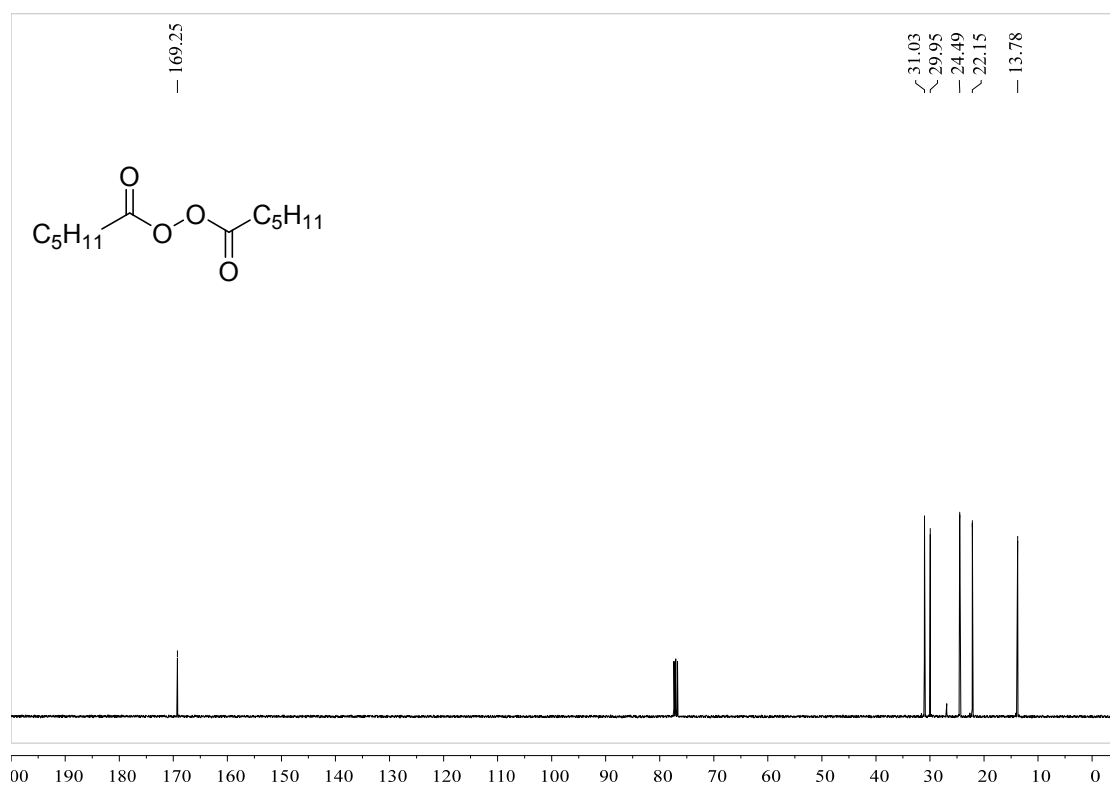


Figure S11. ¹³C NMR spectrum of hexanoic peroxyanhydride, related to **Figure 3**.

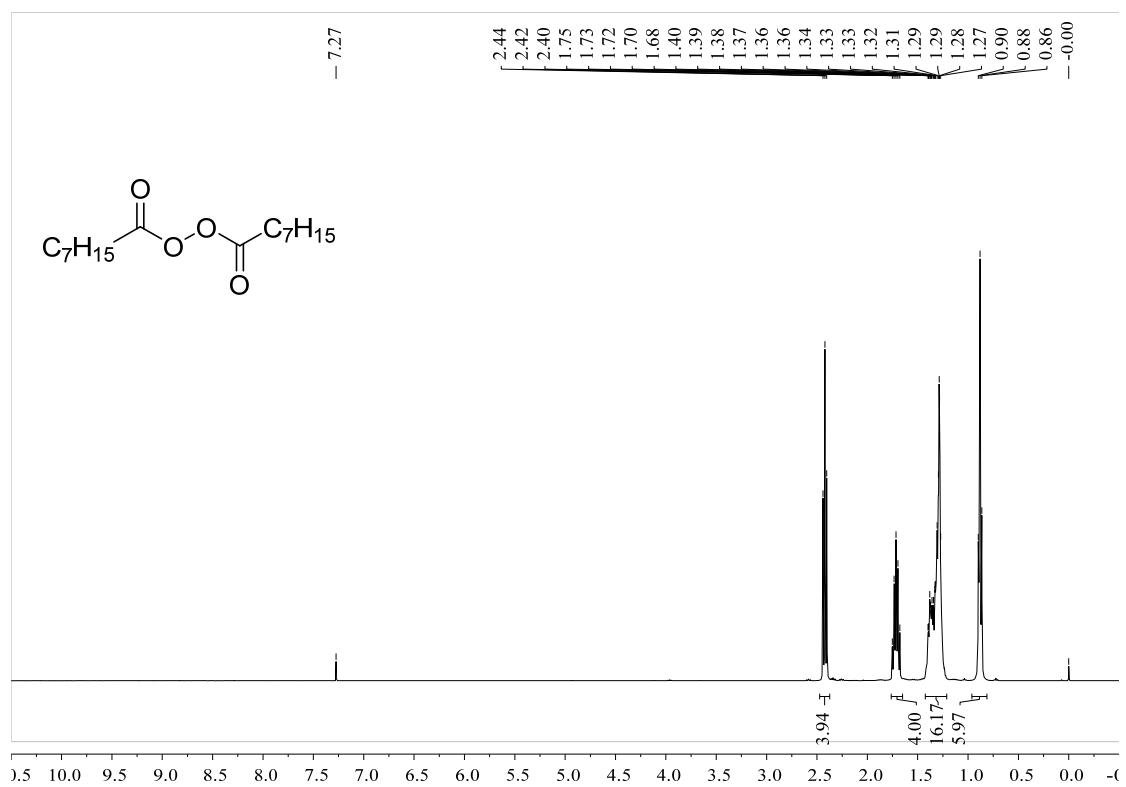


Figure S12. ¹H NMR spectrum of octanoic peroxyanhydride, related to **Figure 3**.

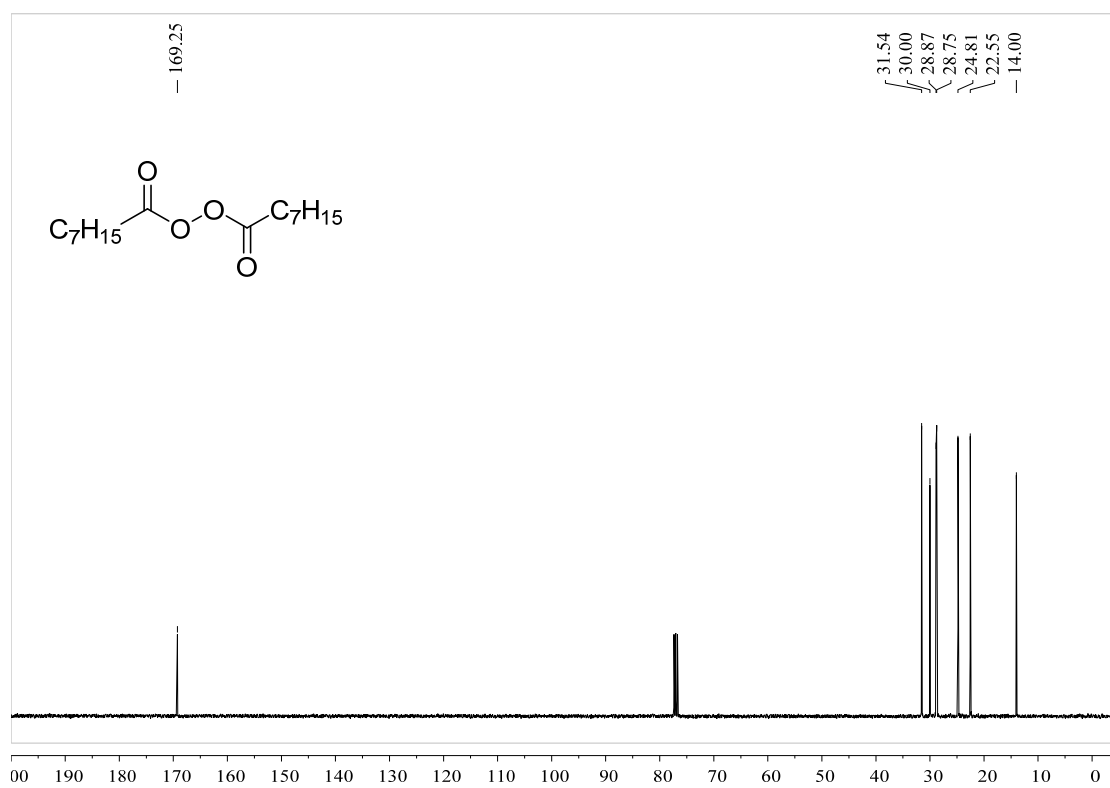


Figure S13. ¹³C NMR spectrum of octanoic peroxyanhydride, related to **Figure 3**.

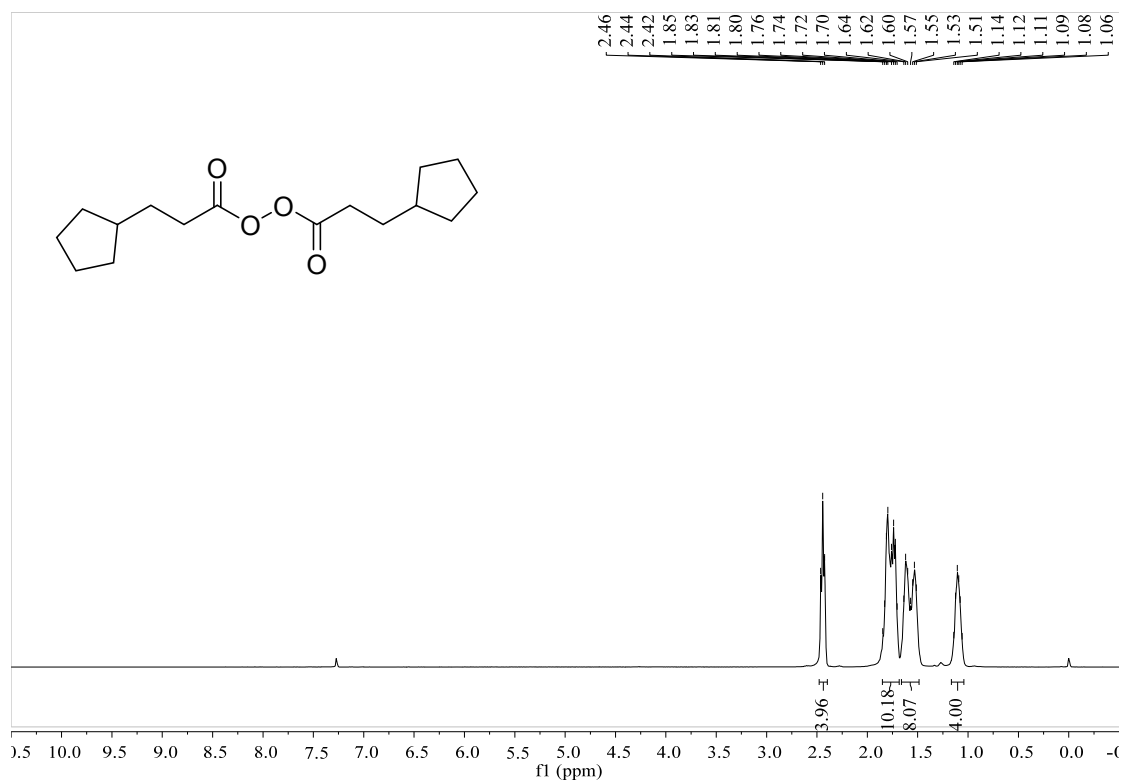


Figure S14. ^1H NMR spectrum of 3-cyclopentylpropanoic peroxyanhydride, related to **Figure 3**.

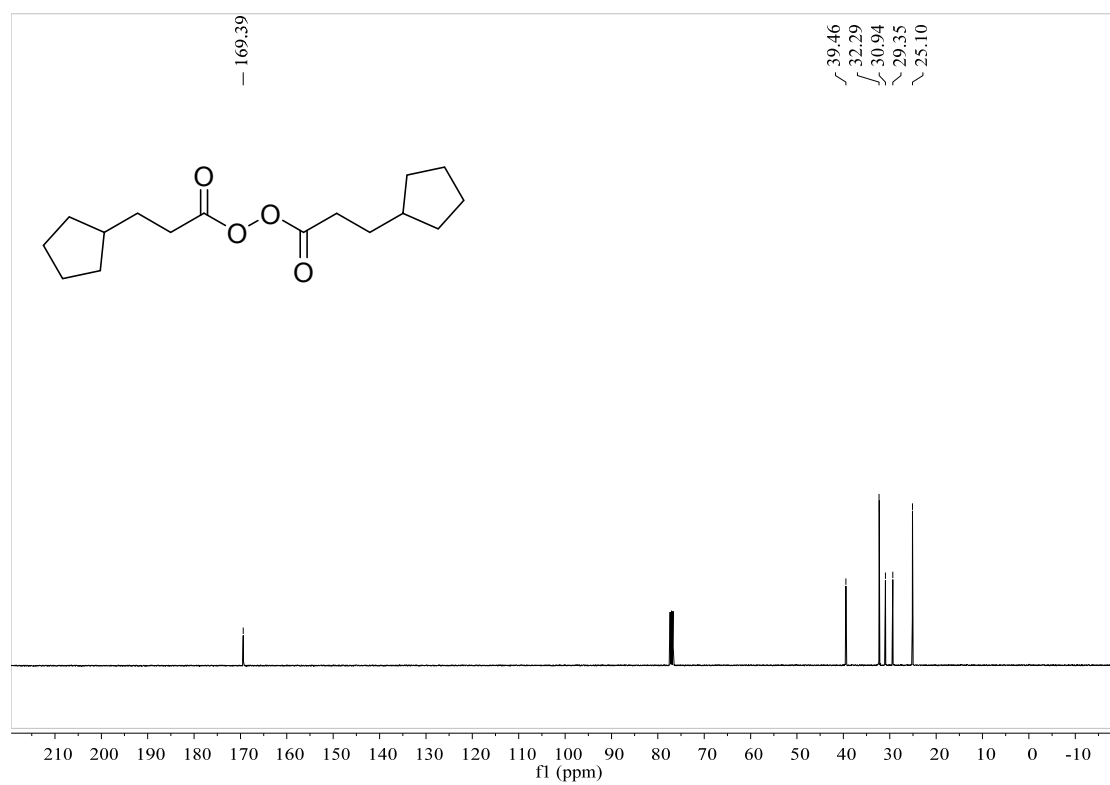


Figure S15. ^{13}C NMR spectrum of 3-cyclopentylpropanoic peroxyanhydride, related to **Figure 3**.

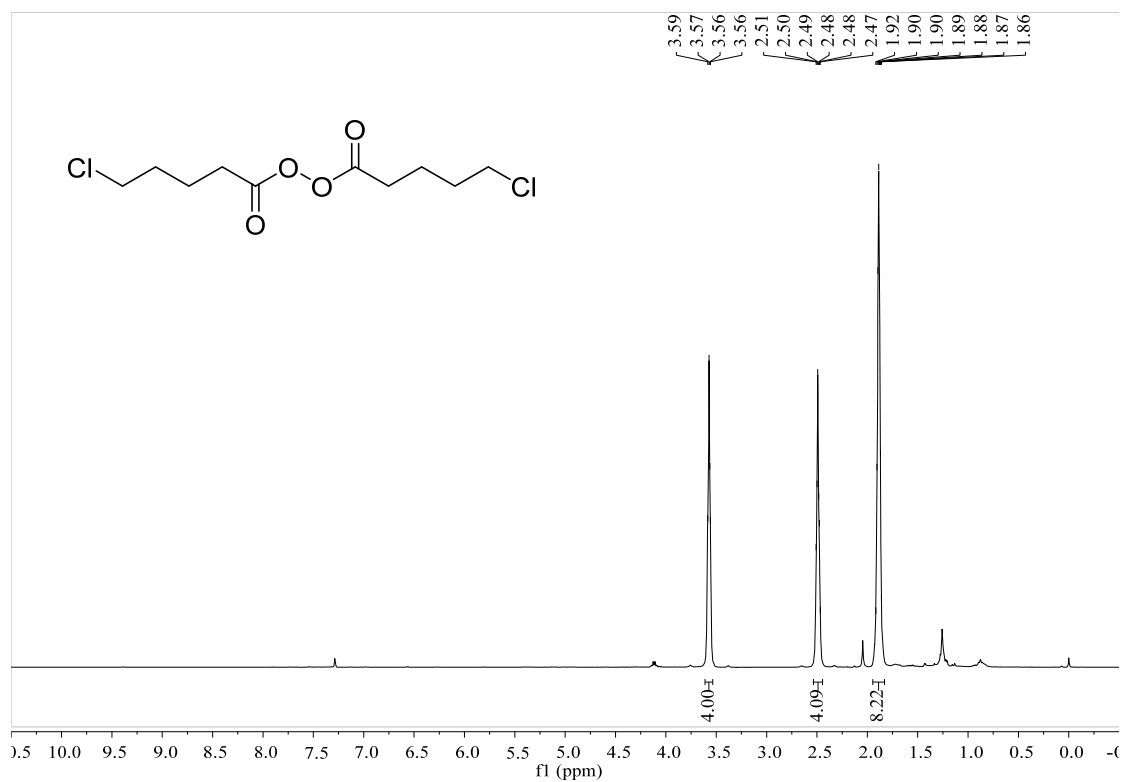


Figure S16. ¹H NMR spectrum of 5-chloropentanoic peroxyanhydride, related to **Figure 3**.

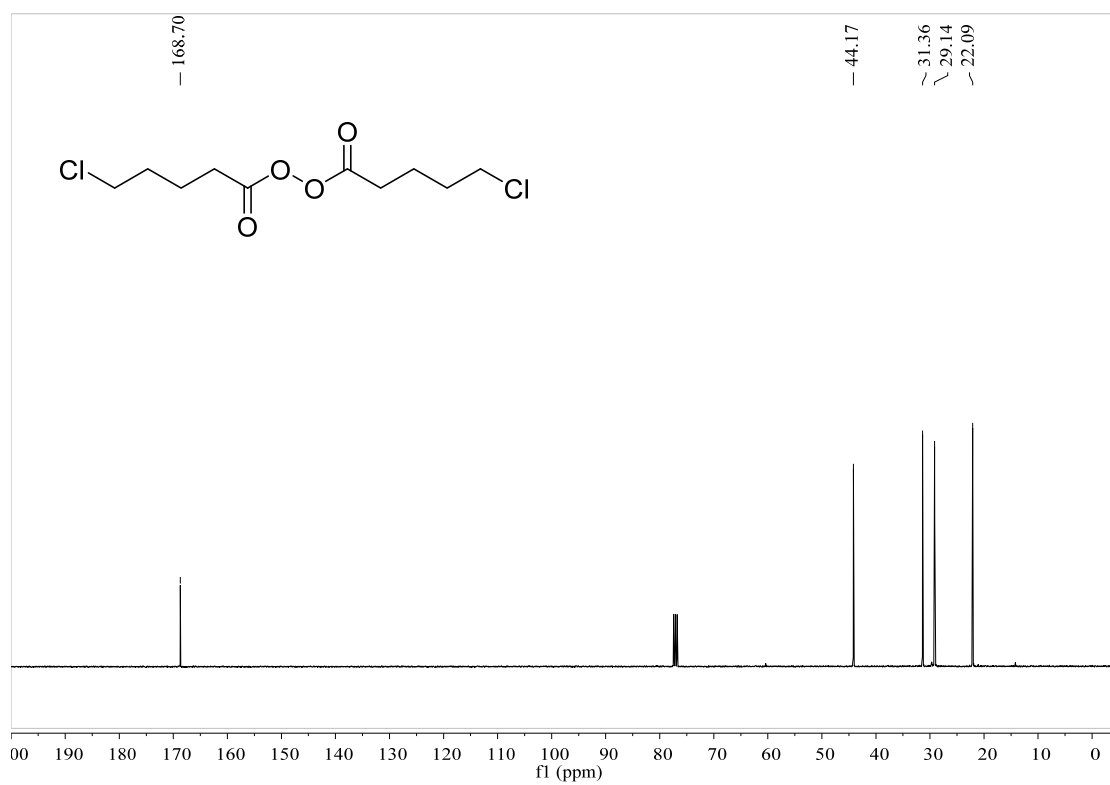


Figure S17. ¹³C NMR spectrum of 5-chloropentanoic peroxyanhydride, related to **Figure 3**.

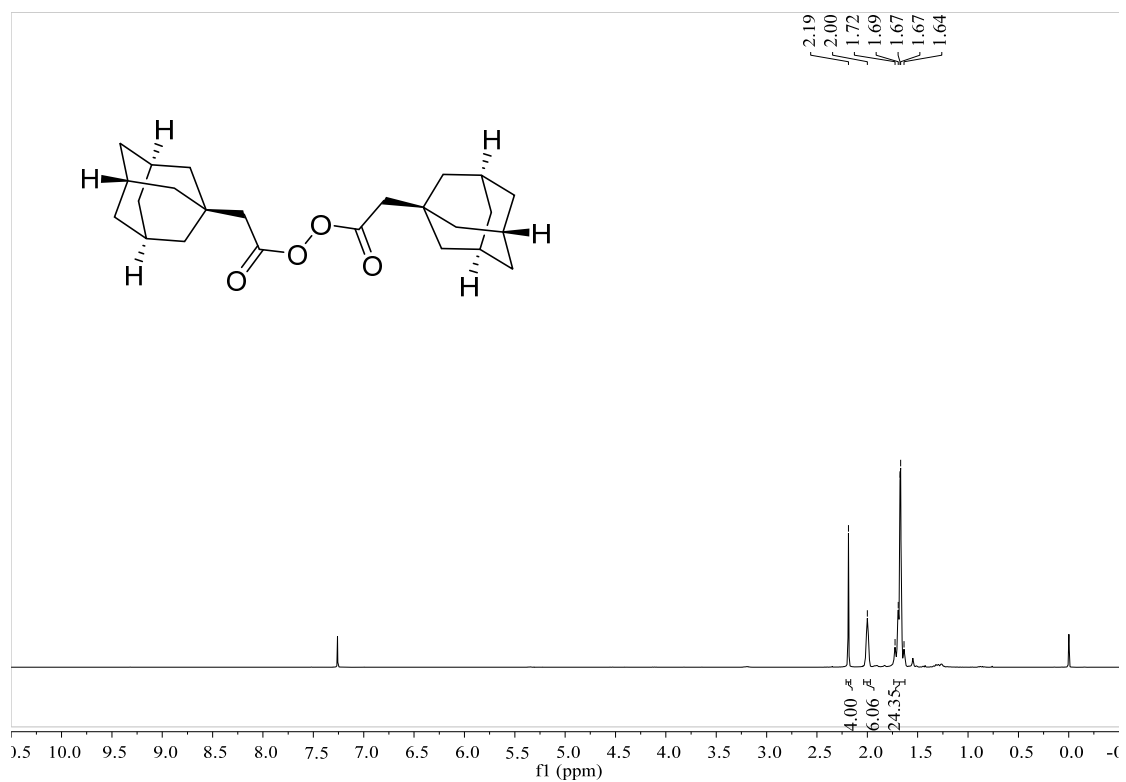


Figure S18. ¹H NMR spectrum of 2-((3*r*,5*r*,7*r*)-adamantan-1-yl)acetic peroxyanhydride, related to **Figure 3**.

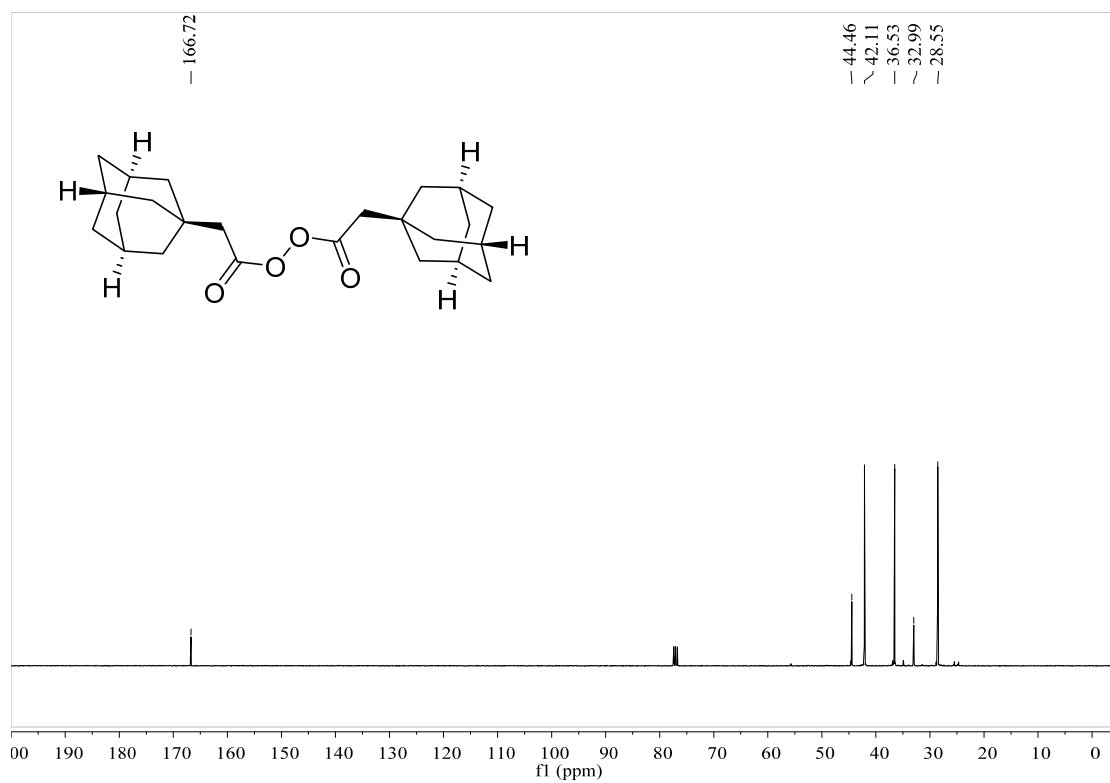


Figure S19. ¹³C NMR spectrum of 2-((3*r*,5*r*,7*r*)-adamantan-1-yl)acetic peroxyanhydride, related to **Figure 3**.

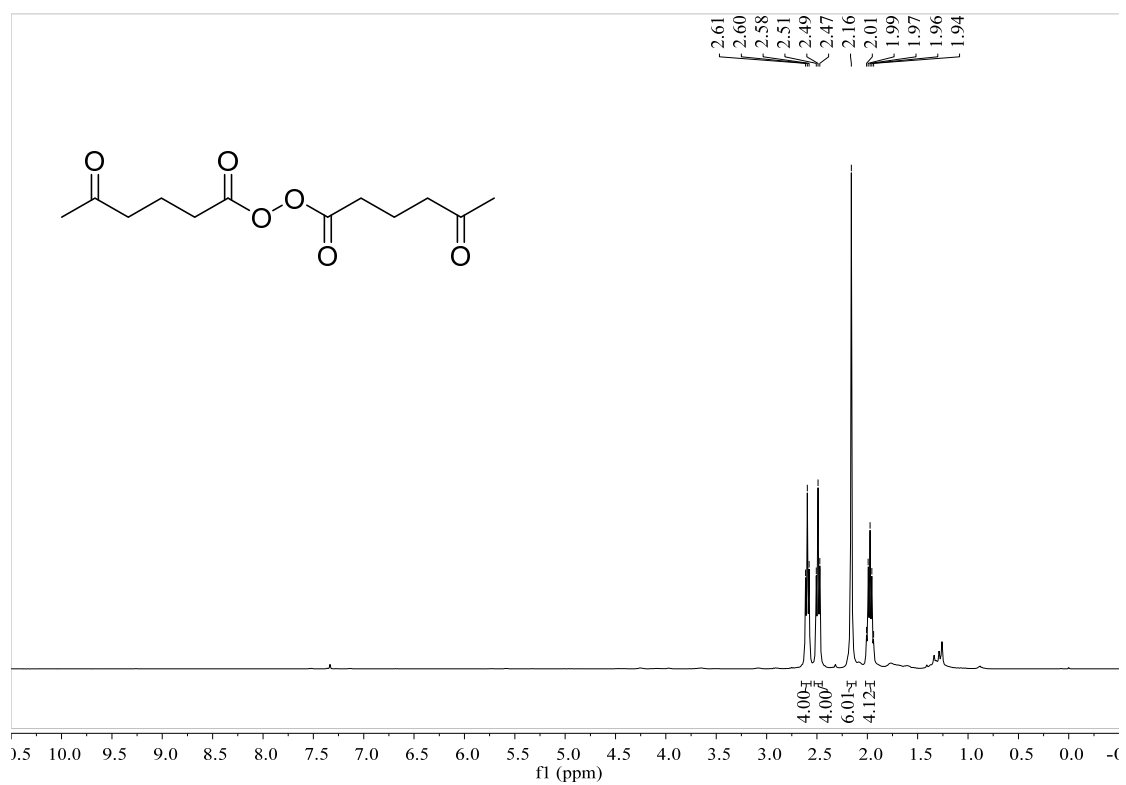


Figure S20. ^1H NMR spectrum of 5-oxohexanoic peroxyanhydride, related to **Figure 3**.

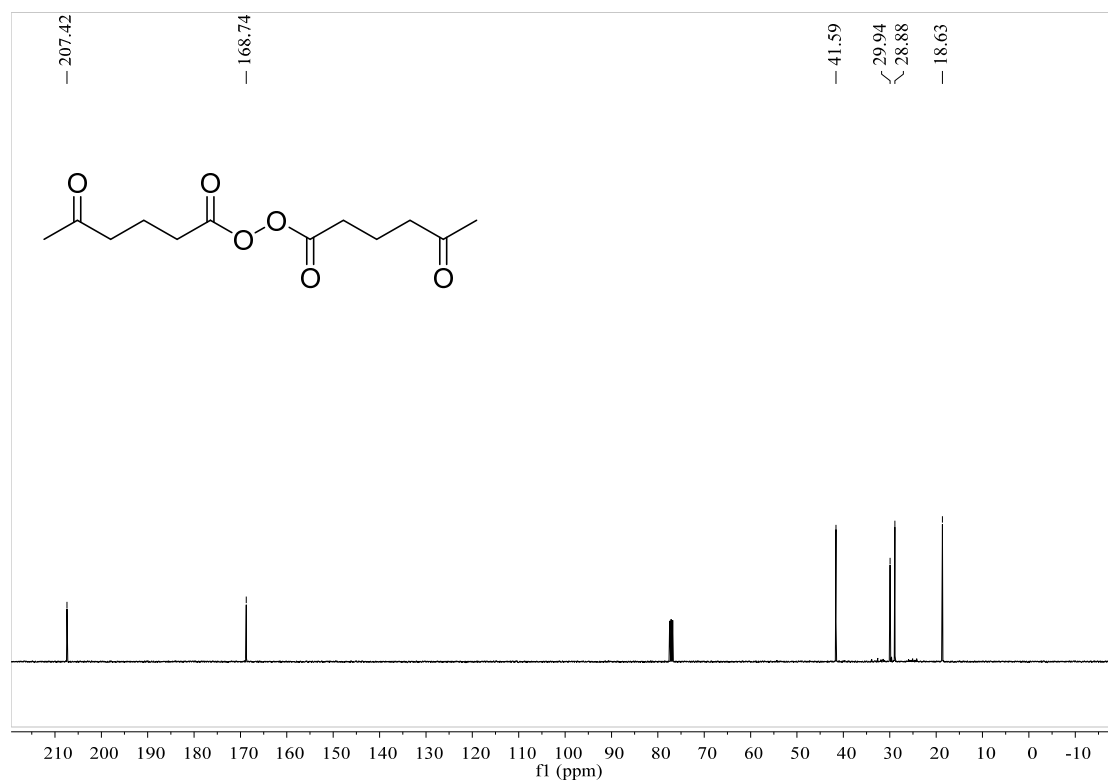


Figure S21. ^{13}C NMR spectrum of 5-oxohexanoic peroxyanhydride, related to **Figure 3**.

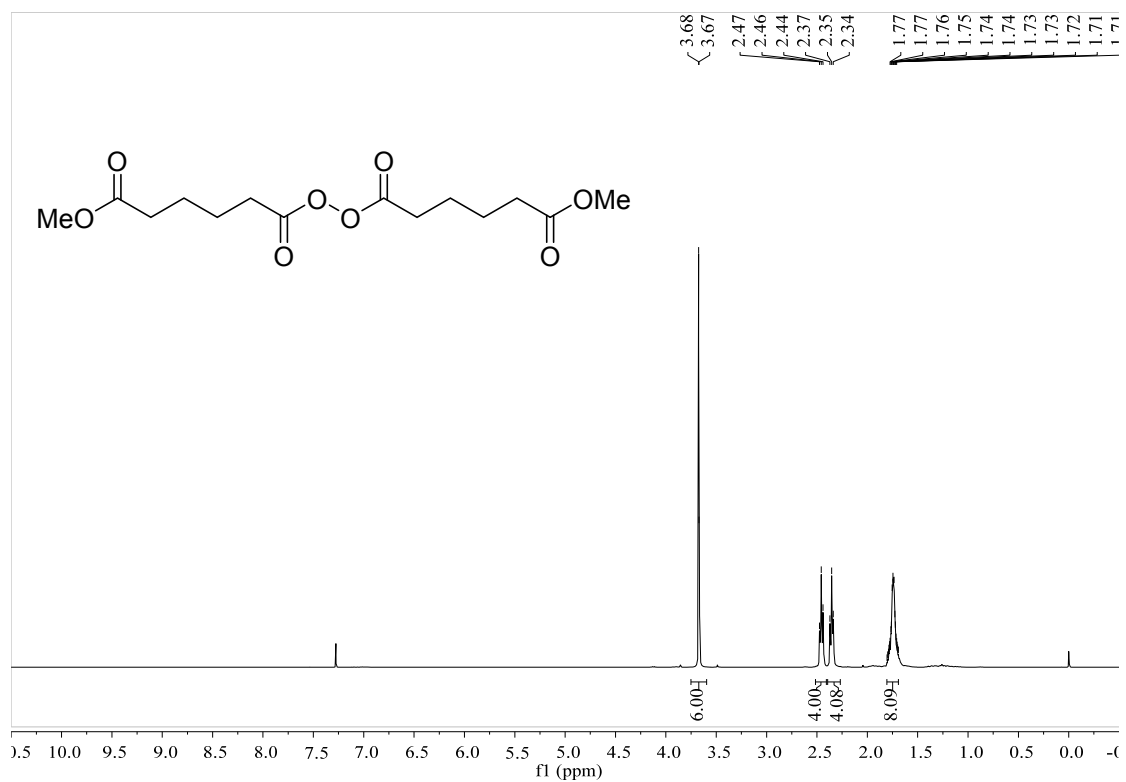


Figure S22. ¹H NMR spectrum of 6-methoxy-6-oxohexanoic peroxyanhydride, related to Figure 3.

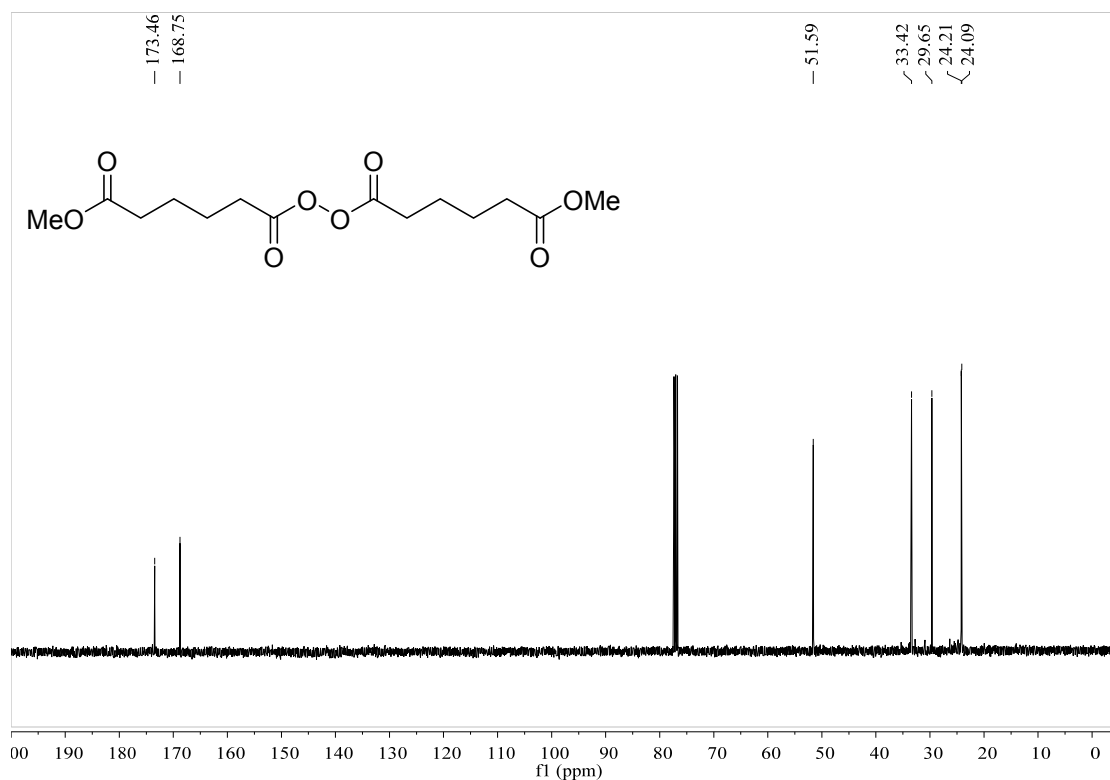


Figure S23. ¹³C NMR spectrum of 6-methoxy-6-oxohexanoic peroxyanhydride, related to Figure 3.

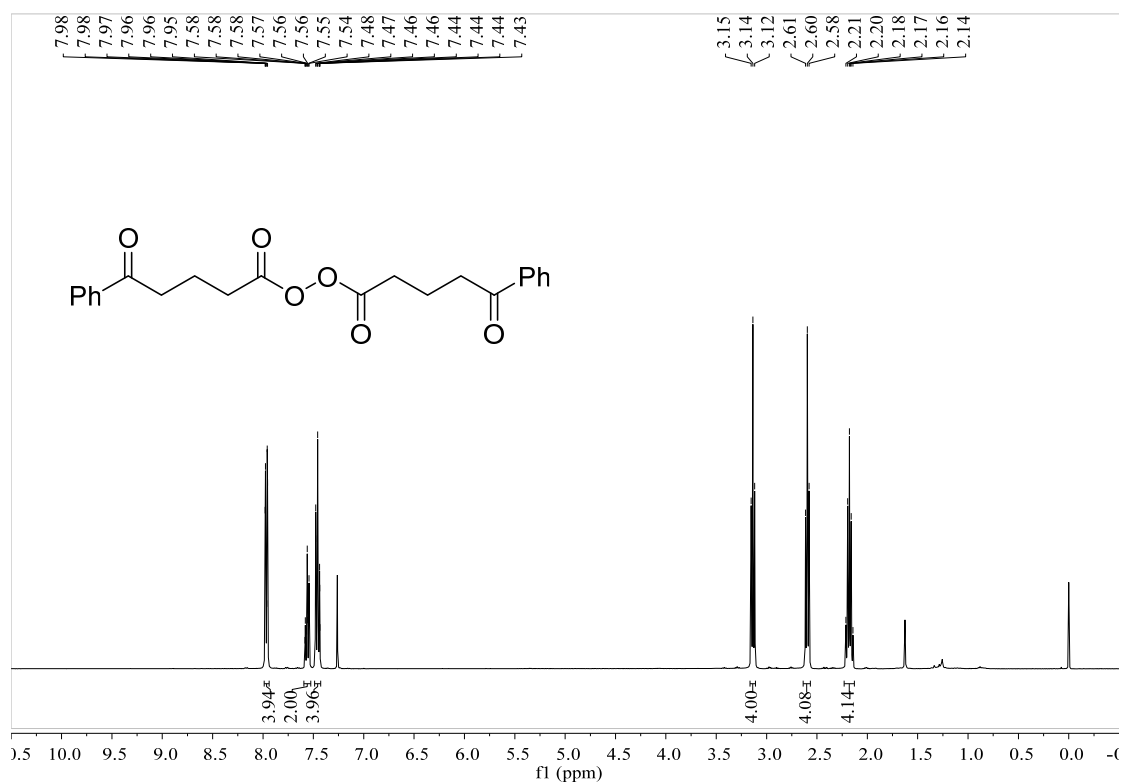


Figure S24. ¹H NMR spectrum of 5-oxo-5-phenylpentanoic peroxyanhydride, related to **Figure 3**.

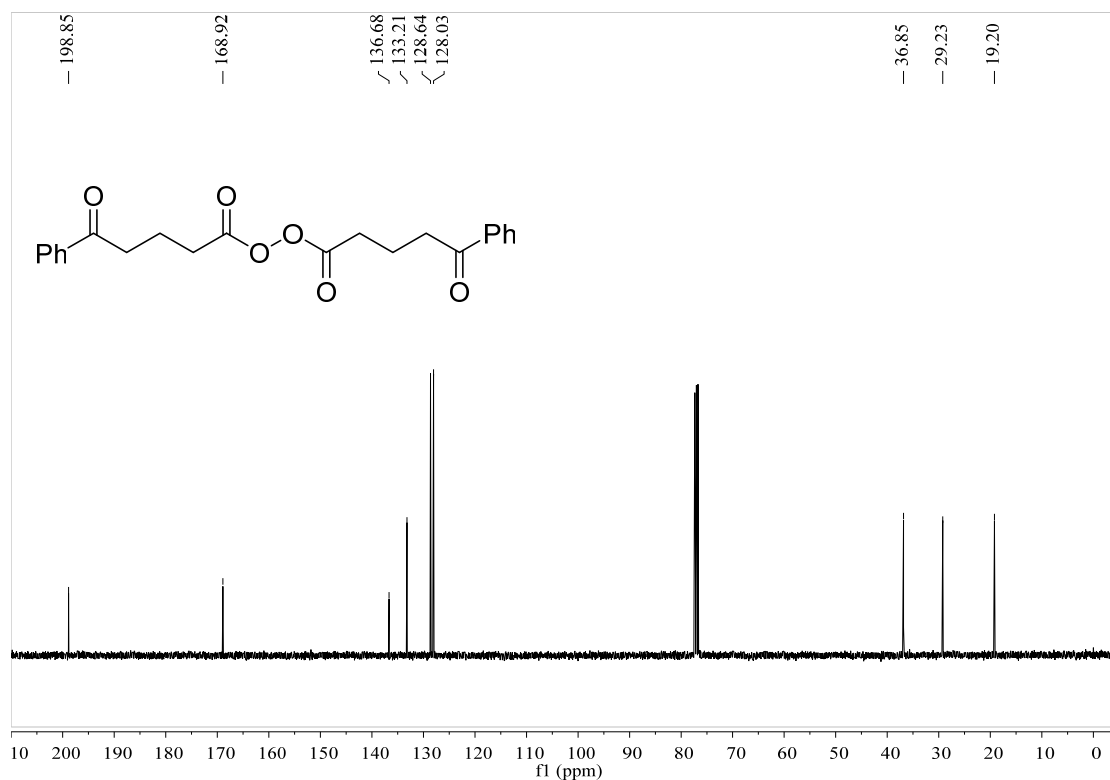


Figure S25. ¹³C NMR spectrum of 5-oxo-5-phenylpentanoic peroxyanhydride, related to **Figure 3**.

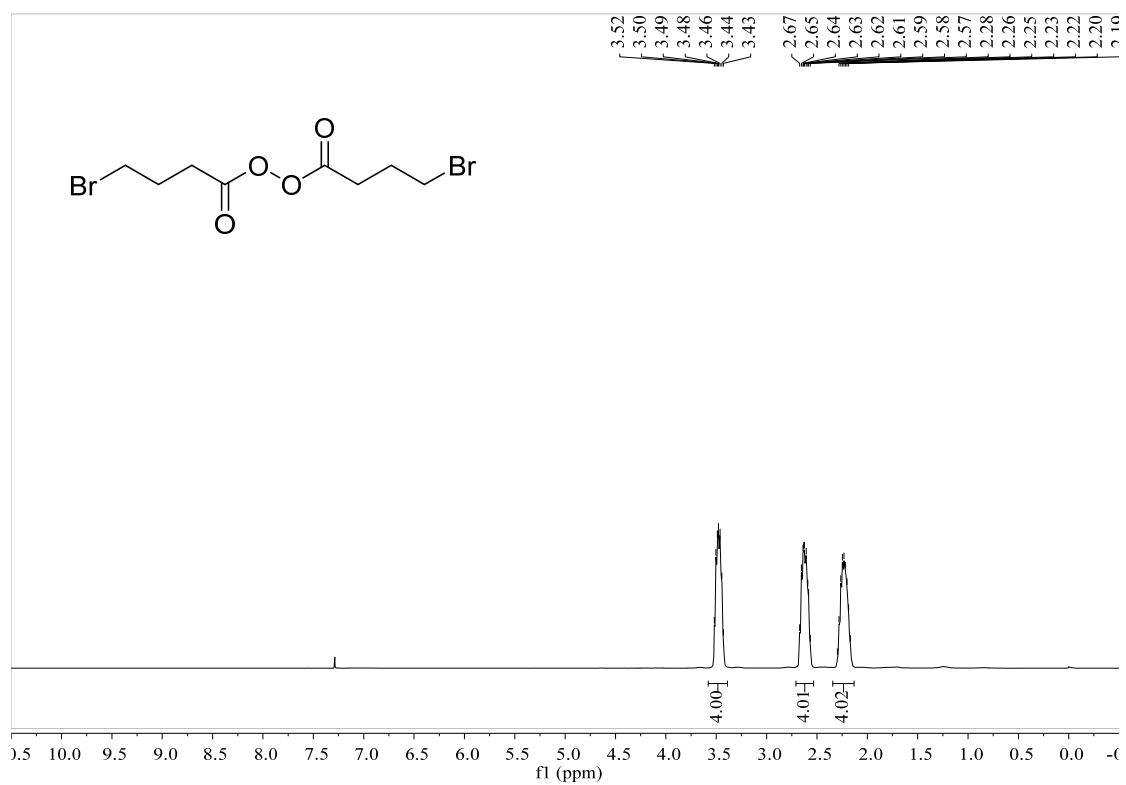


Figure S26. ^1H NMR spectrum of 4-bromobutanoic peroxyanhydride, related to **Figure 3**.

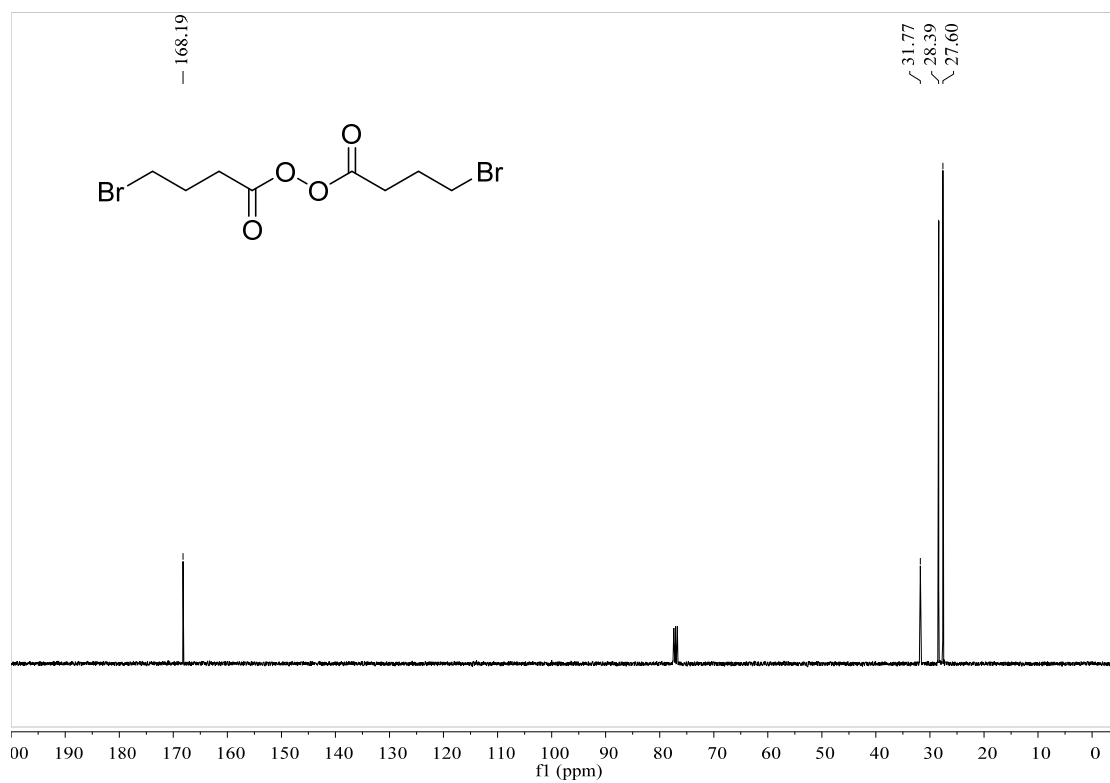


Figure S27. ^{13}C NMR spectrum of 4-bromobutanoic peroxyanhydride, related to **Figure 3**.

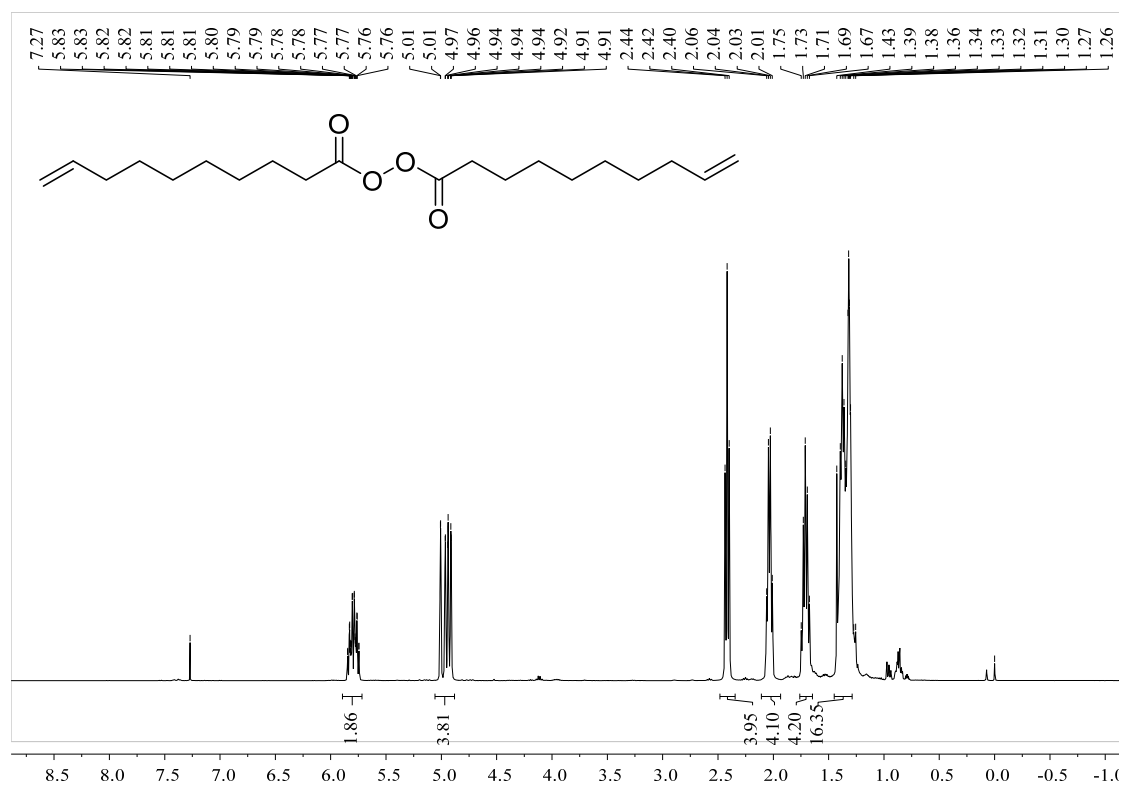


Figure S28. ¹H NMR spectrum of dec-9-enoic peroxyanhydride, related to **Figure 3**.

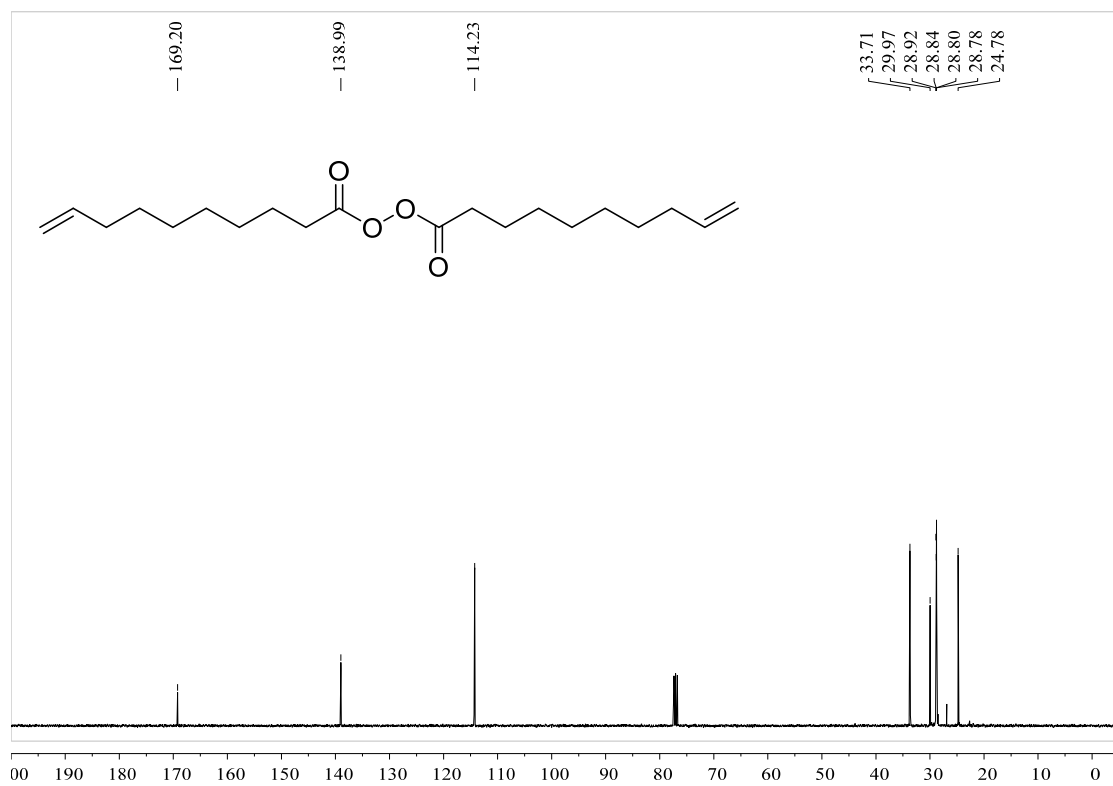


Figure S29. ¹³C NMR spectrum of dec-9-enoic peroxyanhydride, related to **Figure 3**.

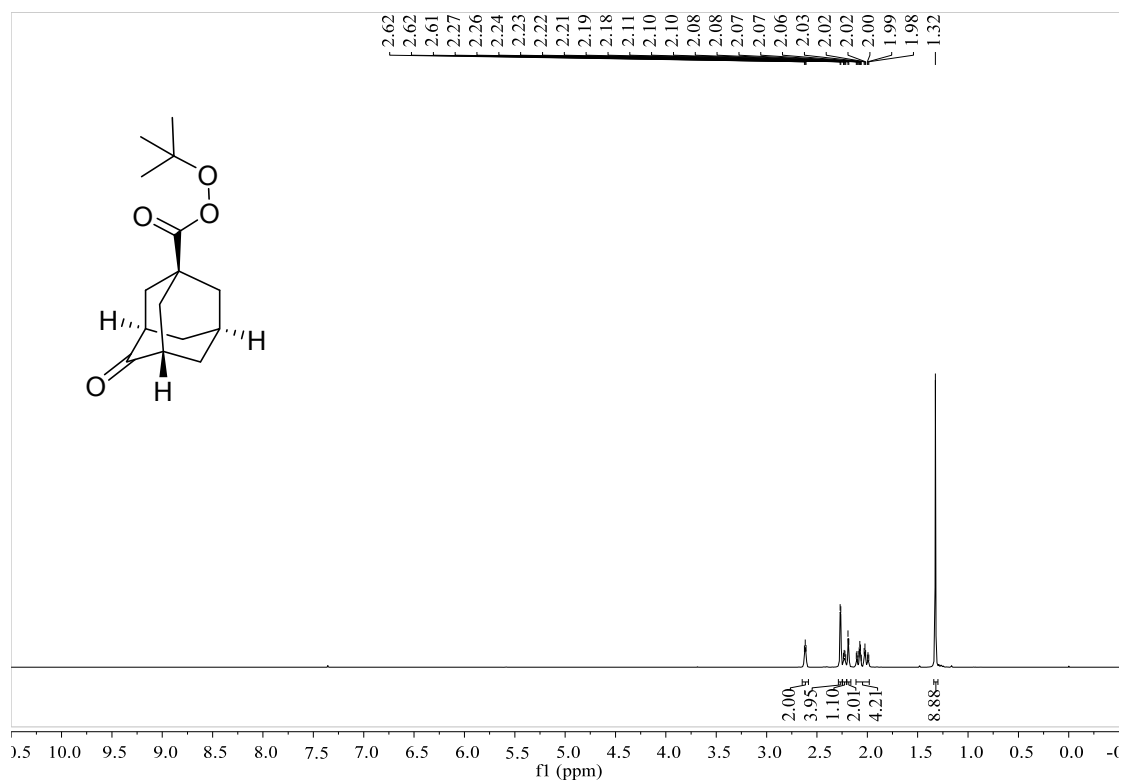


Figure S30. ¹H NMR spectrum of *tert*-butyl(1*s*,3*r*,5*s*,7*s*)-4-oxadamantane-1-carboperoxoate, related to **Figure 2**.

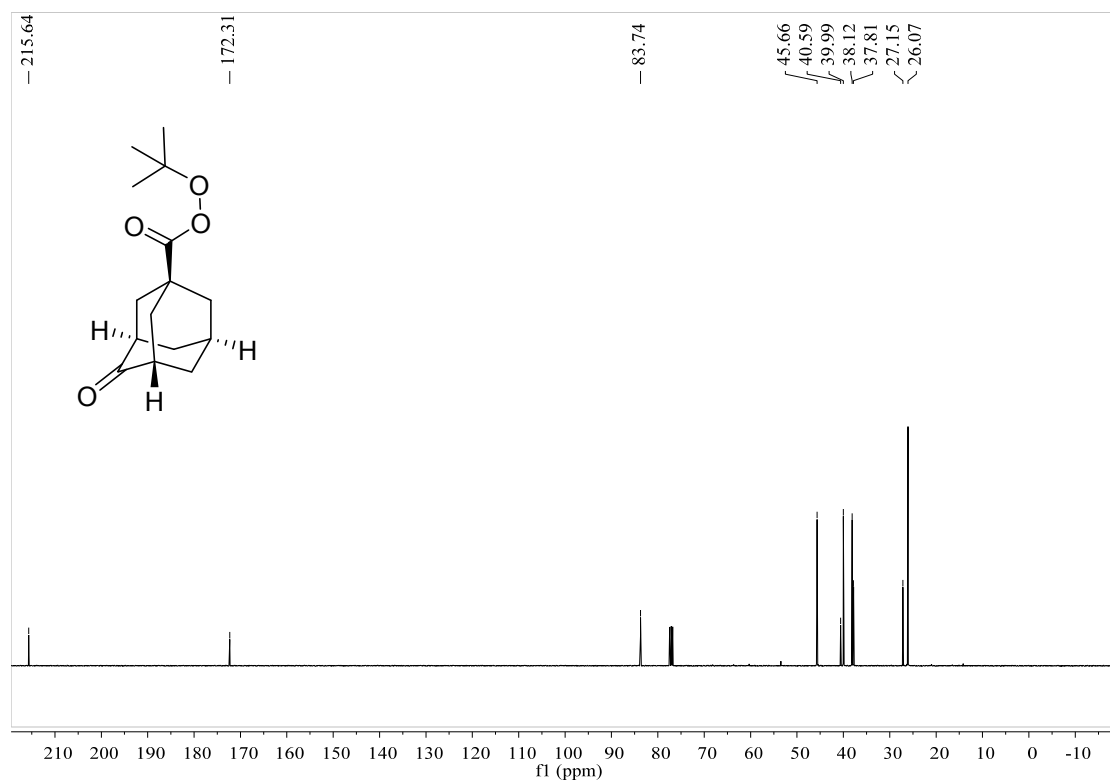


Figure S31. ¹³C NMR spectrum of *tert*-butyl(1*s*,3*r*,5*s*,7*s*)-4-oxadamantane-1-carboperoxoate, related to **Figure 2**.

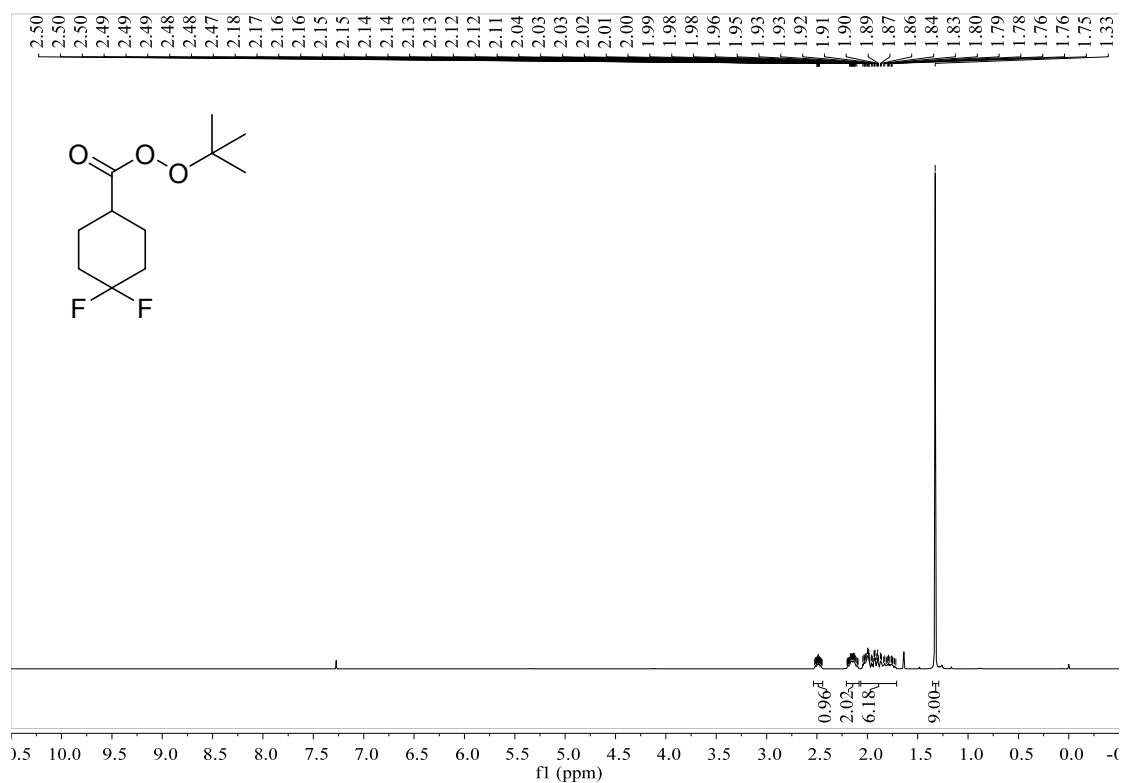


Figure S32. ¹H NMR spectrum of *tert*-butyl 4,4-difluorocyclohexane-1-carboxylate, related to **Figure 2**.

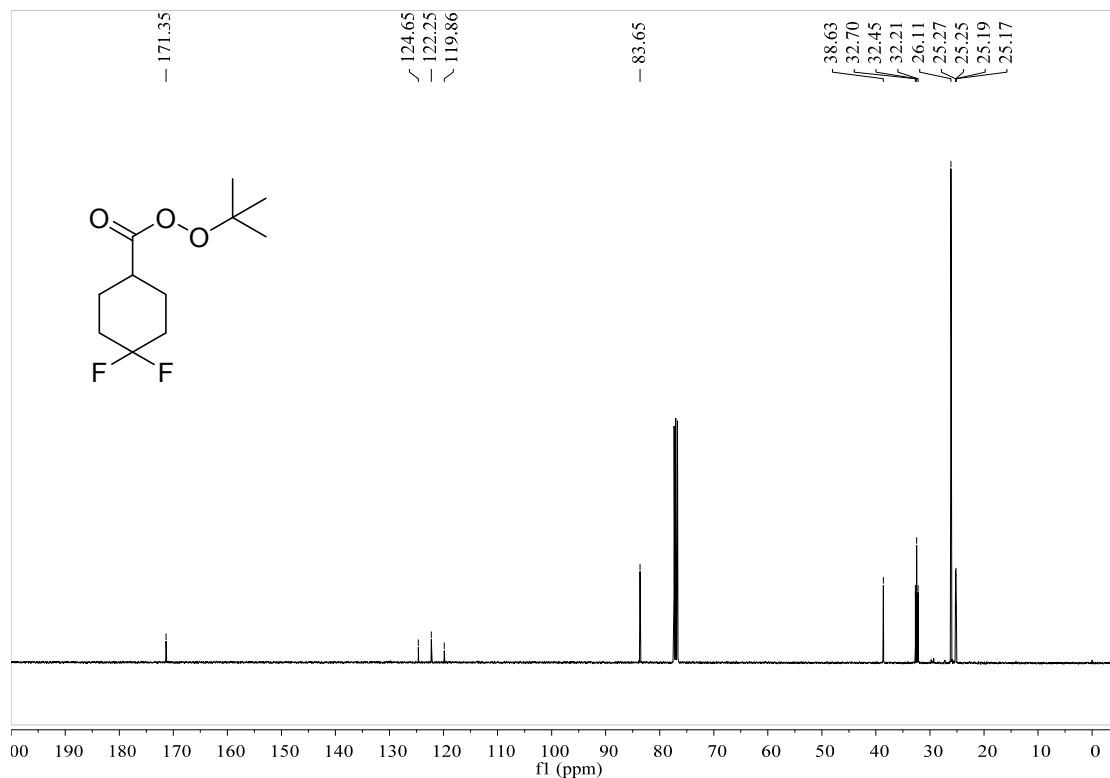


Figure S33. ¹³C NMR spectrum of *tert*-butyl 4,4-difluorocyclohexane-1-carboxylate, related to **Figure 2**.

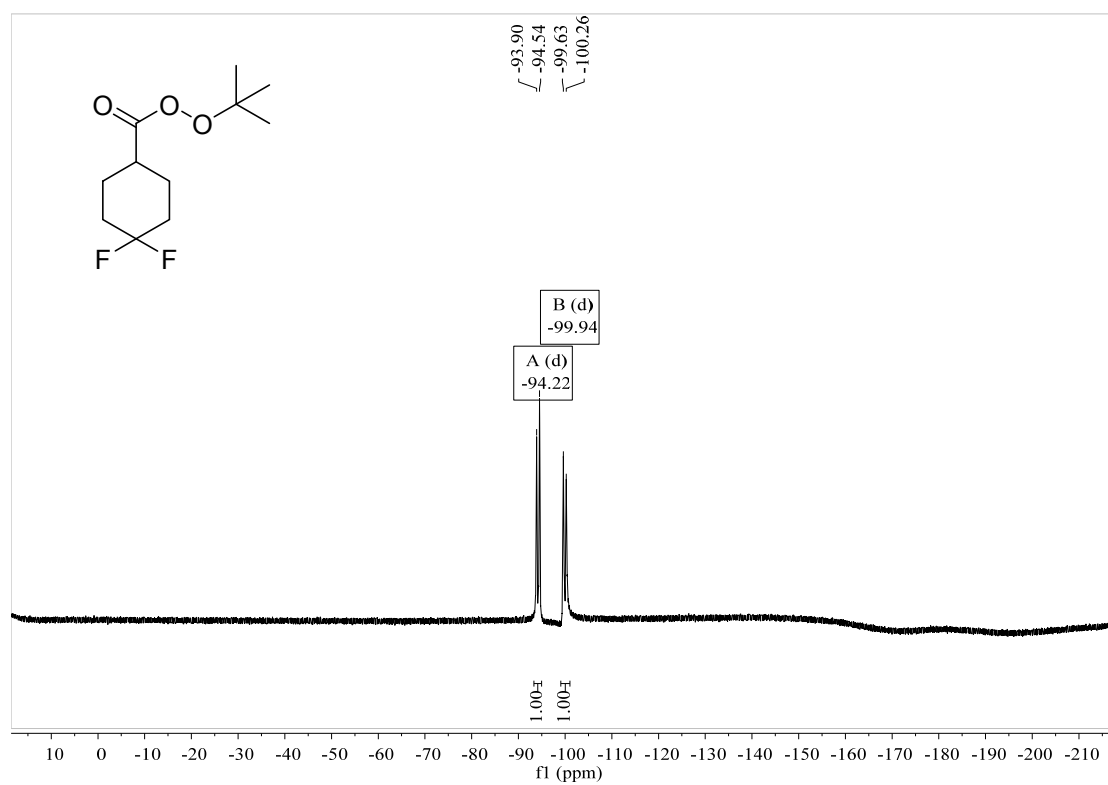


Figure S34. ¹⁹F NMR spectrum of *tert*-butyl 4,4-difluorocyclohexane-1-carboperoxoate, related to **Figure 2**.

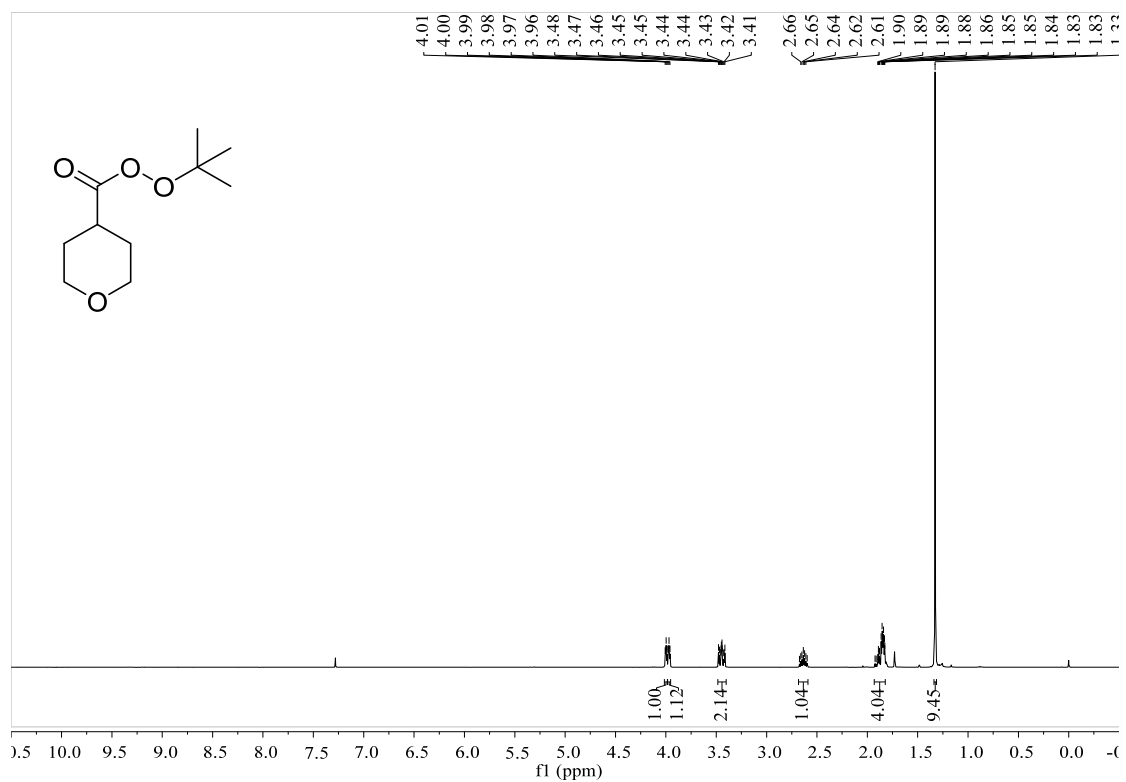


Figure S35. ^1H NMR spectrum of *tert*-butyl tetrahydro-2*H*-pyran-4-carboperoxoate, related to Figure 2.

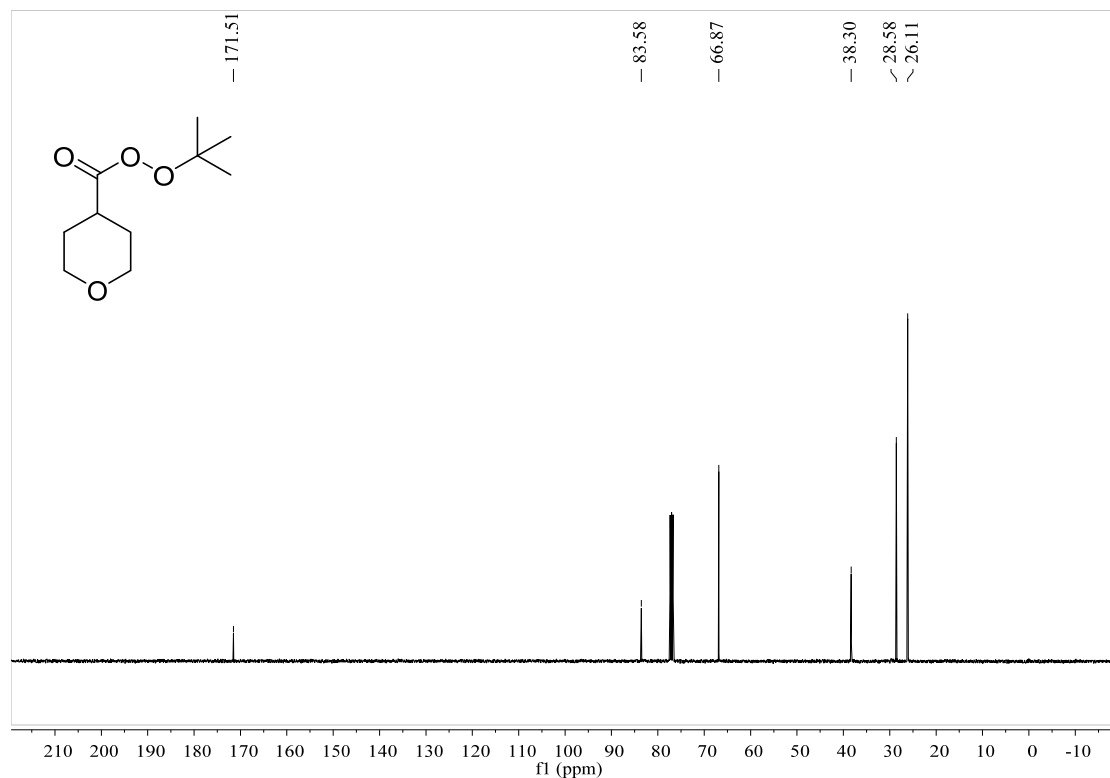


Figure S36. ^{13}C NMR spectrum of *tert*-butyl tetrahydro-2*H*-pyran-4-carboperoxoate, related to Figure 2.

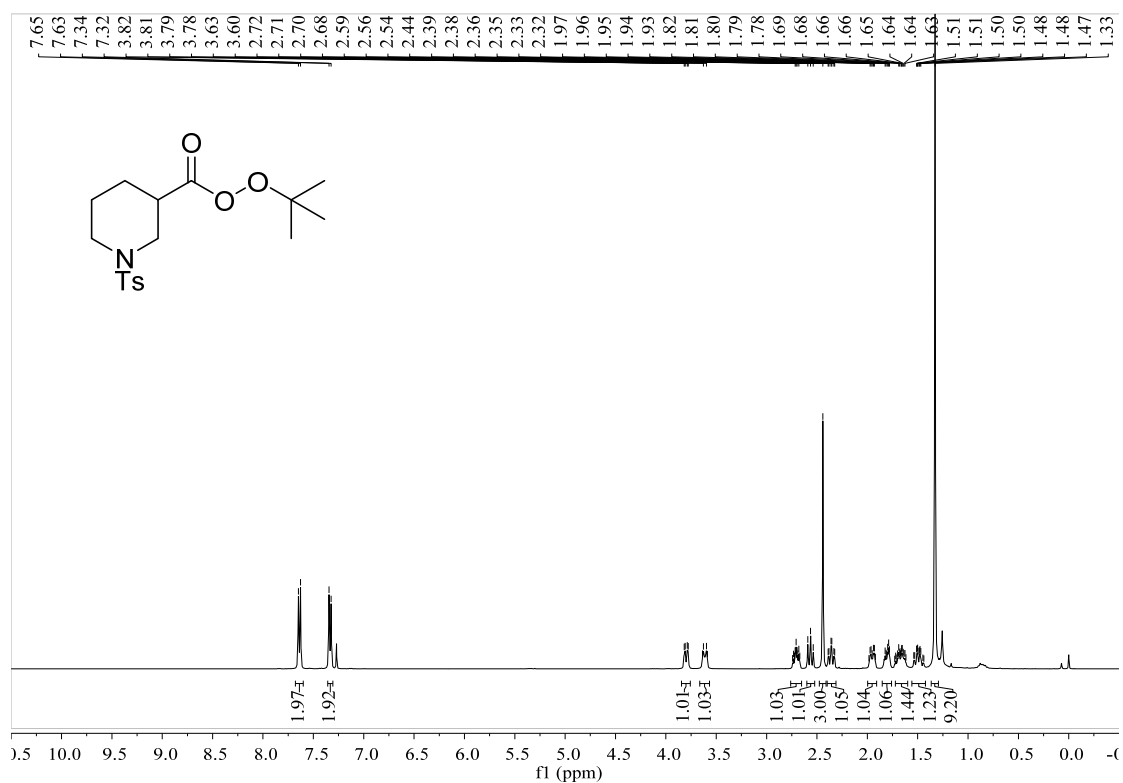


Figure S37. ^1H NMR spectrum of *tert*-butyl 1-tosylpiperidine-3-carboperoxoate, related to Figure 2.

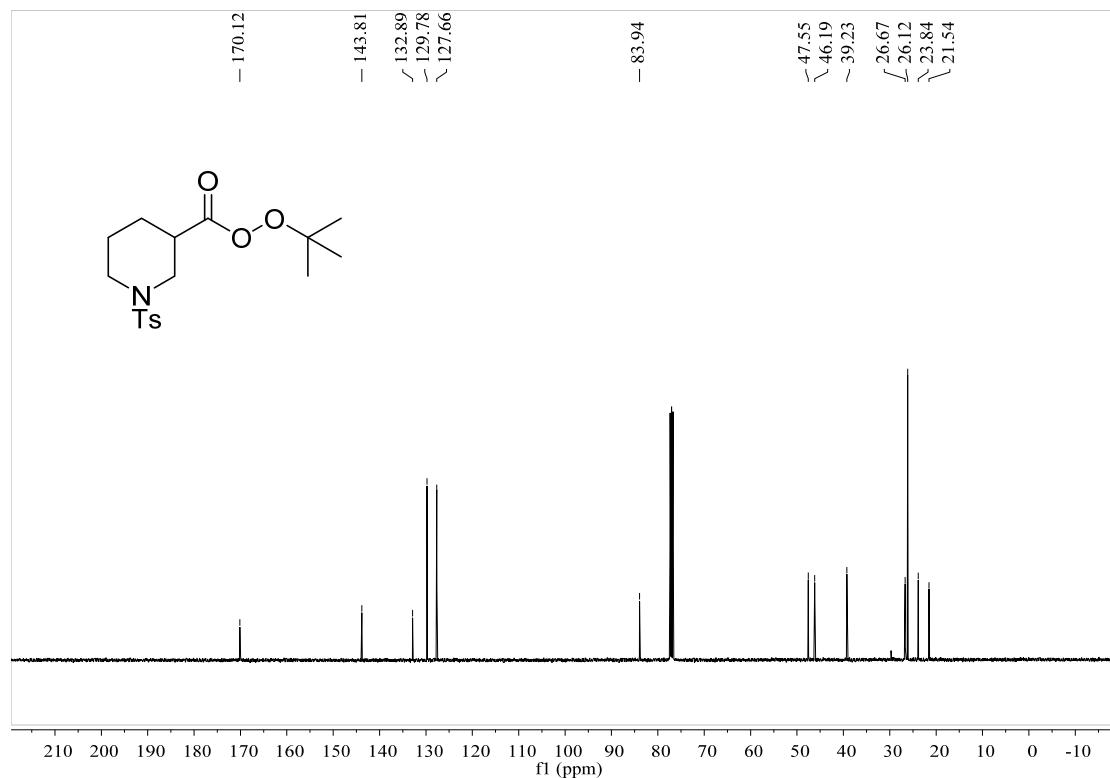


Figure S38. ^{13}C NMR spectrum of *tert*-butyl 1-tosylpiperidine-3-carboperoxoate, related to Figure 2.

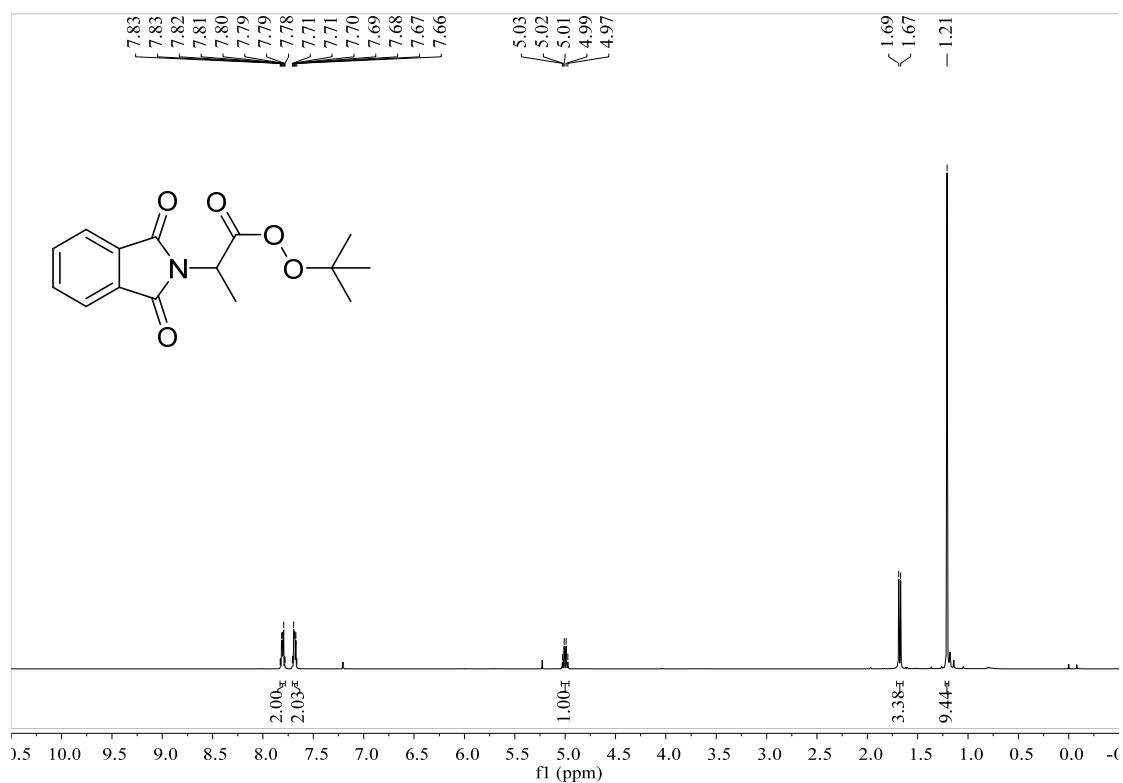


Figure S39. ¹H NMR spectrum of *tert*-butyl 2-(1,3-dioxoisindolin-2-yl)propaneperoxoate, related to **Figure 2**.

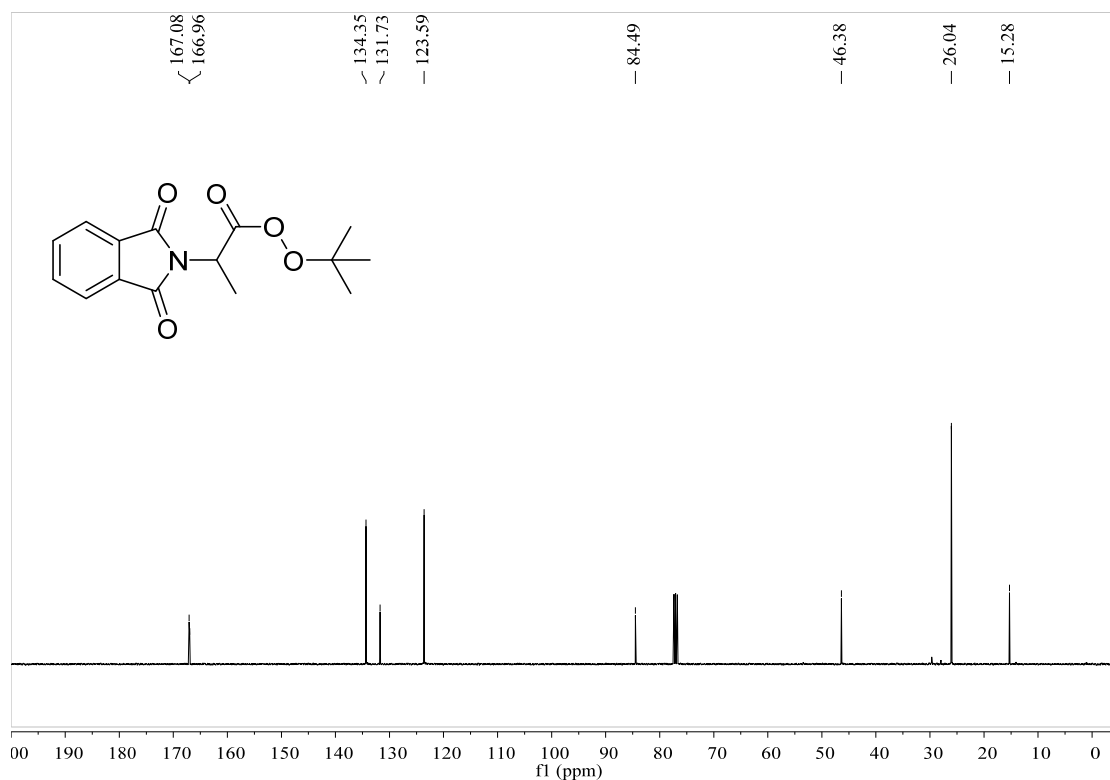


Figure S40. ¹³C NMR spectrum of *tert*-butyl 2-(1,3-dioxoisindolin-2-yl)propaneperoxoate, related to **Figure 2**.

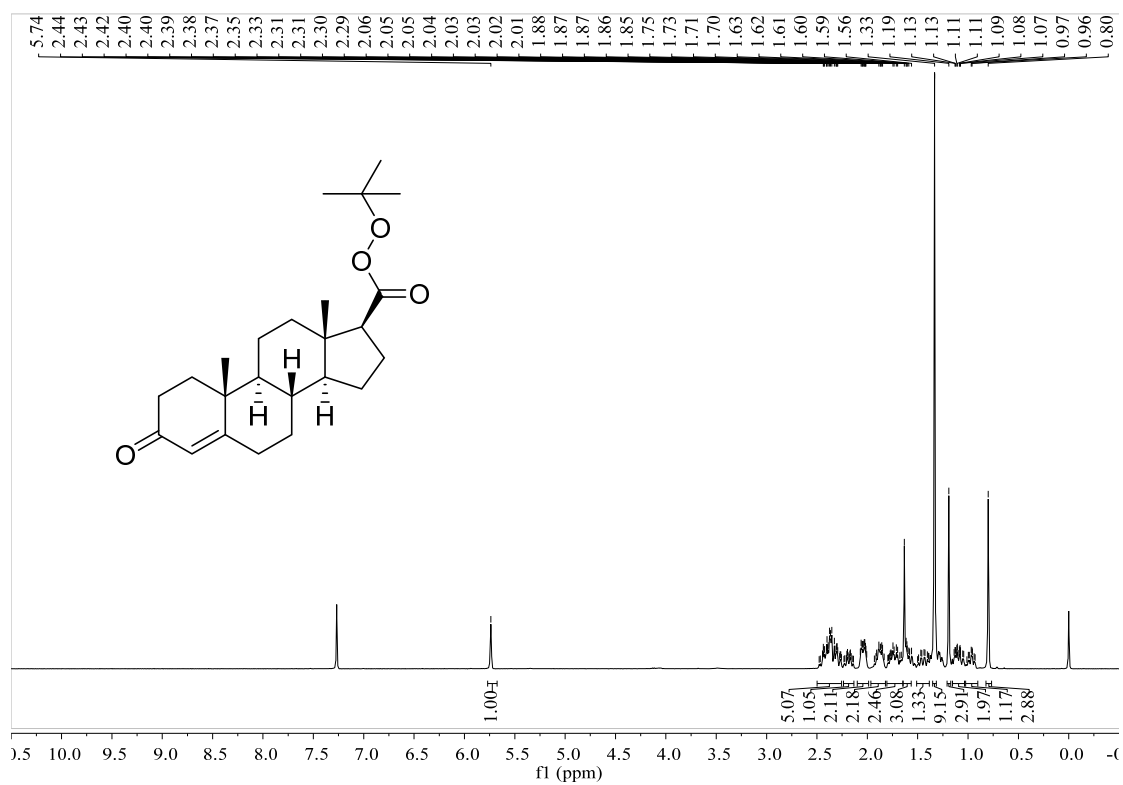


Figure S41. ^1H NMR spectrum of compound 55, related to scheme 2.

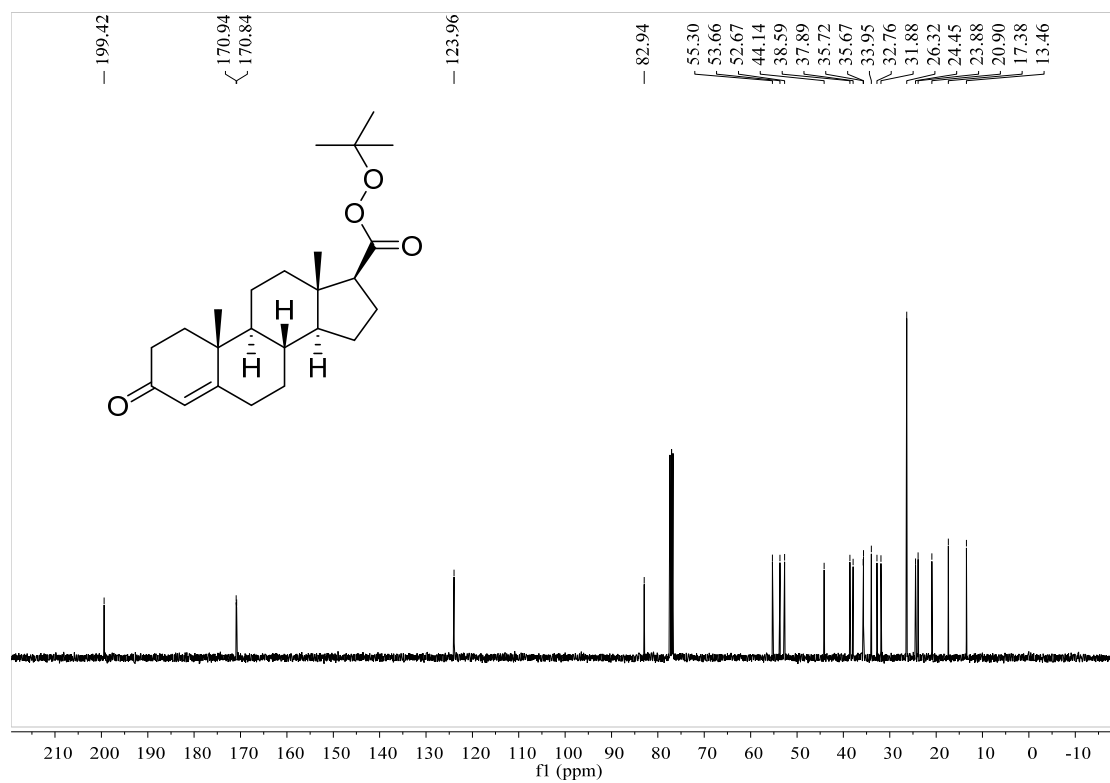


Figure S42. ^{13}C NMR spectrum of compound 55, related to scheme 2.

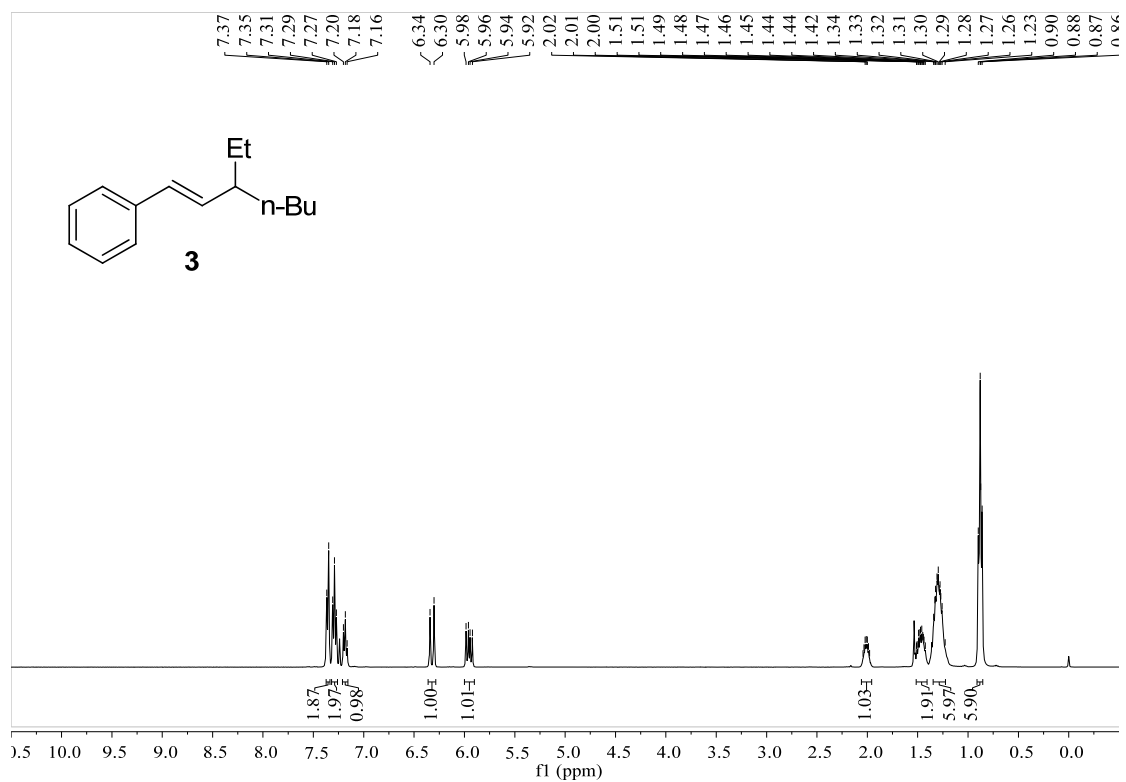


Figure S43. ¹H NMR spectrum of compound **3**, related to Table 1.

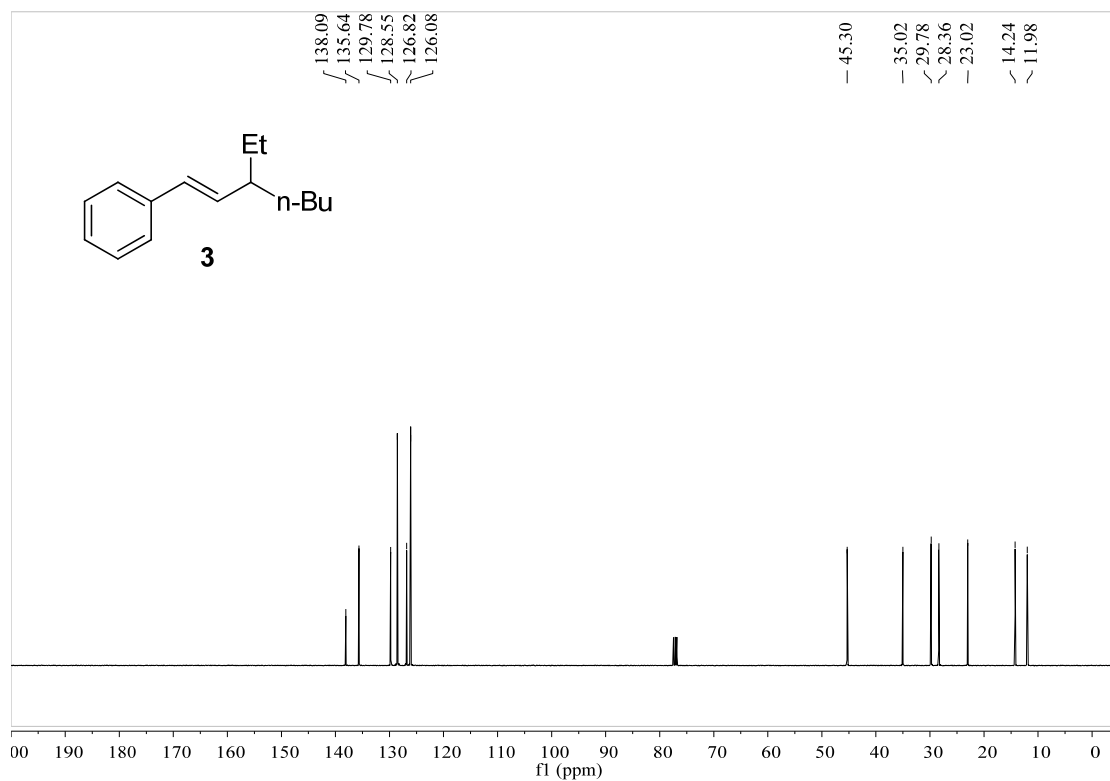


Figure S44. ¹³C NMR spectrum of compound **3**, related to Table 1.

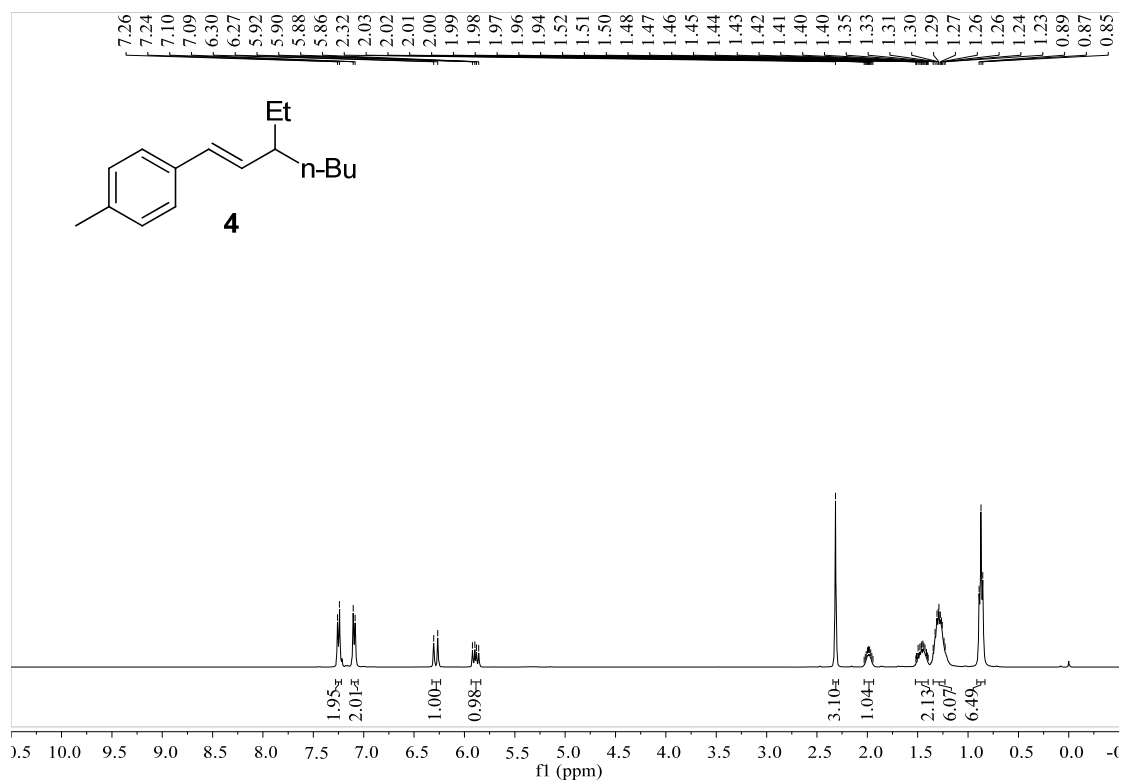


Figure S45. ¹H NMR spectrum of compound 4, related to Figure 1.

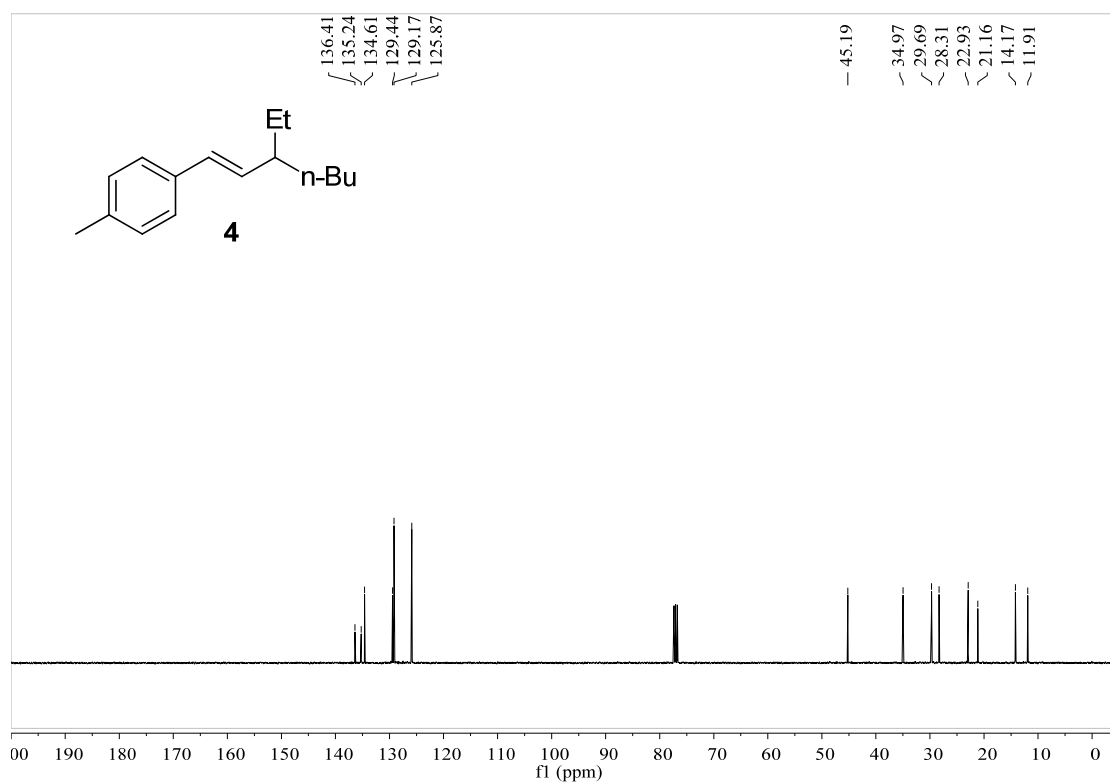


Figure S46. ¹³C NMR spectrum of compound 4, related to Figure 1.

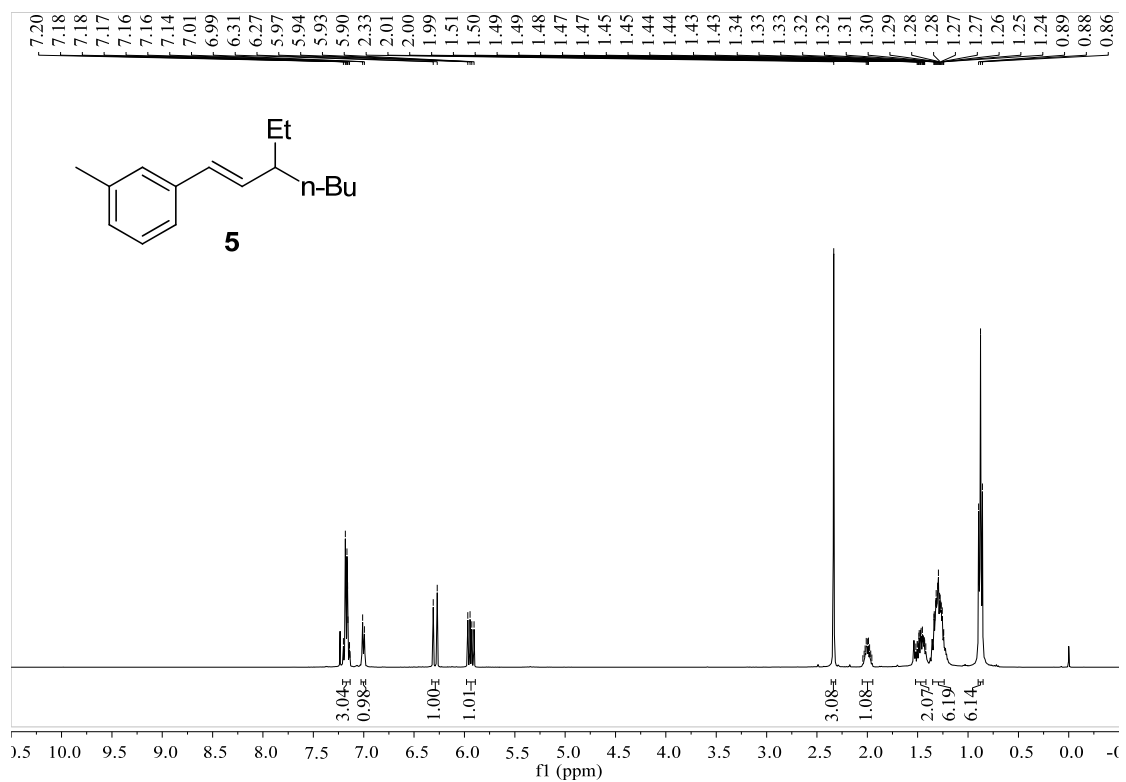


Figure S47. ¹H NMR spectrum of compound 5, related to Figure 1.

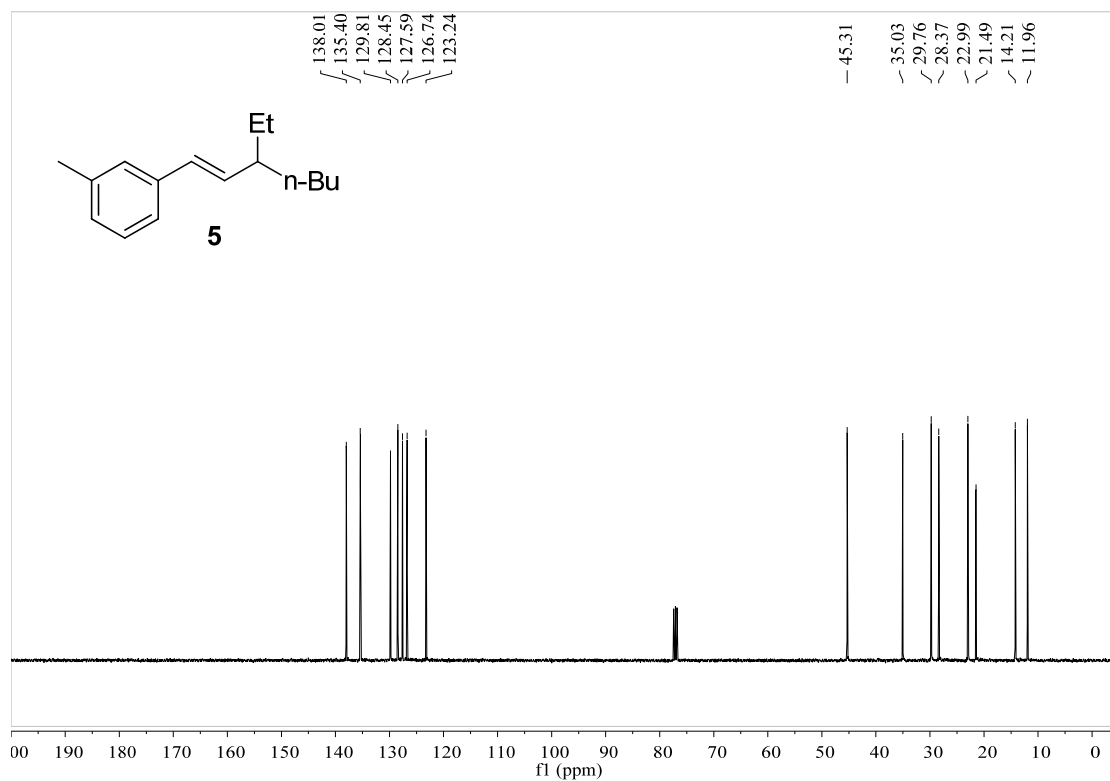


Figure S48. ¹³C NMR spectrum of compound 5, related to Figure 1.

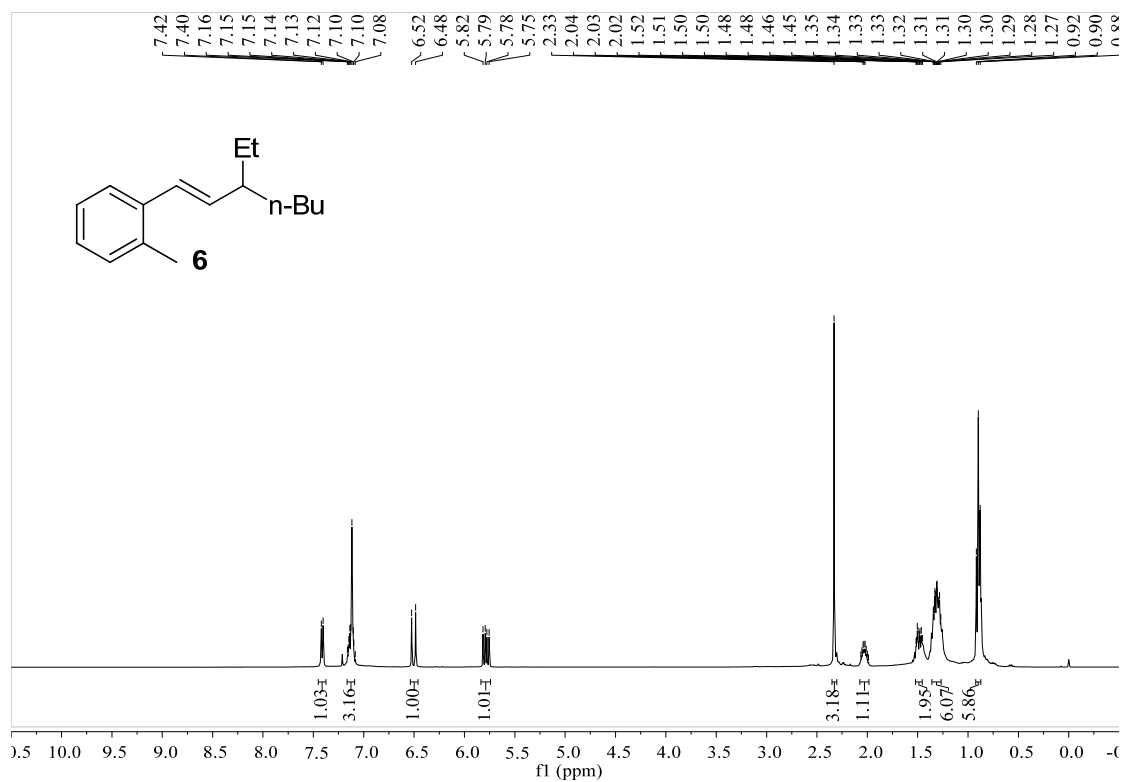


Figure S49. ¹H NMR spectrum of compound **6**, related to Figure 1.

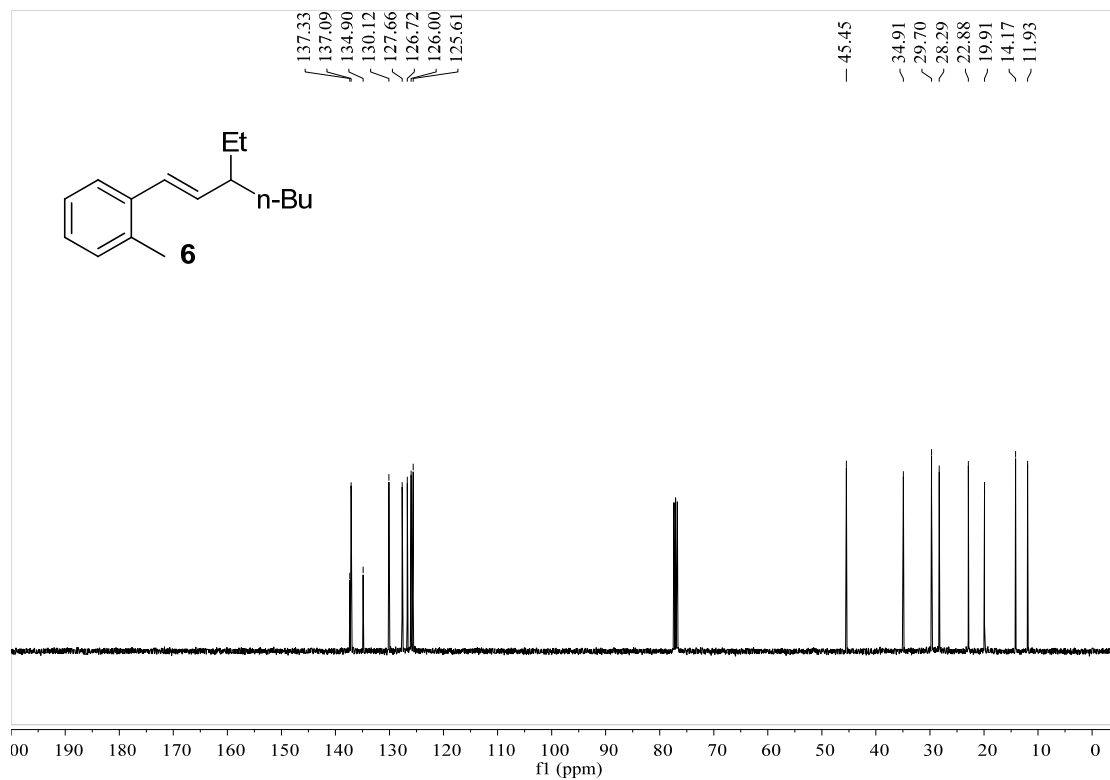


Figure S50. ¹³C NMR spectrum of compound **6**, related to Figure 1.

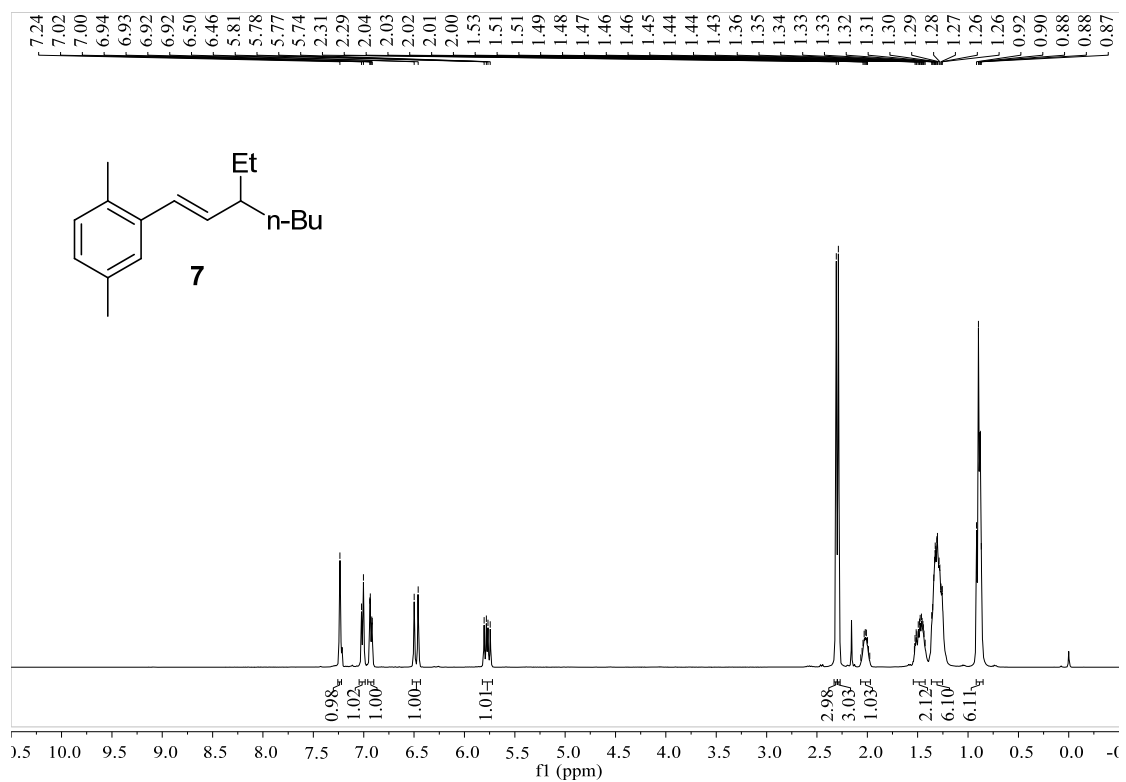


Figure S51. ¹H NMR spectrum of compound 7, related to Figure 1.

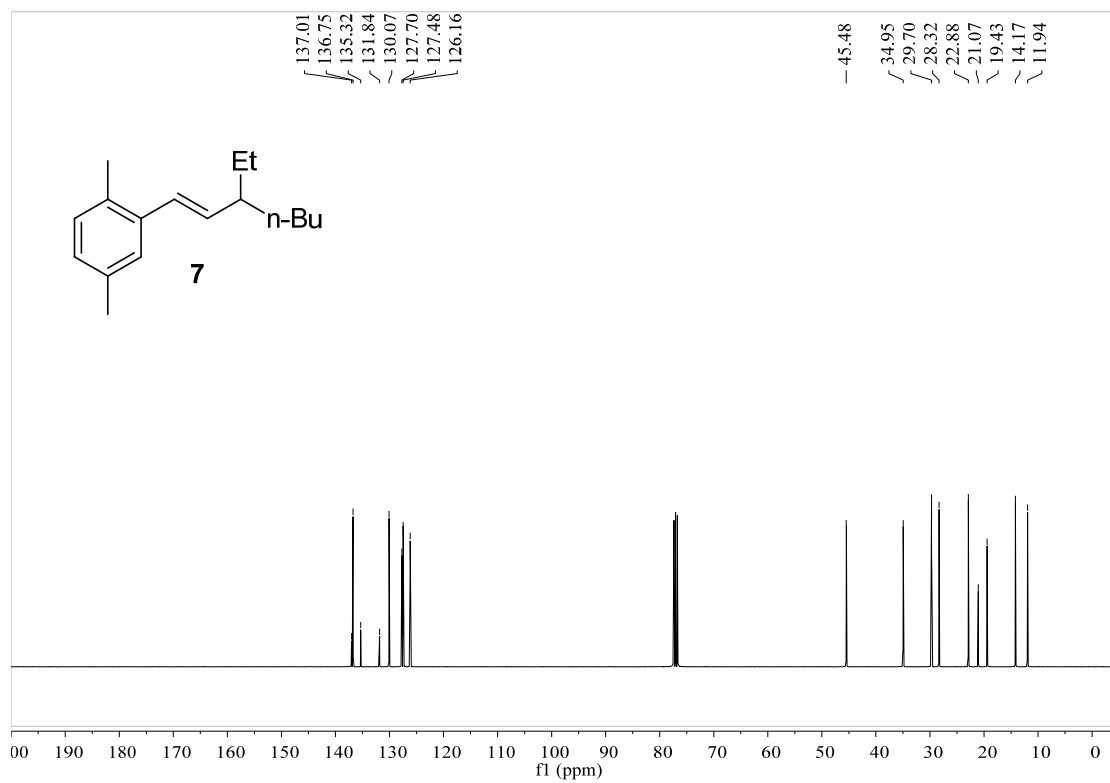


Figure S52. ¹³C NMR spectrum of compound 7, related to Figure 1.

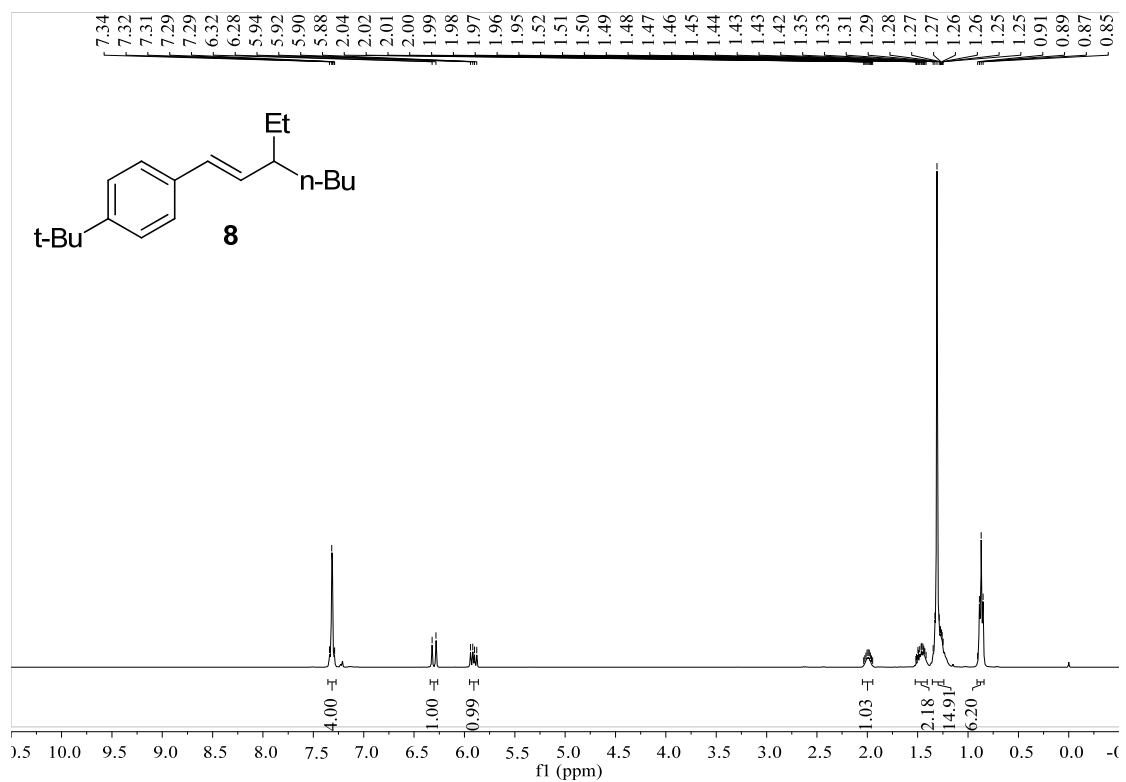


Figure S53. ¹H NMR spectrum of compound **8**, related to Figure 1.

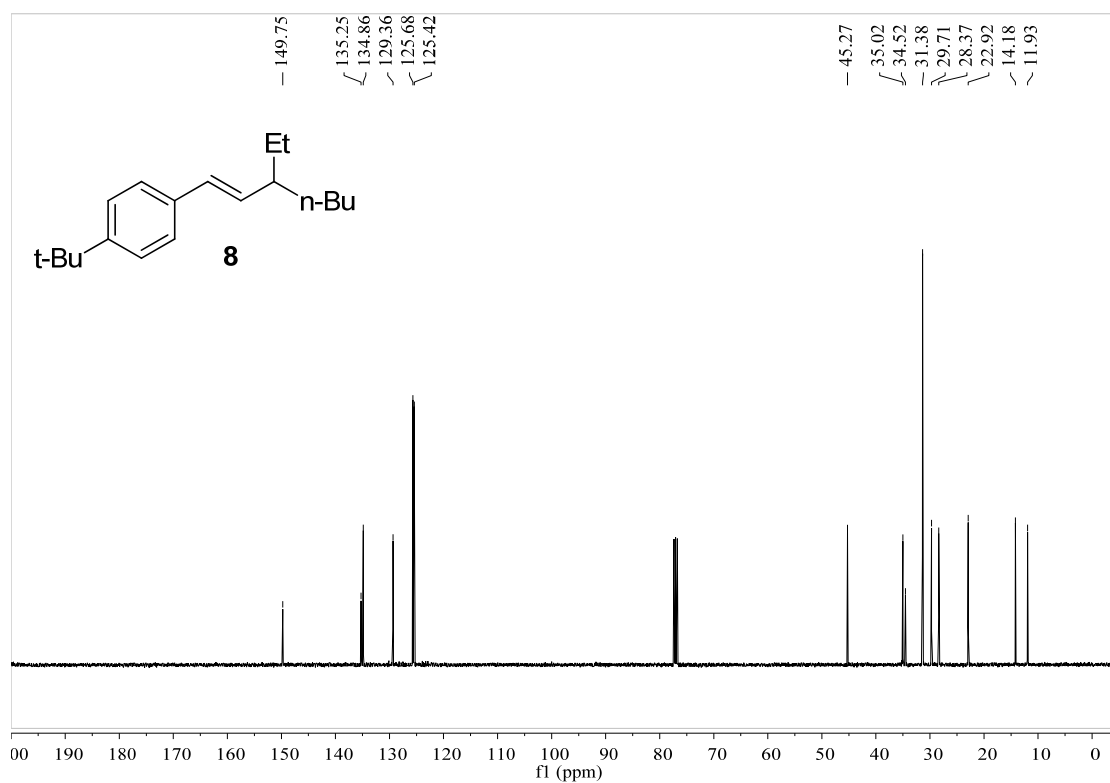


Figure S54. ¹³C NMR spectrum of compound **8**, related to Figure 1.

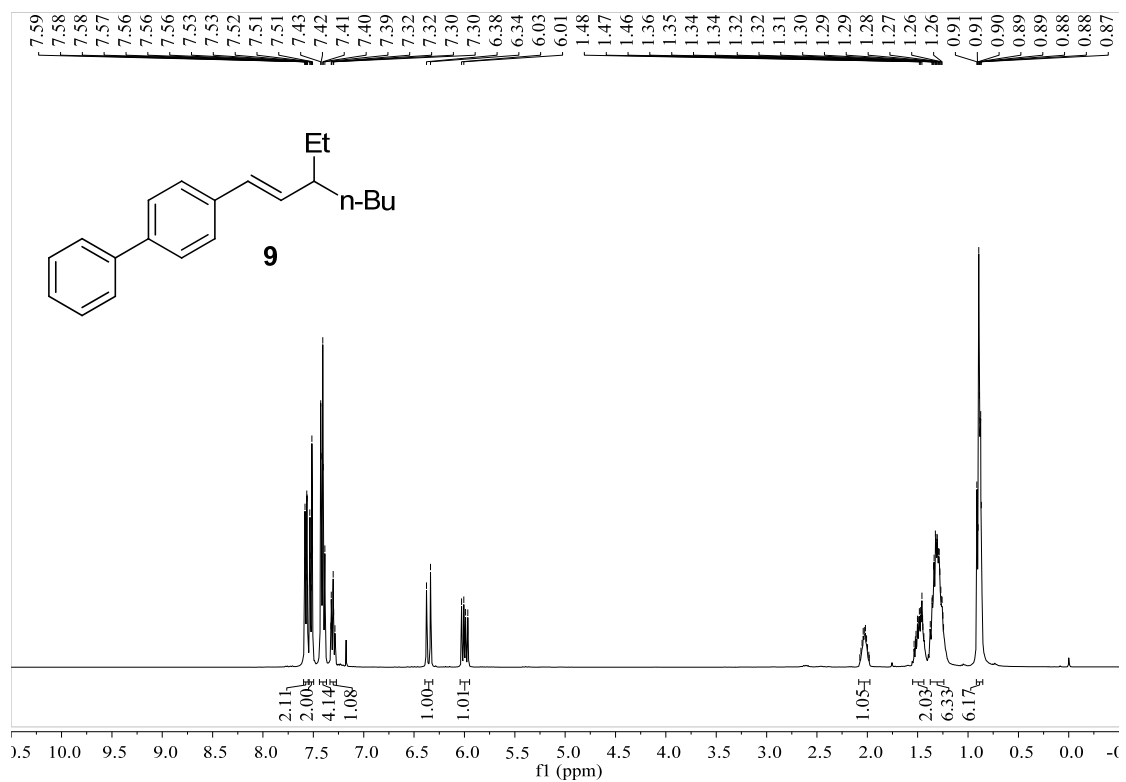


Figure S55. ¹H NMR spectrum of compound **9**, related to **Figure 1**.

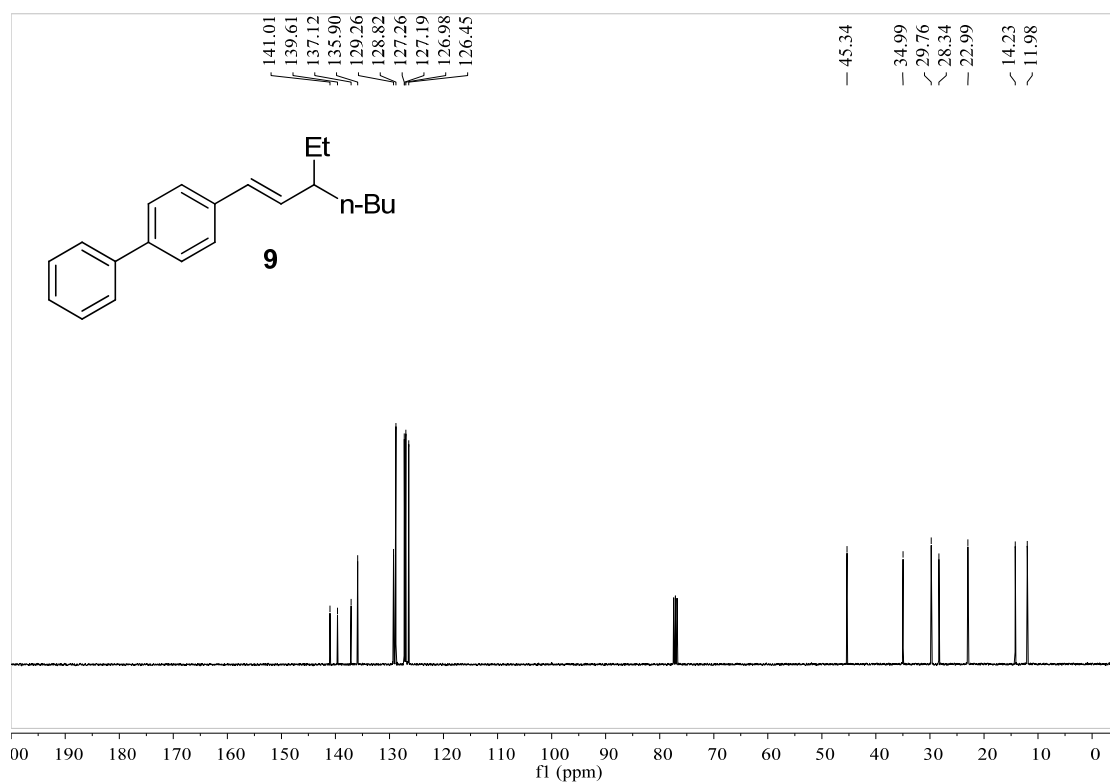


Figure S56. ¹³C NMR spectrum of compound **9**, related to **Figure 1**.

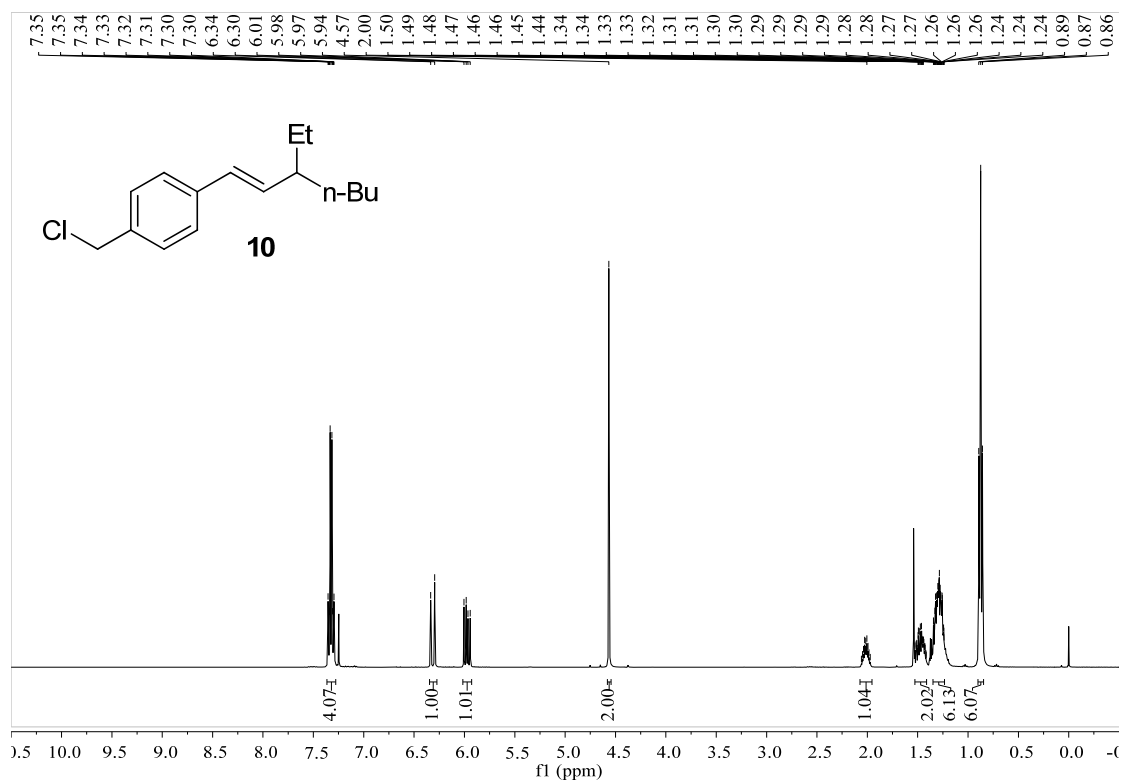


Figure S57. ¹H NMR spectrum of compound **10**, related to Figure 1.

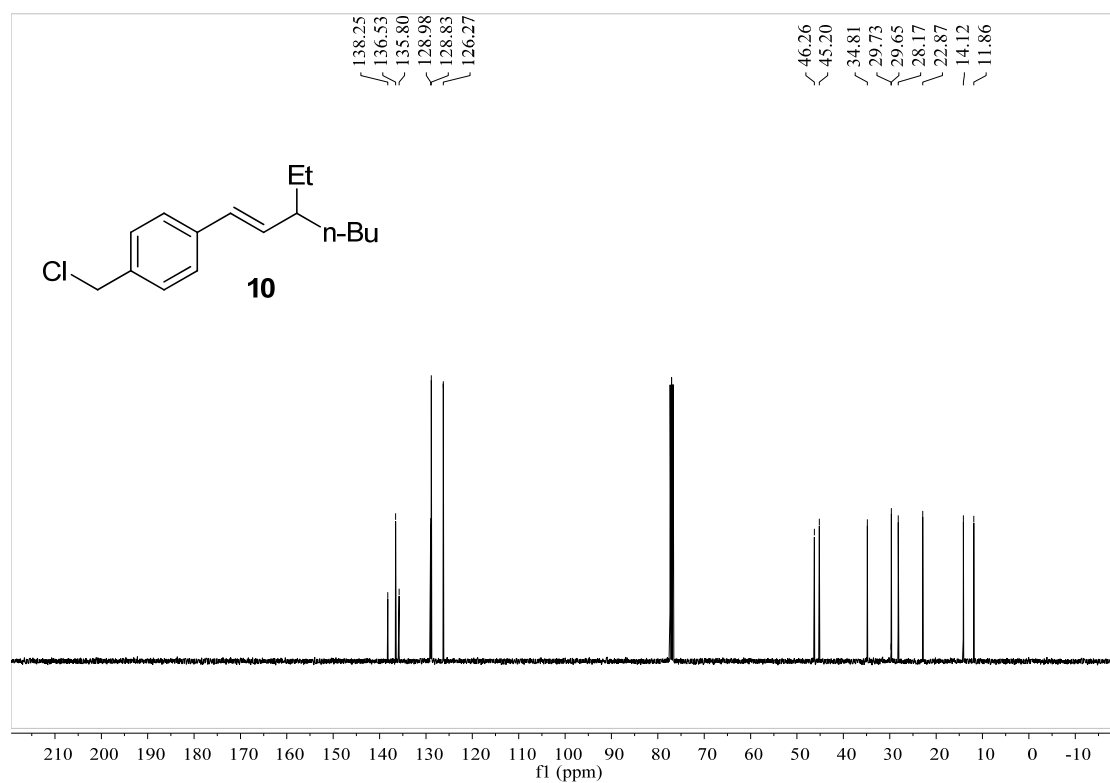


Figure S58. ¹³C NMR spectrum of compound **10**, related to Figure 1.

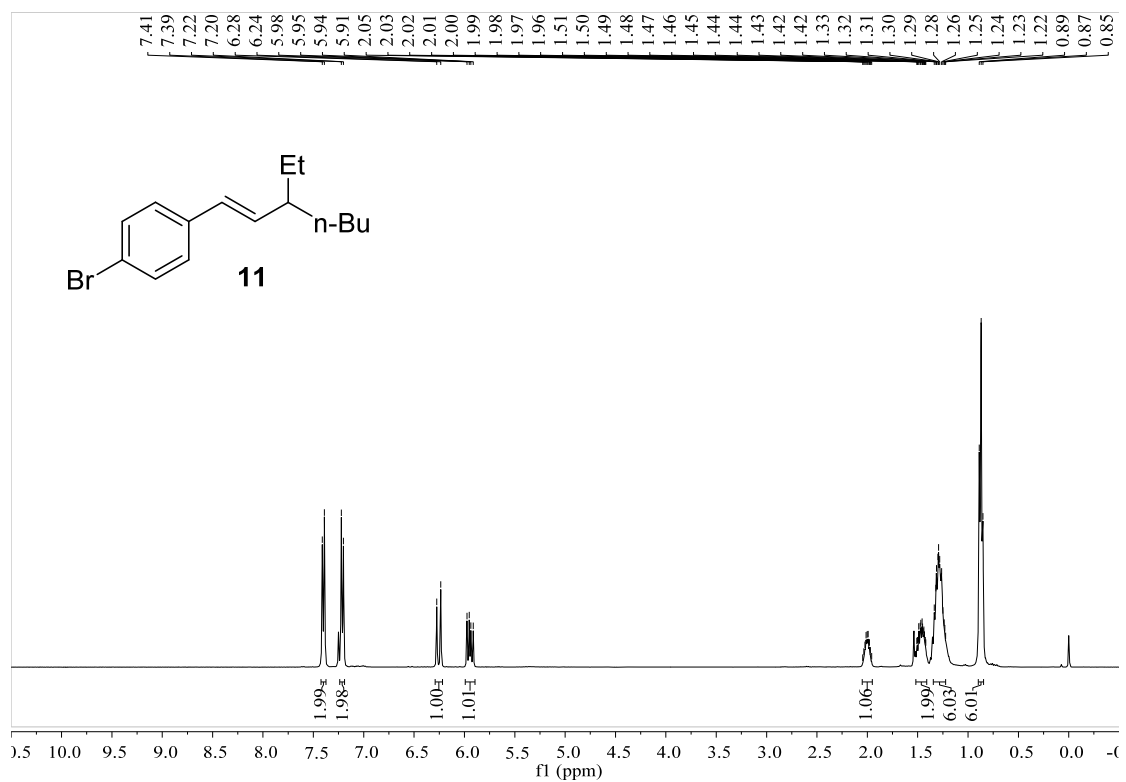


Figure S59. ¹H NMR spectrum of compound **11**, related to **Figure 1**.

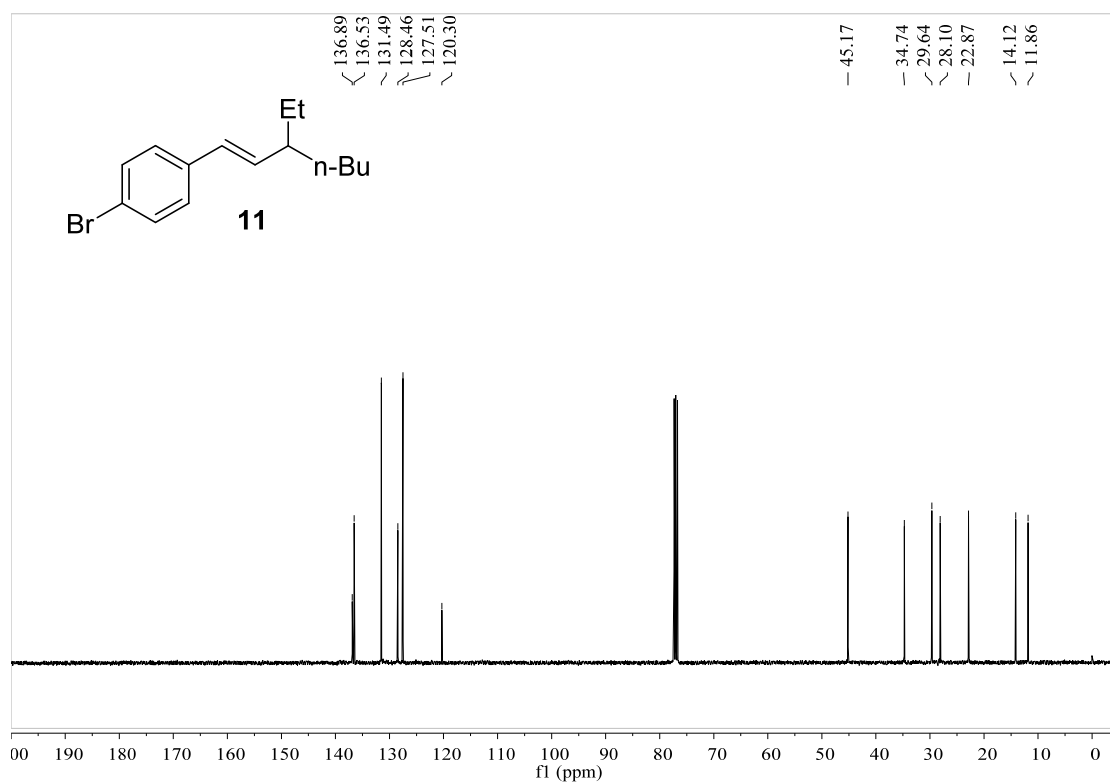


Figure S60. ¹³C NMR spectrum of compound **11**, related to **Figure 1**.

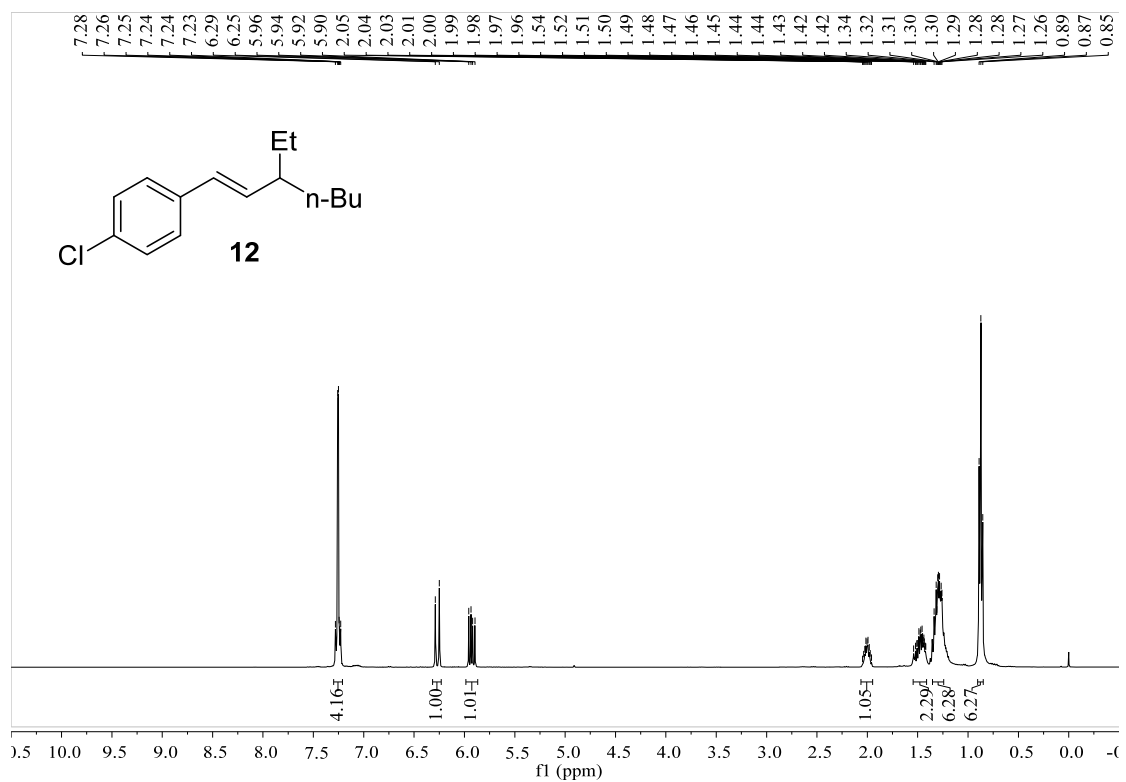


Figure S61. ¹H NMR spectrum of compound **12**, related to **Figure 1**.

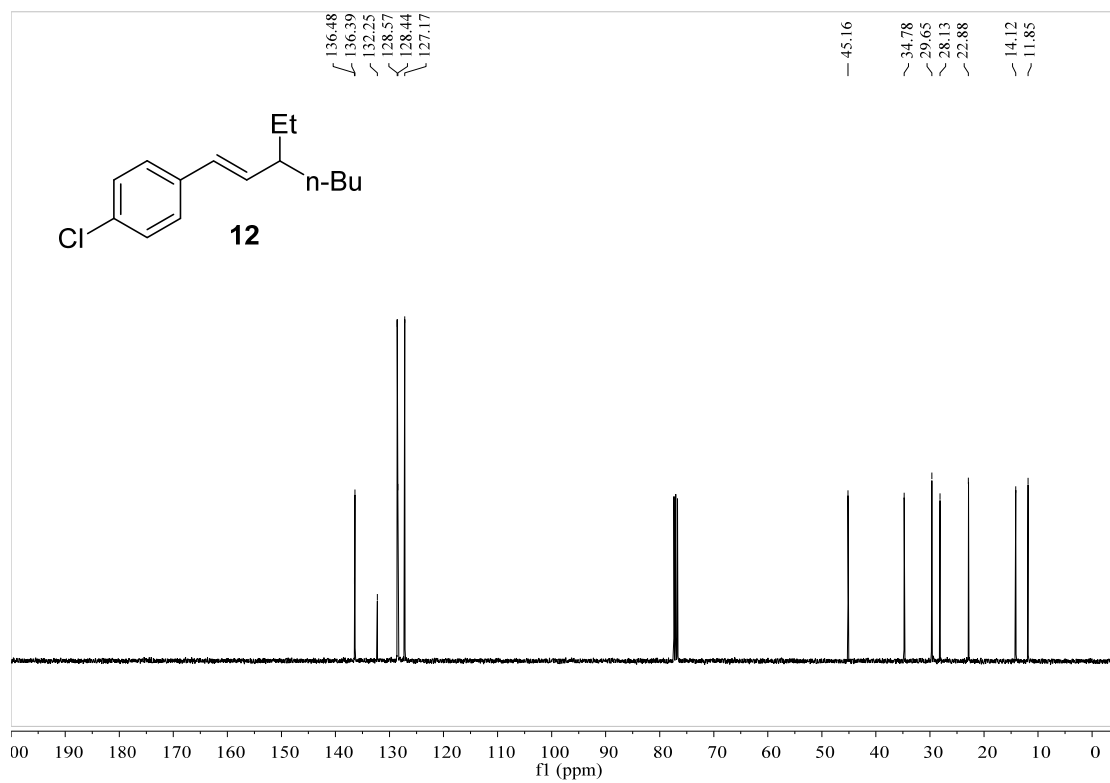


Figure S62. ¹³C NMR spectrum of compound **12**, related to **Figure 1**.

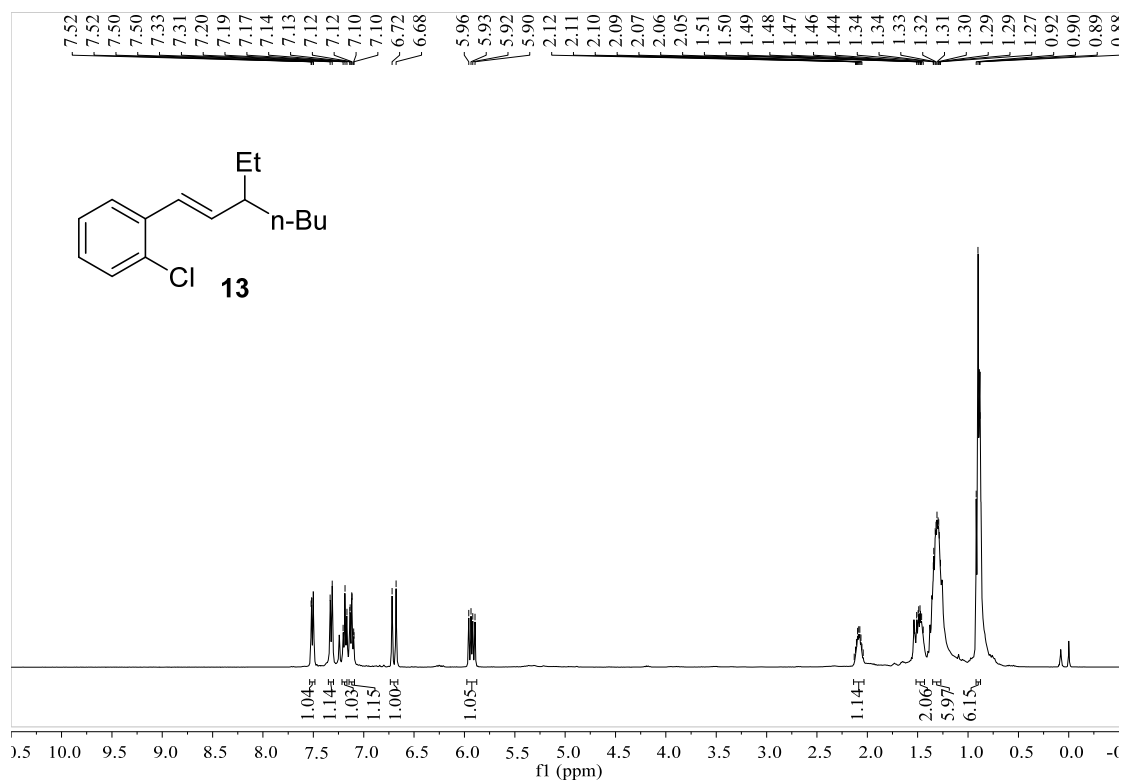


Figure S63. ¹H NMR spectrum of compound **13**, related to **Figure 1**.

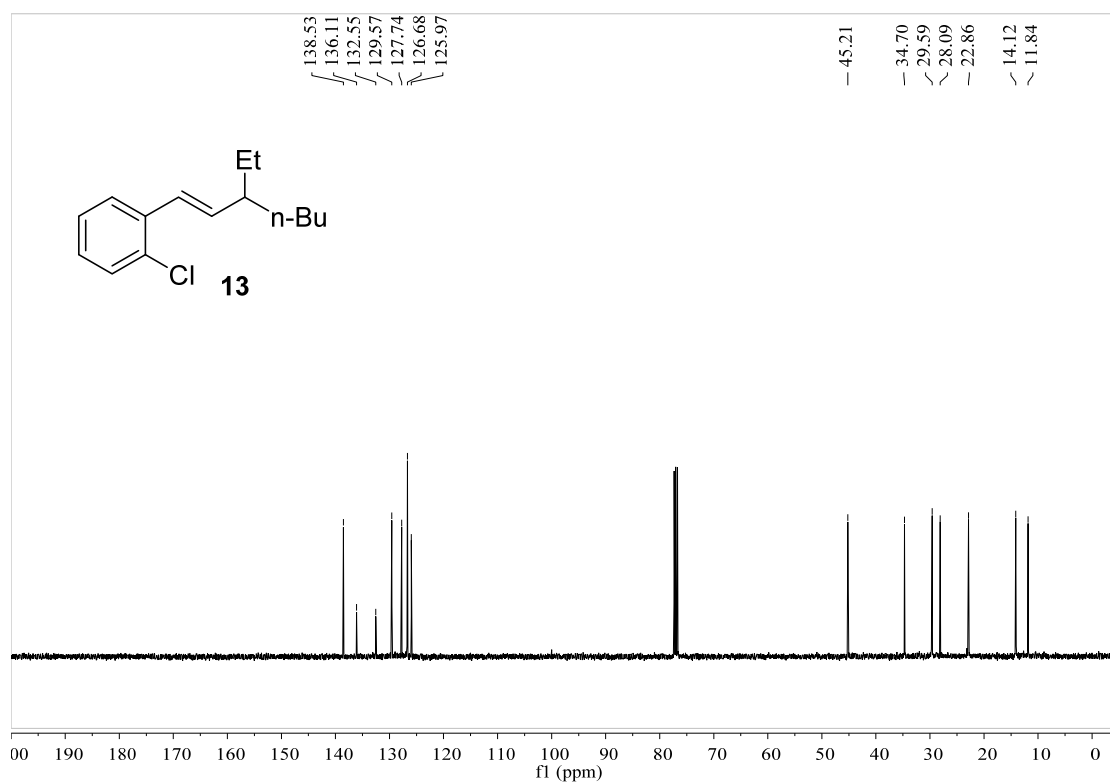
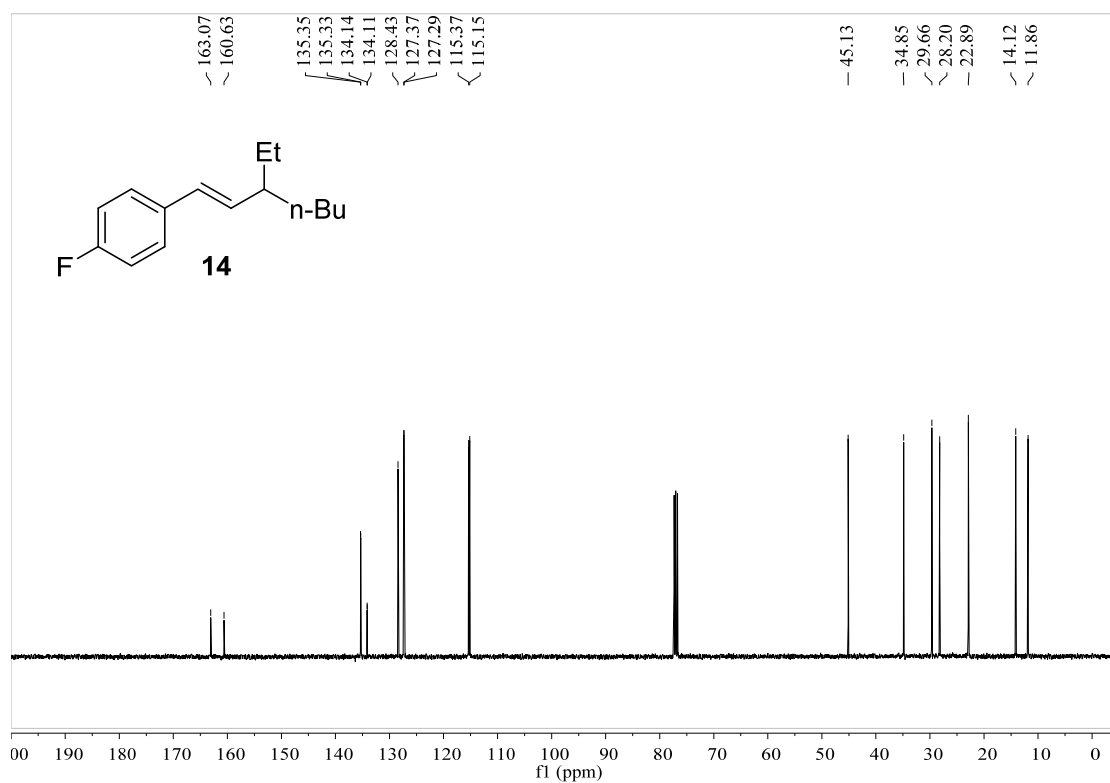
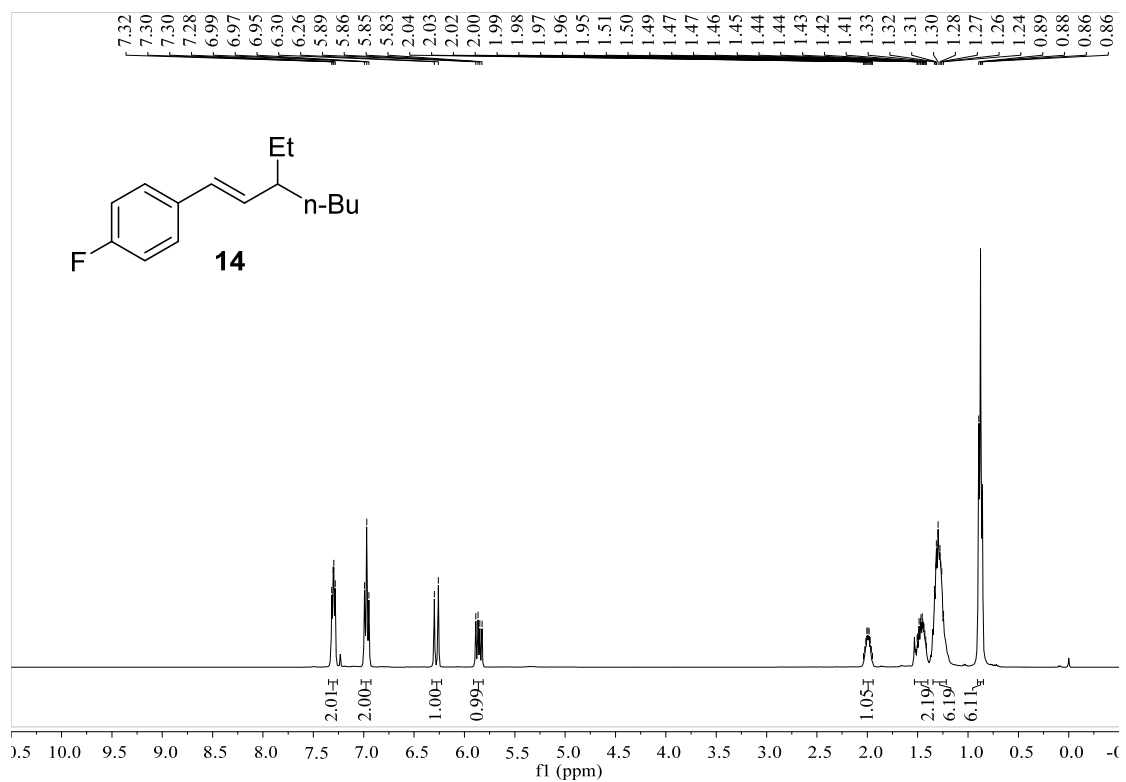


Figure S64. ¹³C NMR spectrum of compound **13**, related to **Figure 1**.



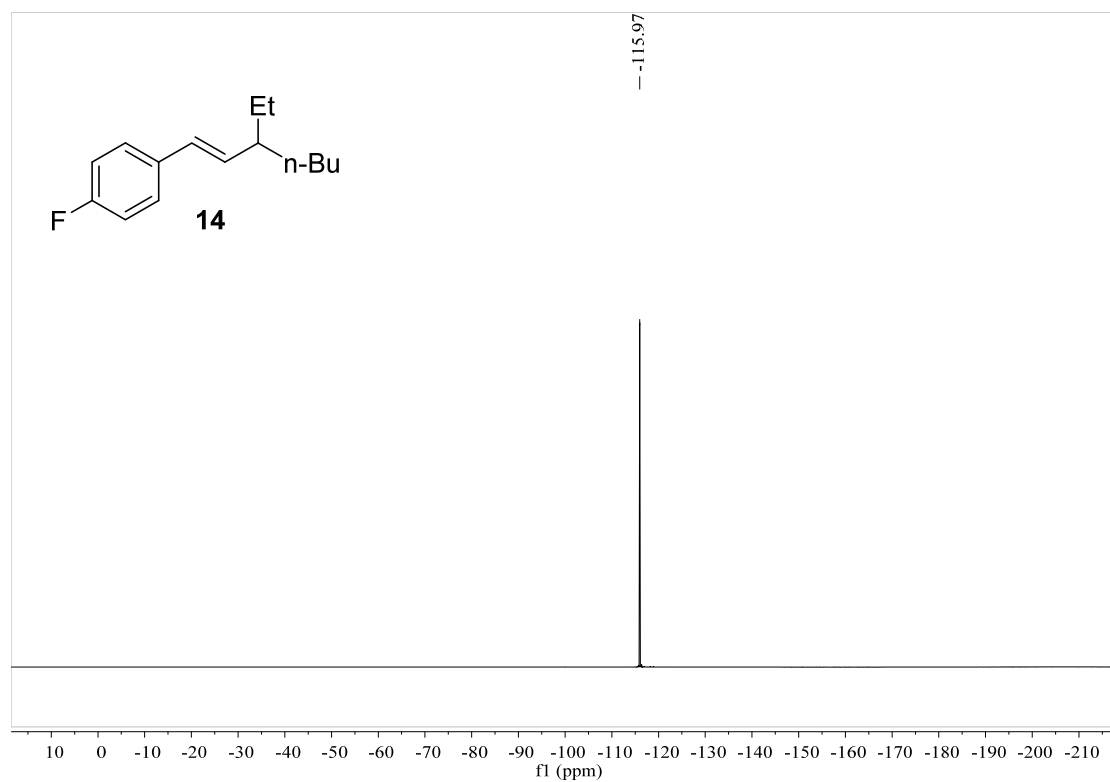


Figure S67. ^{19}F NMR spectrum of compound **14**, related to **Figure 1**.

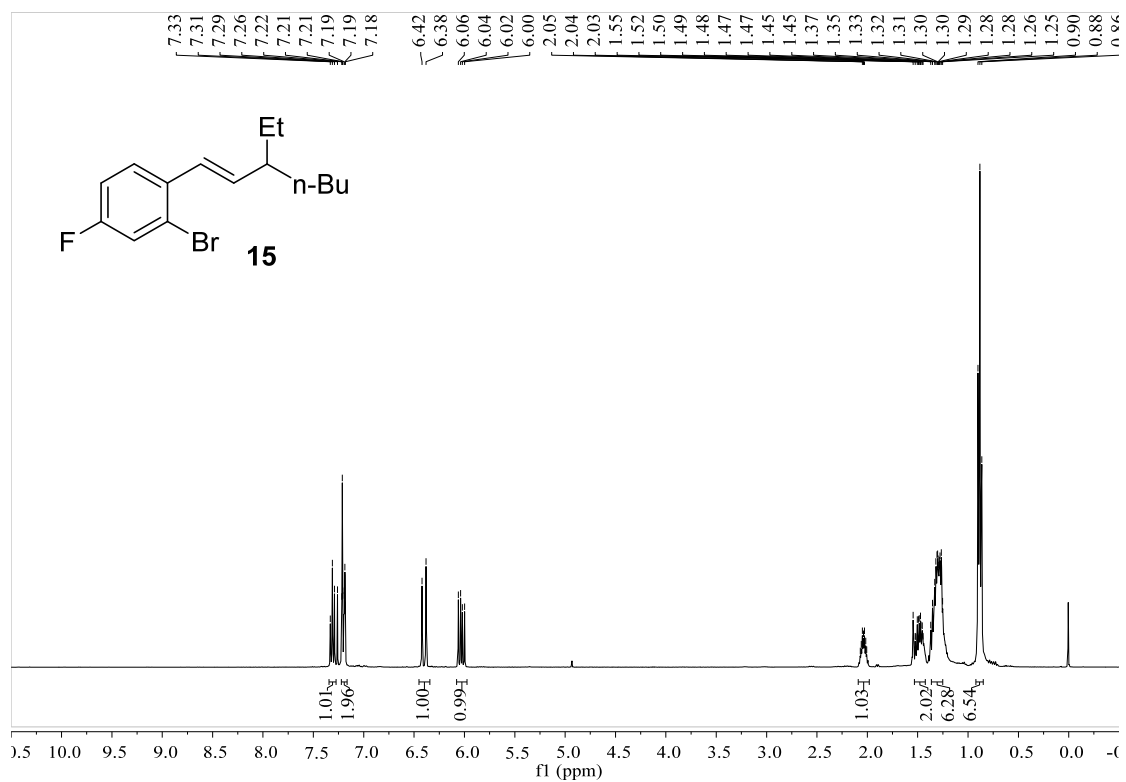


Figure S68. ¹H NMR spectrum of compound **15**, related to Figure 1.

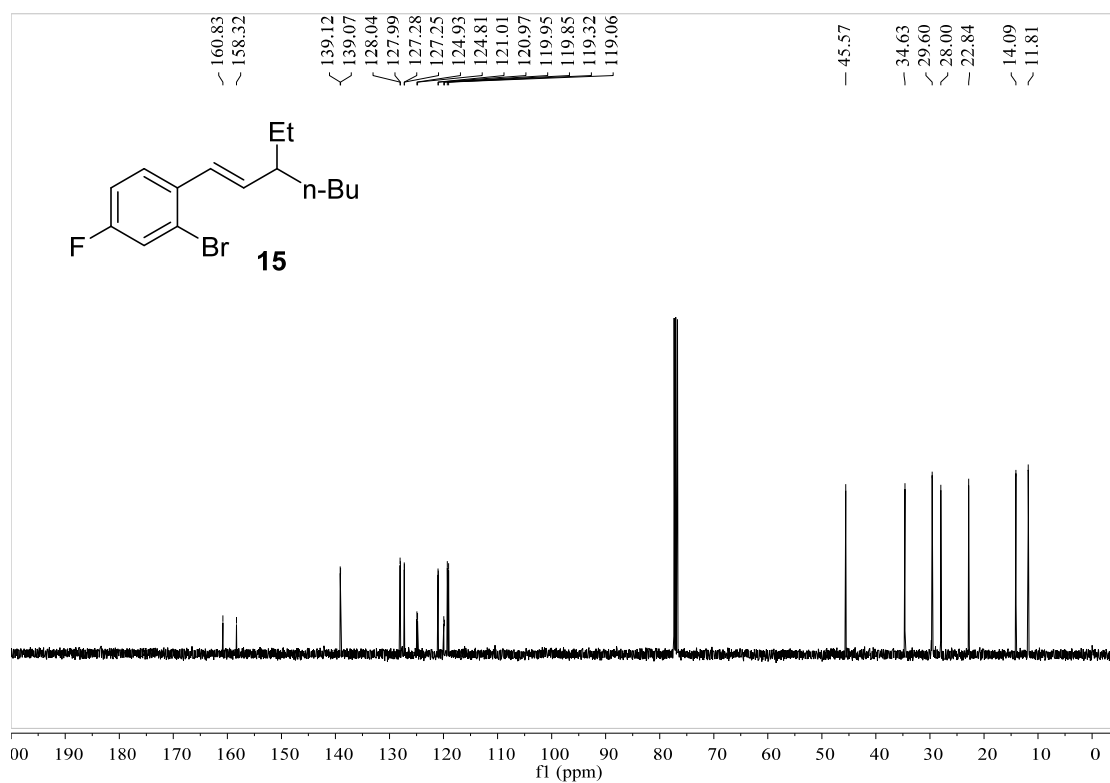


Figure S69. ¹³C NMR spectrum of compound **15**, related to Figure 1.

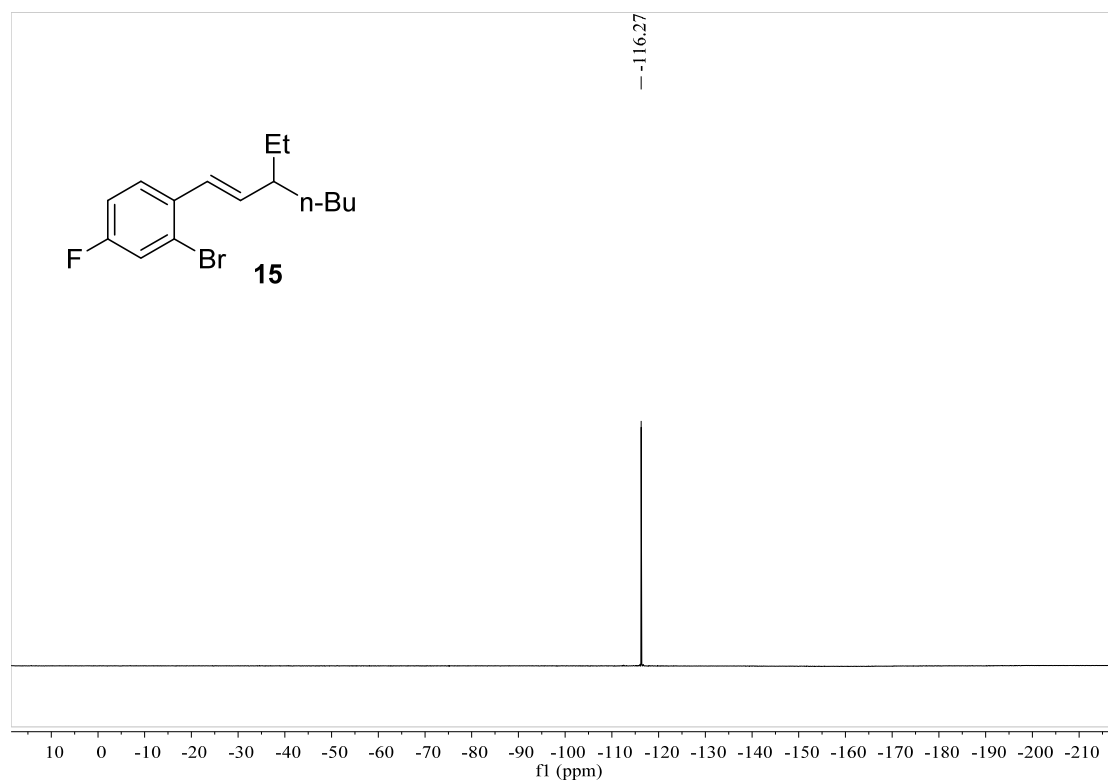
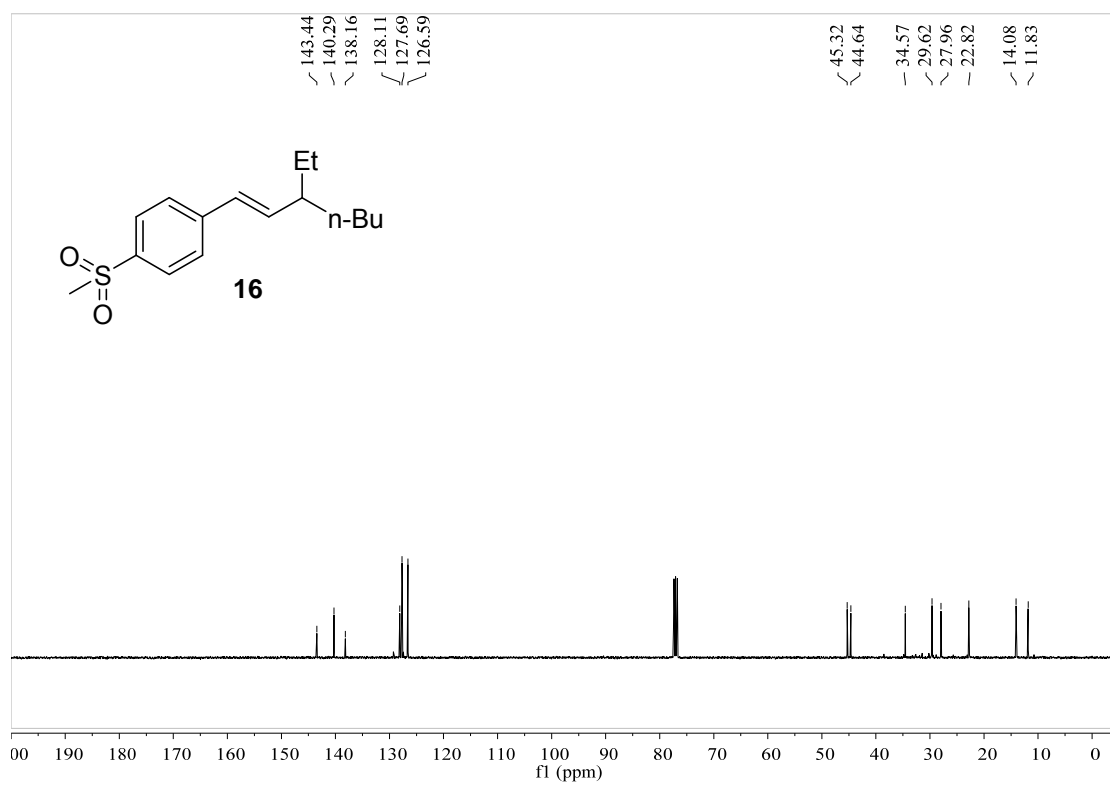
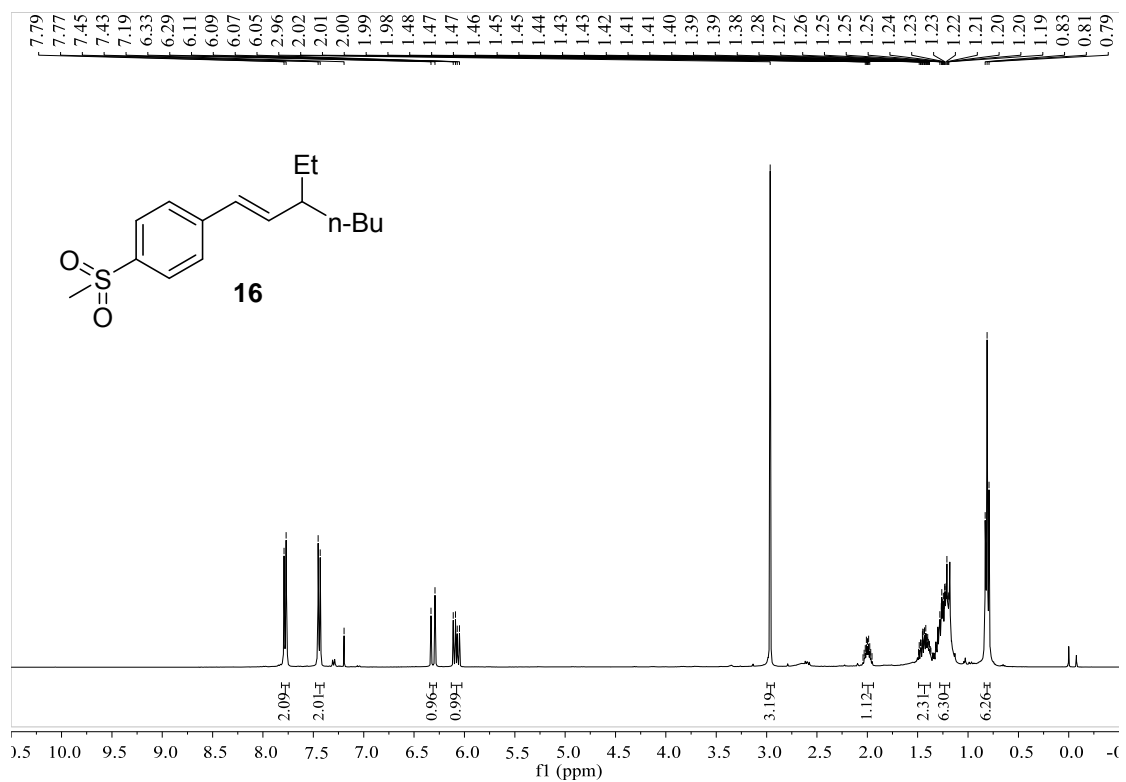


Figure S70. ^{19}F NMR spectrum of compound **15**, related to **Figure 1**.



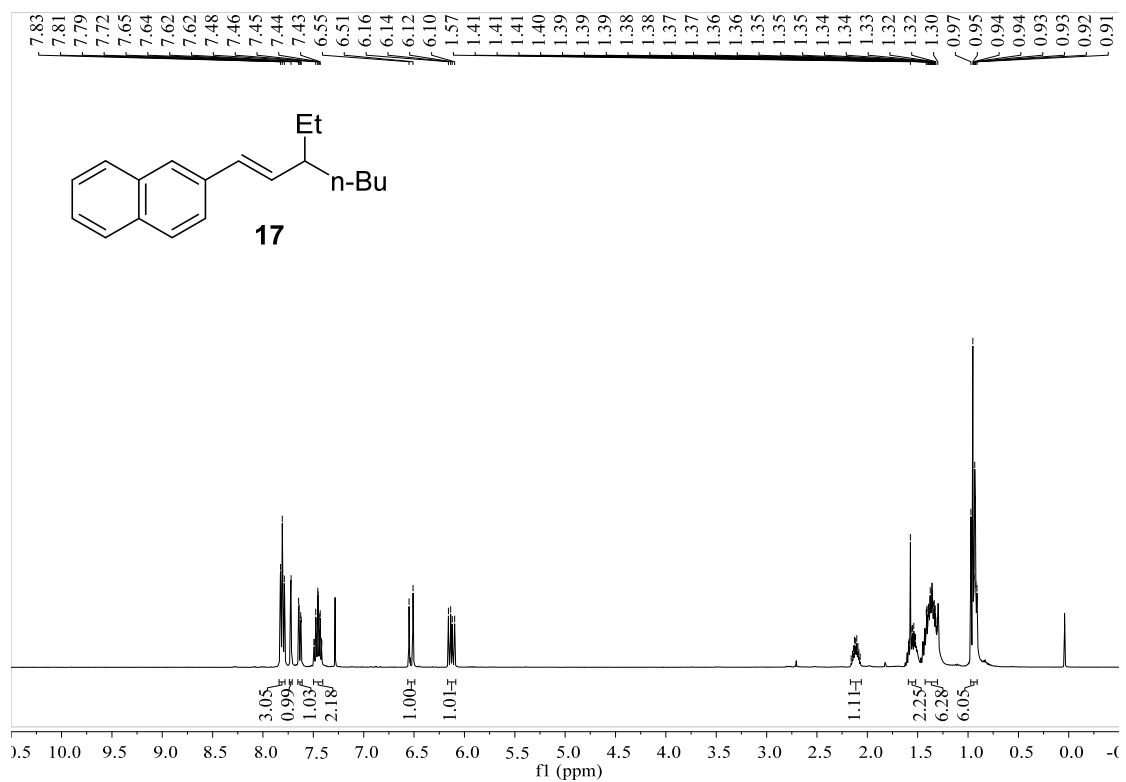


Figure S73. ¹H NMR spectrum of compound 17, related to Figure 1.

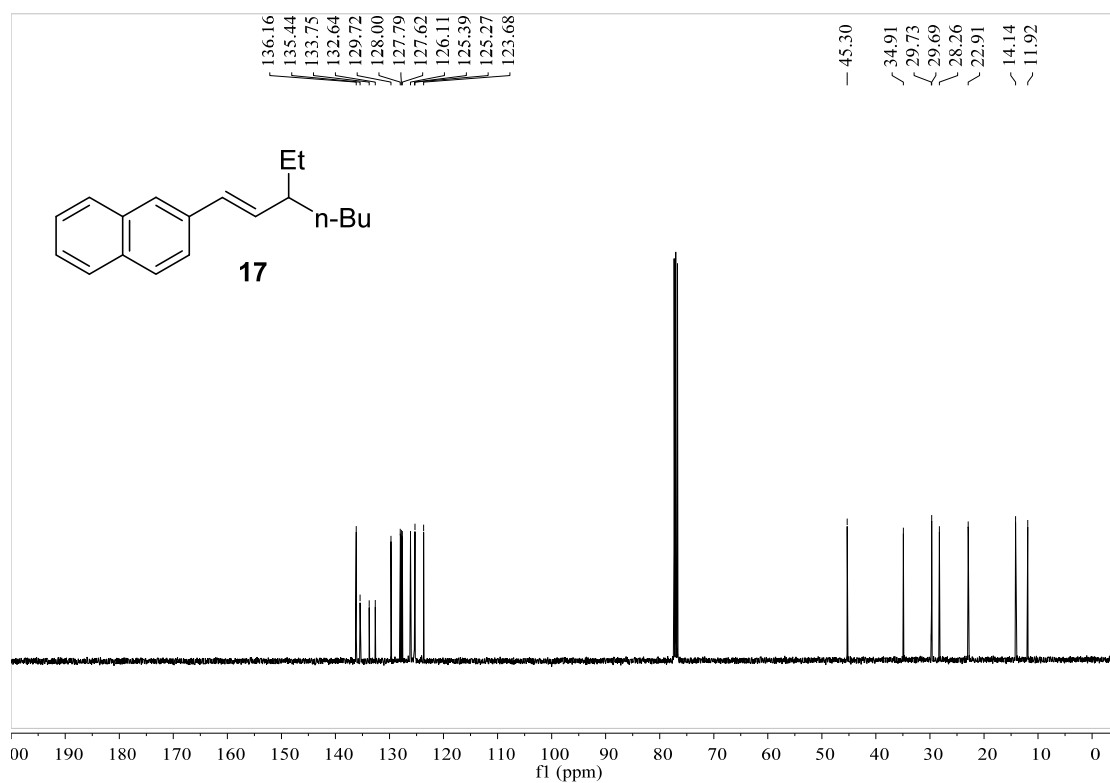
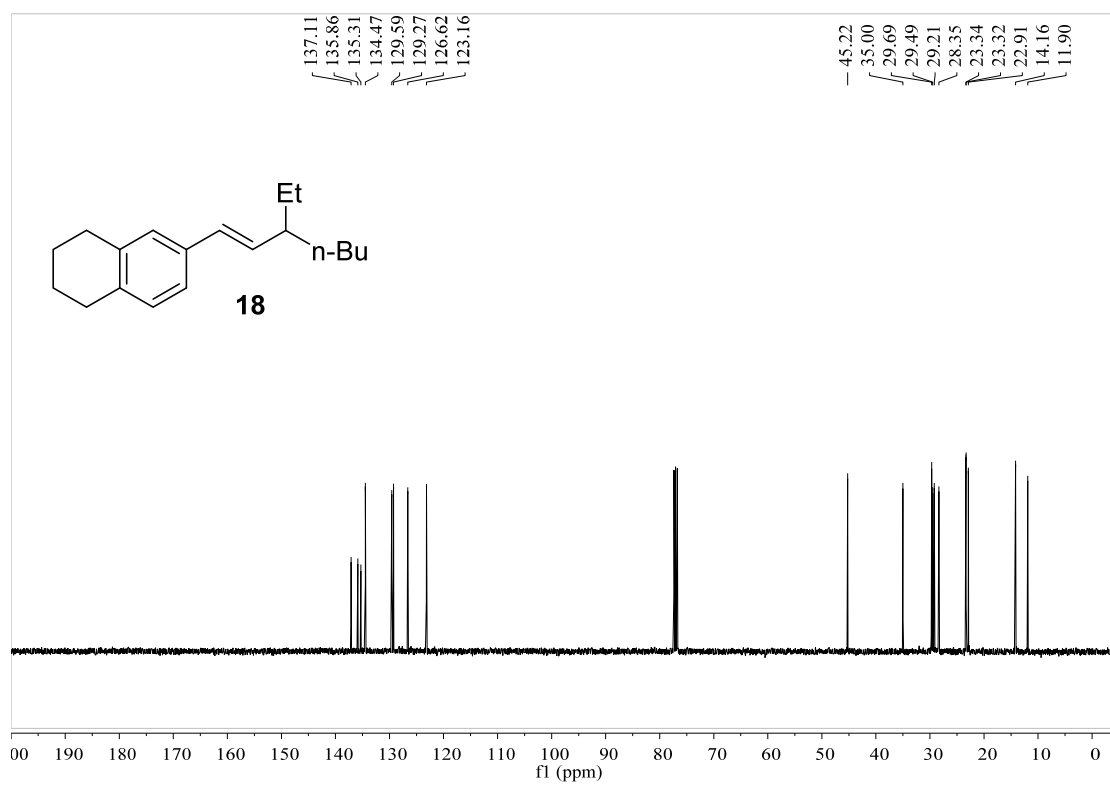
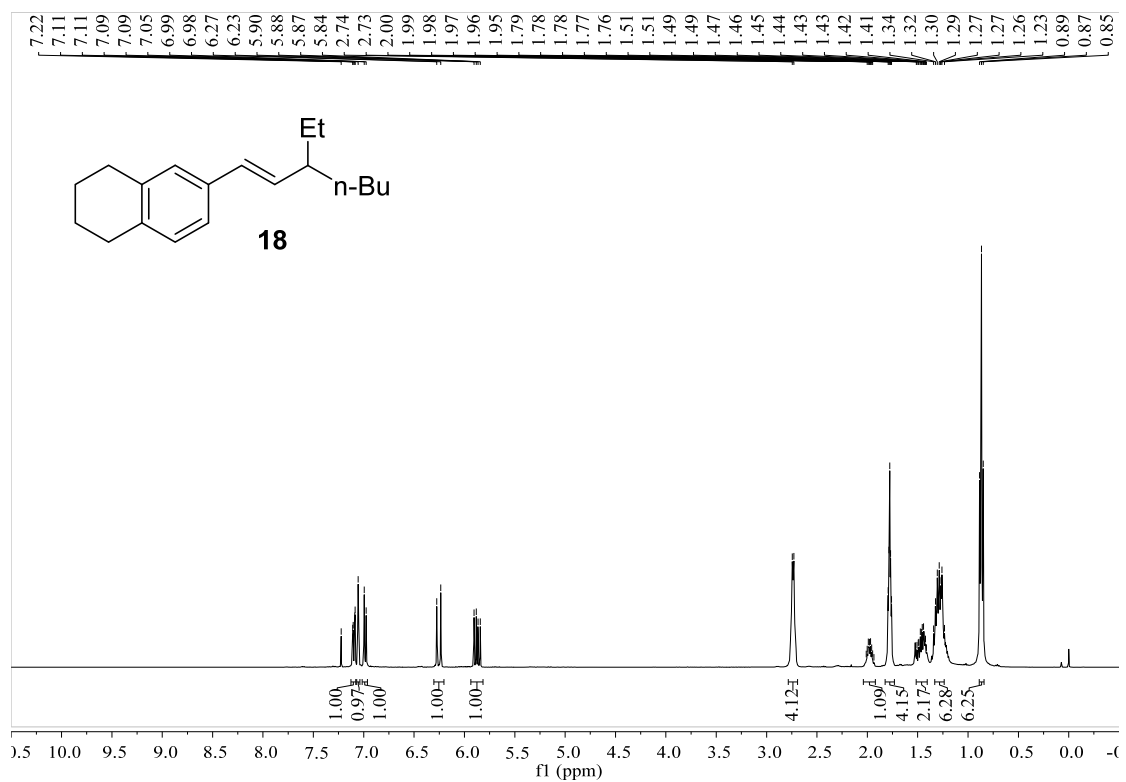


Figure S74. ¹³C NMR spectrum of compound 17, related to Figure 1.



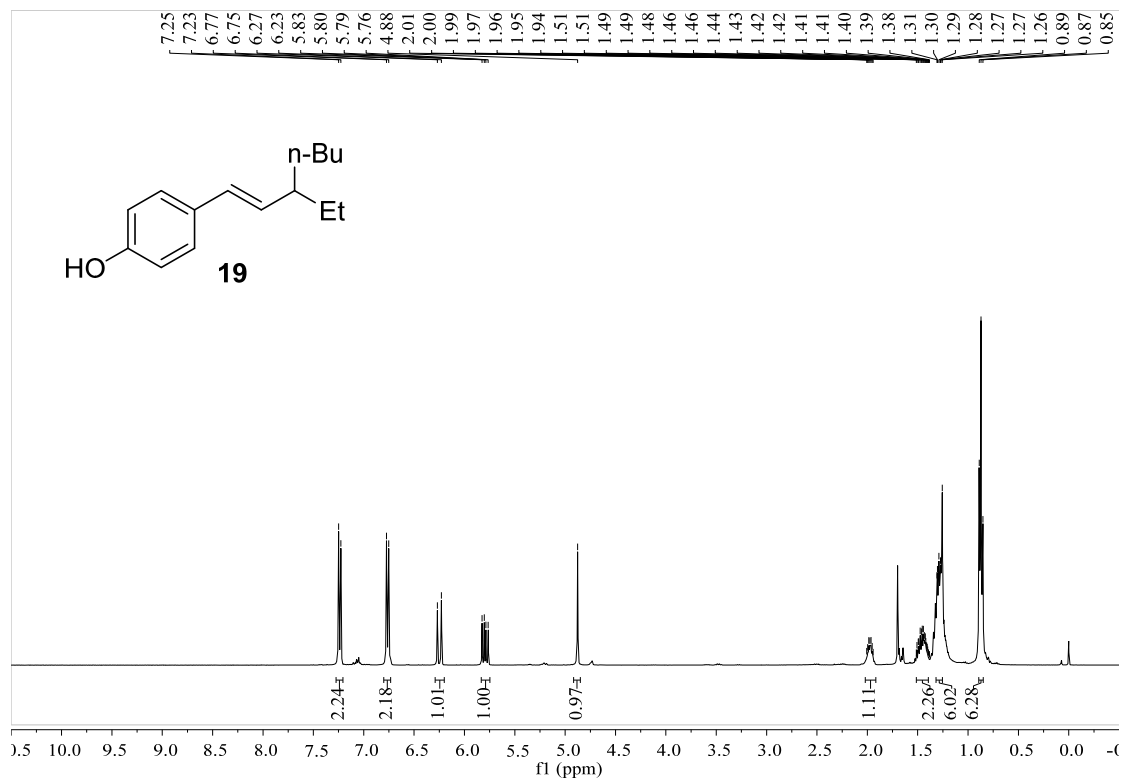


Figure S77. ¹H NMR spectrum of compound **19**, related to **Figure 1**.

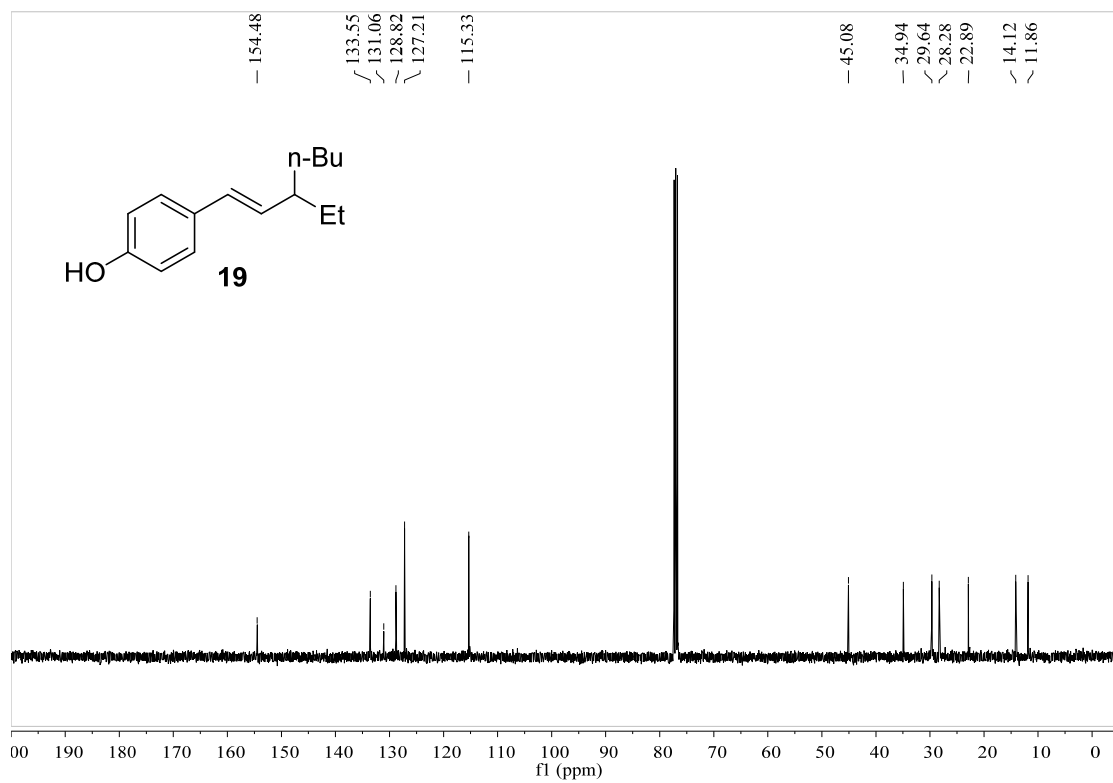


Figure S78. ¹³C NMR spectrum of compound **19**, related to **Figure 1**.

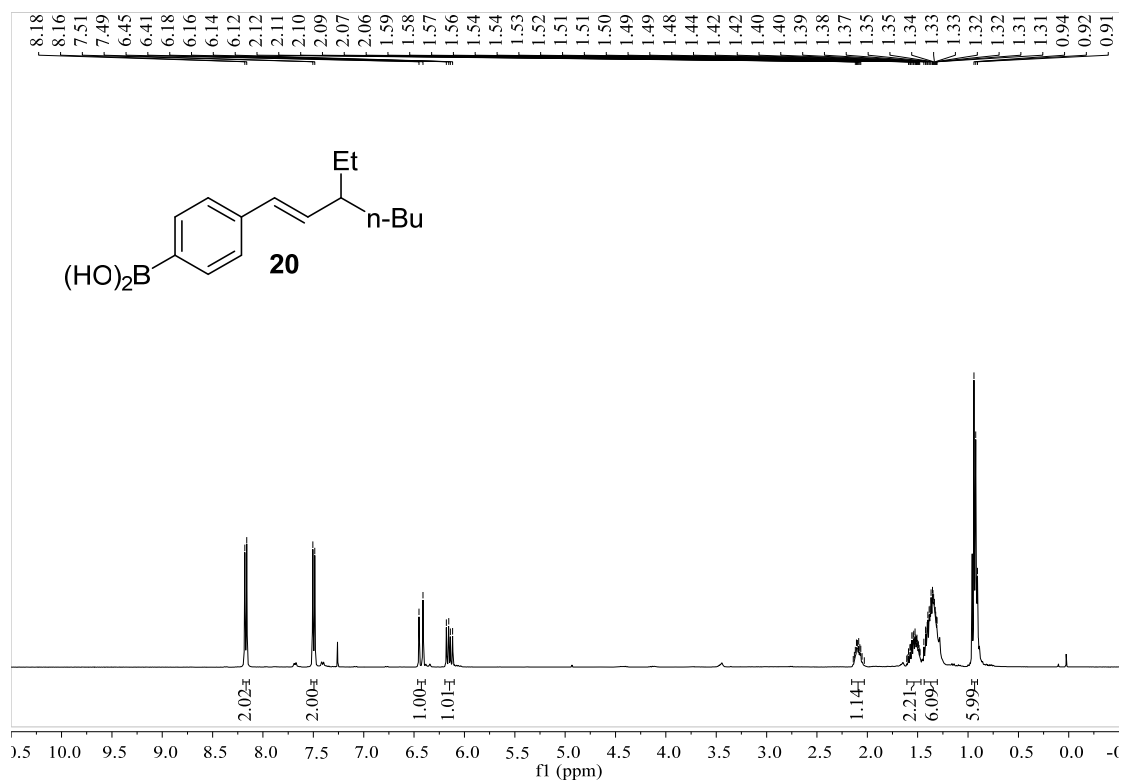


Figure S79. ¹H NMR spectrum of compound **20**, related to **Figure 1**.

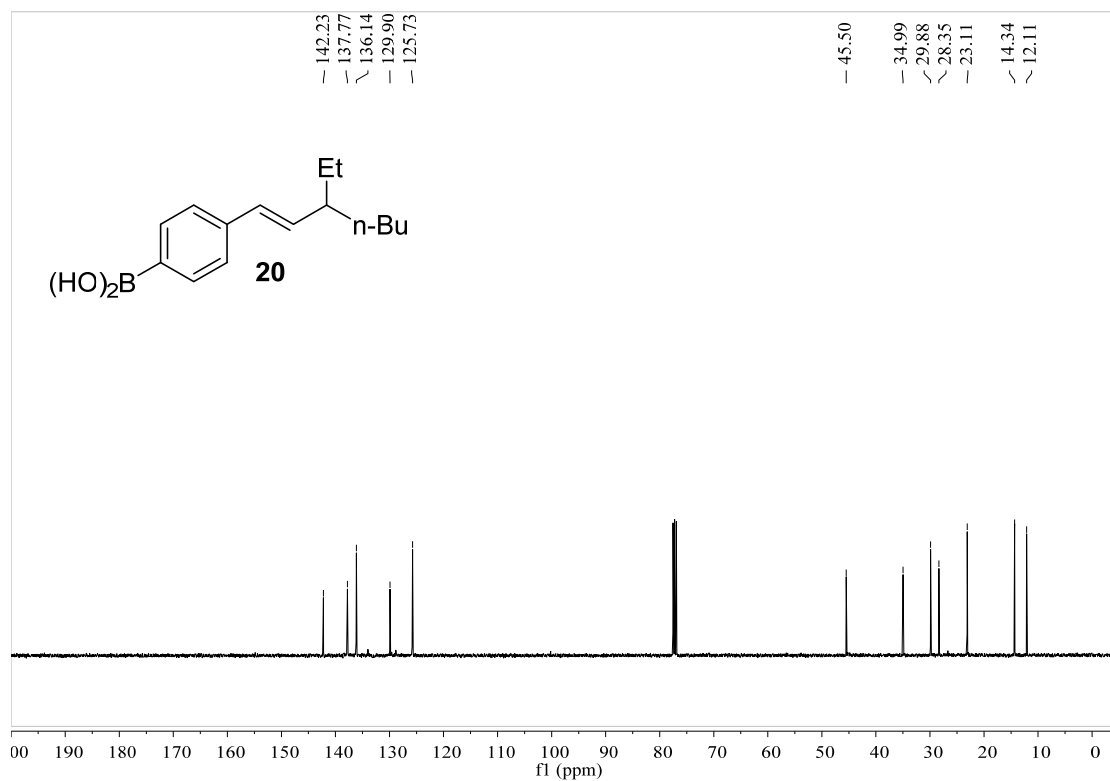


Figure S80. ¹³C NMR spectrum of compound **20**, related to **Figure 1**.

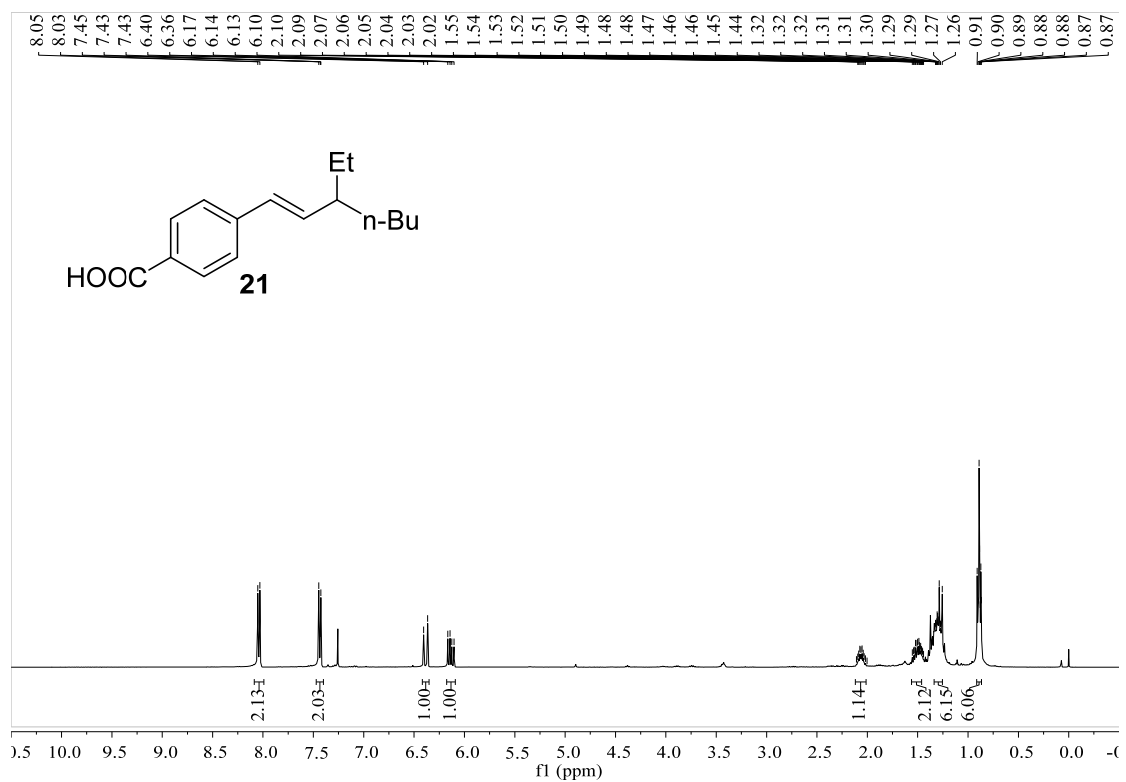


Figure S81. ¹H NMR spectrum of compound **21**, related to **Figure 1**.

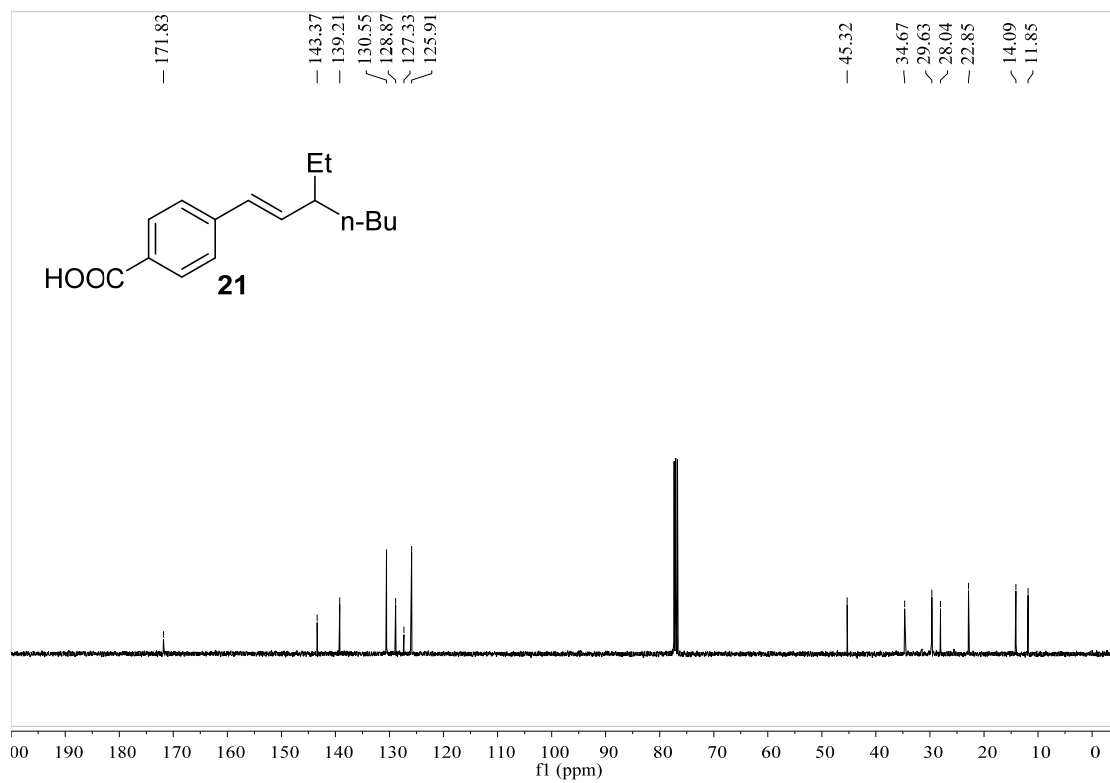


Figure S82. ¹³C NMR spectrum of compound **21**, related to **Figure 1**.

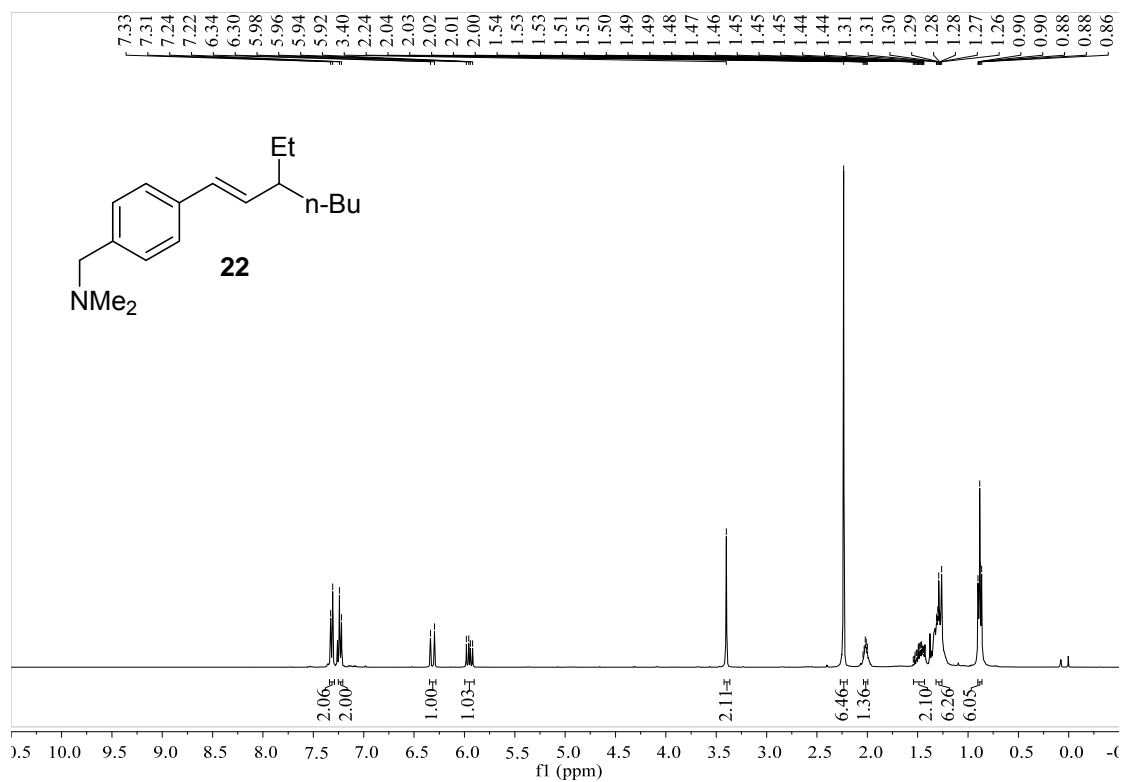


Figure S83. ¹H NMR spectrum of compound **22**, related to **Figure 1**.

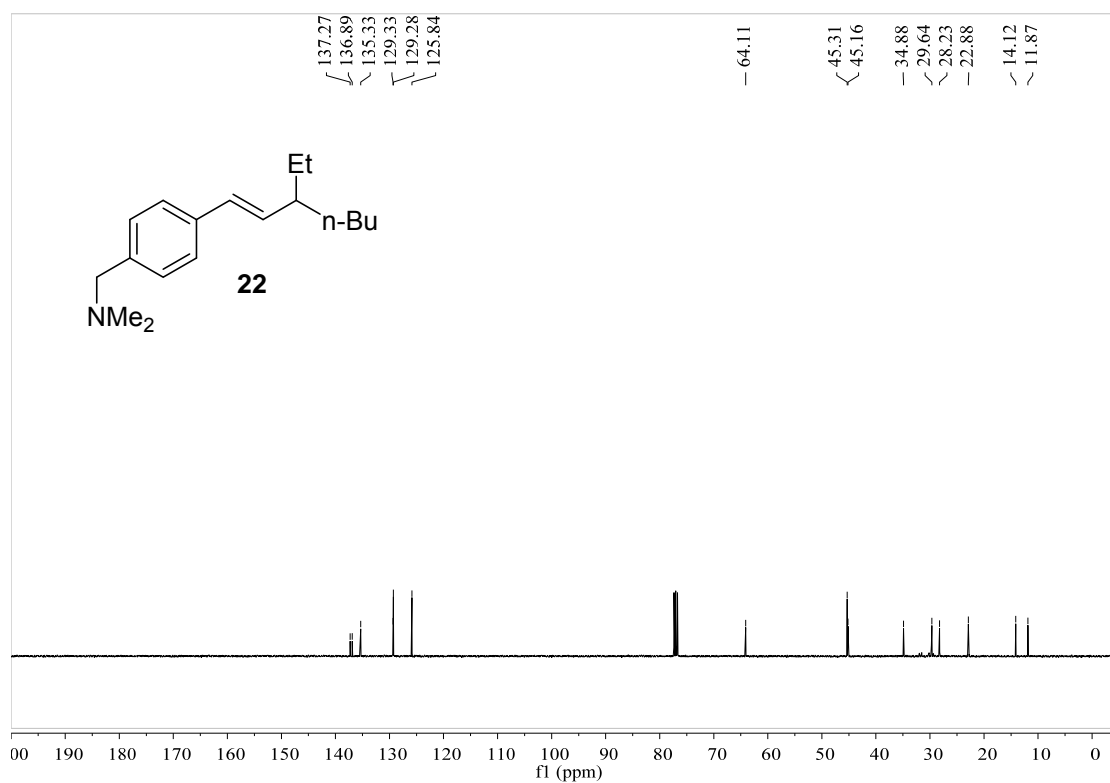


Figure S84. ¹³C NMR spectrum of compound **22**, related to **Figure 1**.

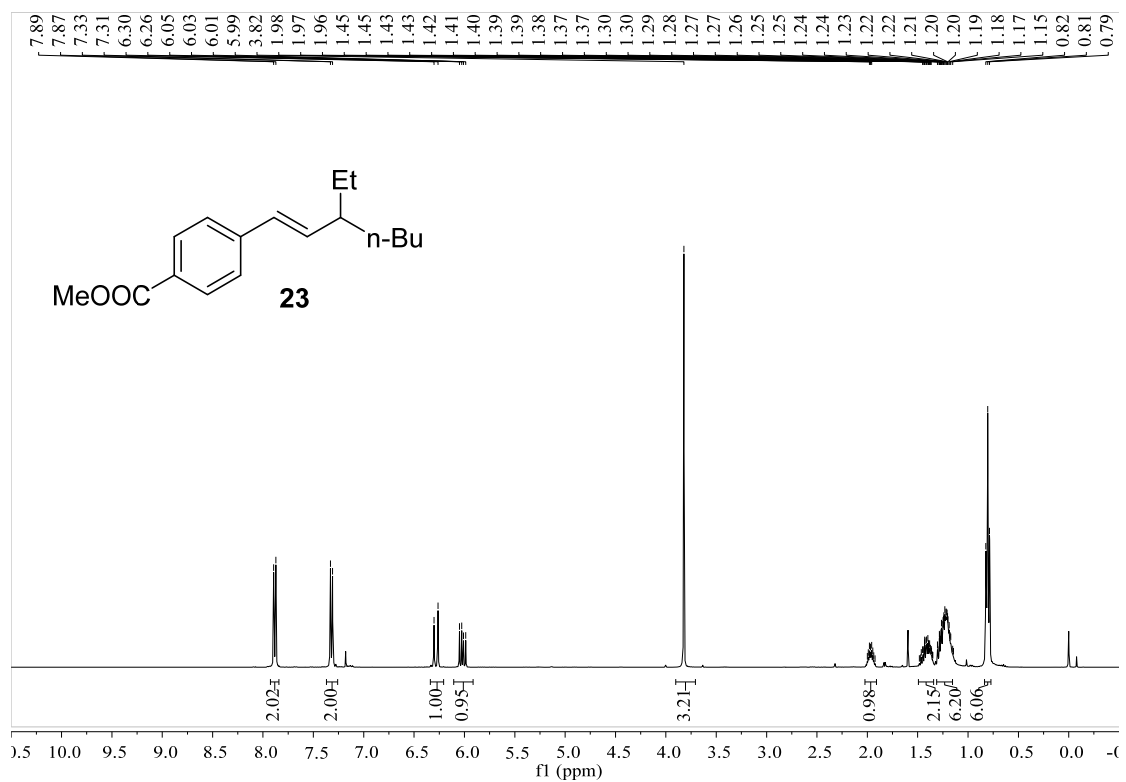


Figure S85. ¹H NMR spectrum of compound **23**, related to **Figure 1**.

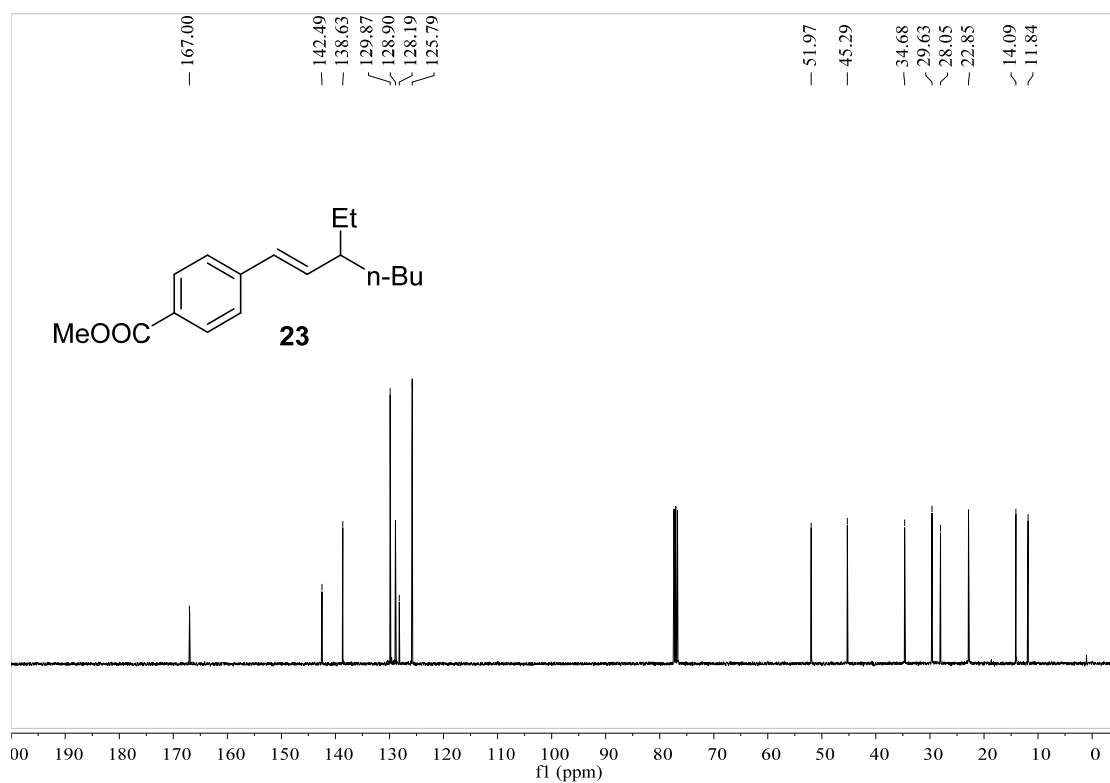


Figure S86. ¹³C NMR spectrum of compound **23**, related to **Figure 1**.

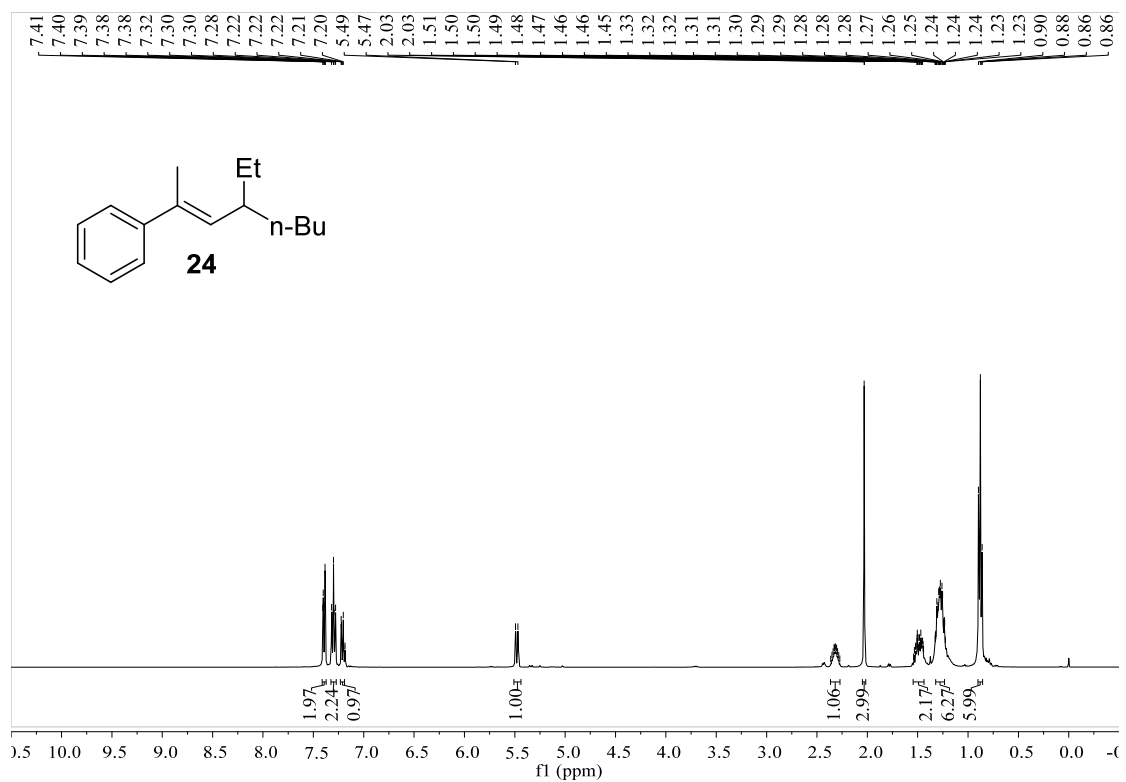


Figure S87. ¹H NMR spectrum of compound **24**, related to **Figure 1**.

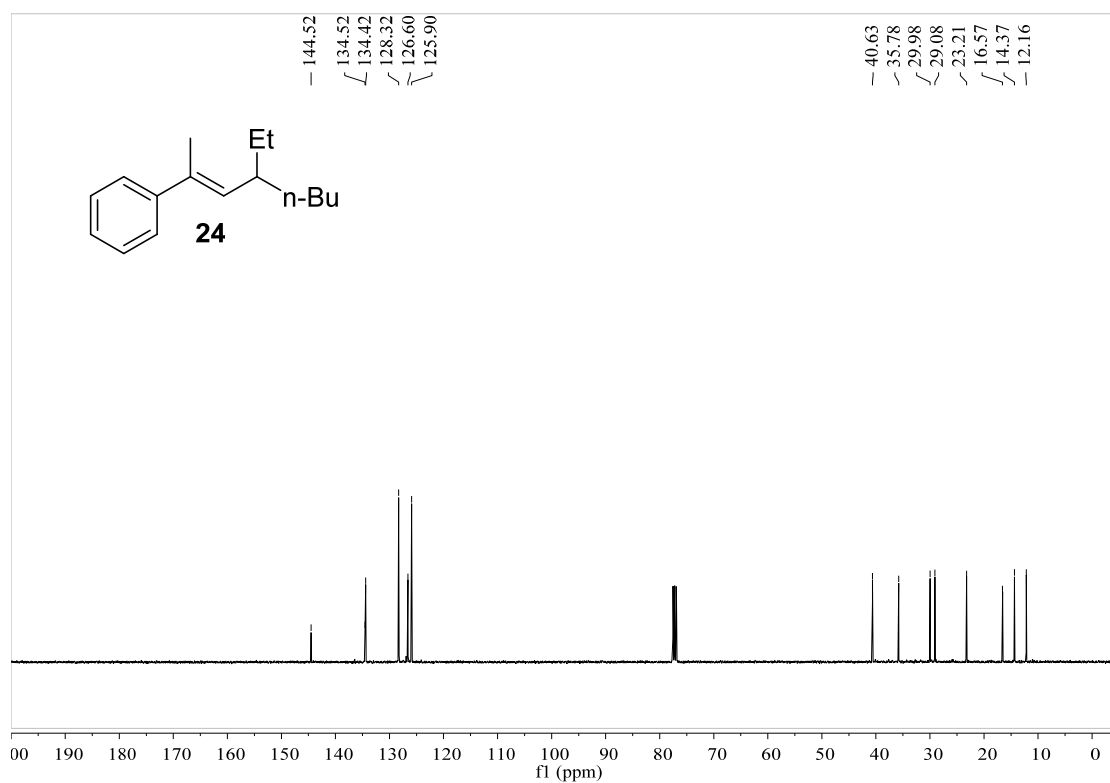


Figure S88. ¹³C NMR spectrum of compound **24**, related to **Figure 1**.

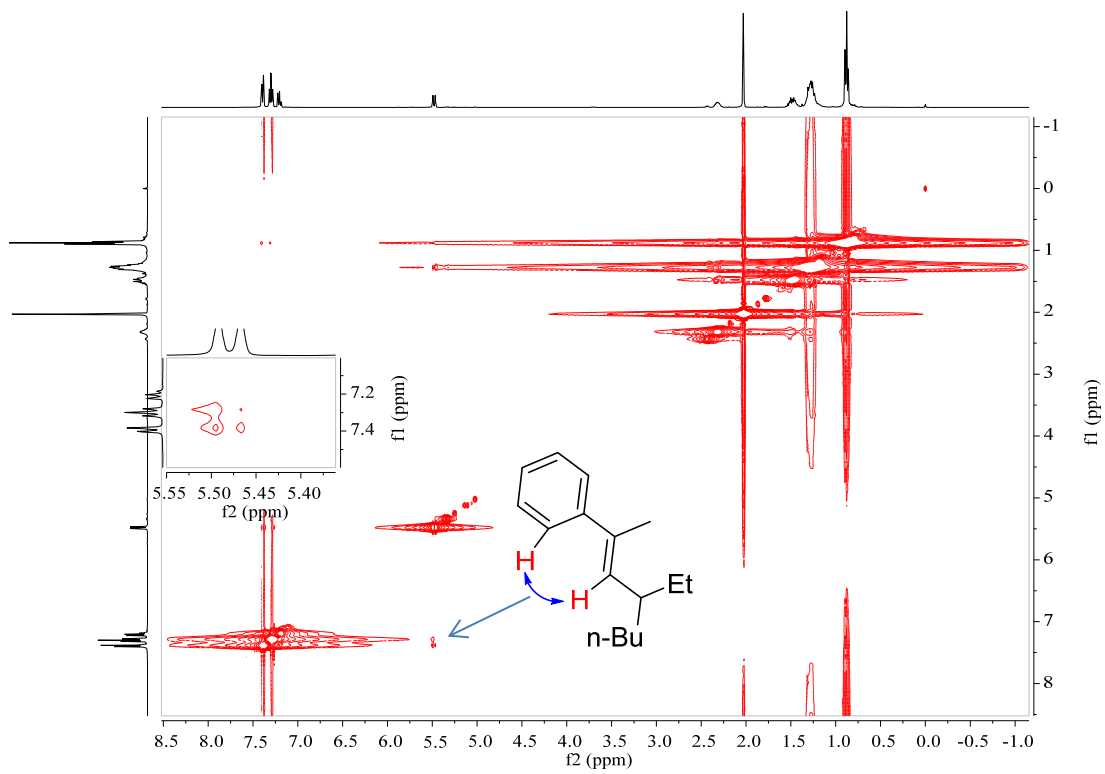


Figure S89. NOE spectrum of compound **24**, related to **Figure 1**.

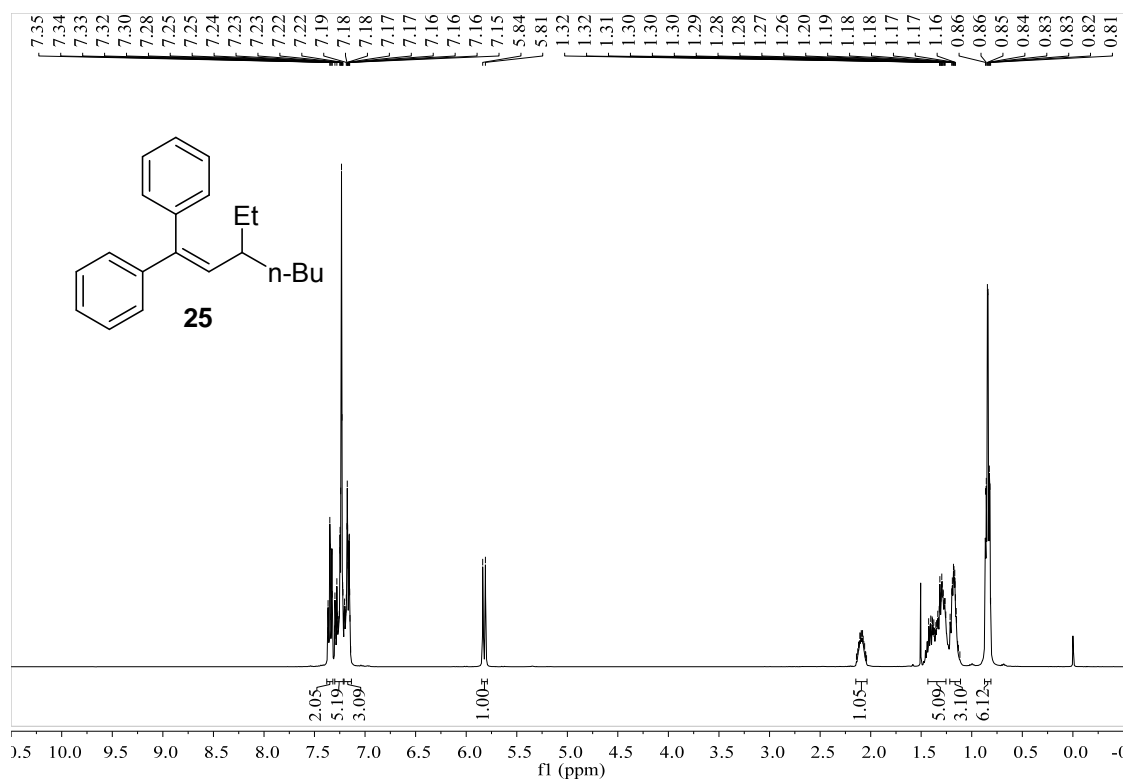


Figure S90. ¹H NMR spectrum of compound **25**, related to **Figure 1**.

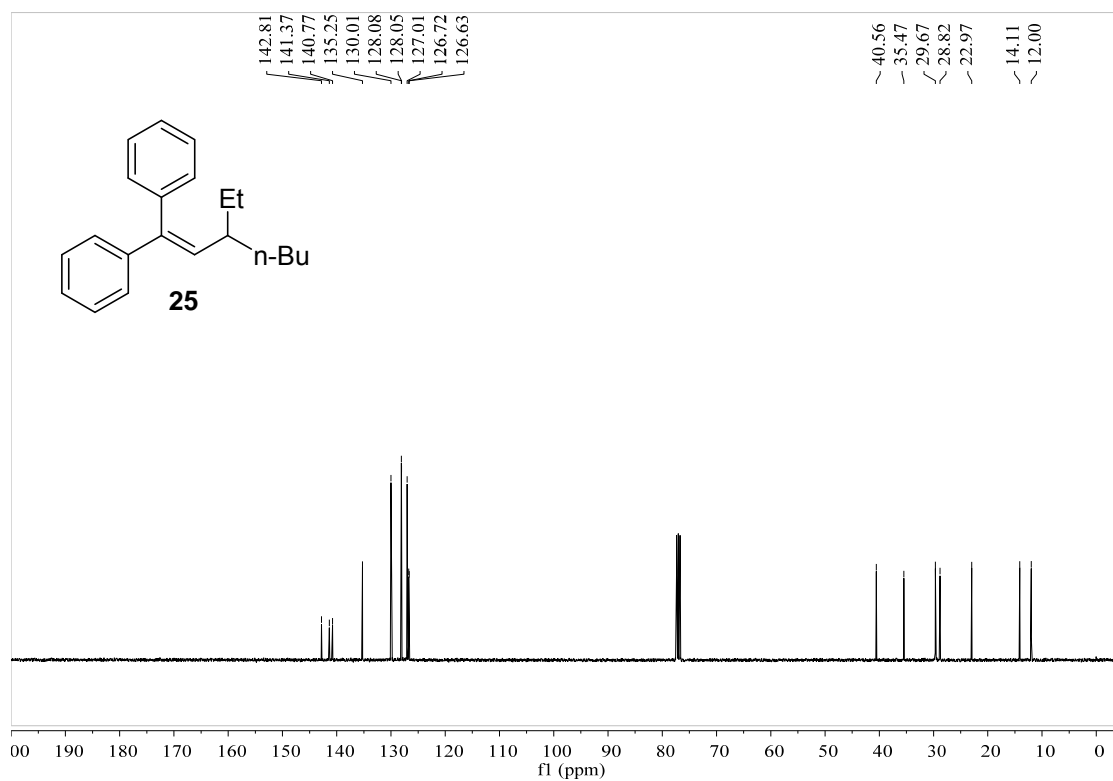


Figure S91. ¹³C NMR spectrum of compound **25**, related to **Figure 1**.

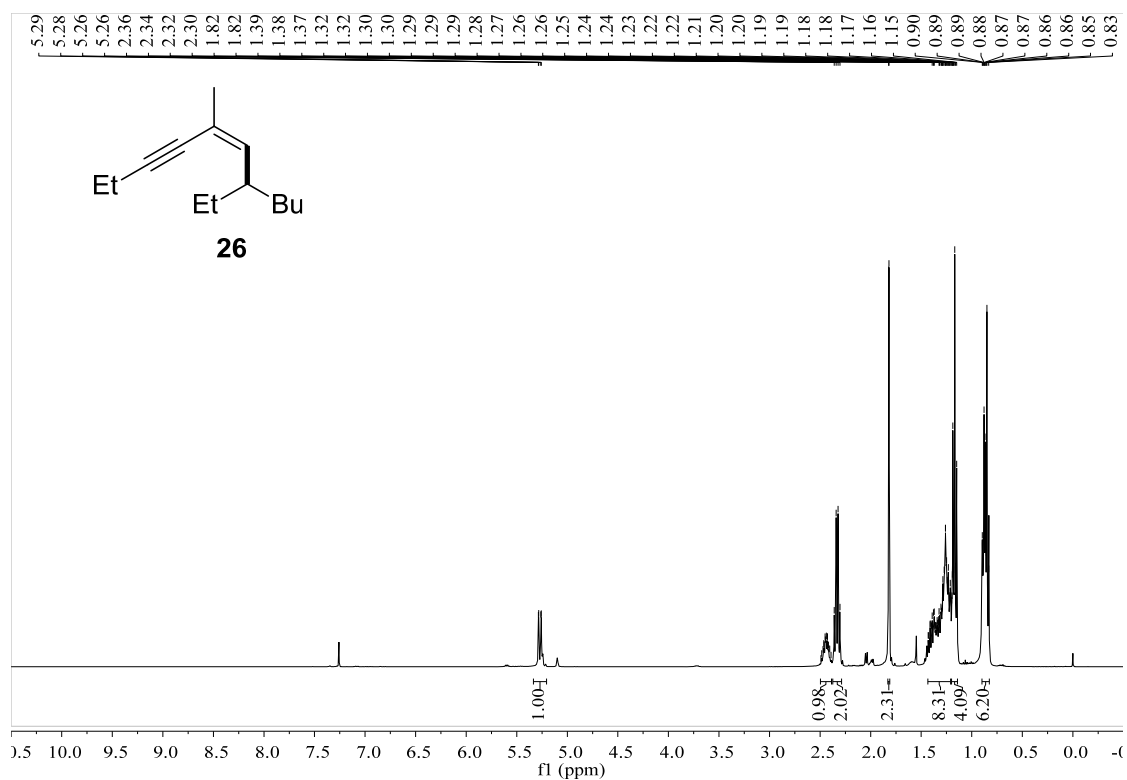


Figure S92. ¹H NMR spectrum of compound **26**, related to Figure 1.

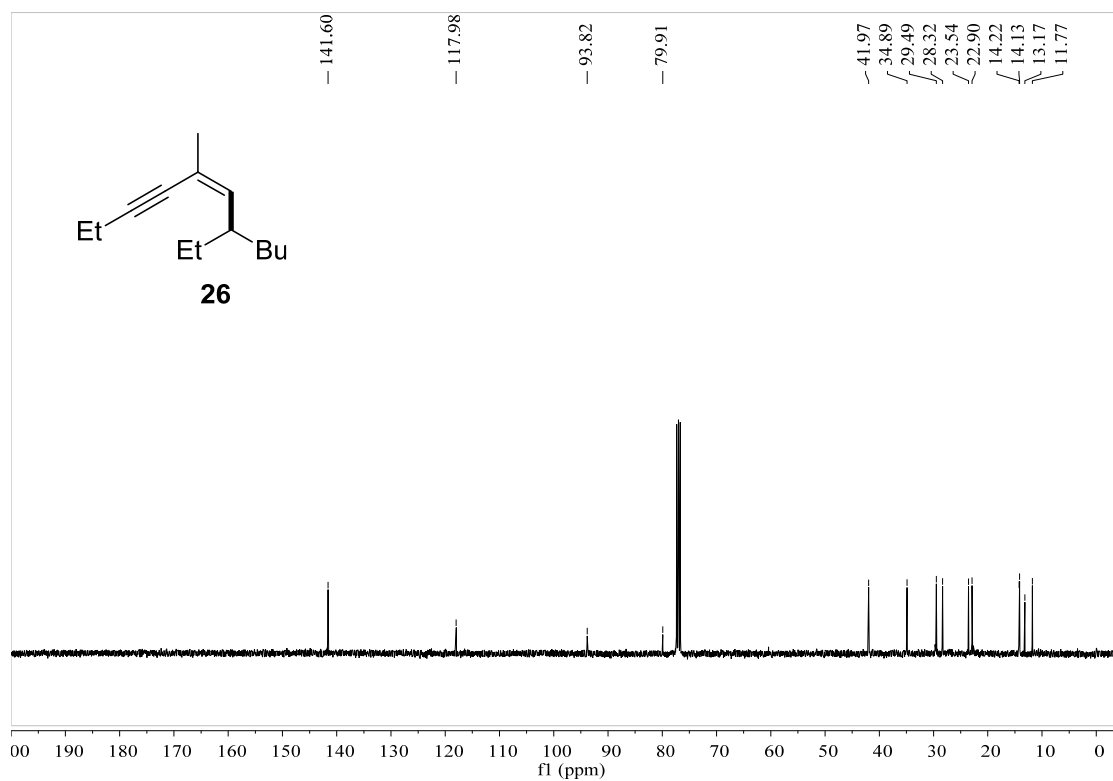


Figure S93. ¹³C NMR spectrum of compound **26**, related to Figure 1.

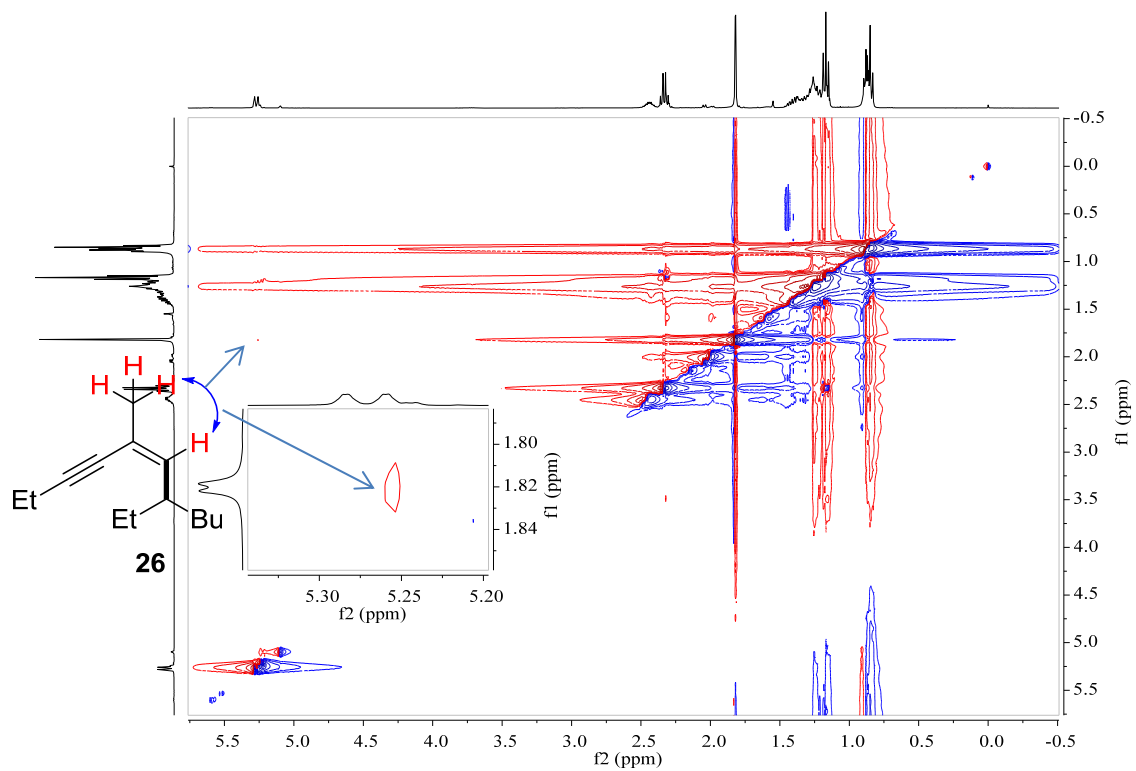


Figure S94. NOE spectrum of compound **26**, related to **Figure 1**.

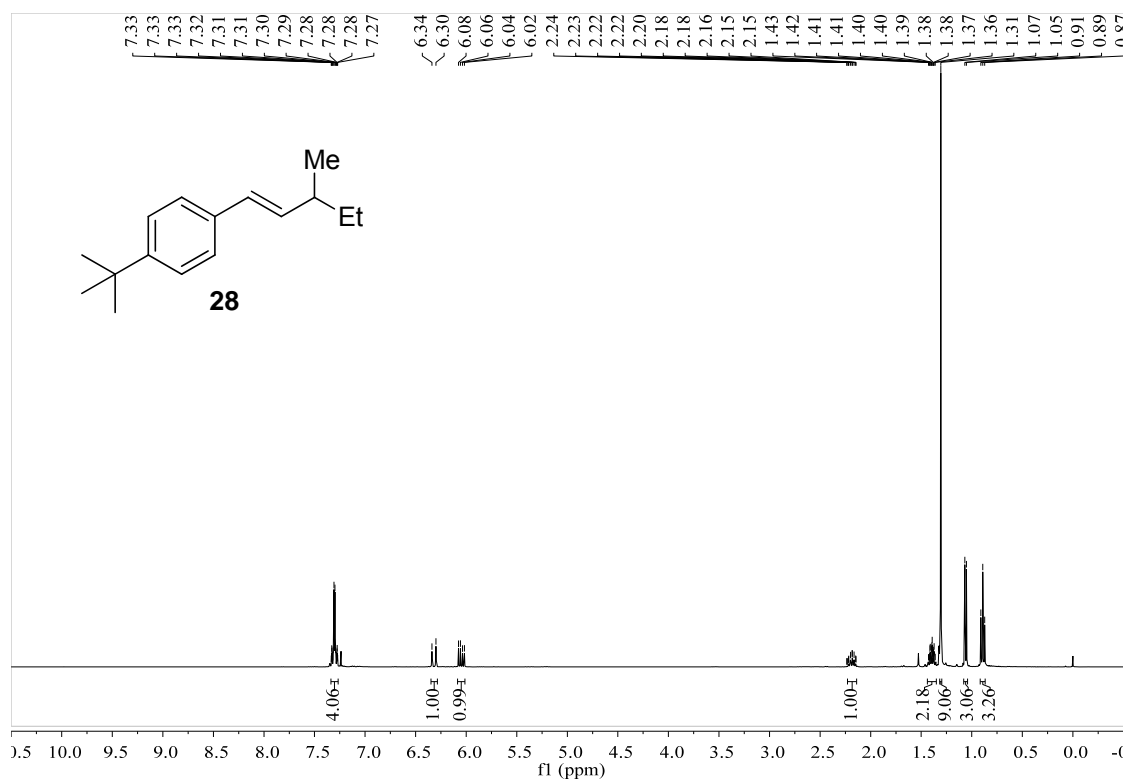


Figure S95. ¹H NMR spectrum of compound **28**, related to Figure 2.

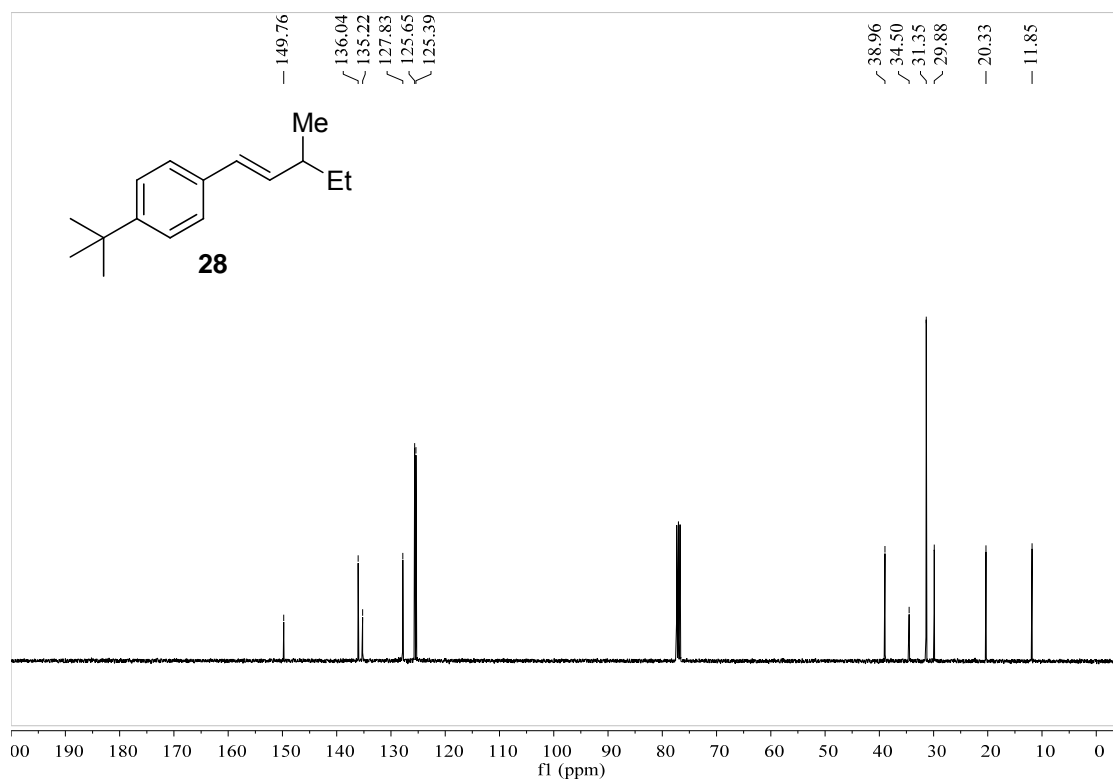


Figure S96. ¹³C NMR spectrum of compound **28**, related to Figure 2.

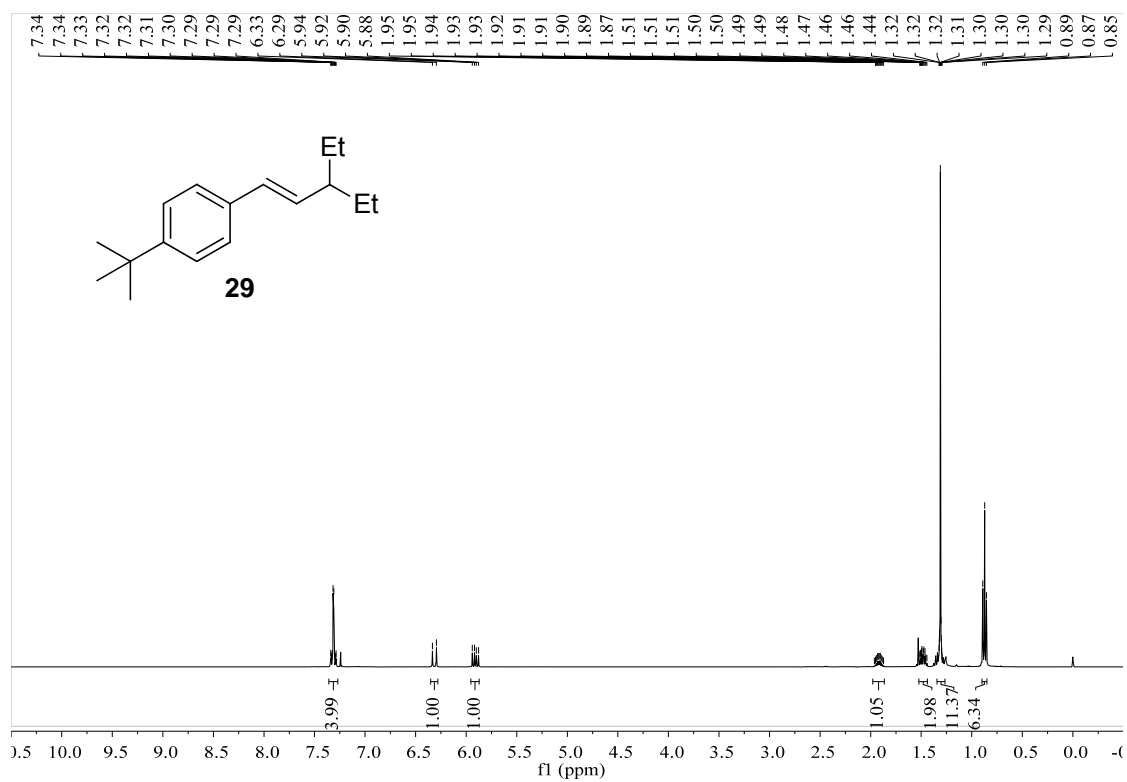


Figure S97. ¹H NMR spectrum of compound **29**, related to Figure 2.

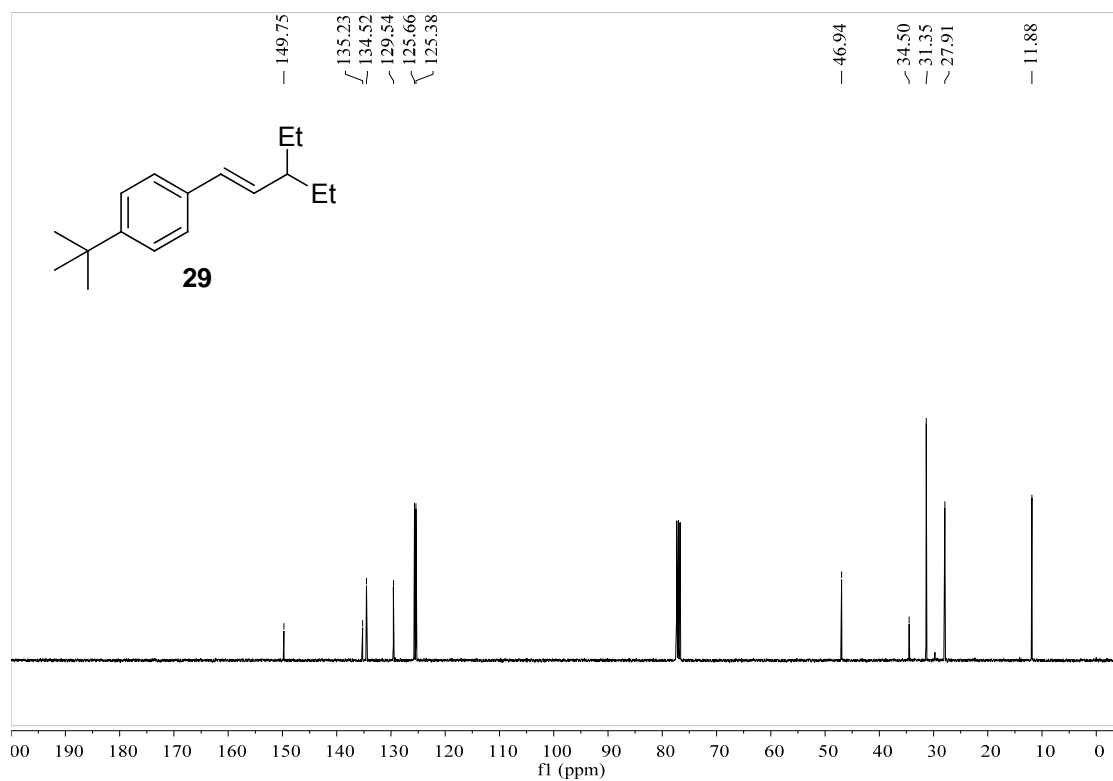


Figure S98. ¹³C NMR spectrum of compound **29**, related to Figure 2.

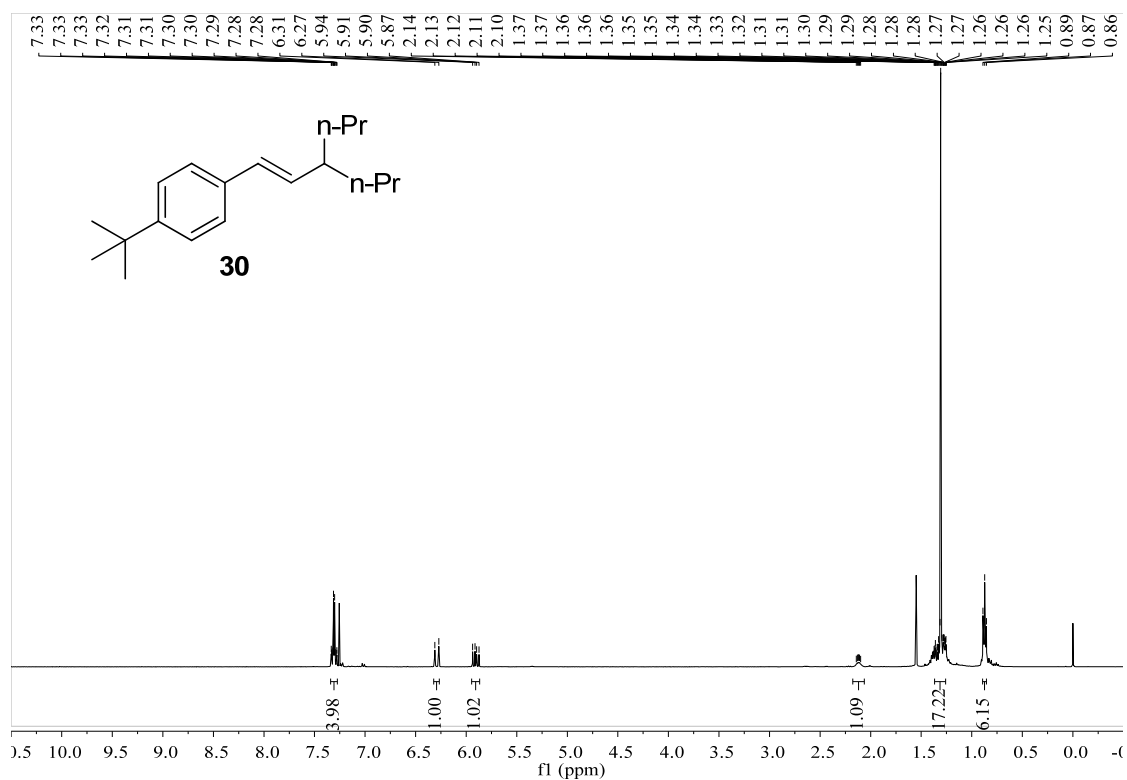


Figure S99. ¹H NMR spectrum of compound **30**, related to **Figure 2**.

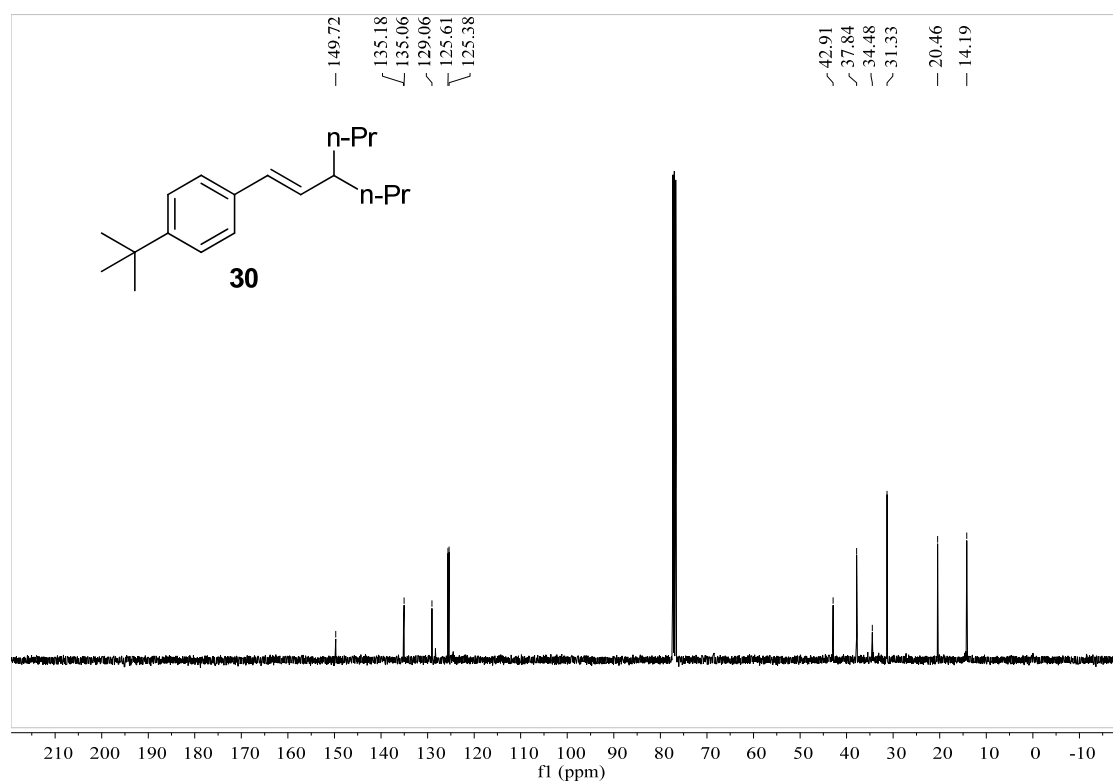


Figure S100. ¹³C NMR spectrum of compound **30**, related to **Figure 2**.

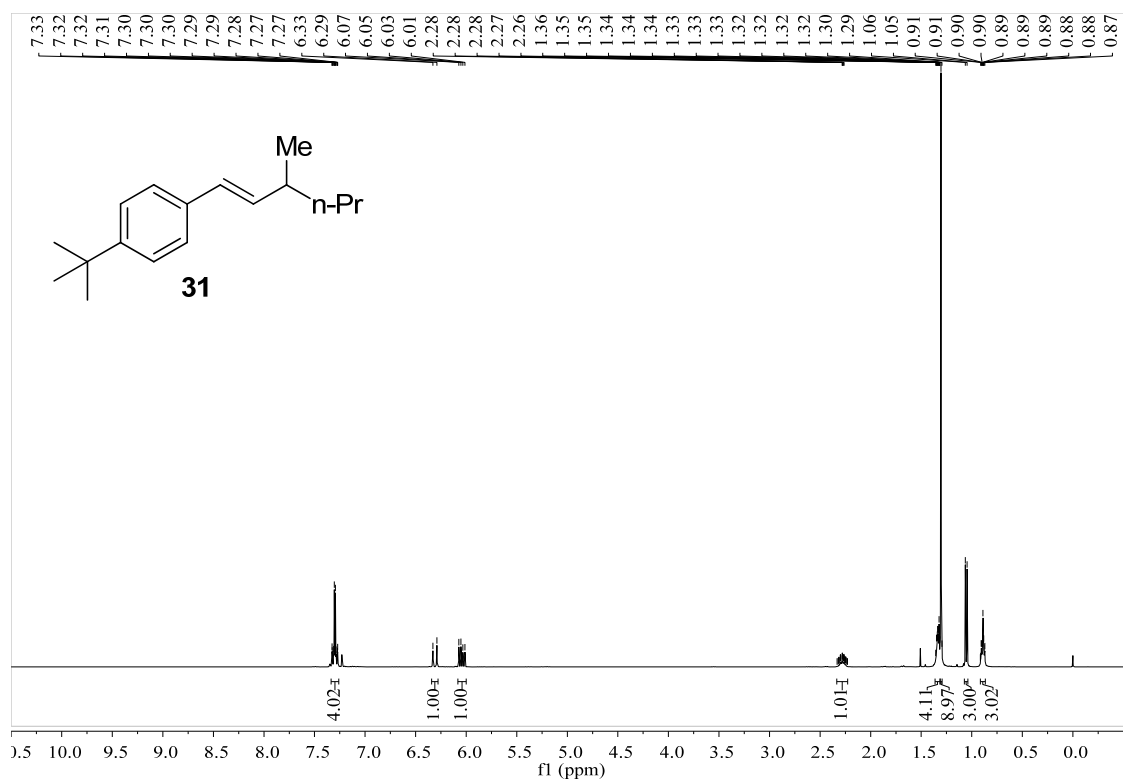


Figure S101. ¹H NMR spectrum of compound **31**, related to **Figure 2**.

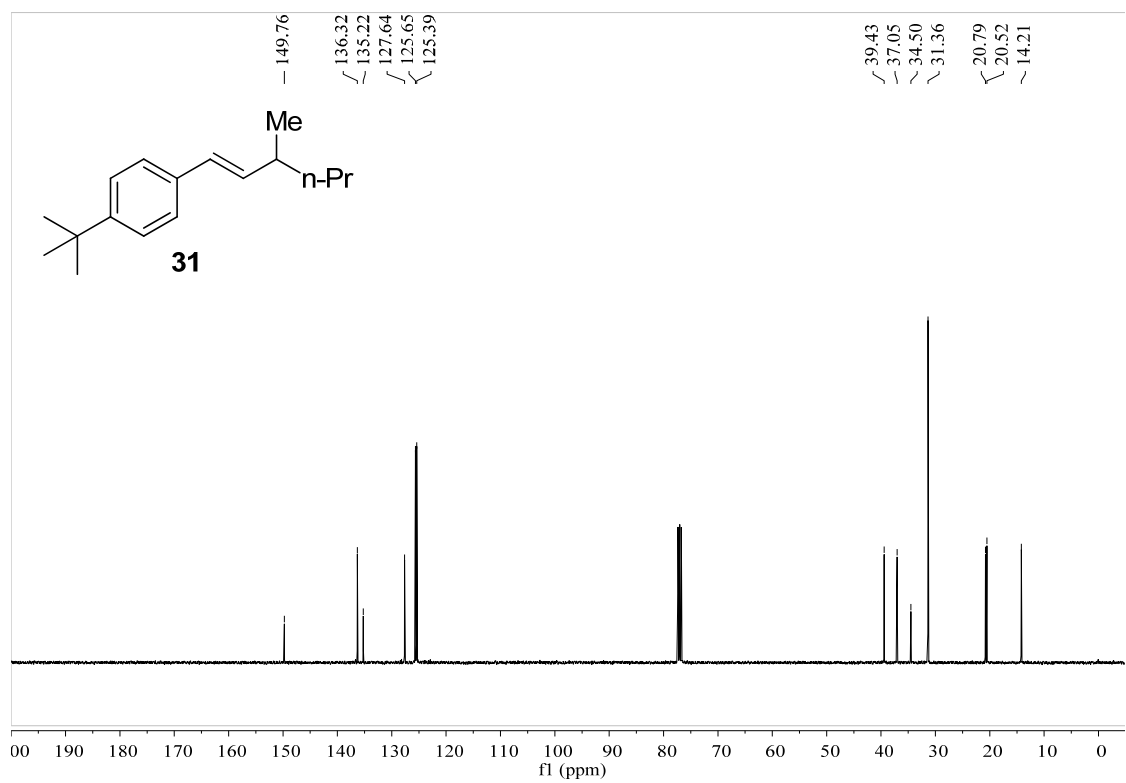


Figure S102. ¹³C NMR spectrum of compound **31**, related to **Figure 2**.

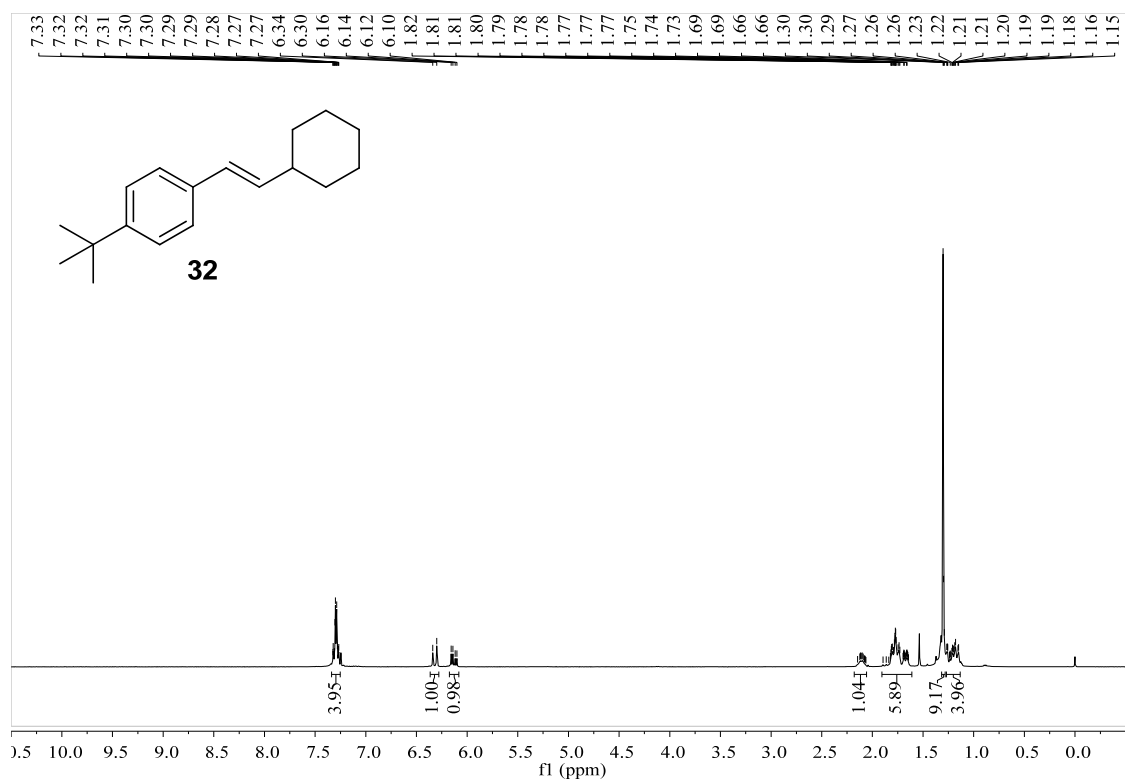


Figure S103. ¹H NMR spectrum of compound **32**, related to **Figure 2**.

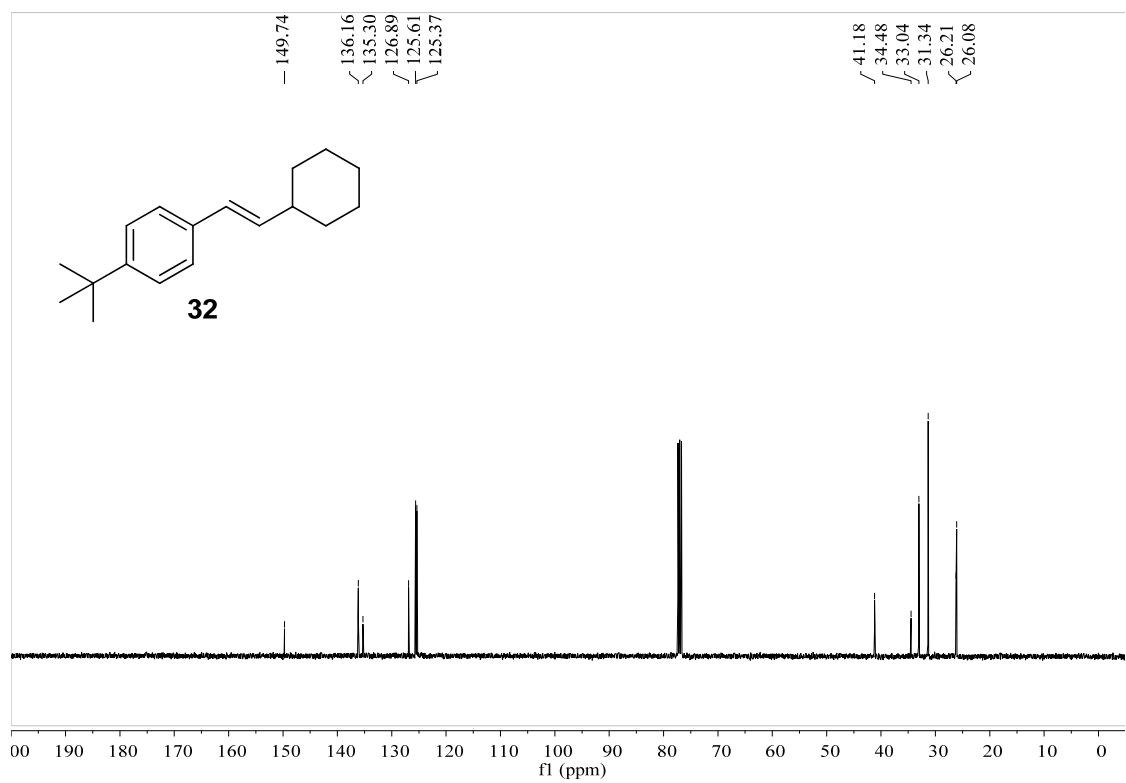


Figure S104. ¹³C NMR spectrum of compound **32**, related to **Figure 2**.

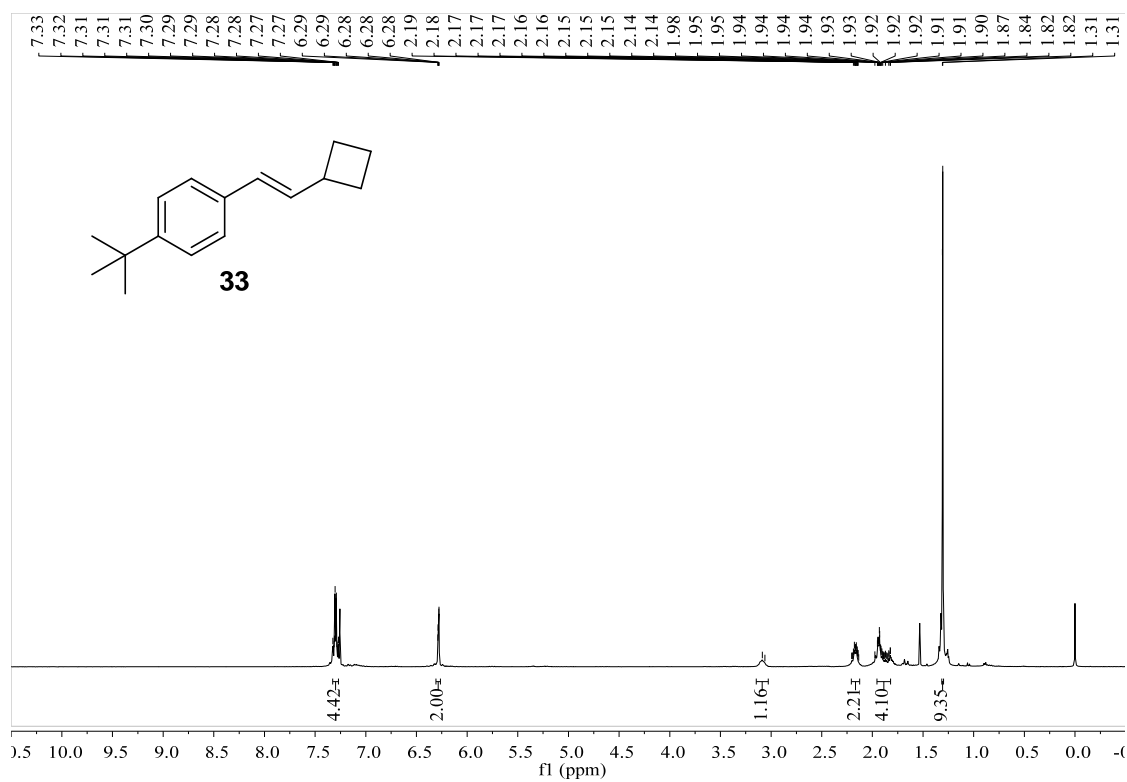


Figure S105. ¹H NMR spectrum of compound **33**, related to **Figure 2**.

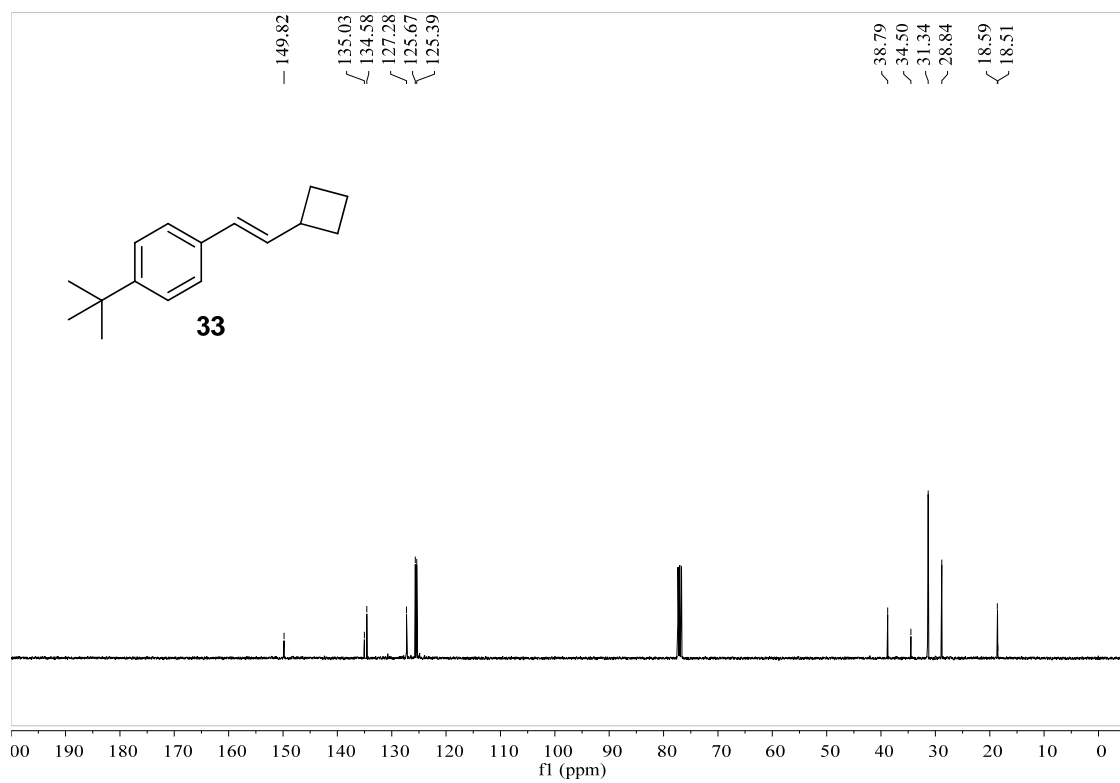


Figure S106. ¹³C NMR spectrum of compound **33**, related to **Figure 2**.

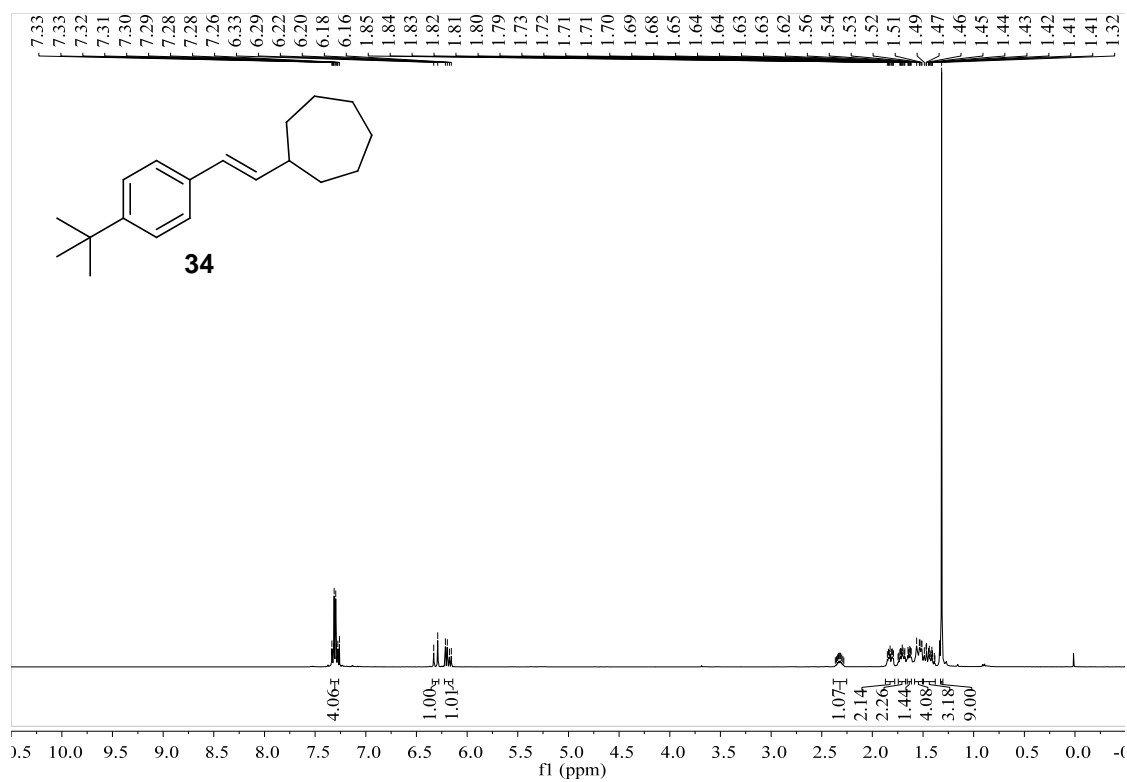


Figure S107. ¹H NMR spectrum of compound **34**, related to Figure 2.

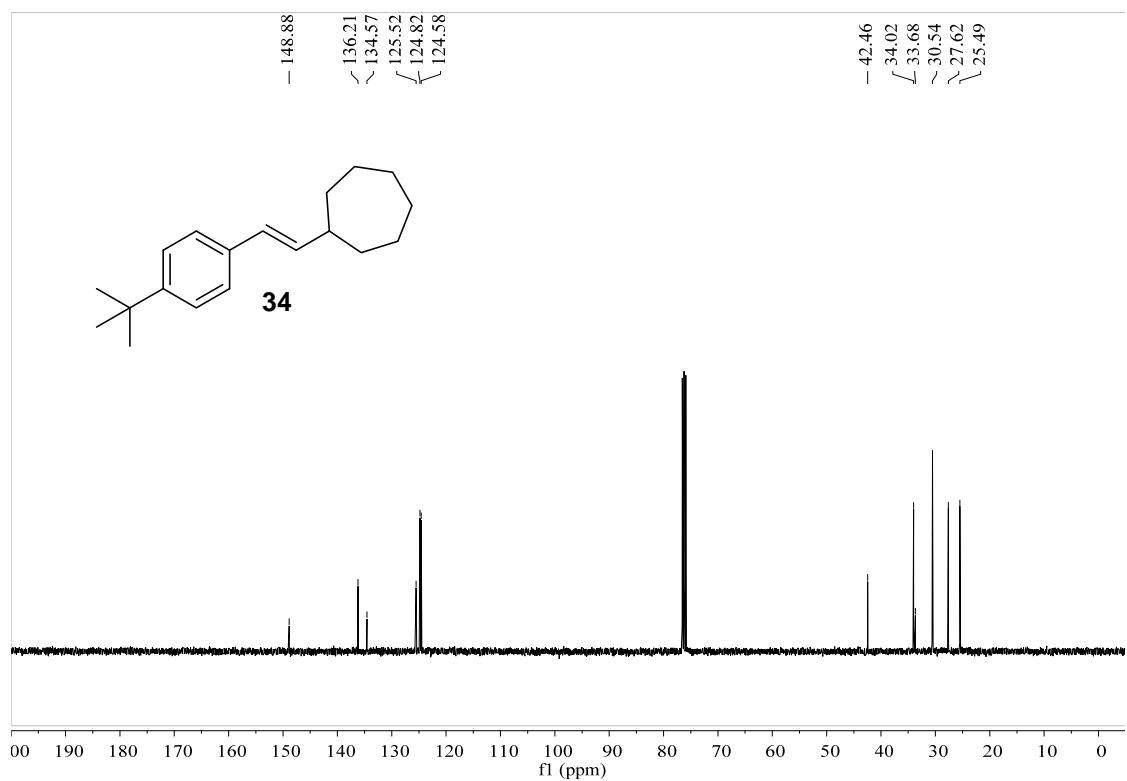
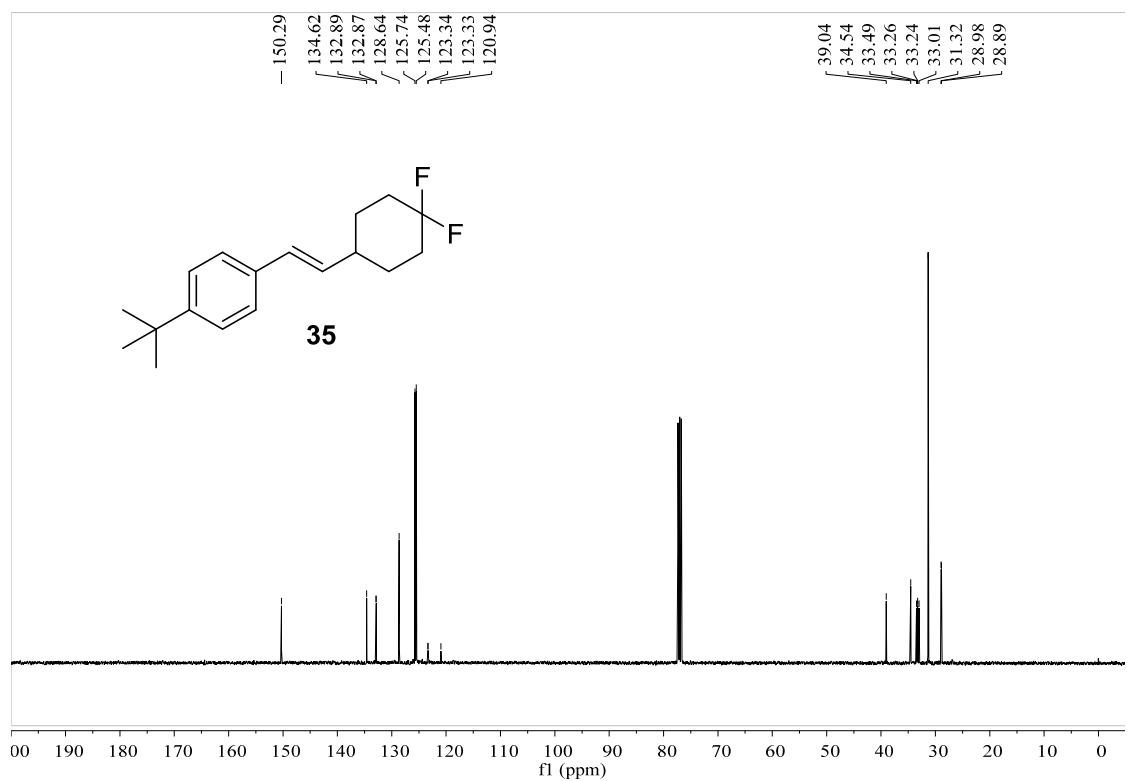
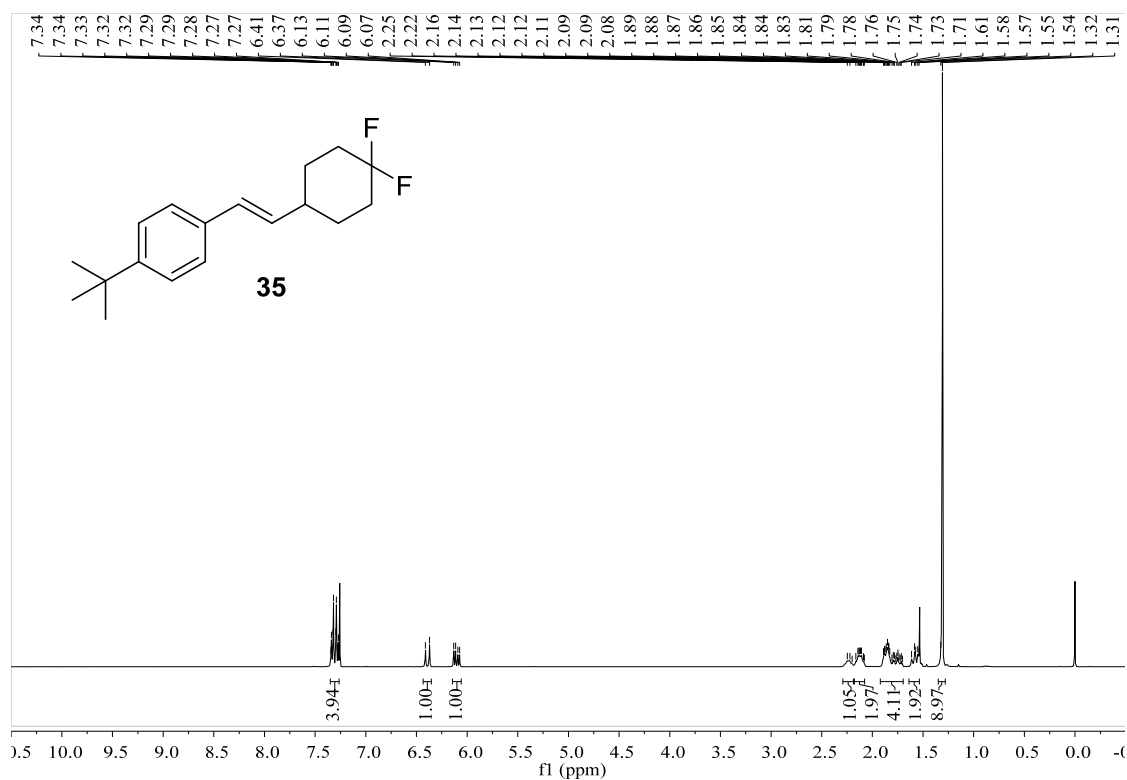


Figure S108. ¹³C NMR spectrum of compound **34**, related to Figure 2.



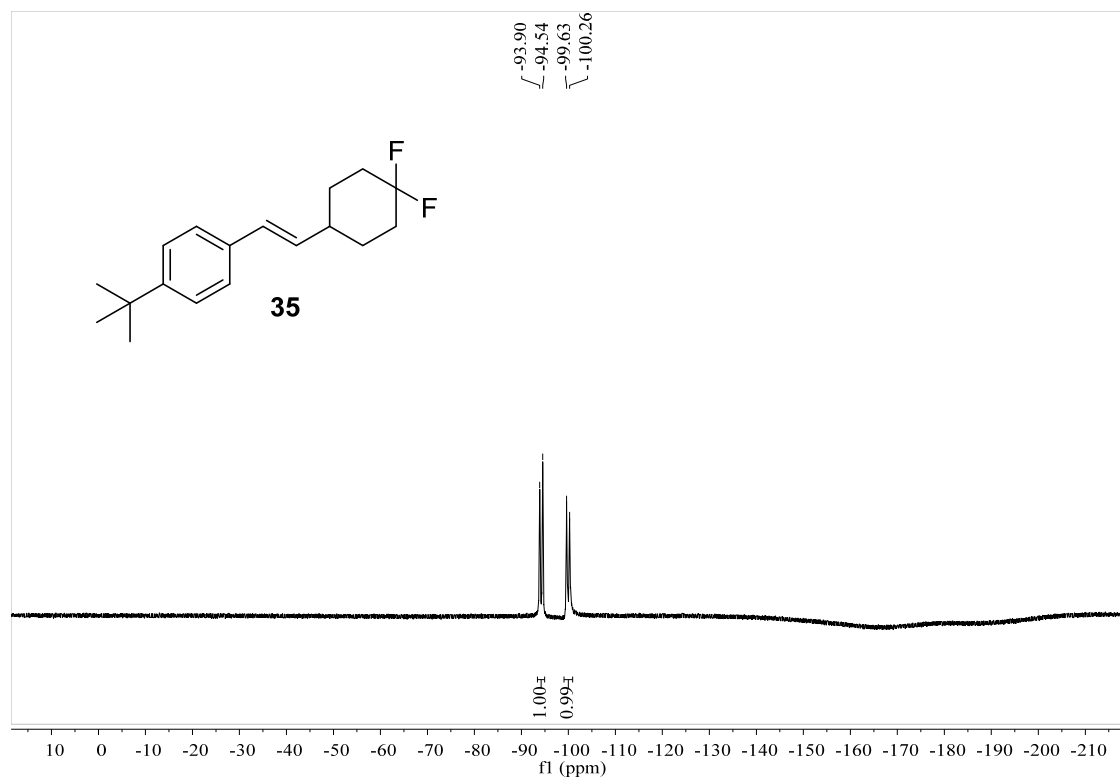


Figure S111. ^{19}F NMR spectrum of compound **35**, related to **Figure 2**.

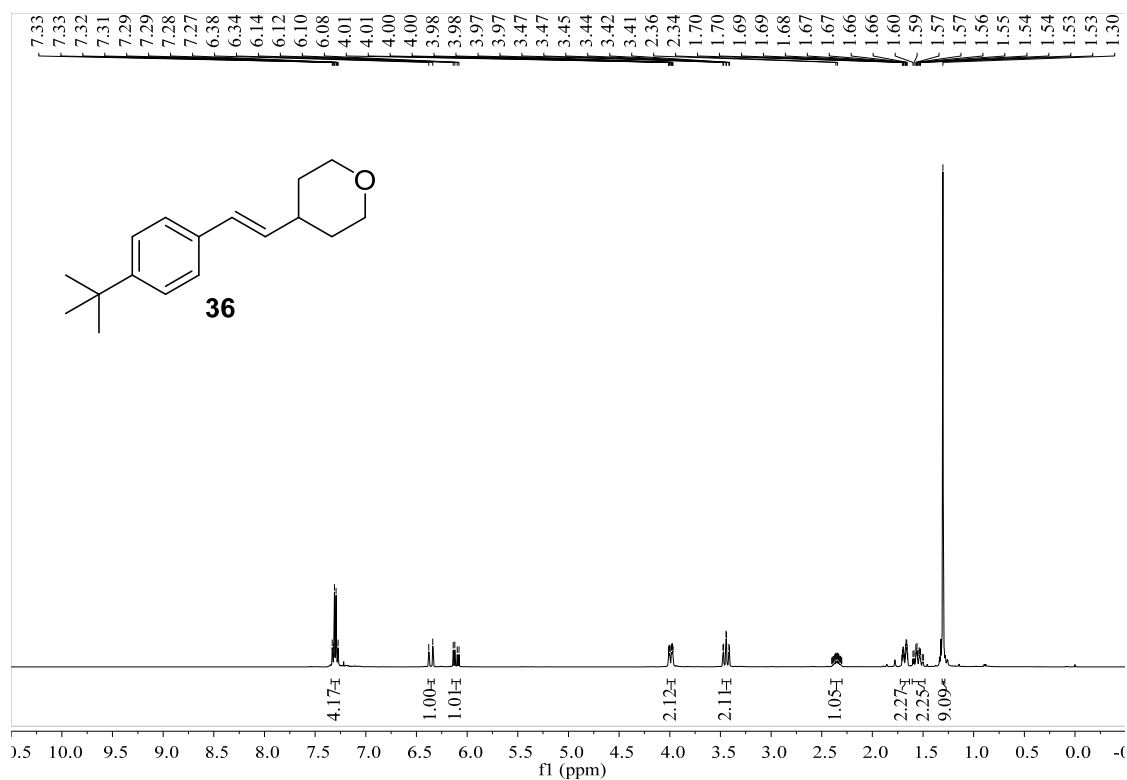


Figure S112. ¹H NMR spectrum of compound **36**, related to Figure 2.

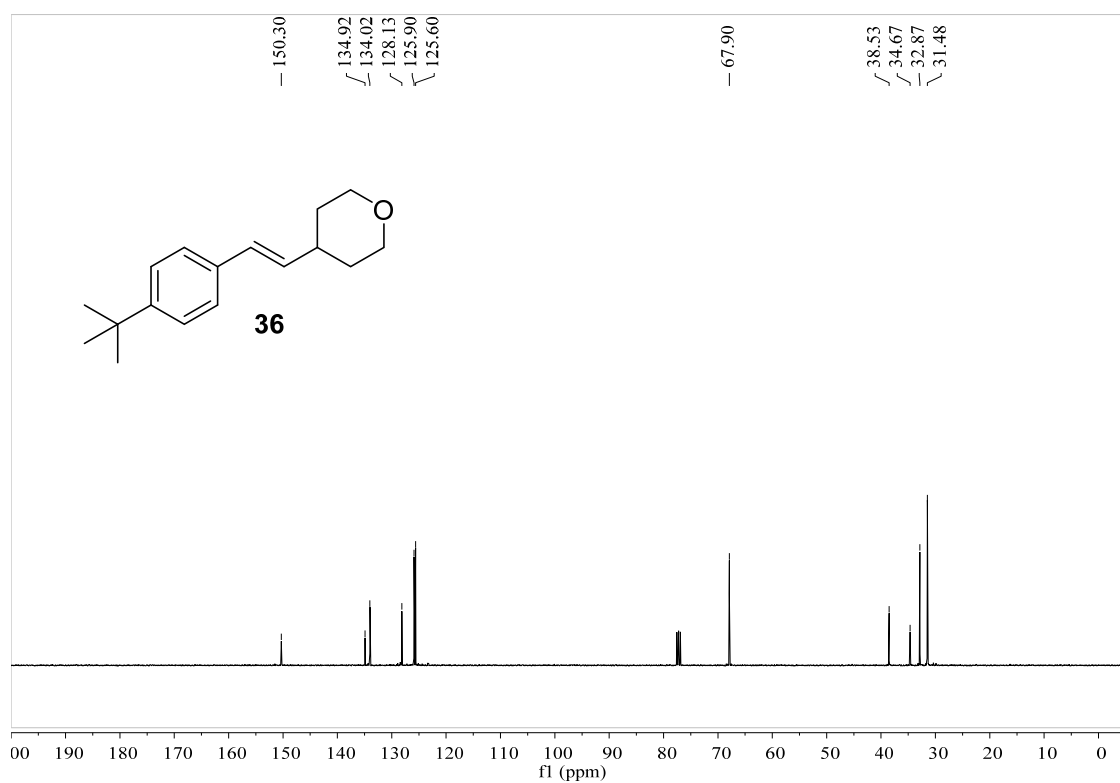


Figure S113. ¹³C NMR spectrum of compound **36**, related to Figure 2.

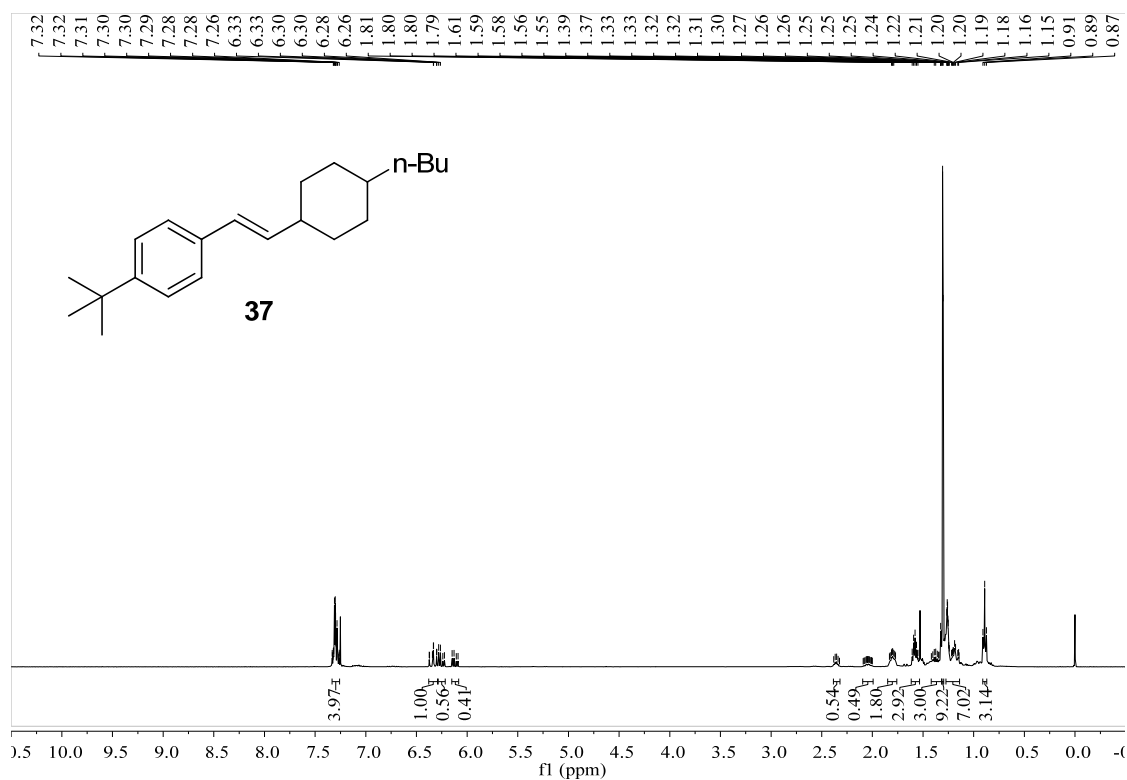


Figure S114. ¹H NMR spectrum of compound **37**, related to Figure 2.

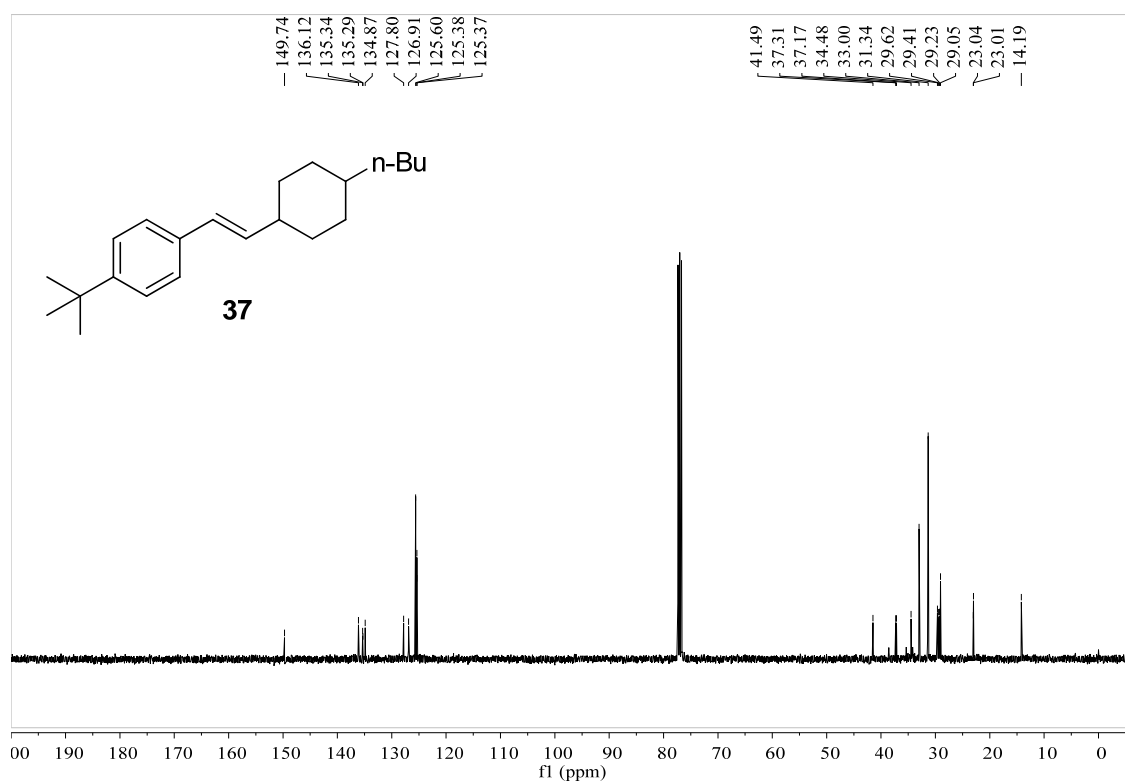


Figure S115. ¹³C NMR spectrum of compound **37**, related to Figure 2.

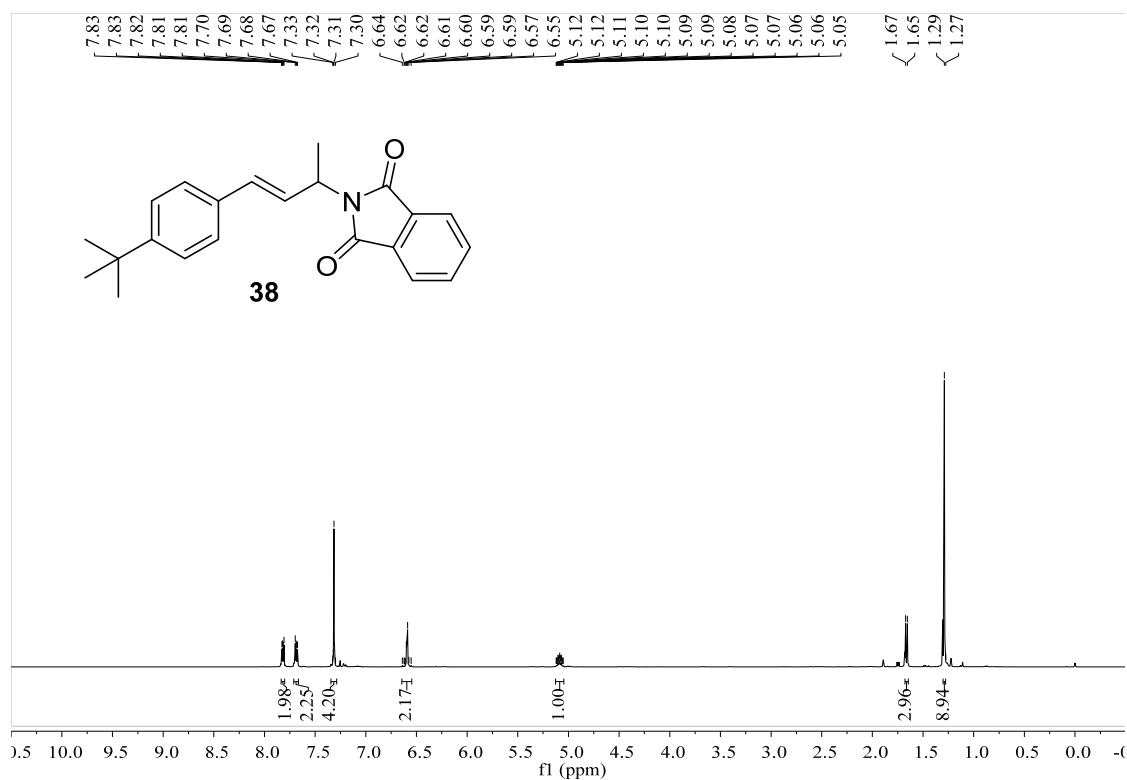


Figure S116. ¹H NMR spectrum of compound **38**, related to **Figure 2**.

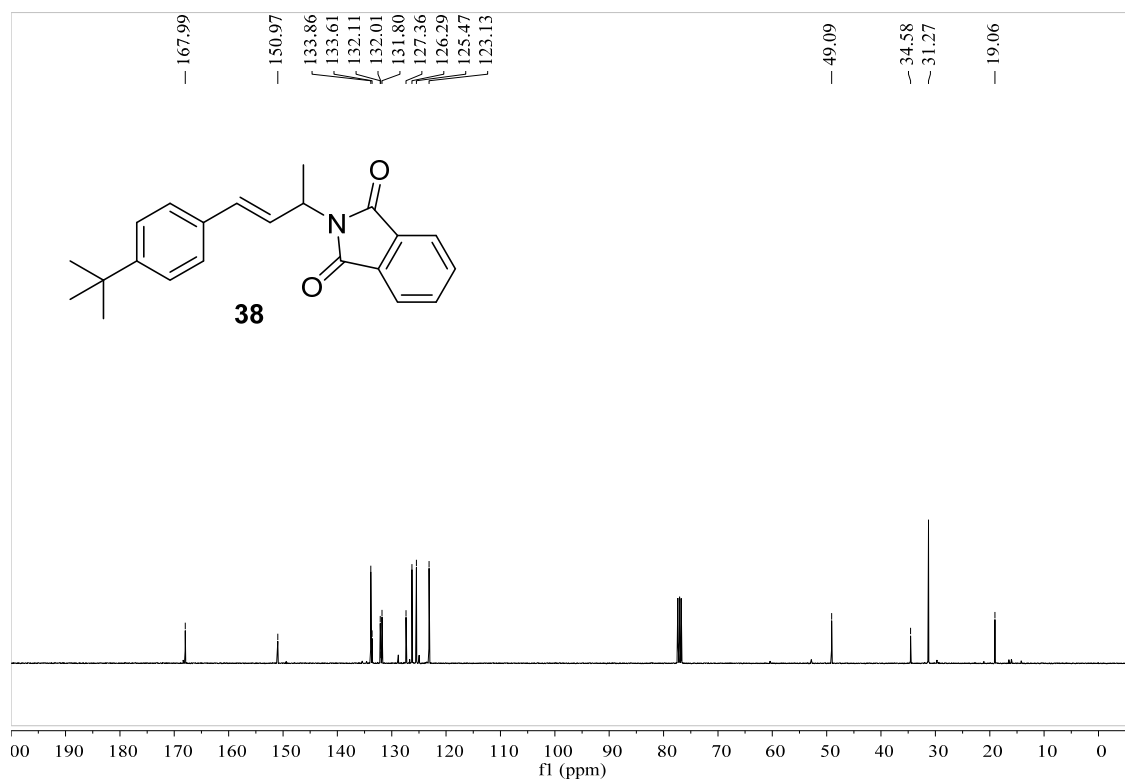


Figure S117. ¹³C NMR spectrum of compound **38**, related to **Figure 2**.

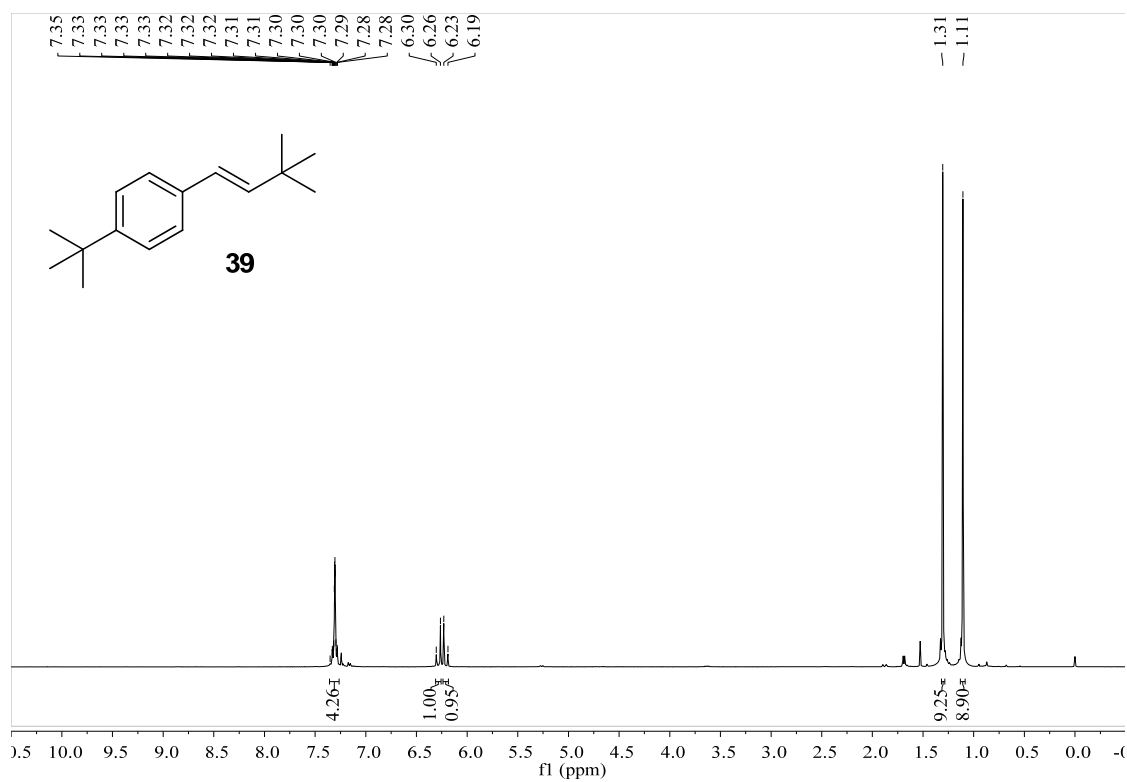


Figure S118. ¹H NMR spectrum of compound **39**, related to **Figure 2**.

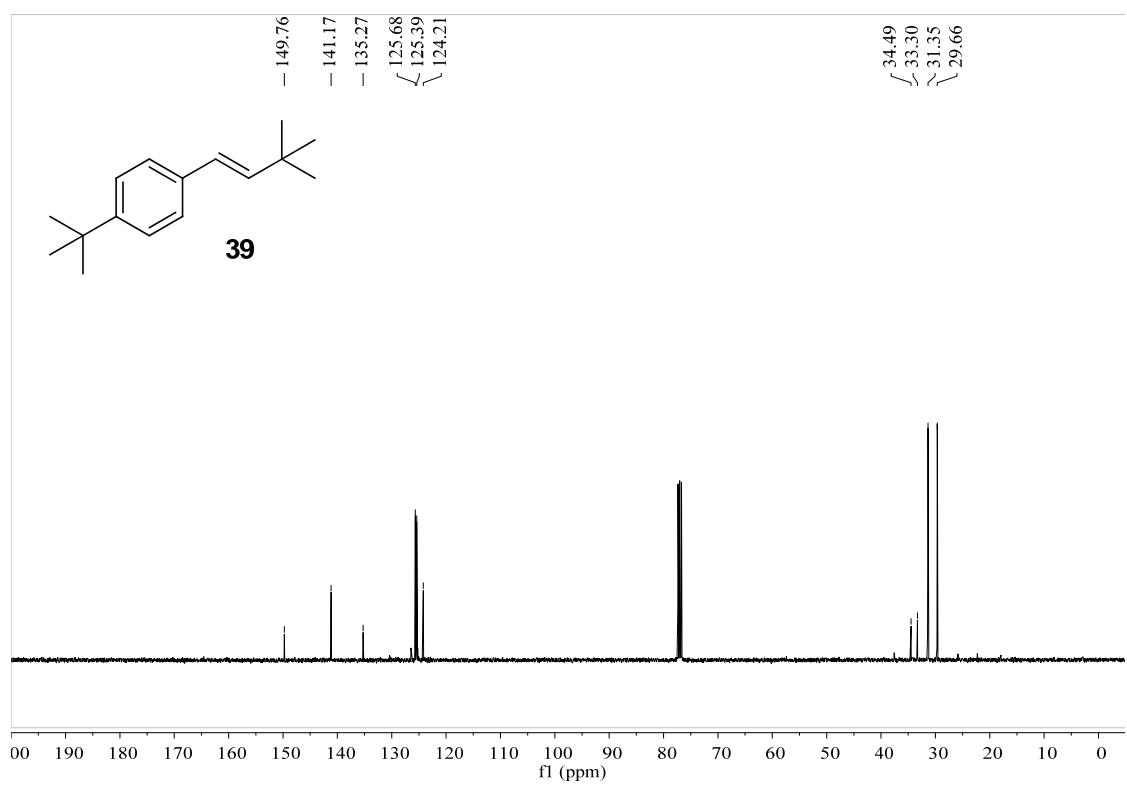


Figure S119. ¹³C NMR spectrum of compound **39**, related to **Figure 2**.

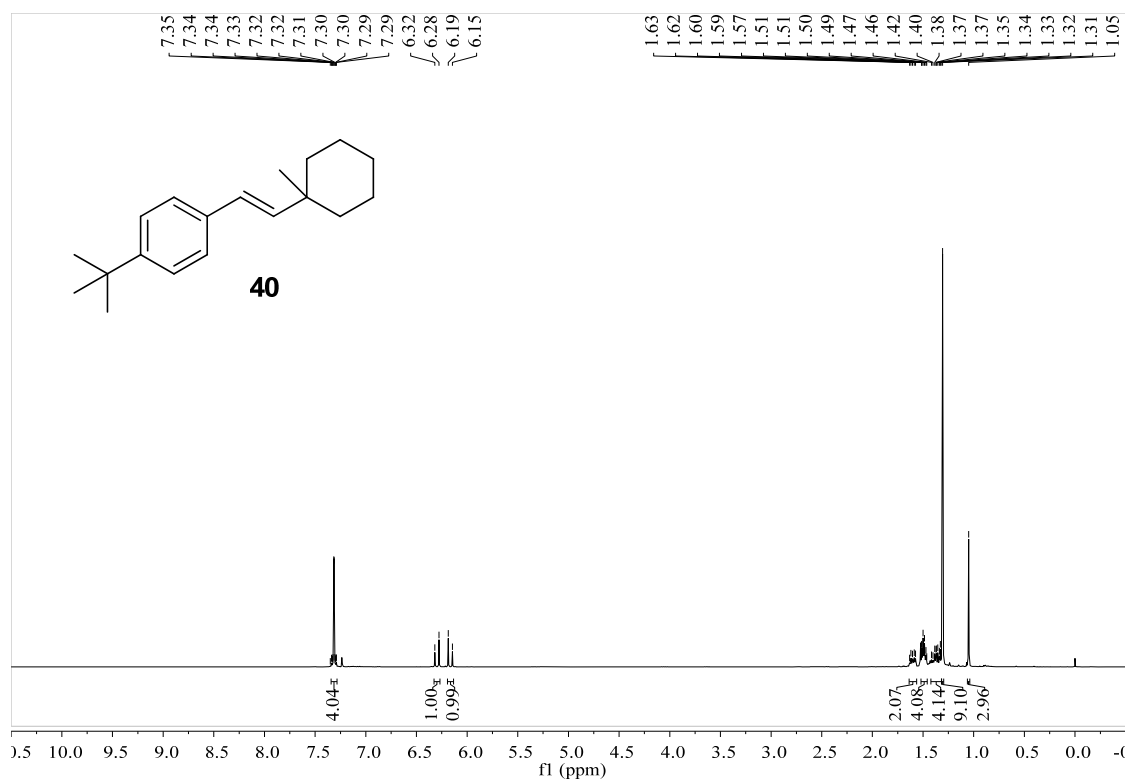


Figure S120. ¹H NMR spectrum of compound **40**, related to **Figure 2**.

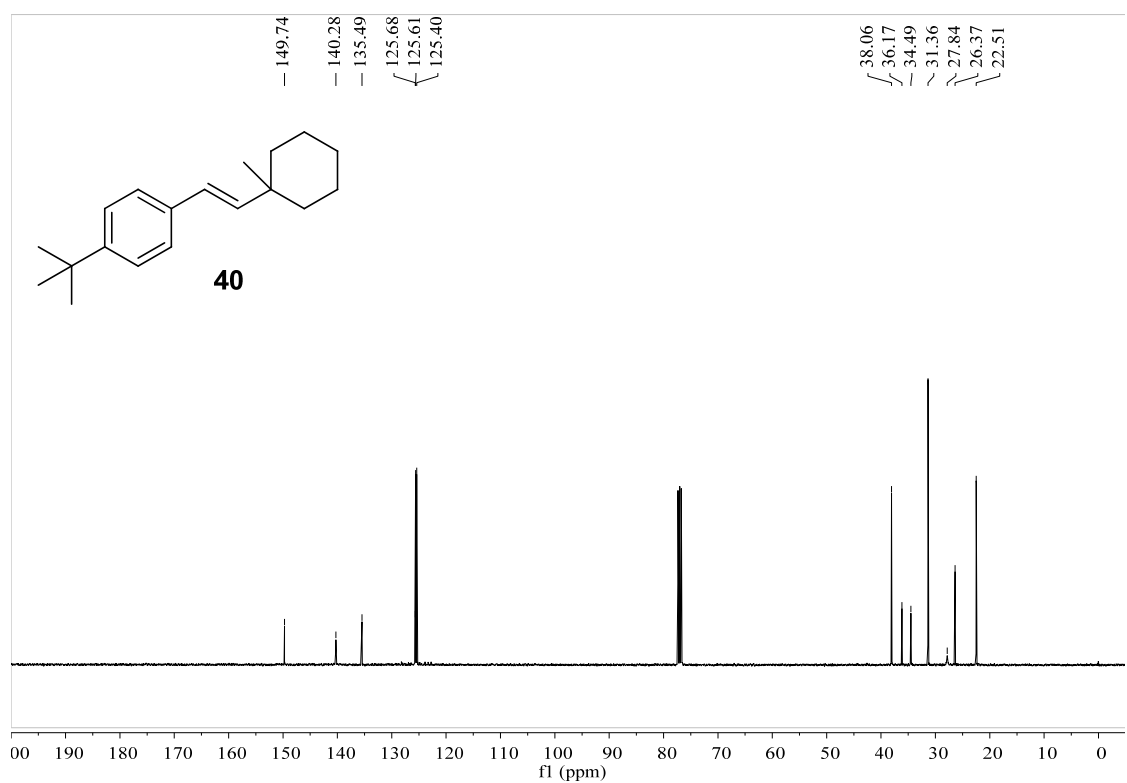


Figure S121. ¹³C NMR spectrum of compound **40**, related to **Figure 2**.

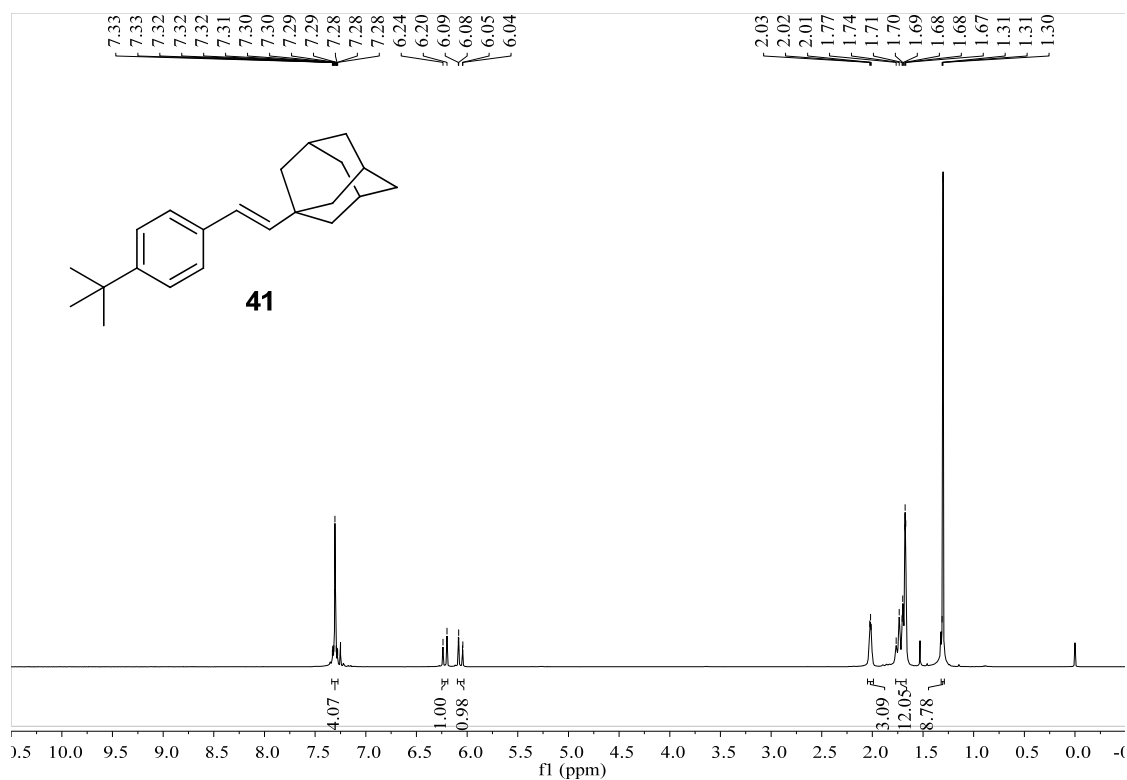


Figure S122. ^1H NMR spectrum of compound **41**, related to **Figure 2**.

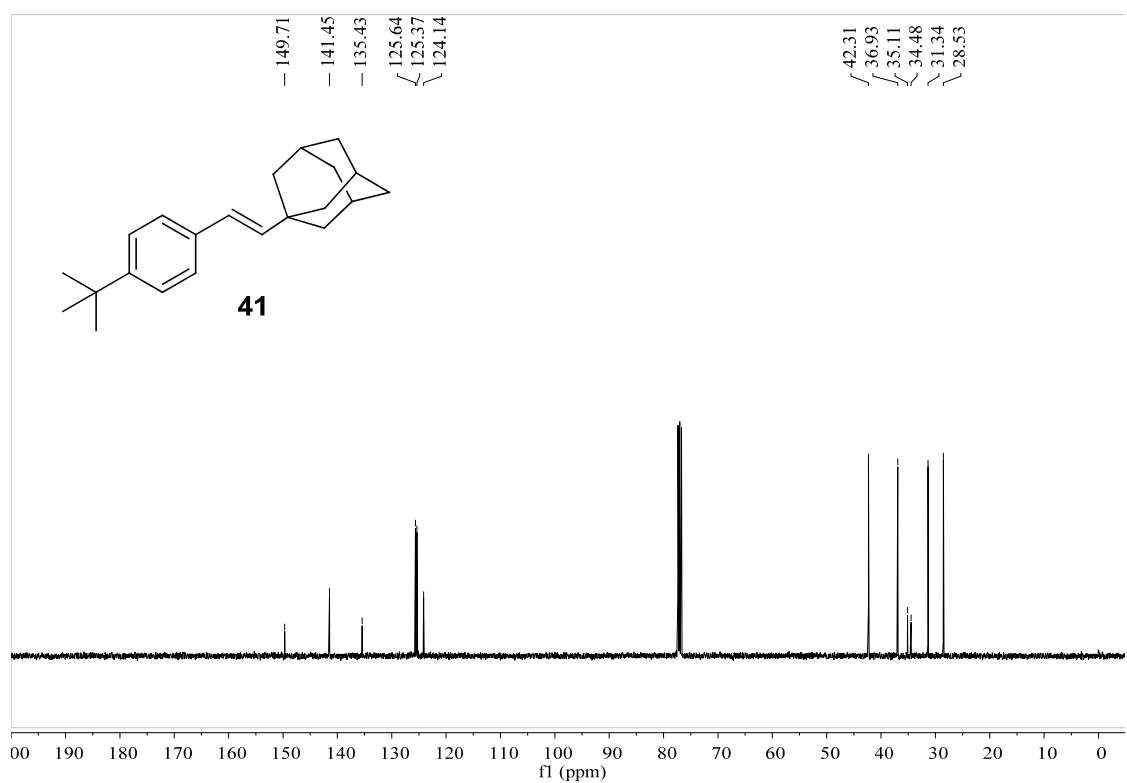


Figure S123. ^{13}C NMR spectrum of compound **41**, related to **Figure 2**.

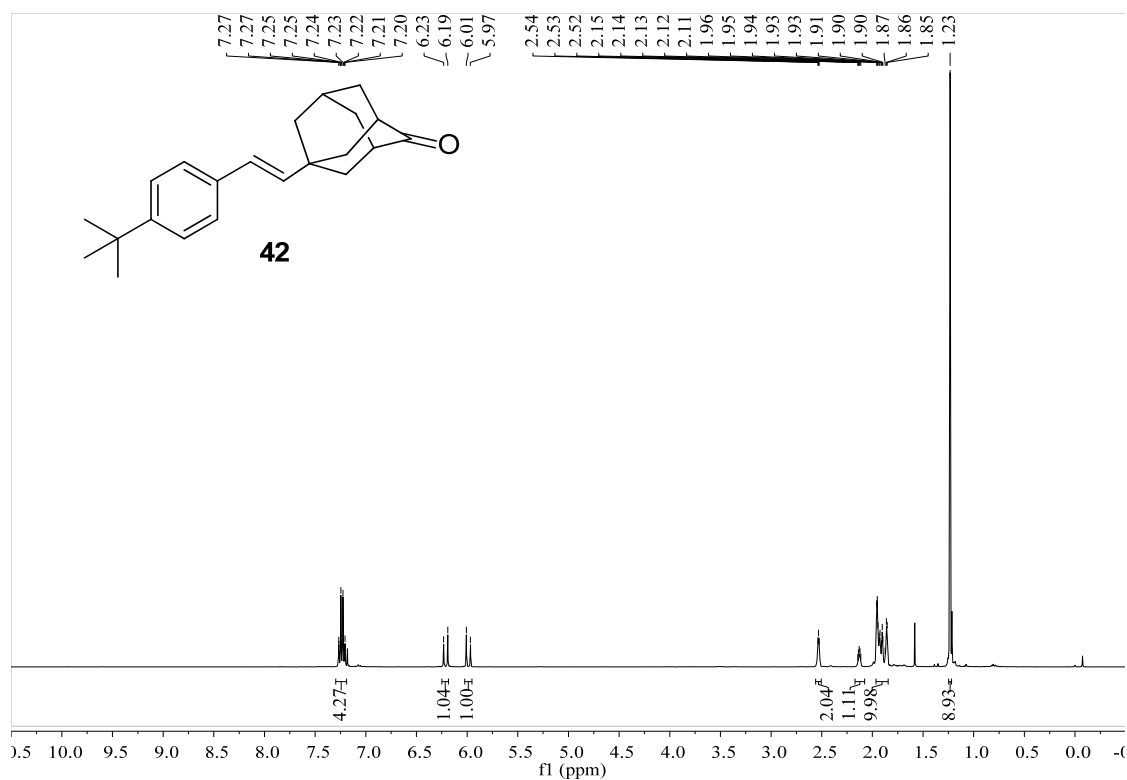


Figure S124. ^1H NMR spectrum of compound **42**, related to **Figure 2**.

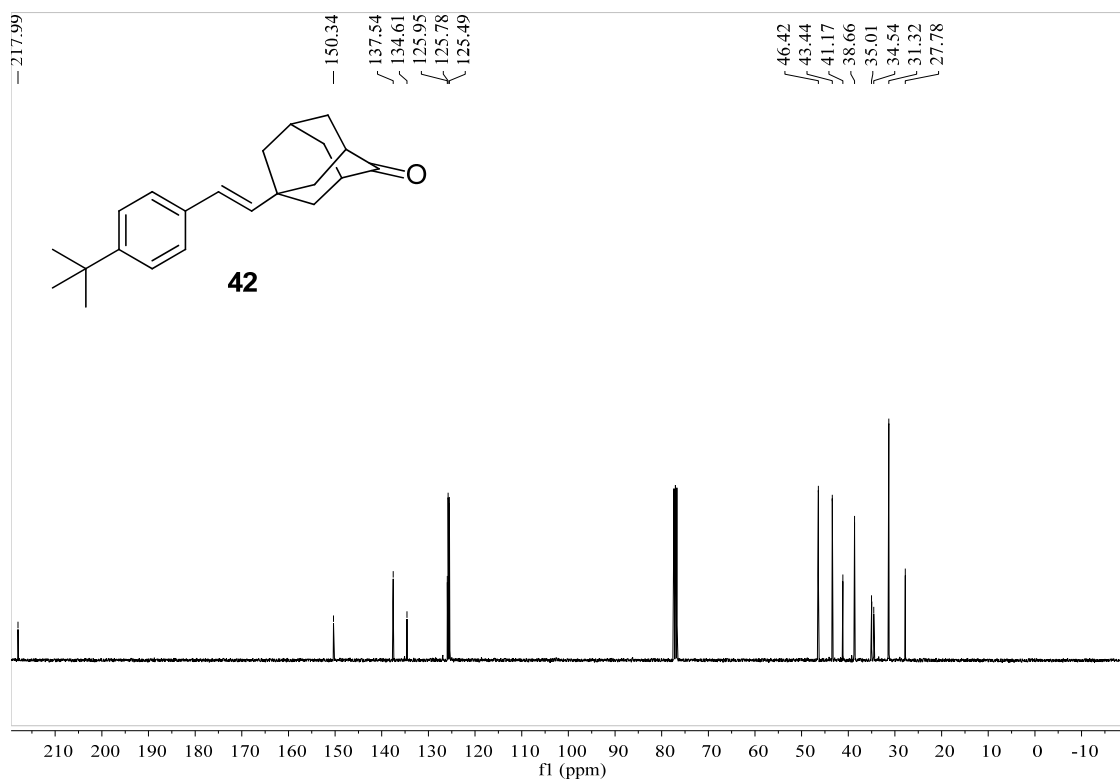


Figure S125. ^{13}C NMR spectrum of compound **42**, related to **Figure 2**.

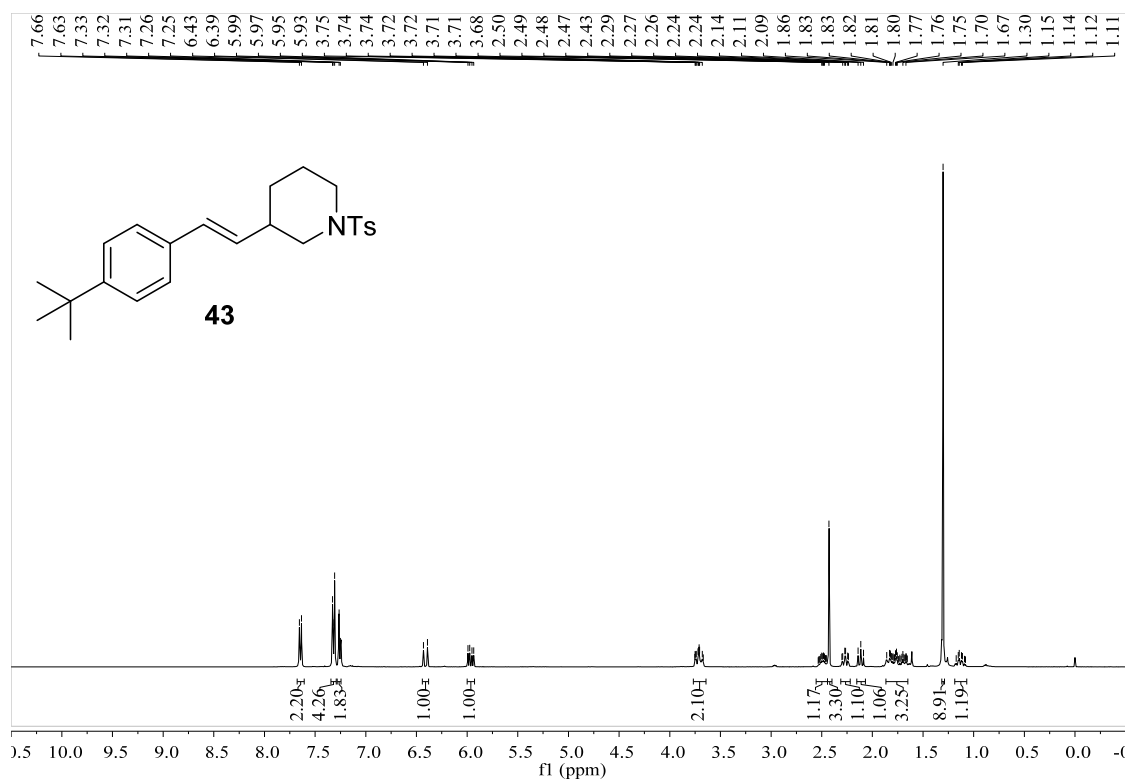


Figure S126. ¹H NMR spectrum of compound 43, related to **Figure 2**.

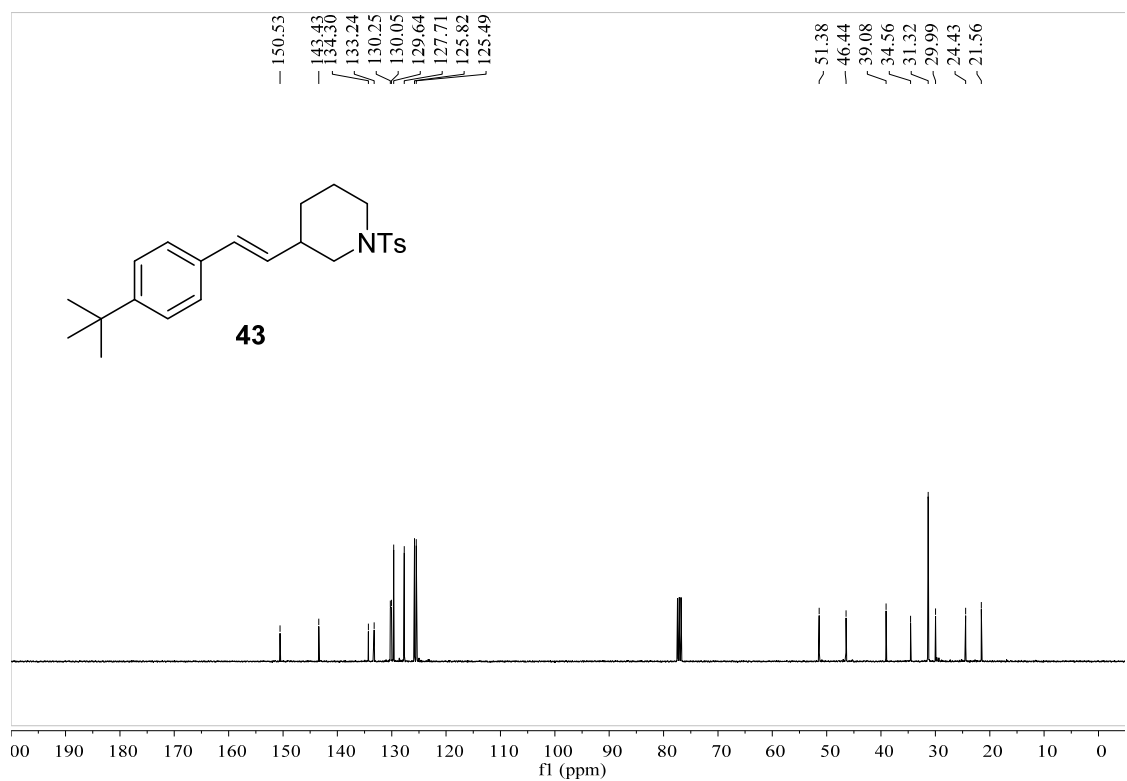


Figure S127. ¹³C NMR spectrum of compound 43, related to **Figure 2**.

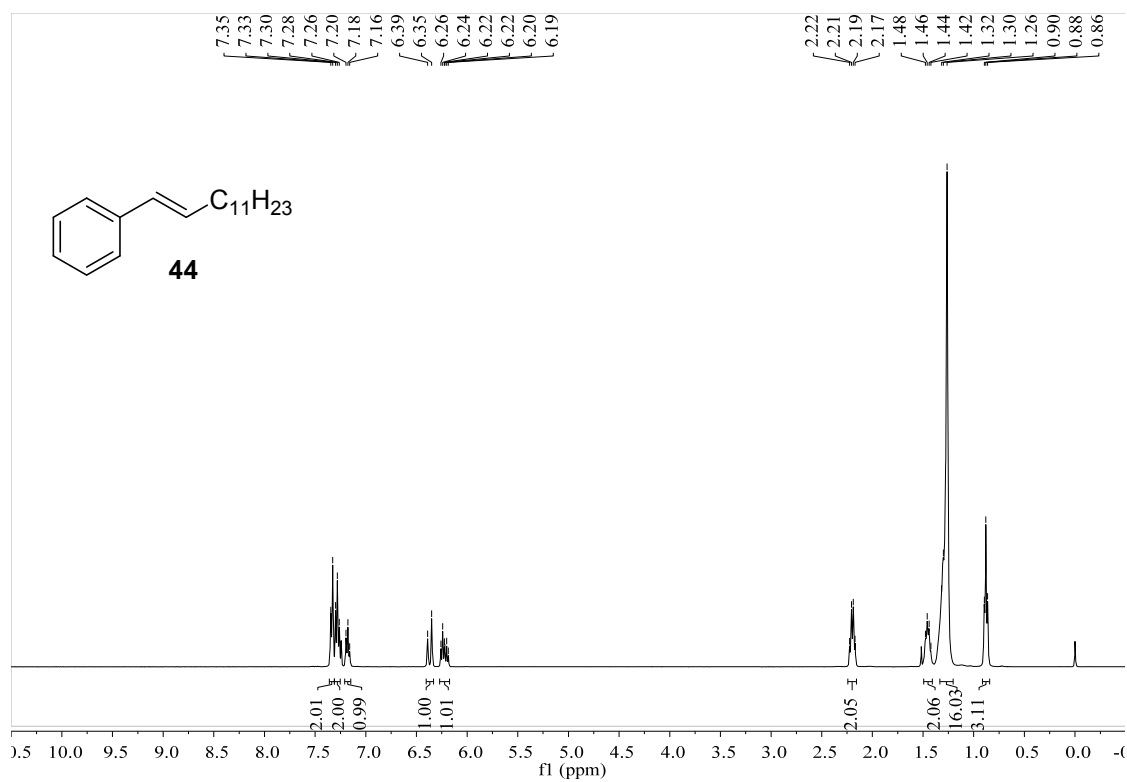


Figure S128. ¹H NMR spectrum of compound **44**, related to Figure 3.

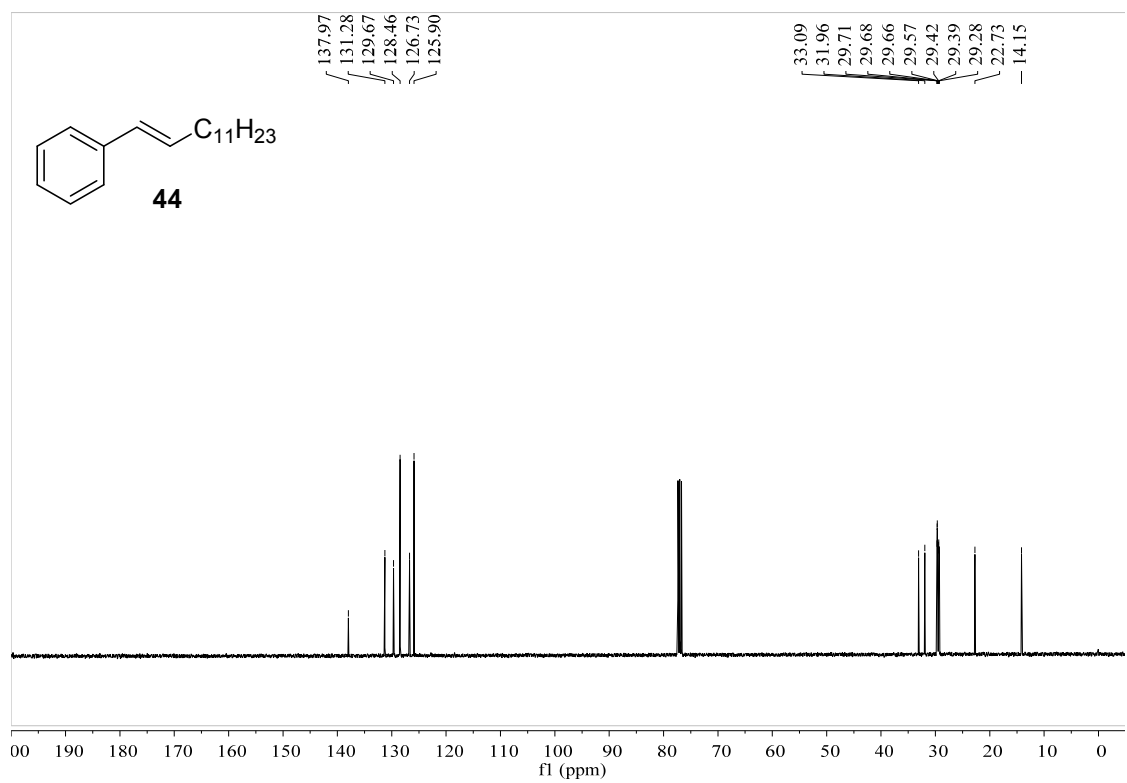


Figure S129. ¹³C NMR spectrum of compound **44**, related to Figure 3.

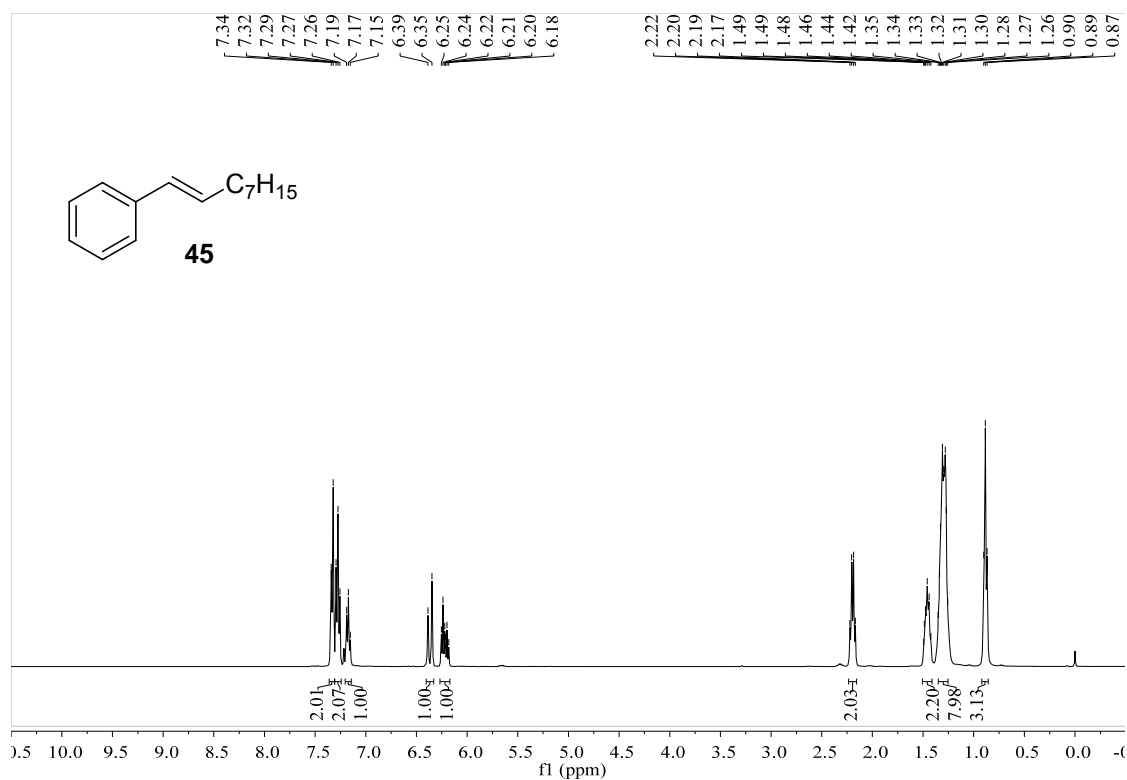


Figure S130. ¹H NMR spectrum of compound 45, related to Figure 3.

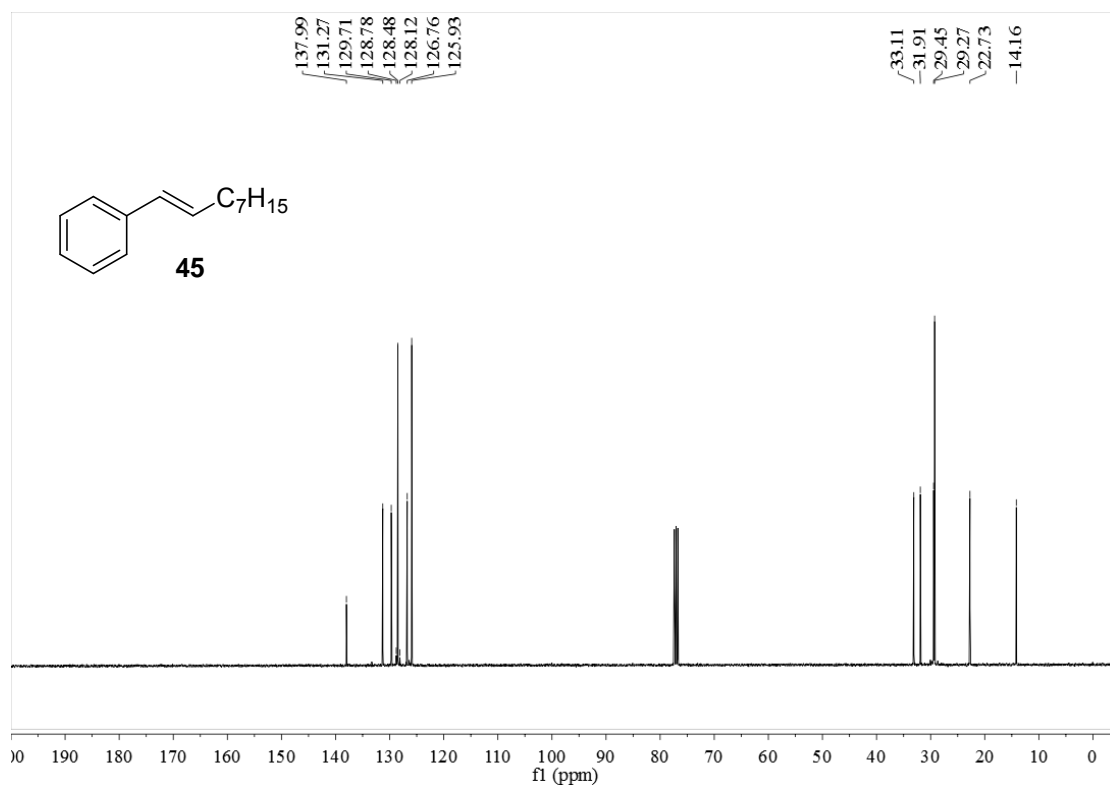


Figure S131. ¹³C NMR spectrum of compound 45, related to Figure 3.

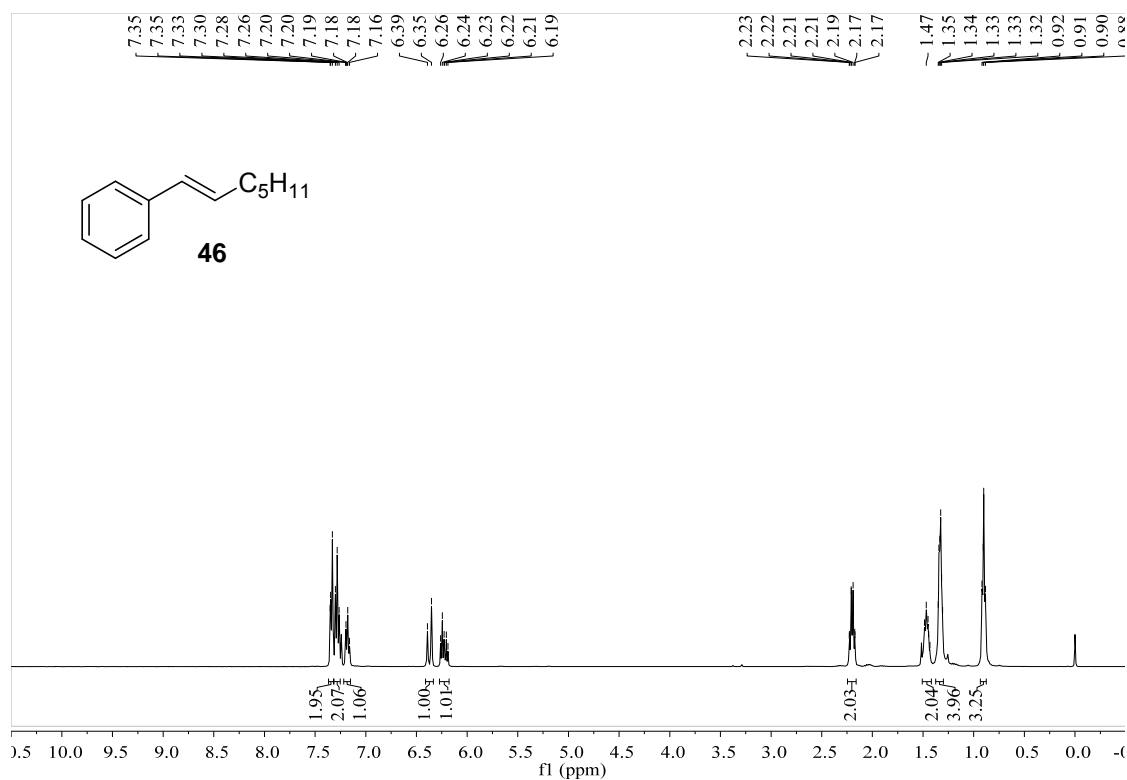


Figure S132. ¹H NMR spectrum of compound 46, related to Figure 3.

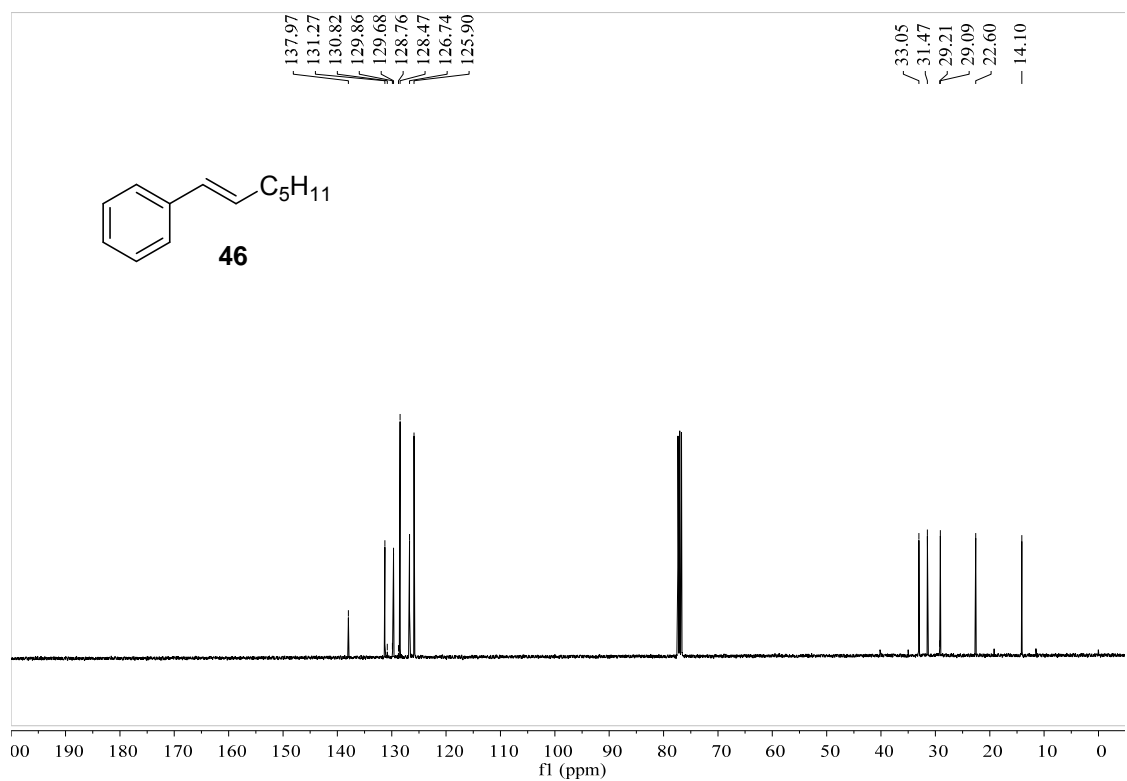


Figure S133. ¹³C NMR spectrum of compound 46, related to Figure 3.

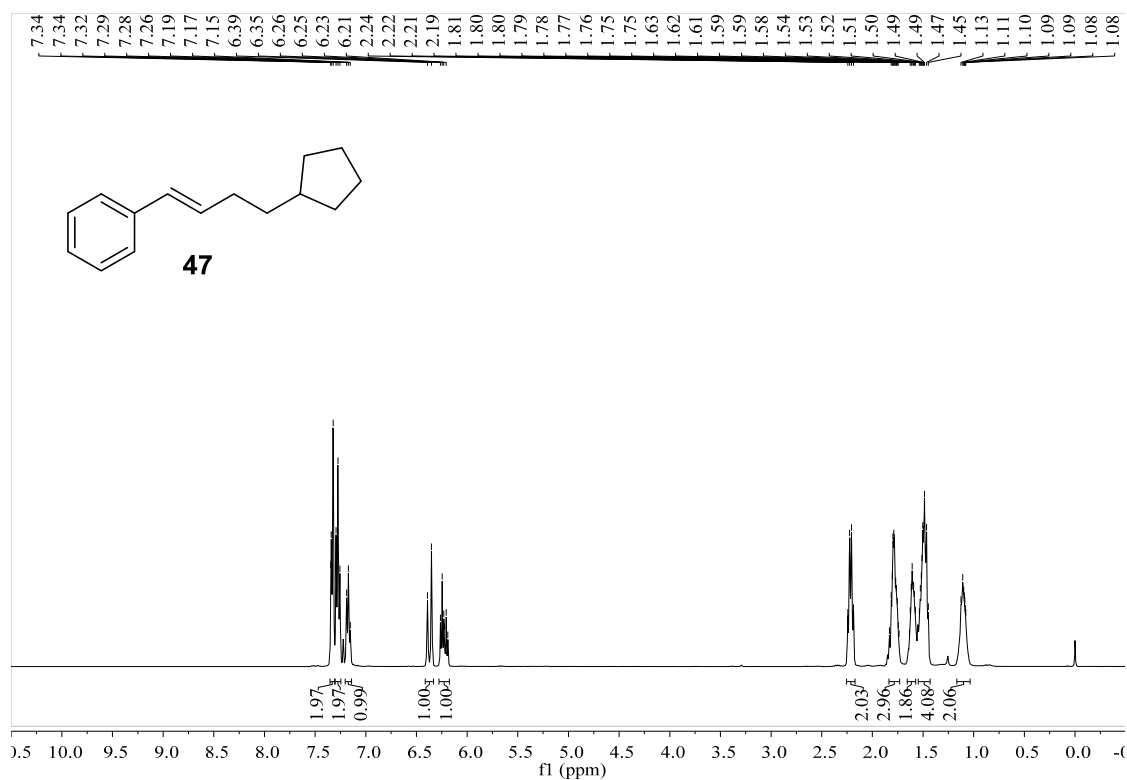


Figure S134. ¹H NMR spectrum of compound 47, related to Figure 3.

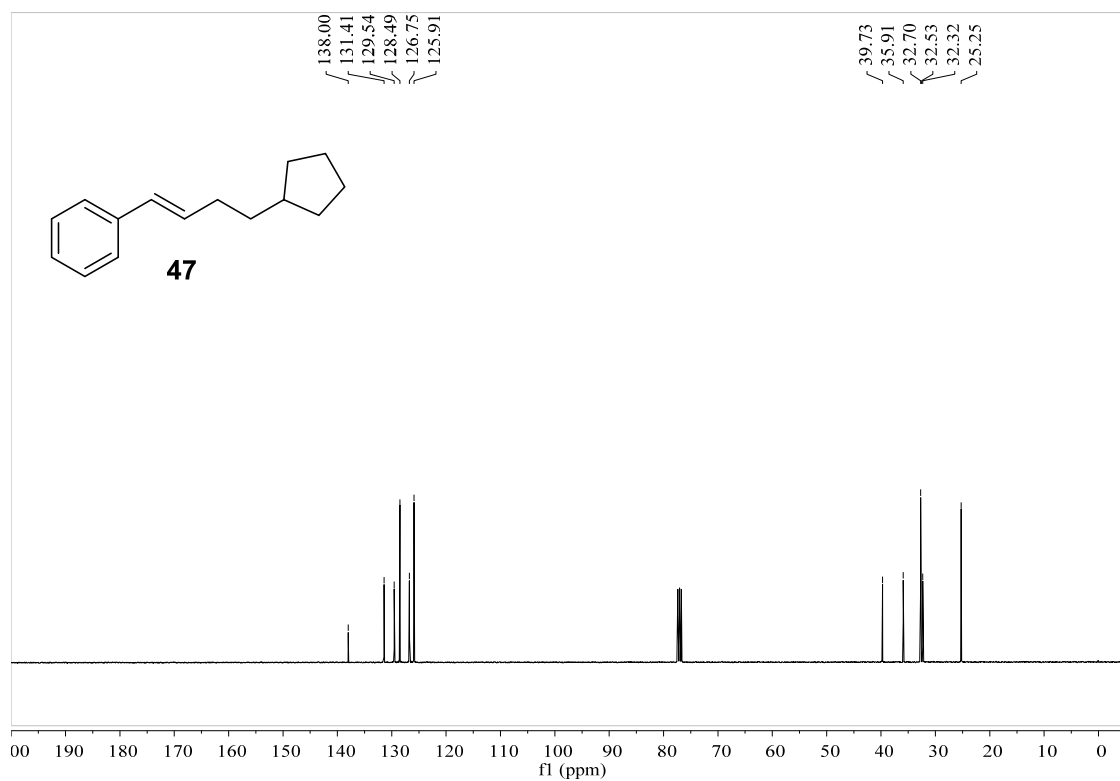


Figure S135. ¹³C NMR spectrum of compound 47, related to Figure 3.

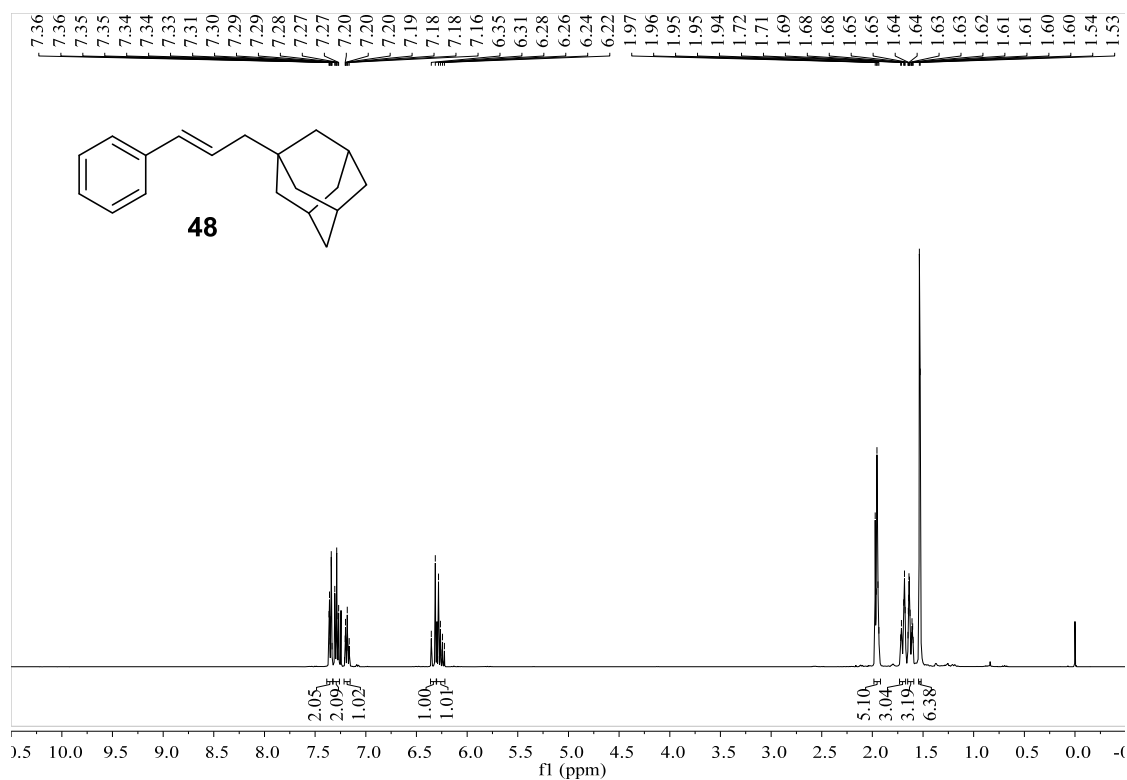


Figure S136. ¹H NMR spectrum of compound **48**, related to **Figure 3**.

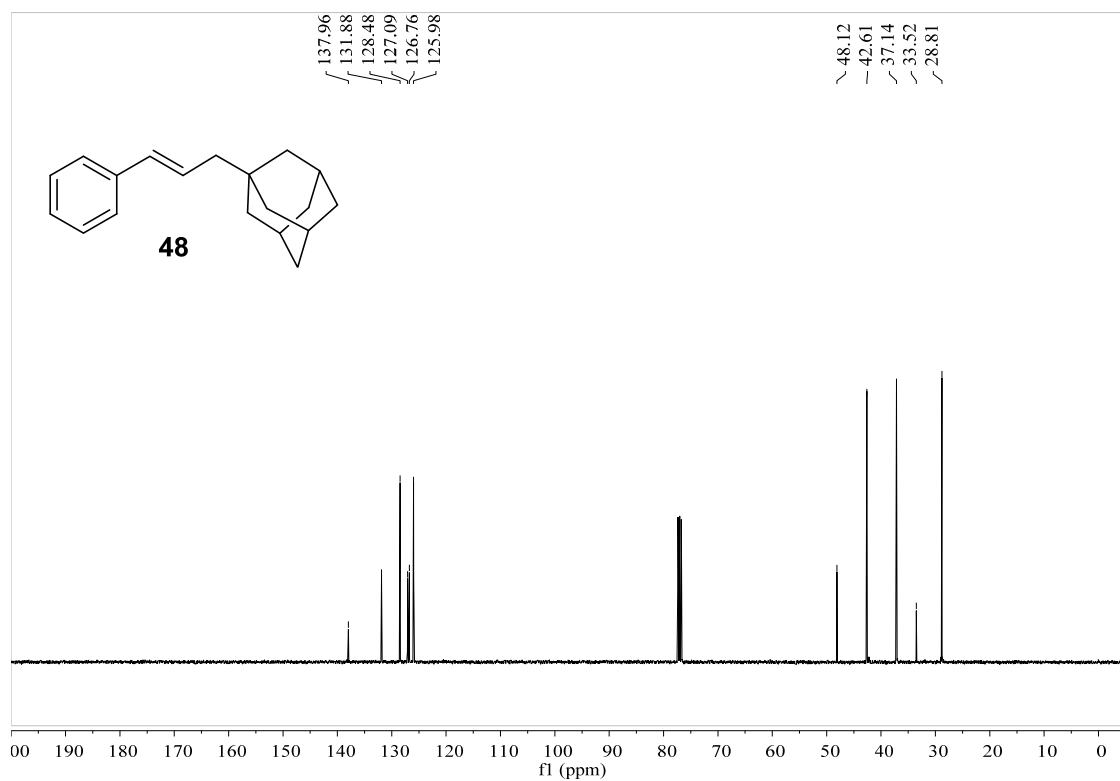


Figure S137. ¹³C NMR spectrum of compound **48**, related to **Figure 3**.

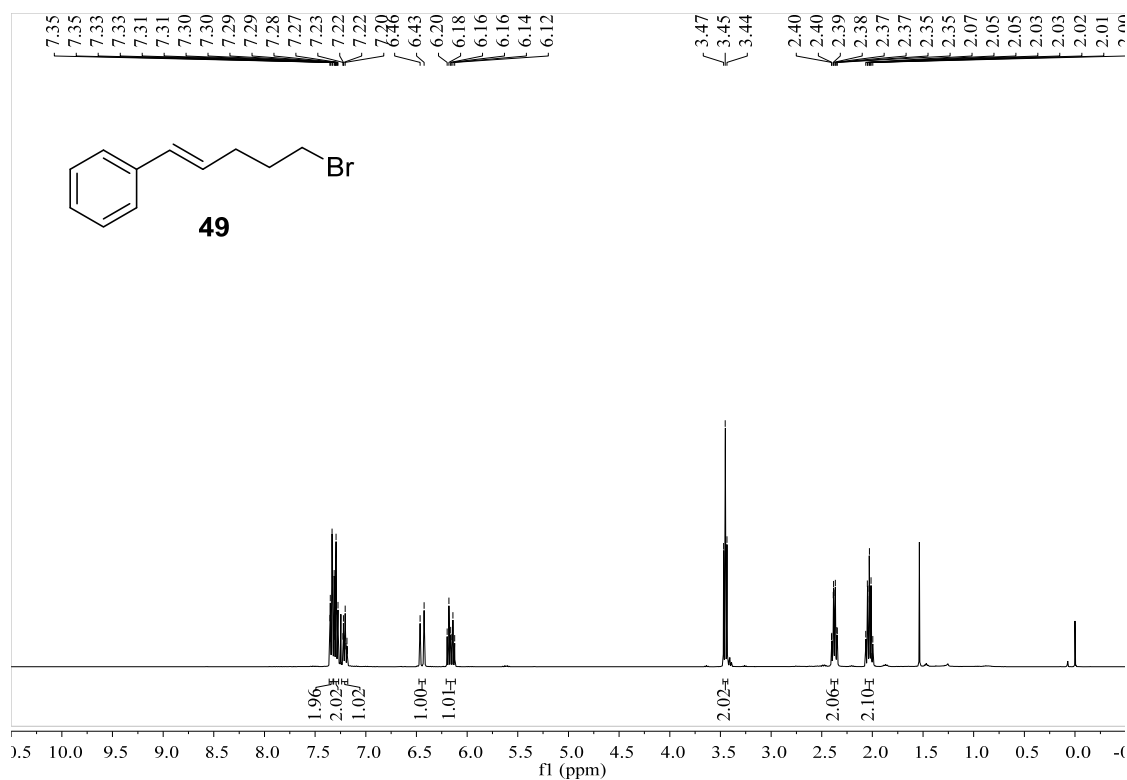


Figure S138. ¹H NMR spectrum of compound 49, related to Figure 3.

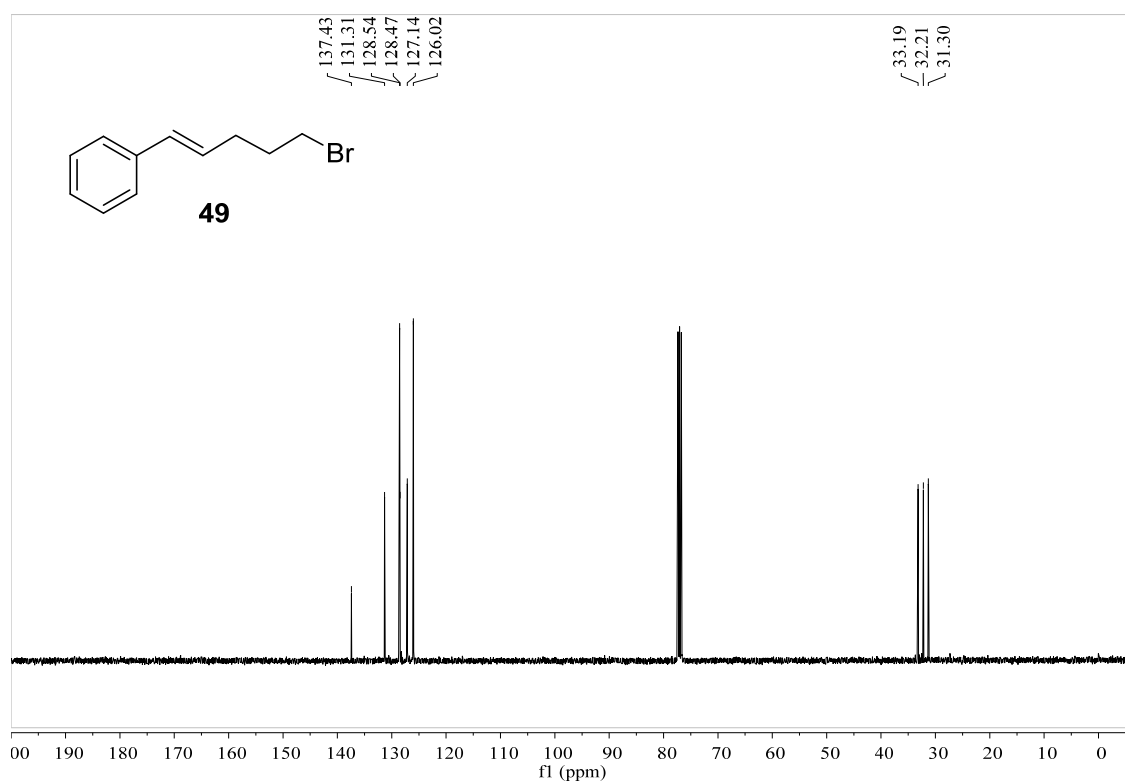


Figure S139. ¹³C NMR spectrum of compound 49, related to Figure 3.

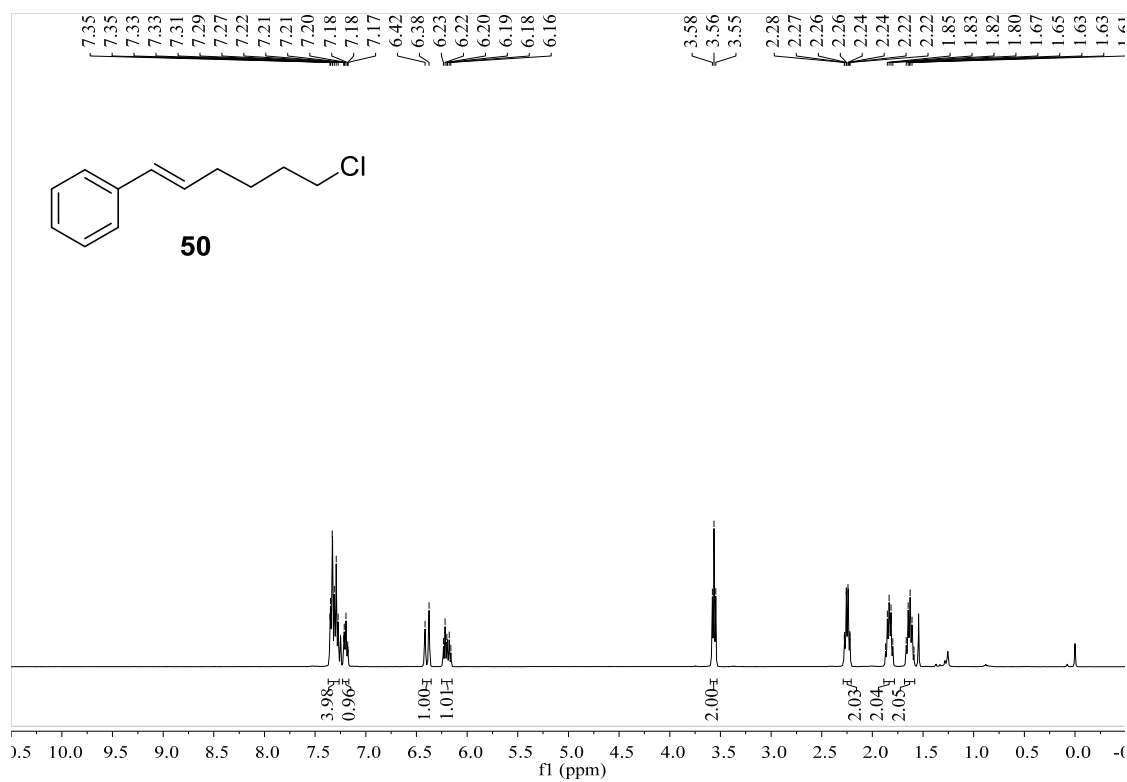


Figure S140. ¹H NMR spectrum of compound **50**, related to **Figure 3**.

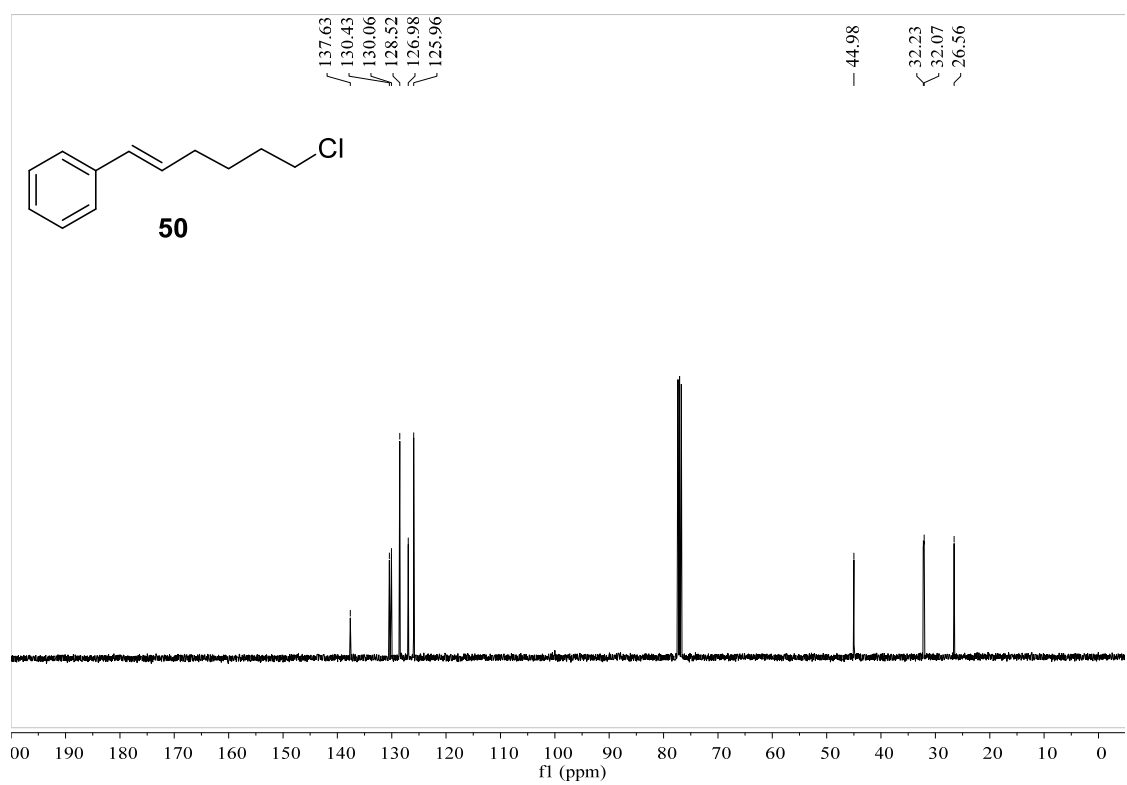


Figure S141. ¹³C NMR spectrum of compound **50**, related to **Figure 3**.

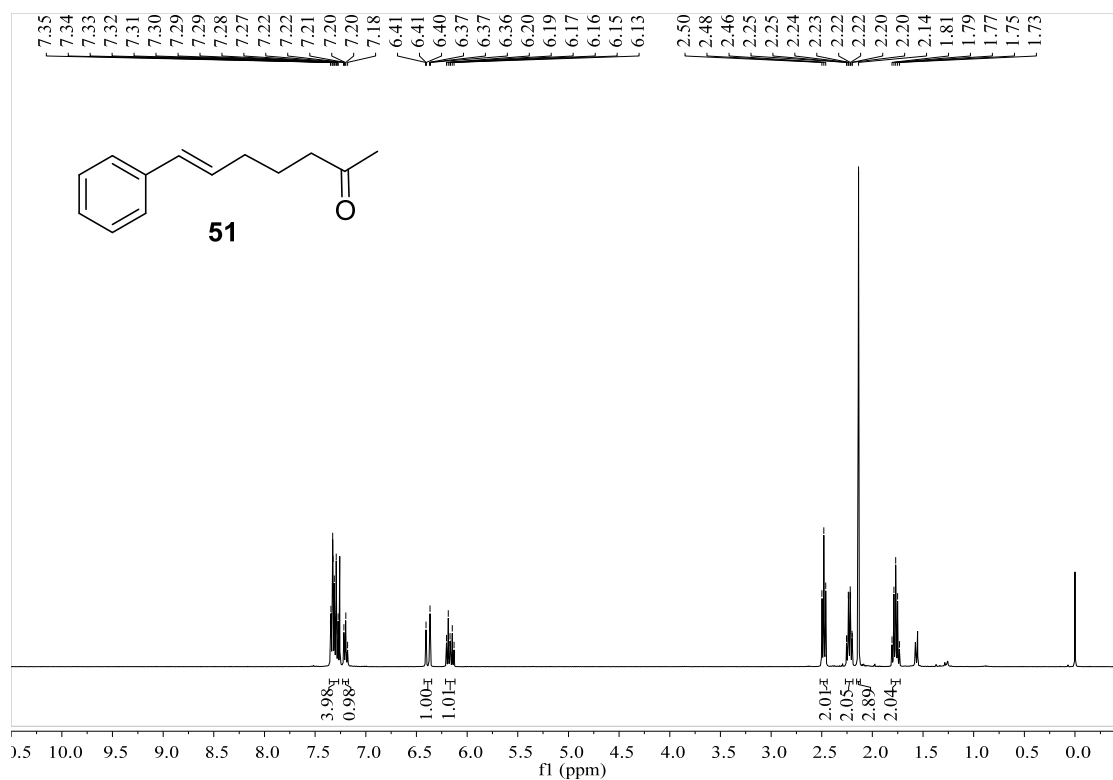


Figure S142. ¹H NMR spectrum of compound **51**, related to Figure 3.

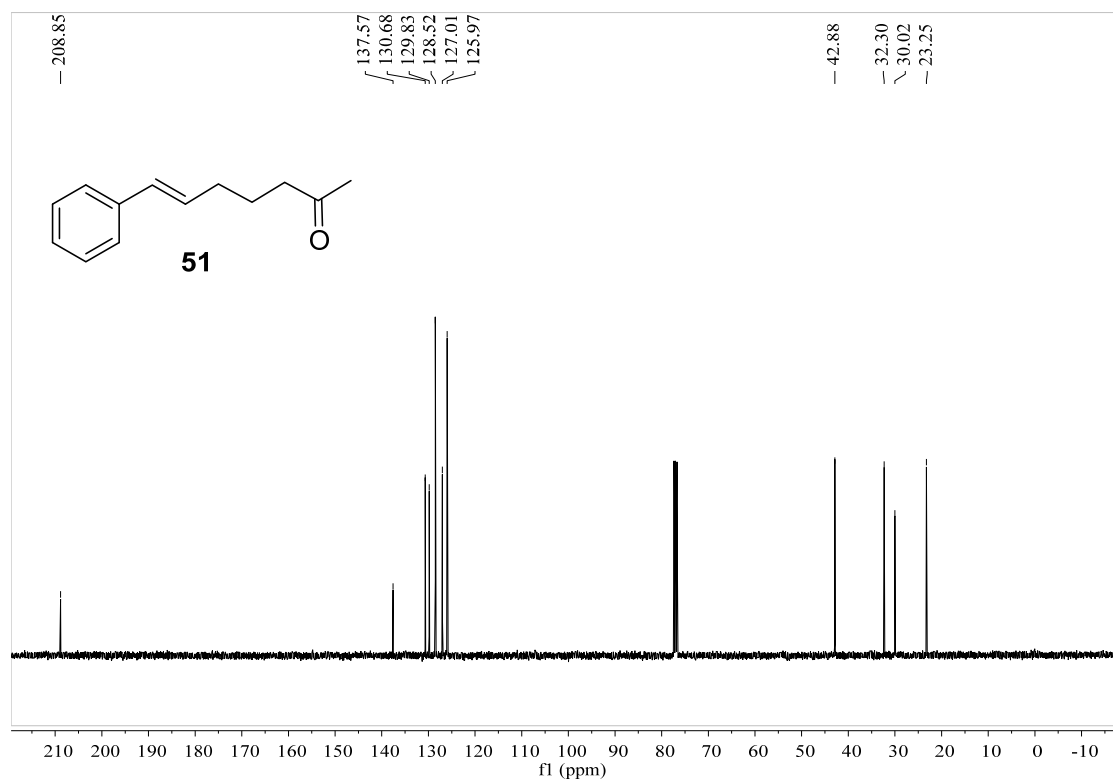


Figure S143. ¹³C NMR spectrum of compound **51**, related to Figure 3.

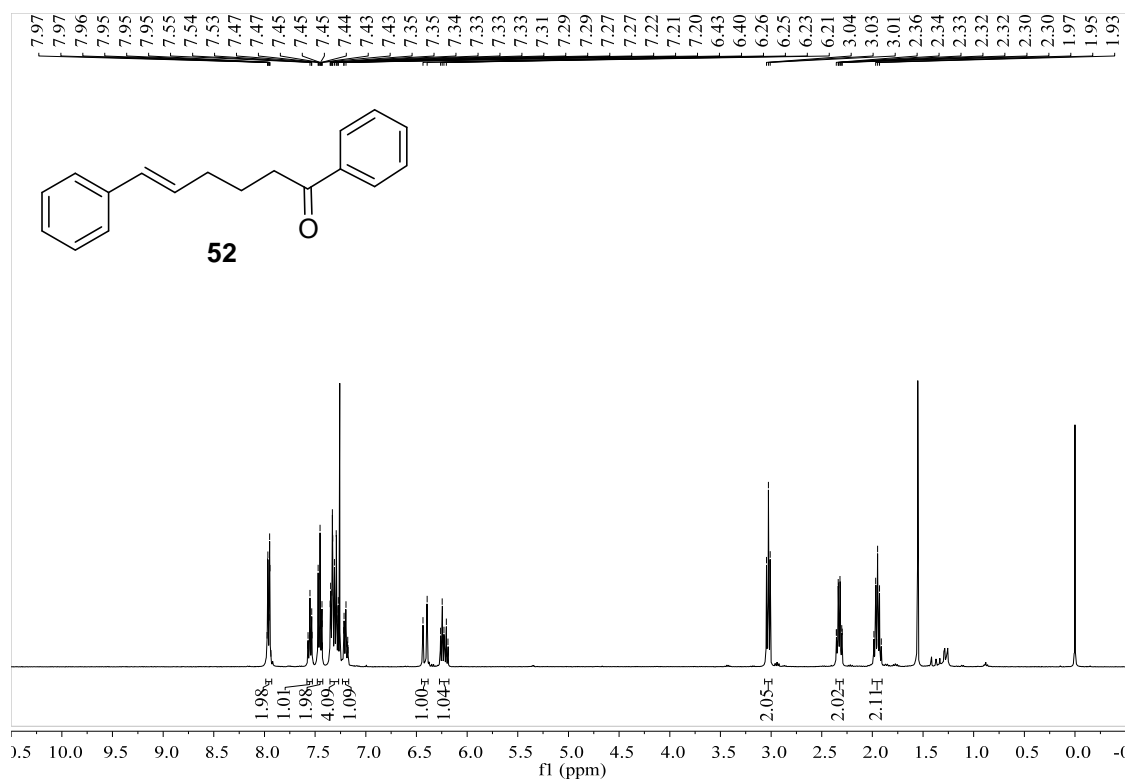


Figure S144. ¹H NMR spectrum of compound **52**, related to Figure 3.

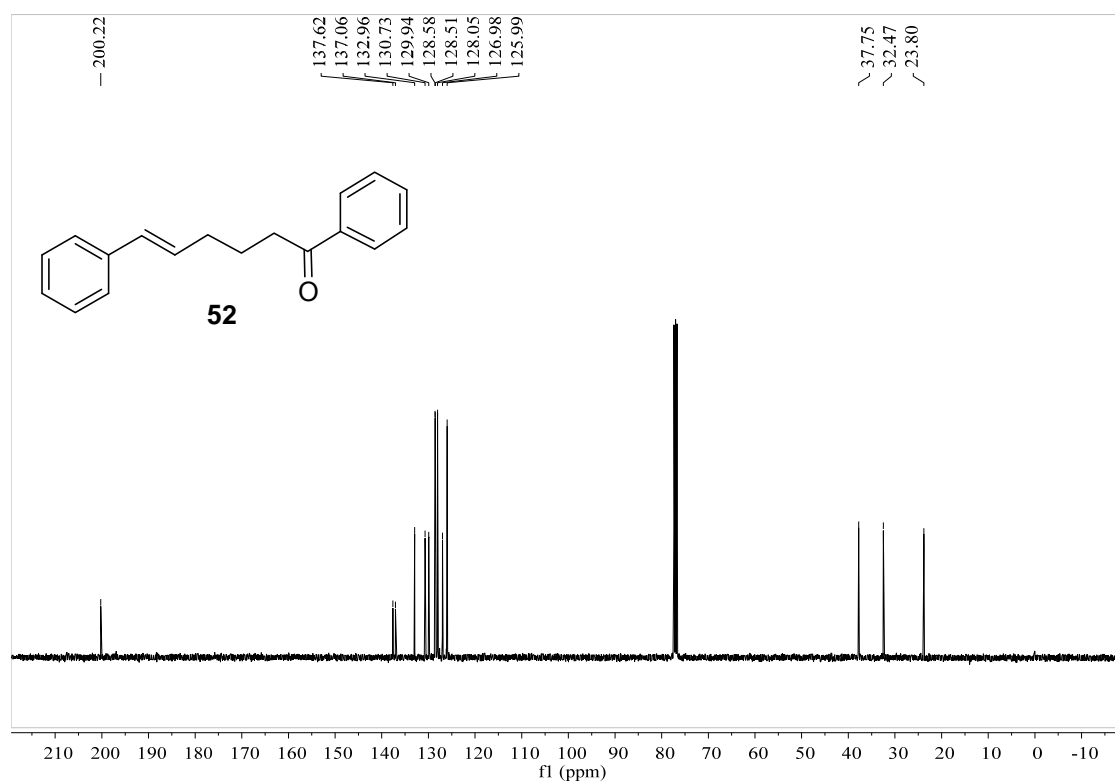


Figure S145. ¹³C NMR spectrum of compound **52**, related to Figure 3.

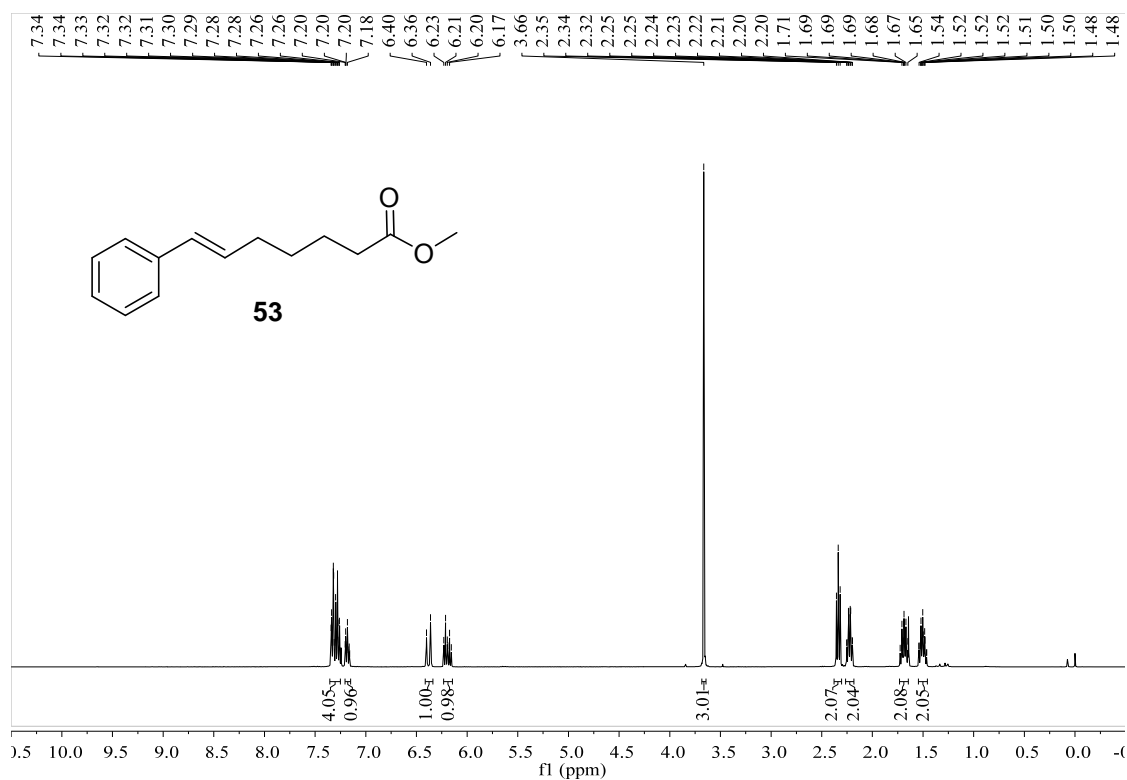


Figure S146. ¹H NMR spectrum of compound 53, related to Figure 3.

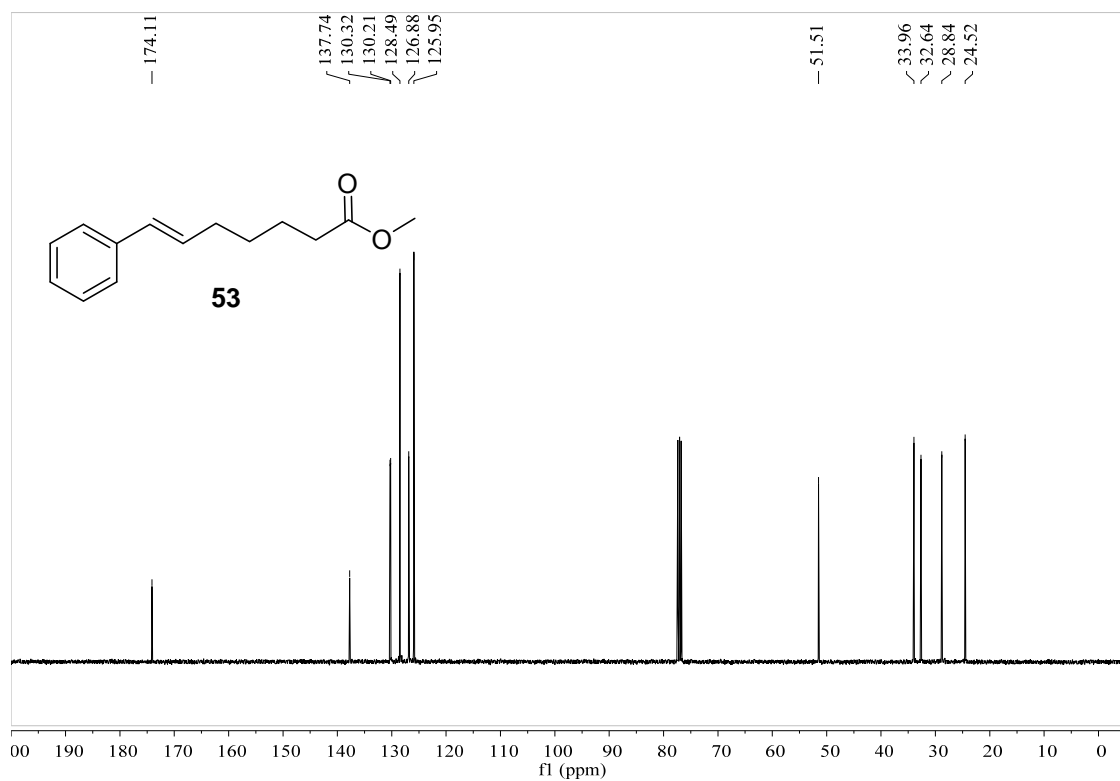
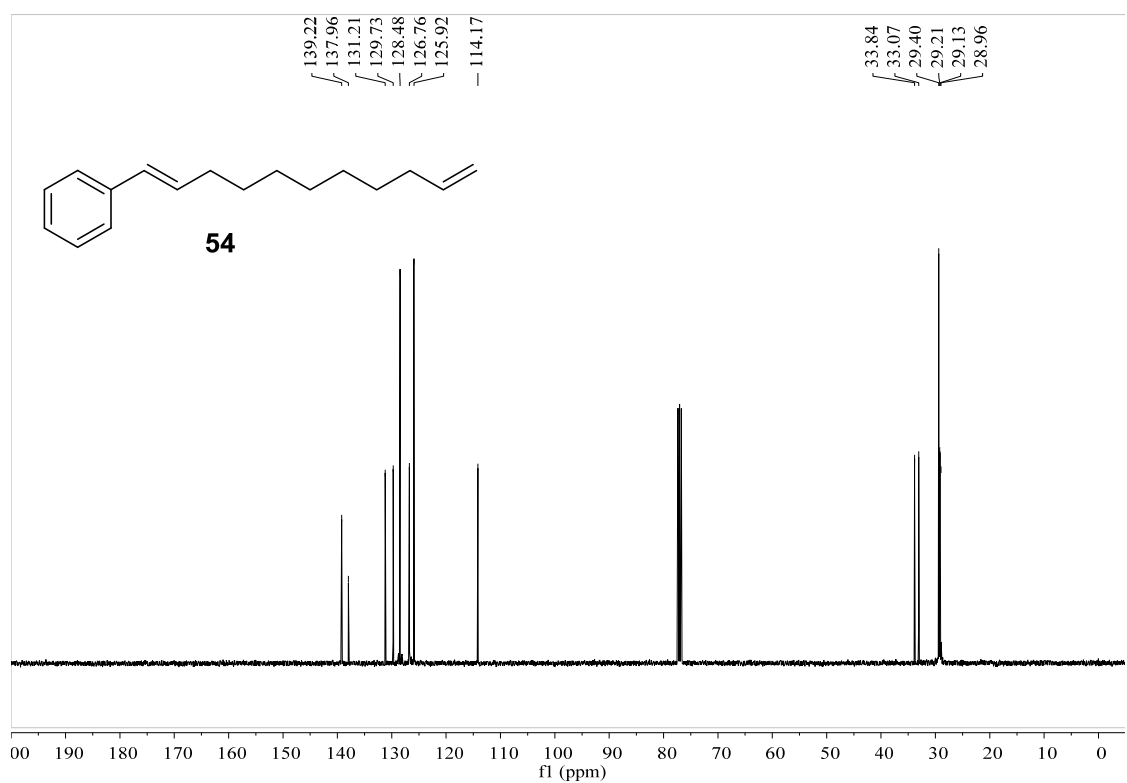
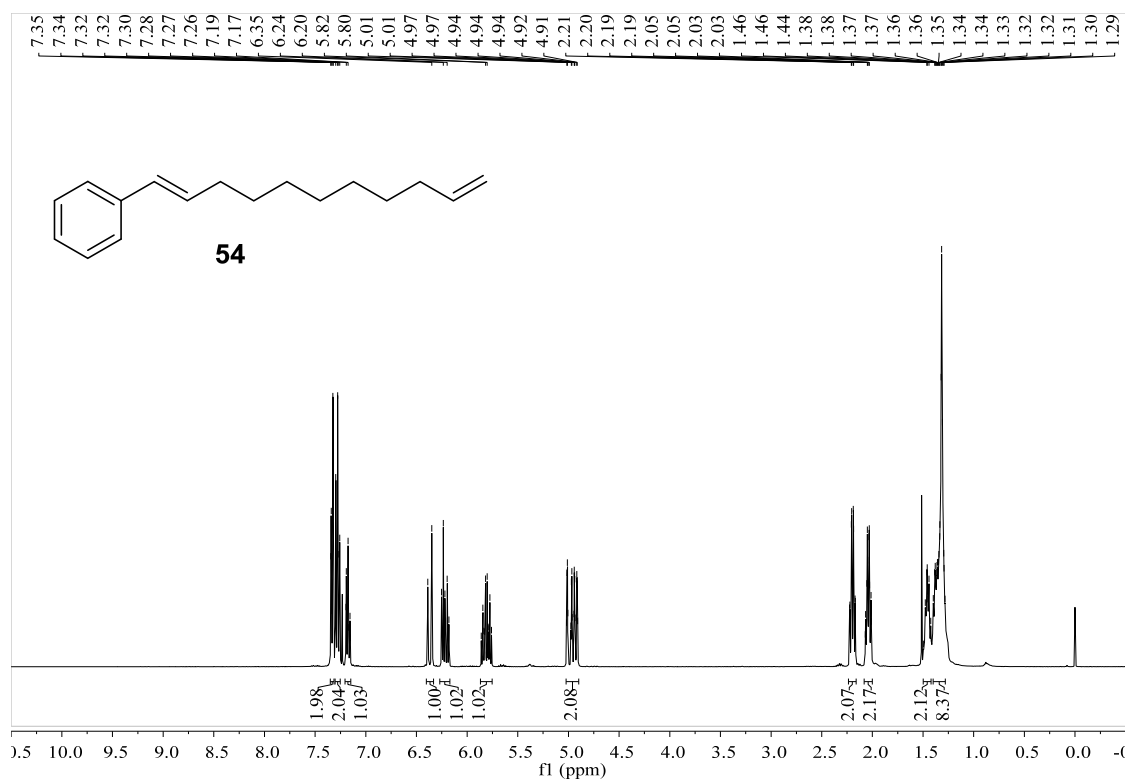


Figure S147. ¹³C NMR spectrum of compound 53, related to Figure 3.



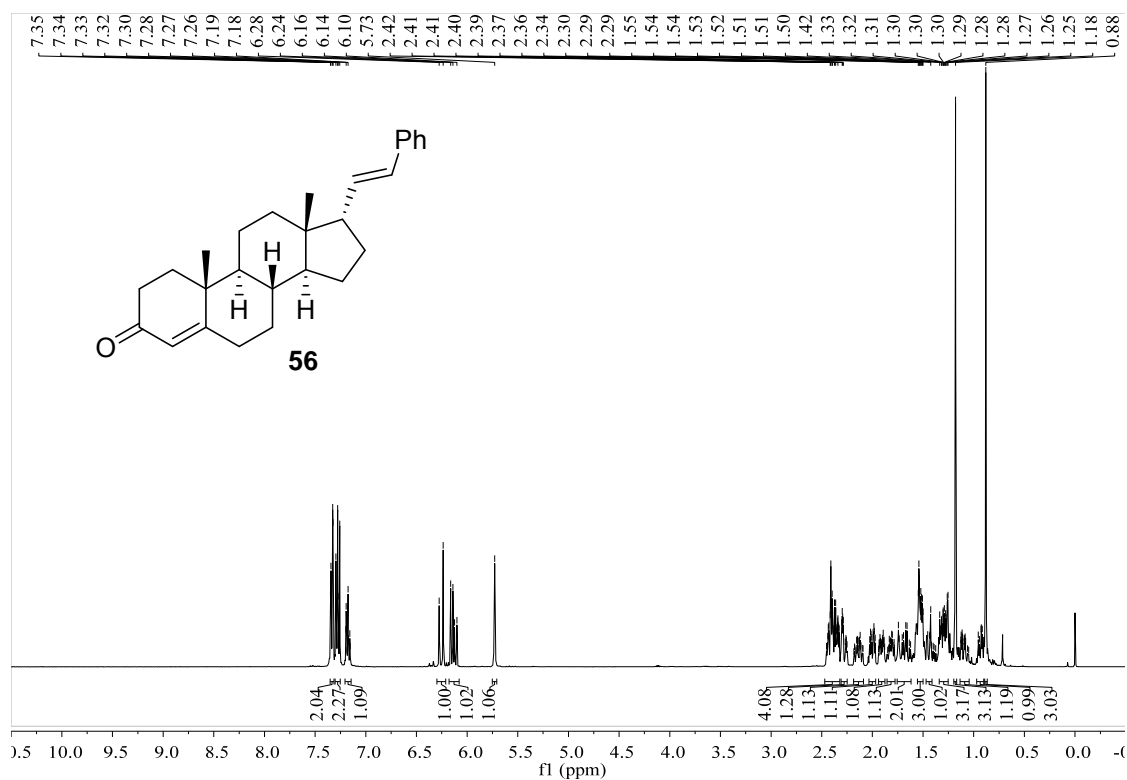


Figure S150. ^1H NMR spectrum of compound **56**, related to **Scheme 2**.

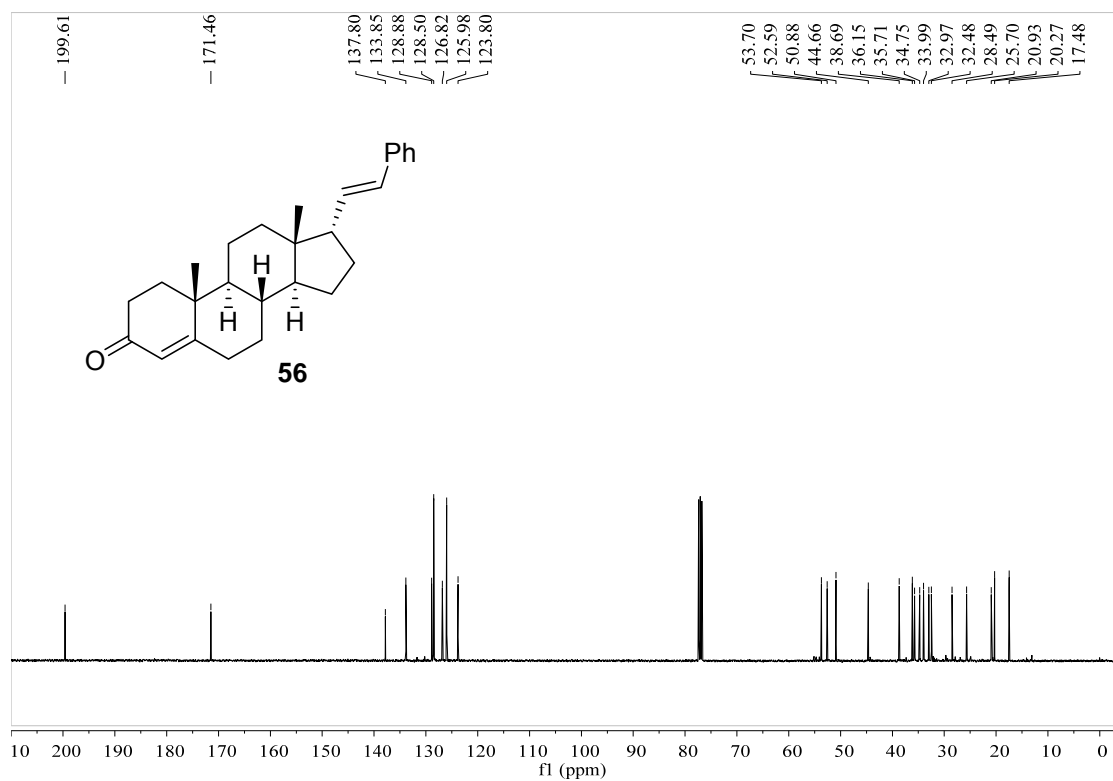


Figure S151. ^{13}C NMR spectrum of compound **56**, related to **Scheme 2**.

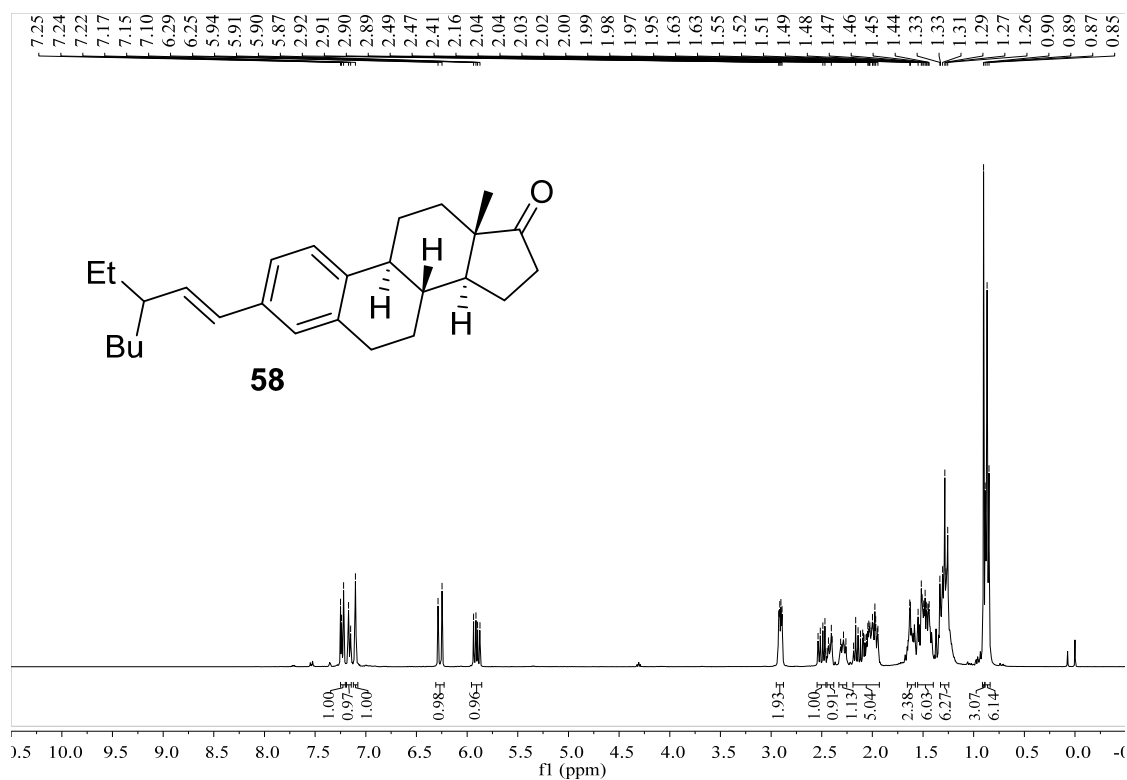


Figure S152. ^1H NMR spectrum of compound **58**, related to **Scheme 2**.

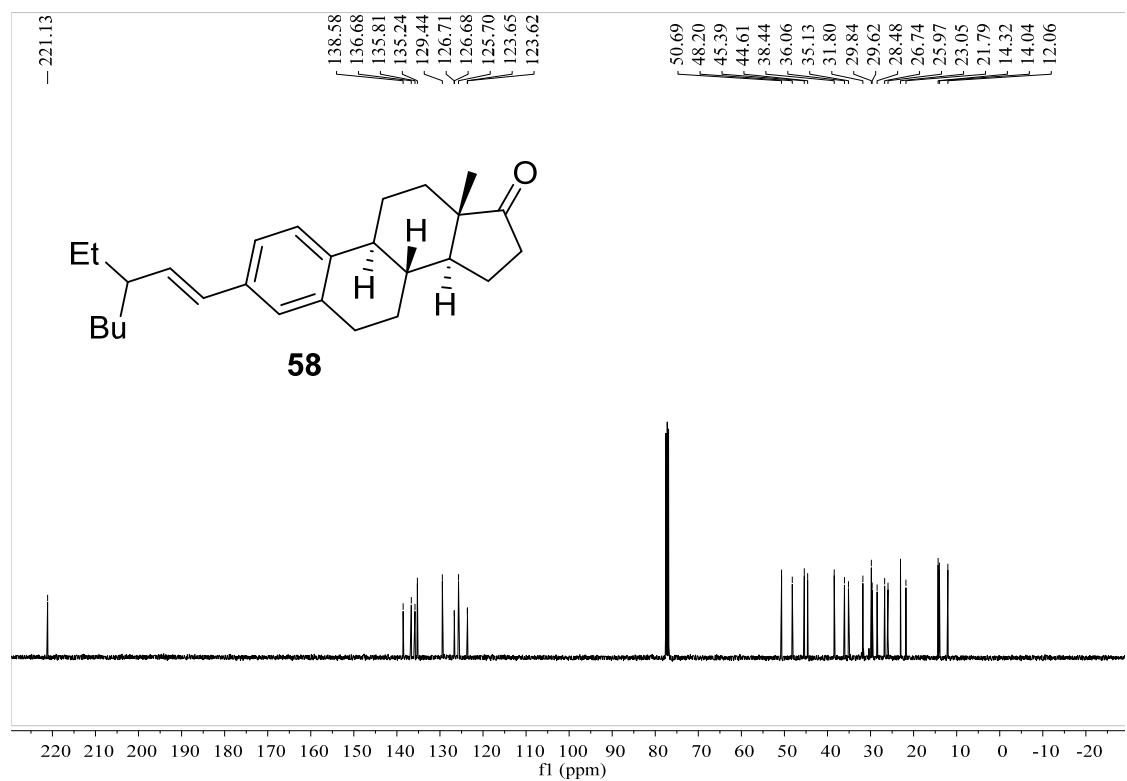


Figure S153. ^{13}C NMR spectrum of compound **58**, related to **Scheme 2**.

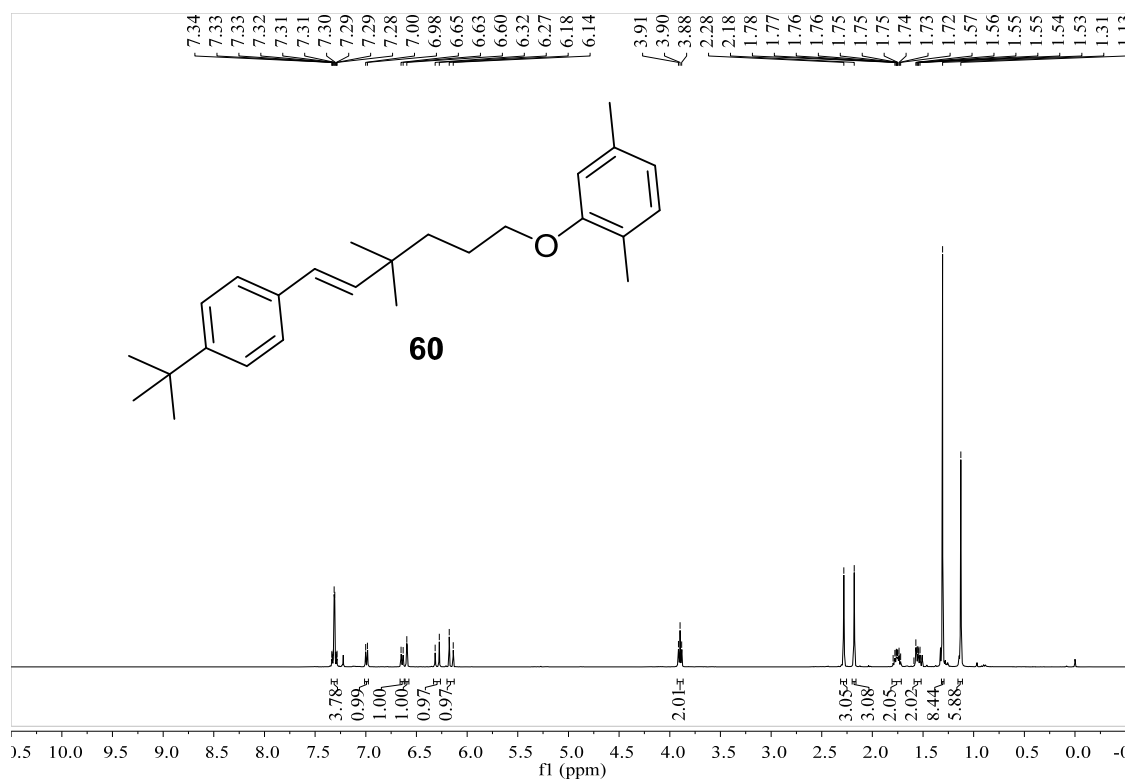


Figure S154. ^1H NMR spectrum of compound **60**, related to Scheme 2.

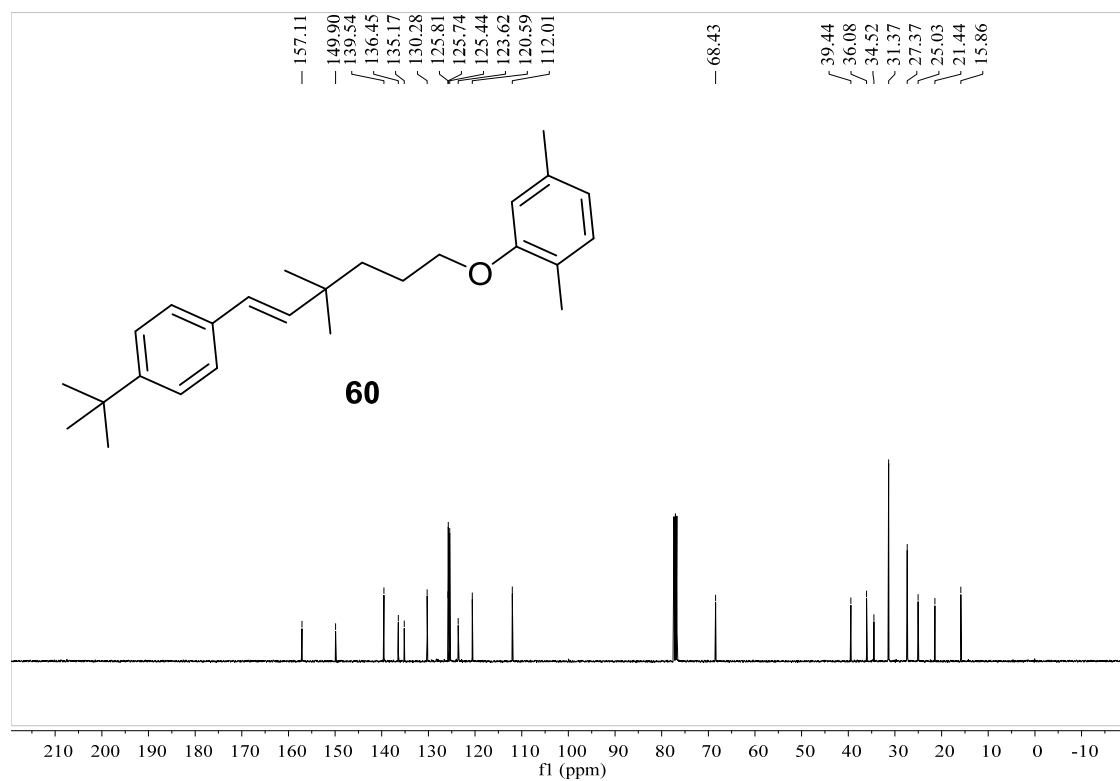


Figure S155. ^{13}C NMR spectrum of compound **60**, related to Scheme 2.

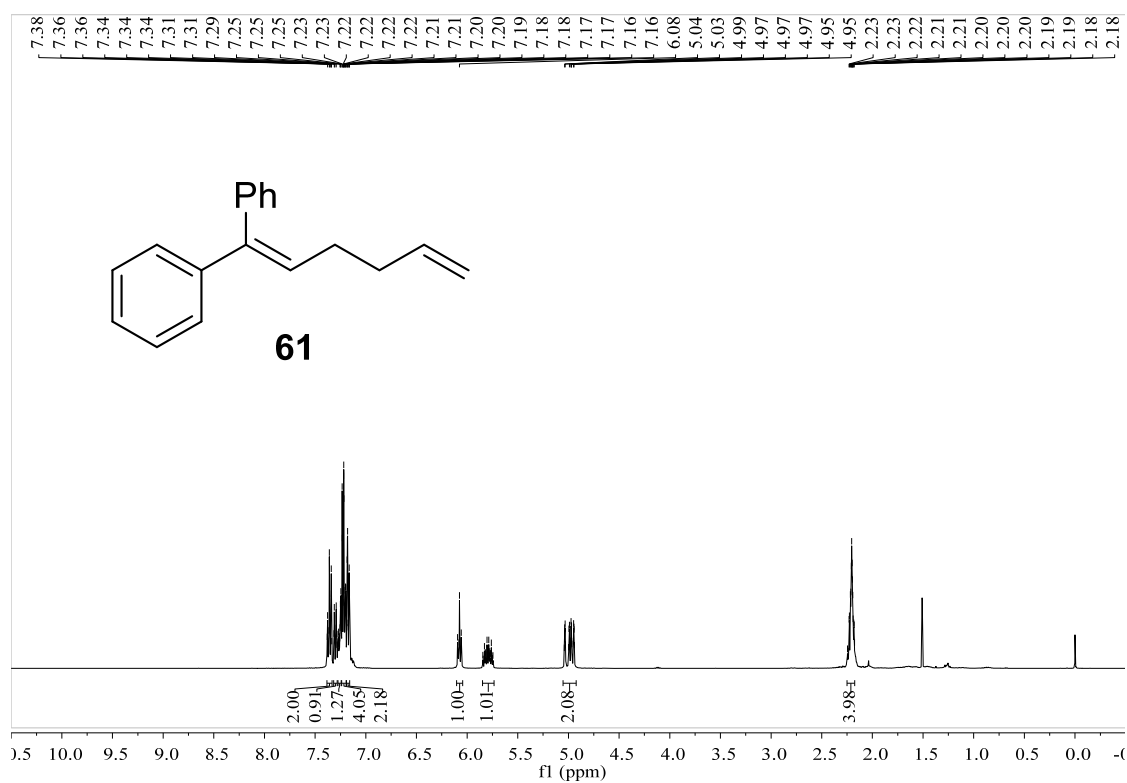


Figure S156. ¹H NMR spectrum of compound **61**, related to Scheme 3A.

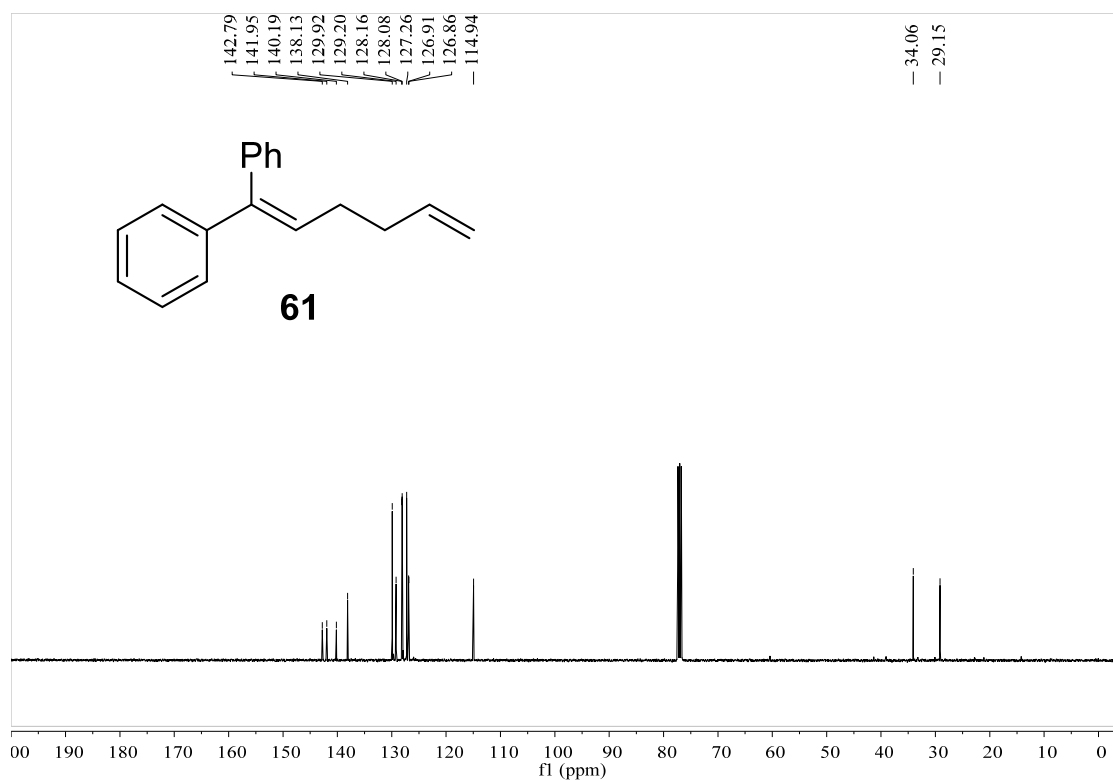


Figure S157. ¹³C NMR spectrum of compound **61**, related to Scheme 3A.

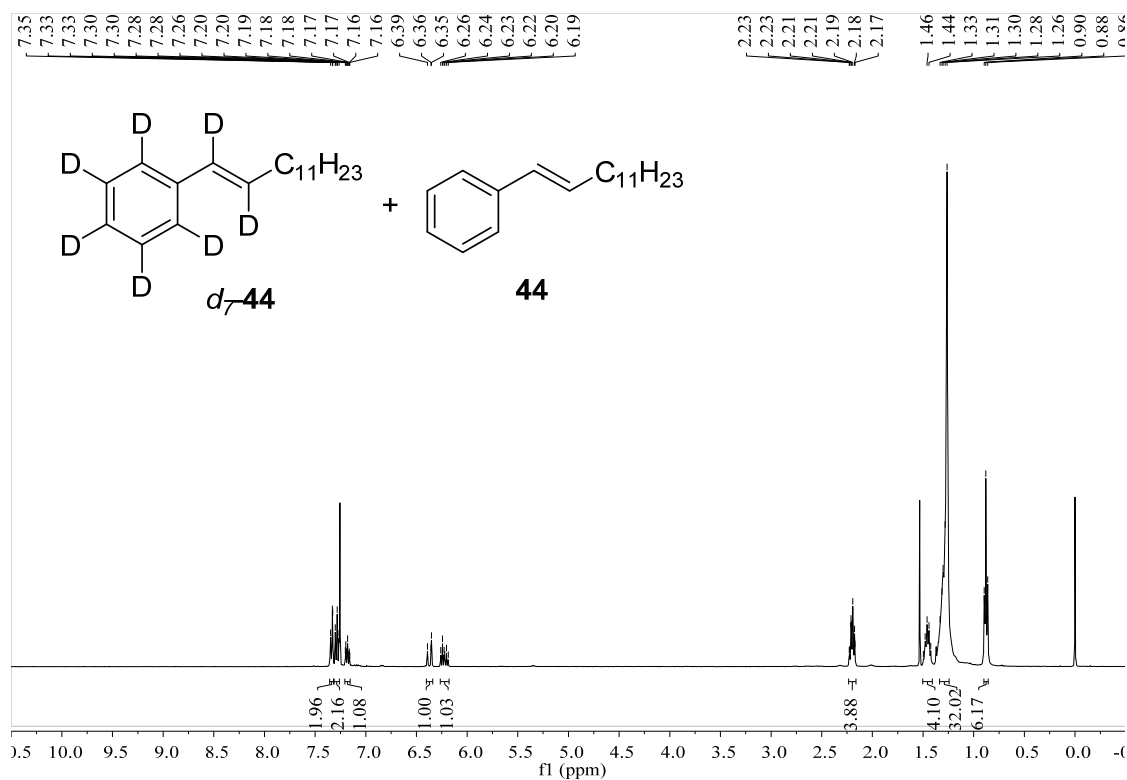


Figure S158. ^1H NMR spectrum of compounds d_7-44 and 44 , related to Scheme 3B.

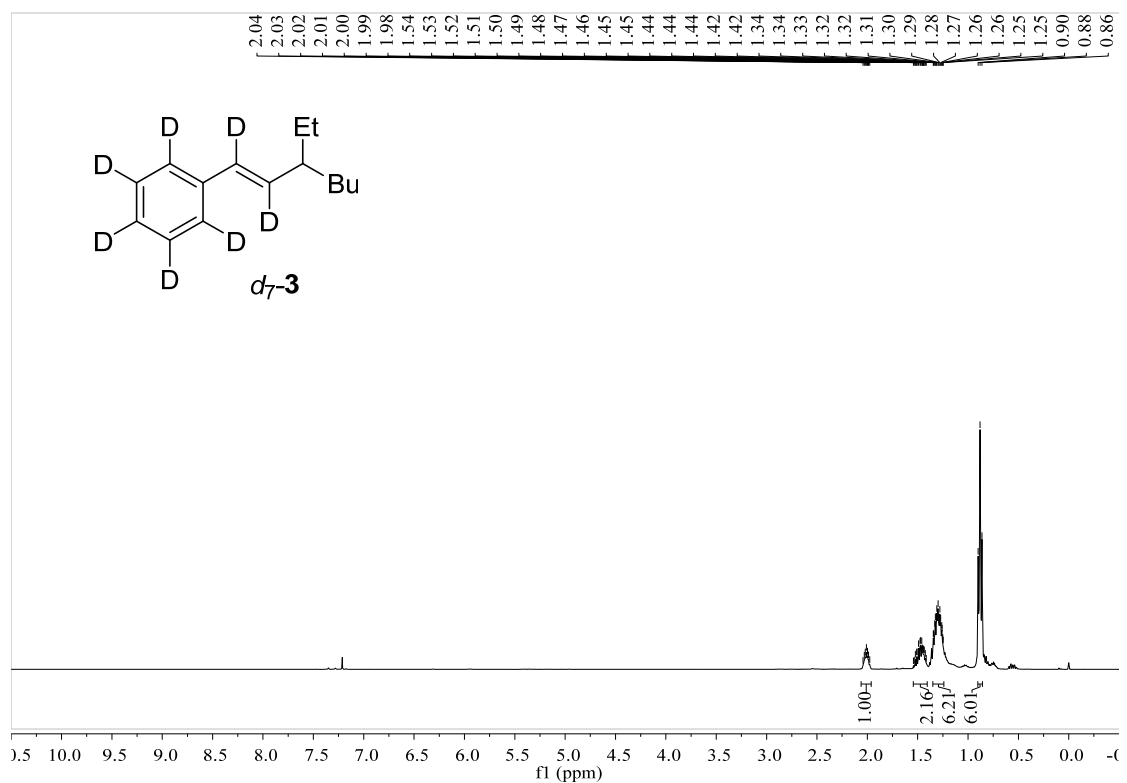


Figure S159. ^1H NMR spectrum of compound d_7-3 , related to Scheme 3B.

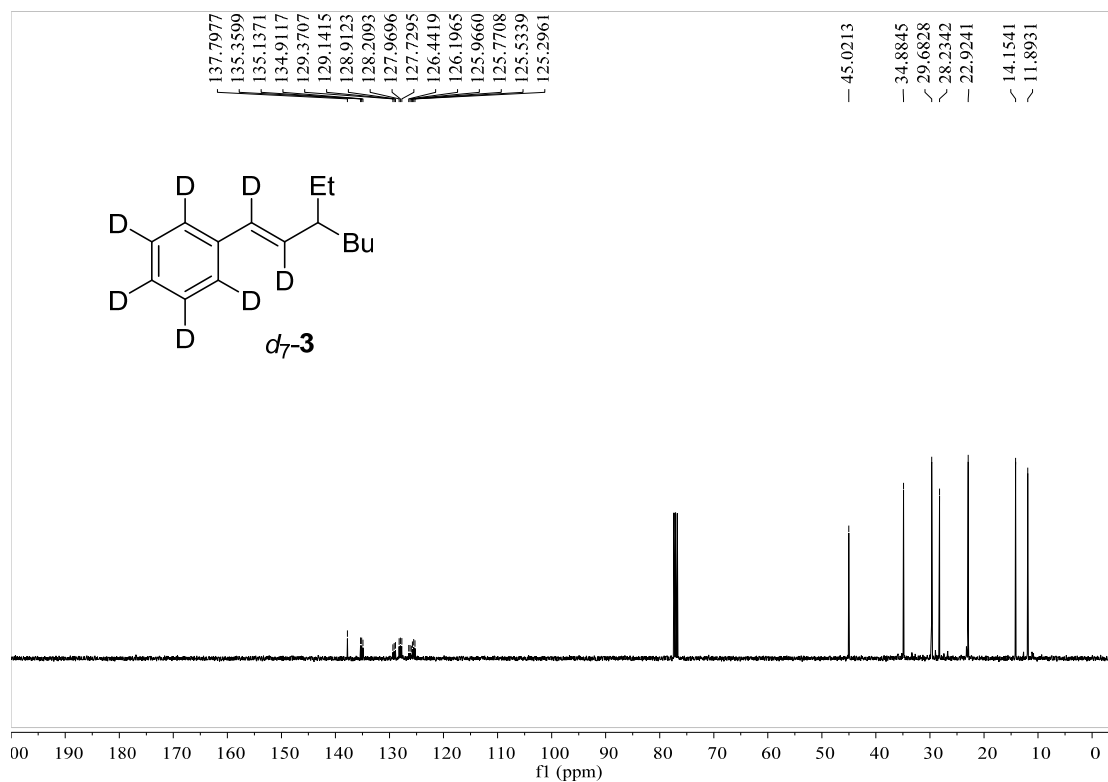


Figure S160. ^{13}C NMR spectrum of compound $d_7\text{-3}$, related to Scheme 3B.

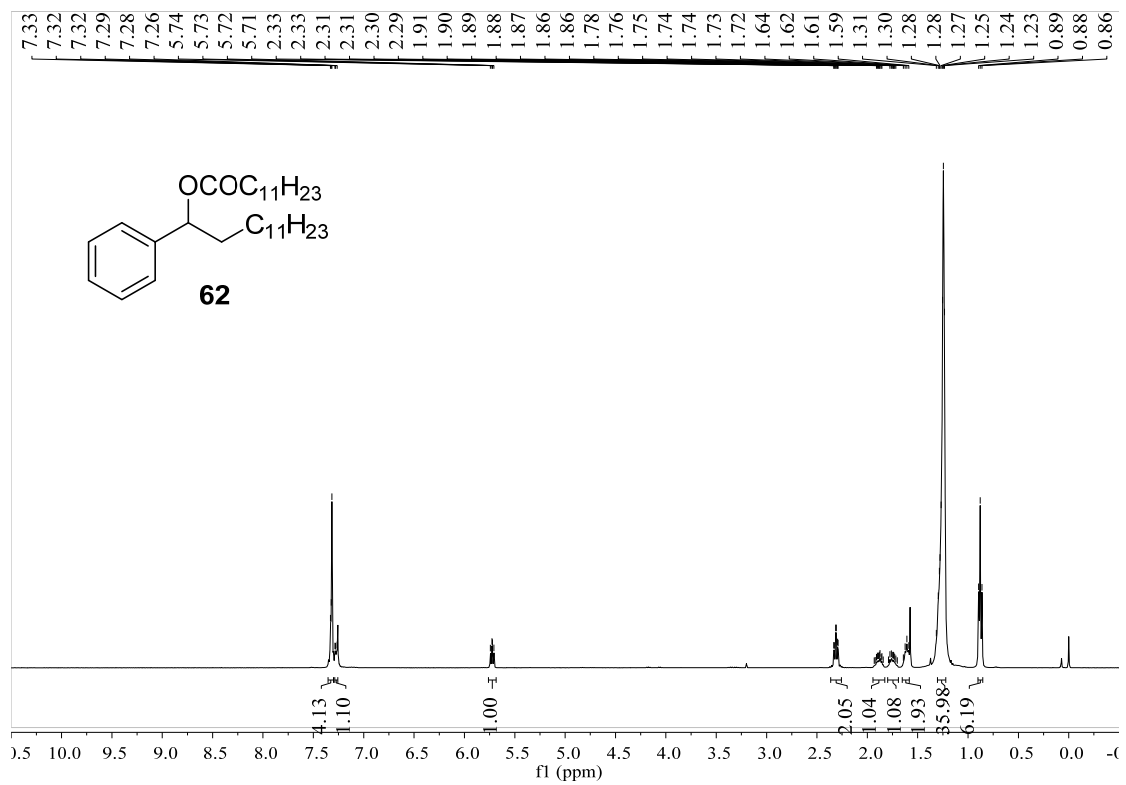


Figure S161. ¹H NMR spectrum of compound **62**, related to **Scheme 3C**.

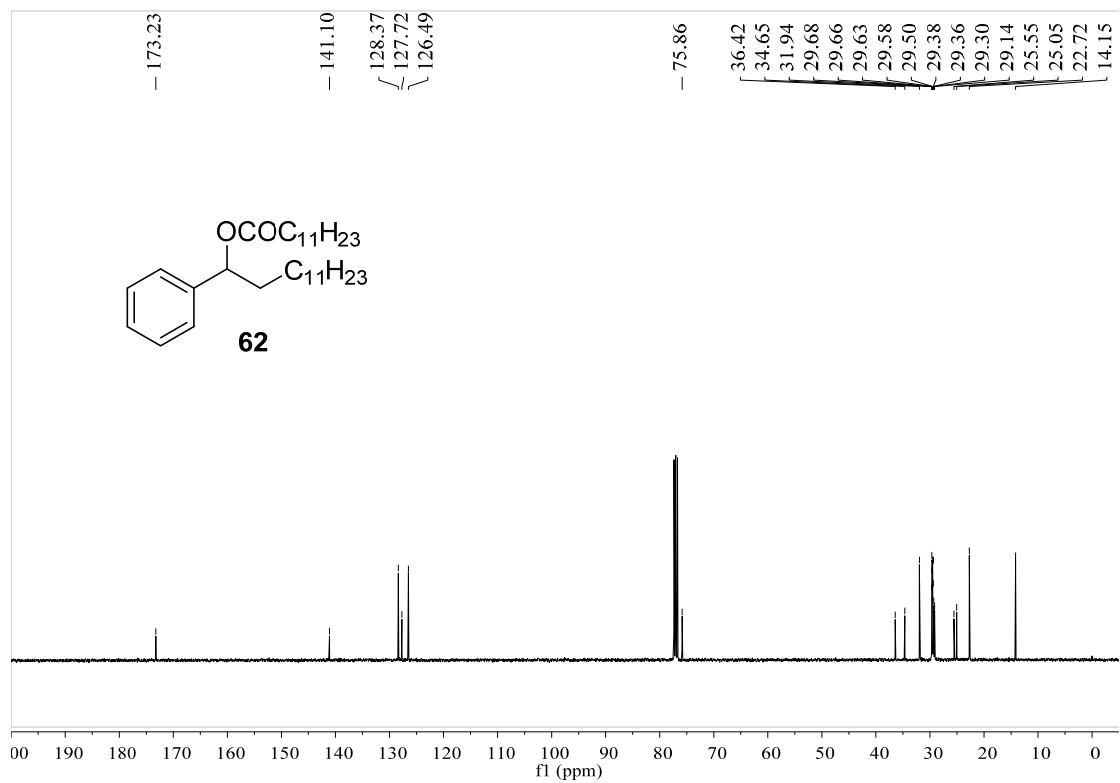


Figure S162. ¹³C NMR spectrum of compound **62**, related to **Scheme 3C**.

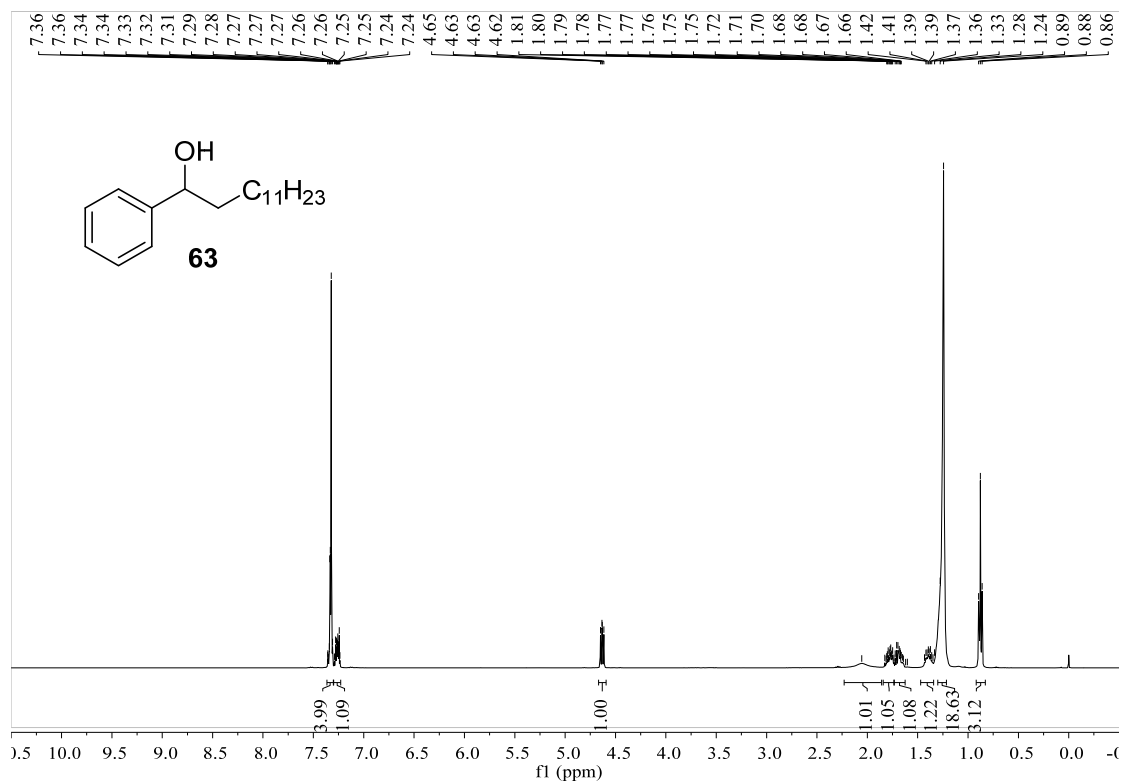


Figure S163. ¹H NMR spectrum of compound **63**, related to **Scheme 3C**.

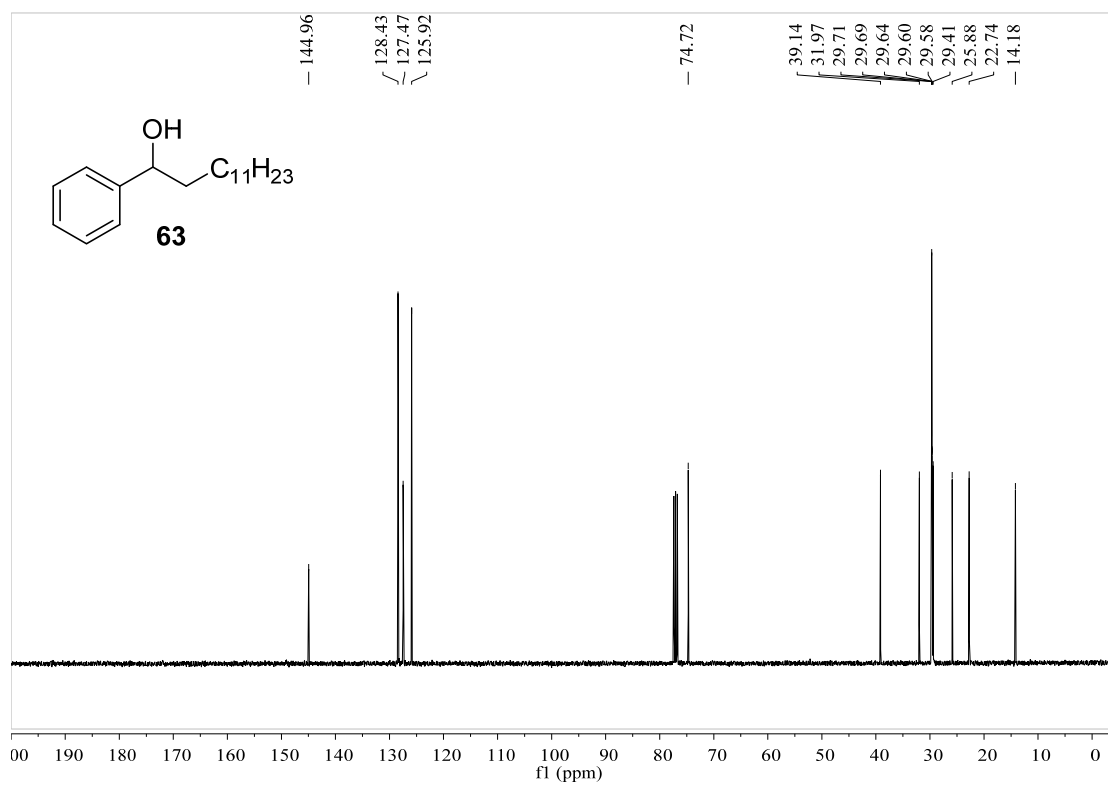
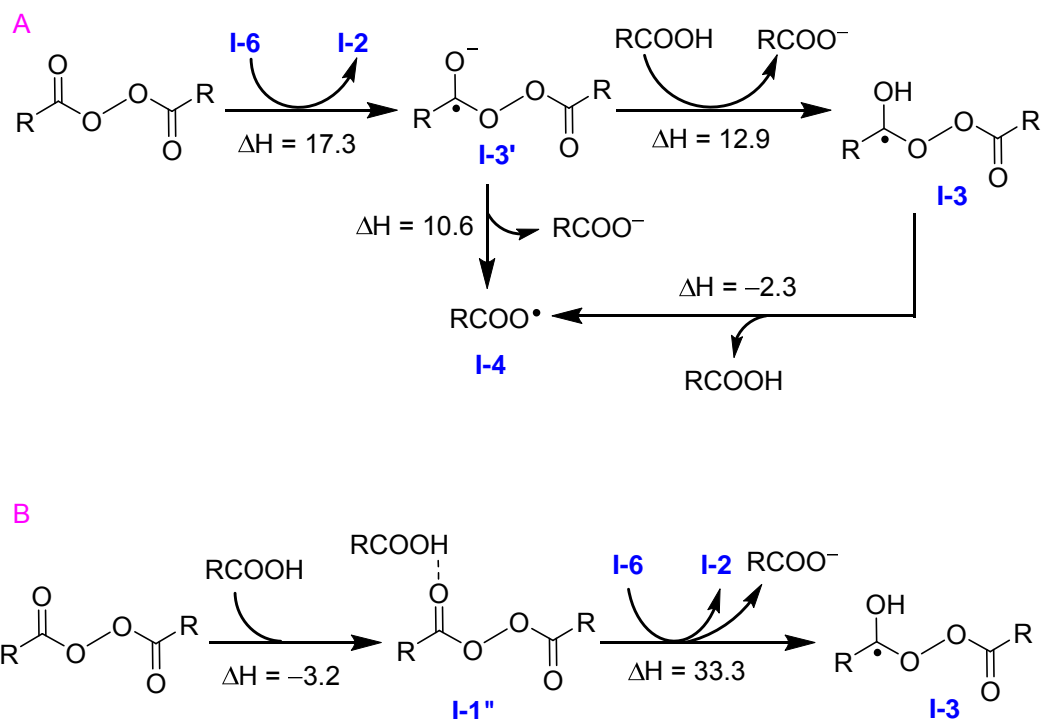


Figure S164. ¹³C NMR spectrum of compound **63**, related to **Scheme 3C**.

Supplemental Schemes

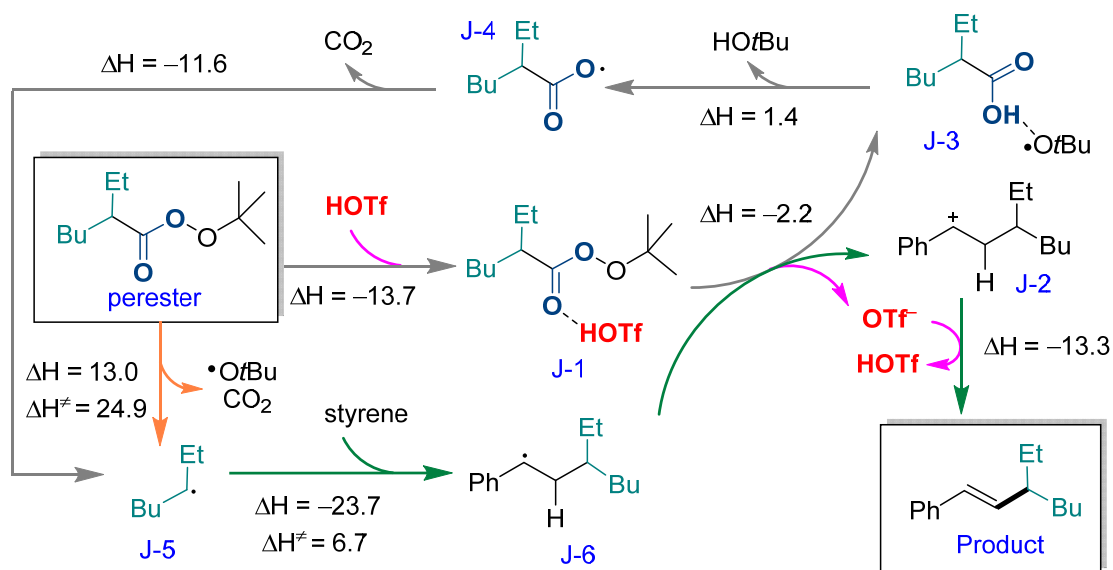
Note: R = *n*-C₅H₁₁ was used for the calculation



Scheme S1. The reaction profiles without HOF. Related to **Scheme 4**.

(A) Direct electron transfer from **I-6** to peroxide requires a high energy of 17.3 kcal/mol. Protonation of **I-2** by RCOOH to form **I-3** is endothermic of 12.9 kcal/mol. Without acid direct O-O cleavage to form **I-4** is also endothermic of 10.6 kcal/mol. Combined with previous energy requirement of electron transfer the overall reaction energies are more than 27 kcal/mol.

(B) Binding a carboxylic acid RCOOH to peroxide forms a weak hydrogen bond of 3.2 kcal/mol. However, electron transfer process requires high energy of 33.3 kcal/mol. As such, both paths are disfavored compared to the HOF involved reactions.



Scheme S2. The reaction profile of perester, Related to **Scheme 4**.

The perester species has a similar mechanism catalyzed by HOTf. Before the catalytic cycle the R• radical **J-5** can be formed by homolytic dissociation of the alkyl diacyl peroxide (perester), which is a very slow step with a high barrier of 24.9 kcal/mol. However, this is considered as the *trigger* to invoke the following catalytic cycle. Attack on the styrene substrate by the active species R• radical **J-5** to form a benzyl radical (**J-6**) leads to energies lower by 23.7 kcal/mol with a small barrier of 6.7 kcal/mol, indicating that such reaction is both thermodynamically and kinetically favourable. In the beginning of the catalytic cycle, LPO binding a molecule of HOTf forms a complex **J-1** with a strong hydrogen bonding of 13.7 kcal/mol. This complex oxidizes benzyl radical (**J-6**) to yield a benzyl cation species (**J-2**), a radical (**J-3**) and an OTf⁻ anion, which is exothermic by 2.2 kcal/mol. Meanwhile, the generated OTf⁻ deprotonates **J-1** to yield the product and regenerate acid HOTf with reaction energy of -13.3 kcal/mol. Thus, from the reactions of LPO and **J-6** to the product and **J-3** stepwise electron and proton transfers are promoted by HOTf, which serves as the driving force and proton source for the reaction. Thereby hydrogen transfer of **J-3** leads to RCOO• radical (**J-4**) and tBuOH, which is nearly thermal neutral of 1.4 kcal/mol without any barrier. Subsequently, C-C cleavage of **J-4** is exothermic by 11.6 kcal/mol in energy which releases the active species R• radical (**J-5**) and CO₂ to close the catalytic cycle.

Supplemental Tables

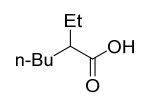
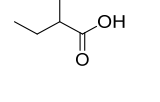
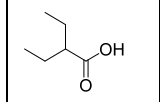
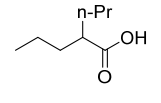
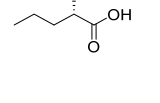
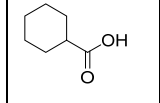
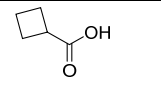
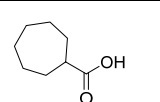
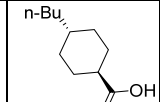
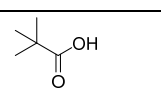
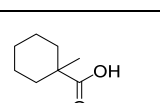
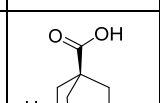
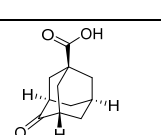
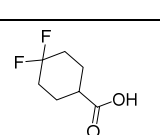
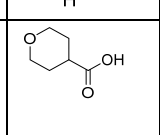
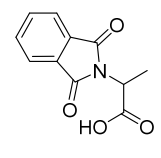
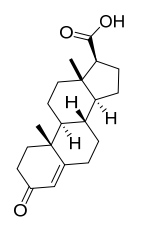
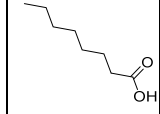
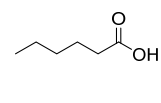
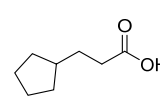
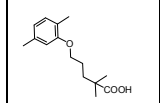
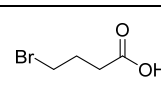
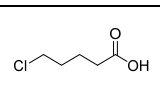
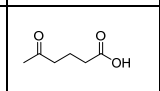
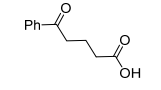
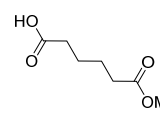
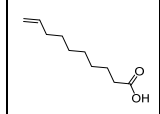
Acids	Company	Acids	Company	Acids	Company
	Energy-chemical		Energy-chemical		Energy-chemical
	Energy-chemical		Energy-chemical		Adamas-beta
	Energy-chemical		Energy-chemical		Adamas-beta
	Energy-chemical		TCI-chemicals		Energy-chemical
	Bide-pharmatech		Bide-pharmatech		Bide-pharmatech
	Aladdin		Heowns		Energy-chemical
	Energy-chemical		Energy-chemical		Energy-chemical
	Inno-chem		Bide-pharmatech		Adamas-beta
	Bide-pharmatech		Energy-chemical		Energy-chemical

Table S1. Sources of acids, related to Figure 2 and Figure 3.

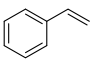
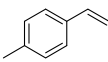
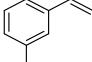
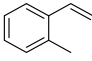
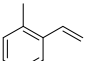
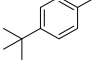
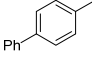
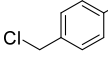
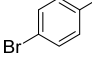
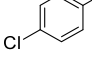
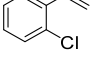
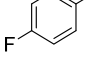
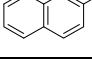
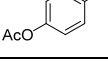
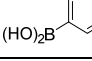
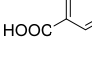
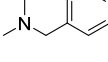
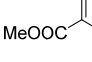
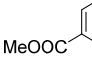
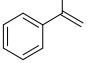
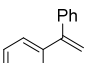
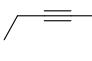
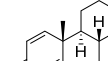
Alkenes	Company	Alkenes	Company	Alkenes	Company
	Energy-chemical		Energy-chemical		Adamas-beta
	Adamas-beta		Alfa Aesar		Energy-chemical
	Energy-chemical		Meryer		Energy-chemical
	Energy-chemical		Energy-chemical		Adamas
	Meryer		Energy-chemical		Energy-chemical
	Energy-chemical		Jkchemical		Energy-chemical
	Energy-chemical		Energy-chemical		Energy-chemical
	Sigma-aldrich		Energy-chemical		

Table S2. Sources of alkenes, related to Figure 1, Figure 2 and Figure 3.

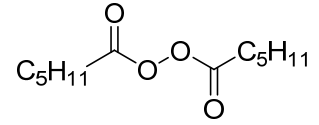
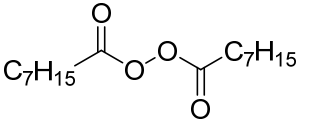
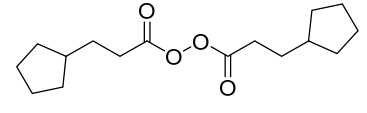
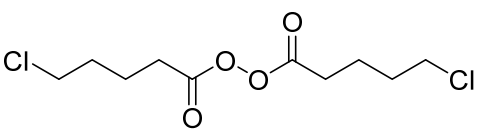
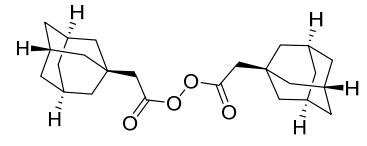
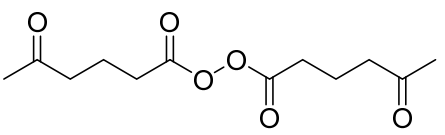
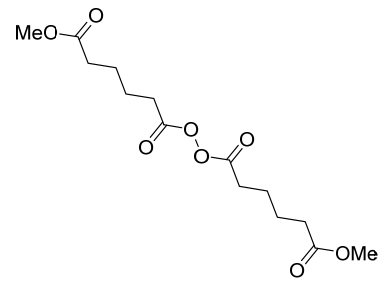
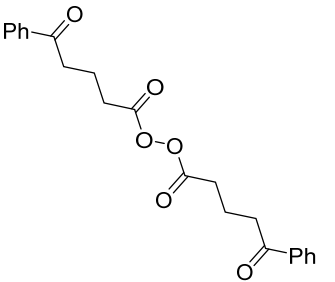
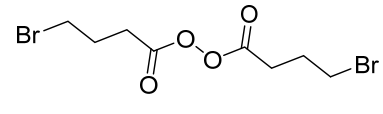
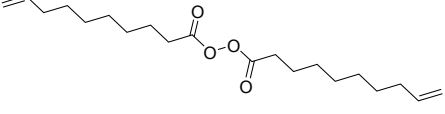
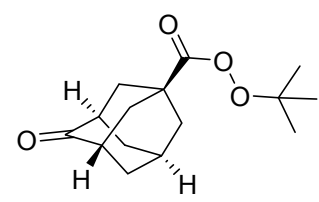
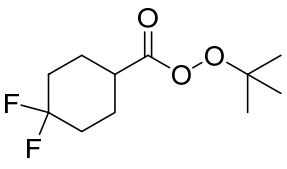
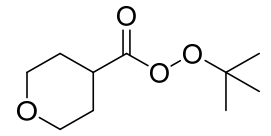
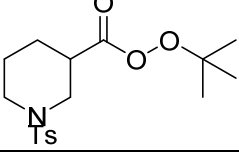
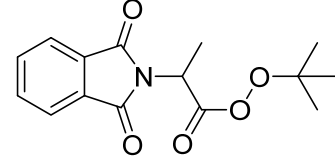
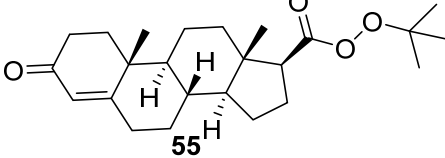
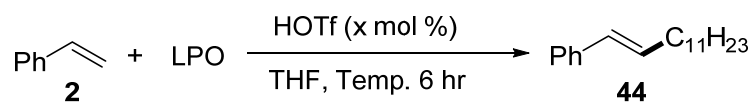
structure	yield	structure	yield
	90%		85%
	84%		65%
	84%		73%
	71%		76%
	55%		76%
	75%		70%
	78%		70%
	64%		80%

Table S3. The synthesis of peroxides, related to Figure 3.



Entry	HOTf (x mol %)	THF (y mL)	Temp.	Yield (%) ^b
1	5 mol %	2 mL	90°C	5%
2	10 mol %	2 mL	90°C	10%
3	15 mol %	2 mL	90°C	36%
4	20 mol %	2 mL	90°C	65%
5	40 mol %	2 mL	90°C	60%
6	50 mol %	2 mL	90°C	76% ^c
7	20 mol %	2 mL	100°C	62%
8 ^d	20 mol %	2 mL	80°C	43%
9 ^d	20 mol %	2 mL	70°C	6%
10	20 mol %	1 mL	90°C	76% (73% ^c)
11 ^e	20 mol %	1 mL	90°C	67%
12 ^f	20 mol %	1 mL	90°C	54%
13 ^g	20 mol %	1 mL	90°C	70%
14 ^h	20 mol %	1 mL	90°C	40%

Table S4. Optimizations of reaction conditions with primary aliphatic acid, Related to **Figure 3**.^a

^a**2** (0.5 mmol), LPO (1.0 mmol).

^bYield detected by GC.

^cIsolated product.

^dReaction with 8 hr.

^e**2** (0.5 mmol), LPO (0.75 mmol).

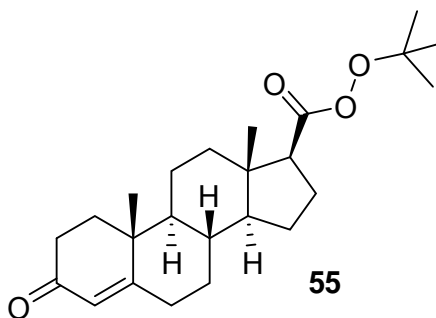
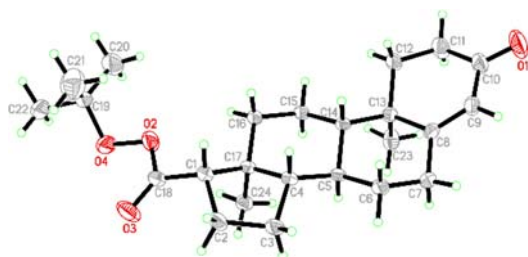
^f**2** (0.5 mmol), LPO (0.5 mmol).

^g**2** (0.6 mmol), LPO (0.5 mmol).

^h**2** (0.75 mmol), LPO (0.5 mmol).

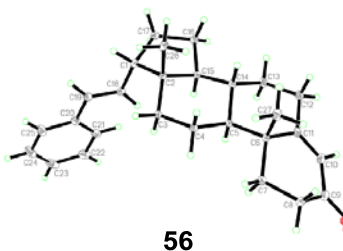
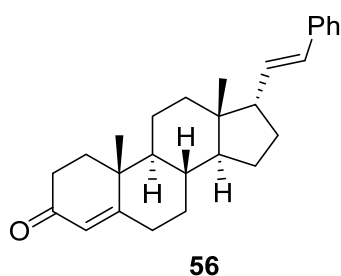
Single Crystal Data of **55** and **56**

Single crystal of **55** and **56** suitable for X-ray diffraction was mounted in Paratone oil onto a glass fiber and frozen under a nitrogen cold stream. The data was collected at 220.0(1) K using a Agilent SuperNova, Dual, Cu at zero, Atlas fitted with Cu K α radiation ($\lambda = 1.54184 \text{ \AA}$). Data collection and unit cell refinement were executed by using CrysAlisPro software. Data processing and absorption correction, giving minimum and maximum transmission factors, were accomplished with CrysAlisPro. The structure was solved with the SHELXT-2014 and refined with the SHELXL-2014 using Least Squares minimisation. All non-hydrogen atoms were refined with anisotropic displacement parameters. All carbon bound hydrogen atom positions were determined by geometry and refined by a riding model. CCDC 1477011 and CCDC 1476738 for **55** and **56** contain the supplementary crystallographic data. Crystal data and structure refinements of **55** and **56** are listed in Table S5 and Table S6. These data can be obtained free of charge from the Cambridge Crystallographic Data Centre via www.ccdc.cam.ac.uk/data_request/cif.



Identification code	55
Empirical formula	C ₂₄ H ₃₆ O ₄
Formula weight	388.53
Temperature	220.0(1) K
Wavelength	1.54184 Å
Crystal system	Orthorhombic
Space group	P 21 21 21
Unit cell dimensions	a = 6.16790(10) Å b = 12.5681(3) Å c = 29.0822(7) Å
Volume	2254.42(8) Å ³
Z	4
Density (calculated)	1.145 Mg/m ³
Absorption coefficient	0.603 mm ⁻¹
F(000)	848
Crystal size	0.220 x 0.200 x 0.170 mm ³
Theta range for data collection	3.831 to 73.663°.
Index ranges	-5 ≤ h ≤ 7, -9 ≤ k ≤ 15, -23 ≤ l ≤ 35
Reflections collected	7382
Independent reflections	3937 [R(int) = 0.0387]
Completeness to theta = 67.684°	99.3 %
Absorption correction	Semi-empirical from equivalents
Max. and min. transmission	1.00000 and 0.60854
Refinement method	Full-matrix least-squares on F ²
Data / restraints / parameters	3937 / 6 / 258
Goodness-of-fit on F ²	1.023
Final R indices [I > 2σ(I)]	R1 = 0.0531, wR2 = 0.1363
R indices (all data)	R1 = 0.0649, wR2 = 0.1499
Absolute structure parameter	0.0(3)
Extinction coefficient	n/a
Largest diff. peak and hole	0.276 and -0.212 e.Å ⁻³

Table S5. Crystal data and structure refinement for **55**, Related to **Scheme 2**.



Identification code	56
Empirical formula	C ₂₇ H ₃₄ O
Formula weight	374.54
Temperature	100.0(2) K
Wavelength	1.54184 Å
Crystal system	Orthorhombic
Space group	P 21 21 21
Unit cell dimensions	a = 6.23490(10) Å b = 28.7978(4) Å c = 11.7959(2) Å
Volume	2117.97(6) Å ³
Z	4
Density (calculated)	1.175 Mg/m ³
Absorption coefficient	0.520 mm ⁻¹
F(000)	816
Crystal size	0.200 x 0.180 x 0.150 mm ³
Theta range for data collection	4.050 to 73.331°.
Index ranges	-7<=h<=2, -31<=k<=35, -14<=l<=7
Reflections collected	5630
Independent reflections	3761 [R(int) = 0.0141]
Completeness to theta = 67.684°	99.9 %
Absorption correction	Semi-empirical from equivalents
Max. and min. transmission	1.00000 and 0.88083
Refinement method	Full-matrix least-squares on F ²
Data / restraints / parameters	3761 / 0 / 256
Goodness-of-fit on F ²	1.025
Final R indices [I>2sigma(I)]	R1 = 0.0291, wR2 = 0.0733
R indices (all data)	R1 = 0.0302, wR2 = 0.0742
Absolute structure parameter	-0.29(15)
Extinction coefficient	0.0041(3)
Largest diff. peak and hole	0.252 and -0.140 e.Å ⁻³

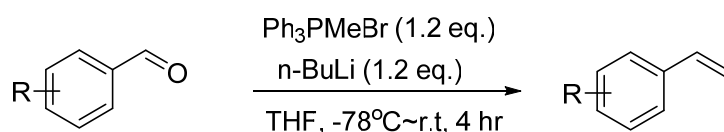
Table S6. Crystal data and structure refinement for **56**, Related to **Scheme 2**.

Transparent Methods

All reactions were carried out under an atmosphere of nitrogen in flame-dried glassware with magnetic stirring unless otherwise indicated. Commercially obtained reagents were used as received. Solvents were dried by Innovative Technology Solvent Purification System. Liquids and solutions were transferred via syringe. All reactions were monitored by thin-layer chromatography. GC-MS data were recorded on Thermo ISQ QD. ^1H , ^{13}C and ^{19}F NMR spectra were recorded on Bruker-BioSpin AVANCE III HD. Data for ^1H NMR spectra are reported relative to chloroform as an internal standard (7.26 ppm) and are reported as follows: chemical shift (ppm), multiplicity, coupling constant (Hz), and integration. Data for ^{13}C NMR spectra are reported relative to chloroform as an internal standard (77.23 ppm) and are reported in terms of chemical shift (ppm). HRMS data were recorded on Waters Micromass GCT Premier or Thermo Fisher Scientific LTQ FTICR-MS.

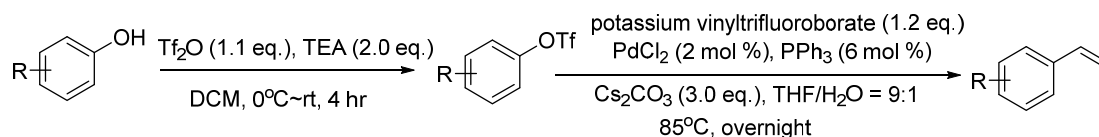
Experimental procedures for synthesis of materials

Procedure A for the synthesis of alkenes



General procedure (Haubenreisser et al., 2016): The reaction vessel was charged with phosphonium salt (1.2 equiv) in dry THF. To the stirred mixture, *n*-butyl lithium (1.2 equiv) was added under N_2 atmosphere at -78°C . The mixture was stirred at 0°C for 5 mins and then substituted aldehyde (1.0 equiv.) in dry THF was added dropwise in over 15 min. After stirring at rt for 4 hr, the mixture was quenched with saturated NH_4Cl , then extracted three times with dichloromethane and water. The combined organic layers were dried over anhydrous sodium sulfate, concentrated and purified by flash column chromatography afford the desired product.

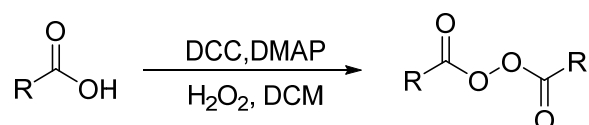
Procedure B for the synthesis of alkenes



General procedure (Huang and Doyle, 2012): A flask was flame dried and charged with phenol (1.0 equiv), dichloromethane, and Et_3N (2.0 equiv). The mixture was cooled in a 0°C ice-water bath, and Tf_2O (1.1 equiv) was added dropwise. The mixture was allowed to warm up to room temperature and stirred at room temperature under argon for 5 hr. The resulting brown mixture was diluted with dichloromethane, washed with sat. NH_4Cl , and the aqueous layer was

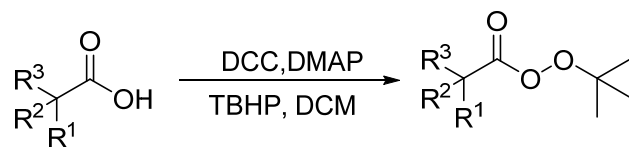
extracted with dichloromethane. The combined organic layers were dried over MgSO₄, and the filtrate was concentrated. The crude was purified with column chromatography to afford triflate. A threaded tube was charged with triflate (1.0 equiv), potassium vinyltrifluoroborate (1.2 equiv), PdCl₂ (2 mol %), PPh₃ (6 mol %), Cs₂CO₃ (3.0 equiv) were added, then THF and water were added under N₂ atmosphere. The mixture was stirred at 85°C for overnight. The resulting dark brown mixture was allowed to cool to room temperature, diluted with dichloromethane, and washed with water. The aqueous layer was extracted with dichloromethane. The combined organic layers were dried over MgSO₄, and the filtrate was concentrated. The crude was purified with column chromatography to afford the desired product.

Procedure C for the synthesis of diacyl peroxides



General procedure (Jian et al., 2017): A solution of DMAP (10 mol %), 30% hydrogen peroxide (1.2 equiv), and acid in CH₂Cl₂ was cooled to -5°C for about 10 min. Then DCC (1.2 equiv) was added. Then the mixture was stirred at -5°C to room temperature for 1.5 ~4 hr. The solution was concentrated on a rotary evaporator under vacuum at 10~15°C and the residue was chromatographed on silica gel to give the diacyl peroxide.

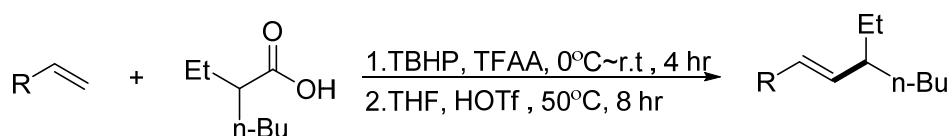
Procedure D for the synthesis of peresters



General procedure (Zhu et al., 2017): A solution of DMAP (10 mol %), TBHP (aqueous solution, 1.2 equiv), and acid in CH₂Cl₂ was cooled to -5°C for about 10 min. Then DCC (1.2 equiv) was added. Then the mixture was stirred at -5°C to room temperature for 4 hr. The solution was concentrated on a rotary evaporator under vacuum at 20~25°C and the residue was chromatographed on silica gel to give the perester.

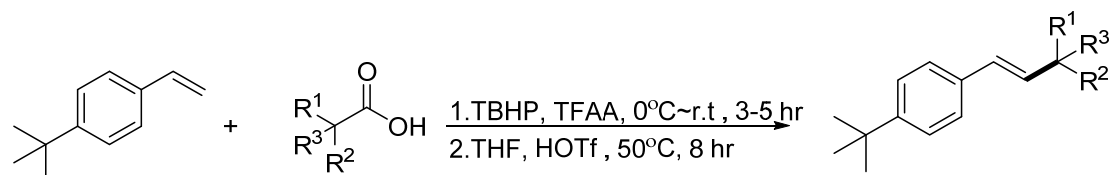
General procedure for the alkyl-Heck-type reaction

Procedure E for the alkyl-Heck-type reaction of alkenes



To a flame-dried Schlenk tube were added 2-ethylhexanoic acid (1.5 mmol, 3.0 equiv), TBHP (1.5 mmol, 3.0 equiv, in decane) and TFAA (2.0 mmol, 4.0 equiv) at 0°C under the atmosphere of nitrogen. The mixture was then stirred at rt for 4 hours. After completion, THF (2 mL), alkene (0.5 mmol, 1.0 equiv) and HOTf (0.05 mmol, 10 mol %) were added into the Schlenk tube under the atmosphere of nitrogen. The mixture was then stirred at 50°C for 8 hr. After completion detected by TLC, the solvent was removed by rotary evaporation under vacuum, and the residue was chromatographed on silica gel to give the desired product.

Procedure F for the alkyl-Heck-type reaction of secondary and tertiary aliphatic acids



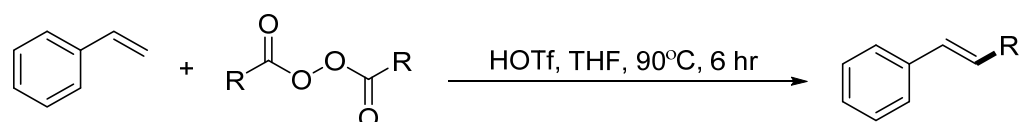
General procedure: To a flame-dried Schlenk tube were added acid (1.5 mmol, 3.0 equiv), TBHP (1.5 mmol, 3.0 equiv, in decane) and TFAA (2.0 mmol, 4.0 equiv) at 0°C under the atmosphere of nitrogen. The mixture was then stirred at rt for 3-5 hours. After completion, THF (2 mL), 4-*tert*-butylstyrene (0.5 mmol, 1.0 equiv) and HOTf (0.05 mmol, 10 mol %) were added into the Schlenk tube under the atmosphere of nitrogen. The mixture was then stirred at 50°C for 8 hours. After completion detected by TLC, the solvent was removed by rotary evaporation under vacuum, and the residue was chromatographed on silica gel to give the desired product.

Procedure G for the alkyl-Heck-type reaction with peresters



To a flame-dried Schlenk tube were added THF (2 mL), 4-*tert*-butylstyrene (0.5 mmol, 1.0 equiv), perester (1.25 mmol, 2.5 equiv) and HOTf (0.1 mmol, 20 mol %) under the atmosphere of nitrogen. The mixture was then stirred at 80°C for 6 hours. After completion detected by TLC, the solvent was removed by rotary evaporation under vacuum, and the residue was chromatographed on silica gel to give the desired product.

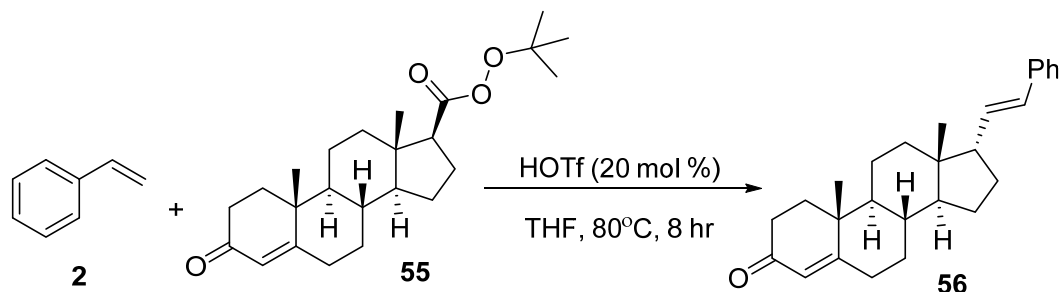
Procedure H for the alkyl-Heck-type reaction with diacyl peroxides



To a flame-dried Schlenk tube were added THF (1 mL), styrene (0.5 mmol, 1.0 equiv) diacyl peroxides (1.0 mmol, 2.0 equiv) and HOTf (0.1 mmol, 20 mol %) under the atmosphere of nitrogen. The mixture was then stirred at 90°C for 6 hr. After completion detected by TLC, the solvent was removed by rotary evaporation under vacuum, and the residue was chromatographed on silica gel to give the desired product.

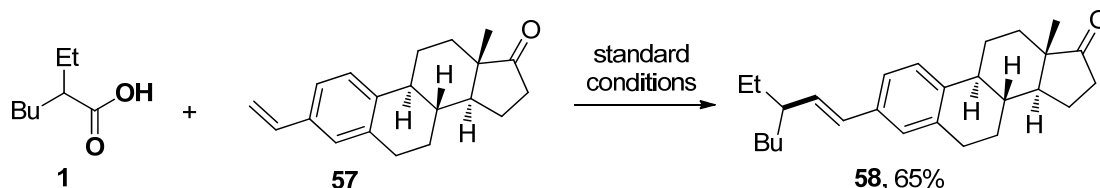
Experimental procedures for synthetic applications

(i)



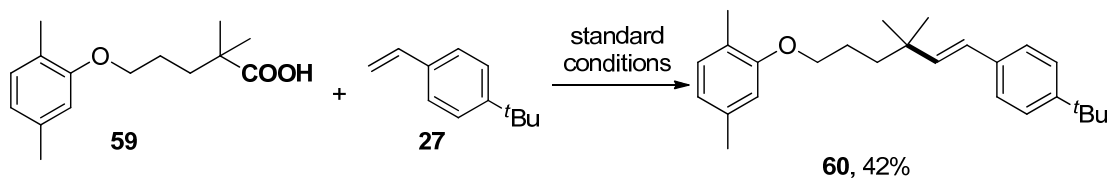
To a flame-dried Schlenk tube were added THF (2 mL), styrene **2** (0.5 mmol, 1.0 equiv) perester **55** (1.25 mmol, 2.5 equiv) and HOTf (0.1 mmol, 20 mol %) under the atmosphere of nitrogen. The mixture was then stirred at 80°C for 8 hr. After completion detected by TLC, the solvent was removed by rotary evaporation under vacuum, and the residue was chromatographed on silica gel to give the desired product **56**.

(ii)



To a flame-dried Schlenk tube were added acid **1** (1.5 mmol, 3.0 equiv), TBHP (1.5 mmol, 3.0 equiv) and TFAA (2.0 mmol, 4.0 equiv) at 0°C under the atmosphere of nitrogen. The mixture was then stirred at rt for 5 hr. After completion, THF (2 mL), alkene **57** (0.5 mmol, 1.0 equiv) and HOTf (0.05 mmol, 10 mol %) were added into the Schlenk tube under the atmosphere of nitrogen. The mixture was then stirred at 50°C for 8 hr. After completion detected by TLC, the solvent was removed by rotary evaporation under vacuum, and the residue was chromatographed on silica gel to give the desired product **58**.

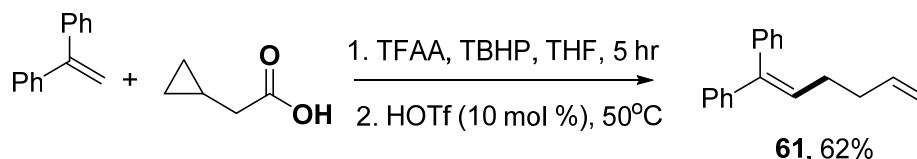
(iii)



To a flame-dried Schlenk tube were added acid **59** (1.5 mmol, 3.0 equiv), TBHP (1.5 mmol, 3.0 equiv) and TFAA (2.0 mmol, 4.0 equiv) at 0°C under the atmosphere of nitrogen. The mixture was then stirred at rt for 5 hr. After completion THF (2 mL), 4-*tert*-butylstyrene **27** (0.5 mmol, 1.0 equiv) and HOTf (0.05 mmol, 10 mol %) were added into the Schlenk tube under the atmosphere of nitrogen. The mixture was then stirred at 50°C for 8 hr. After completion detected by TLC, the solvent was removed by rotary evaporation under vacuum, and the residue was chromatographed on silica gel to give the desired product **60**.

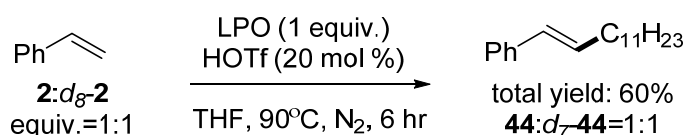
Experimental procedures for preliminary mechanistic studies

Radical clock experiment

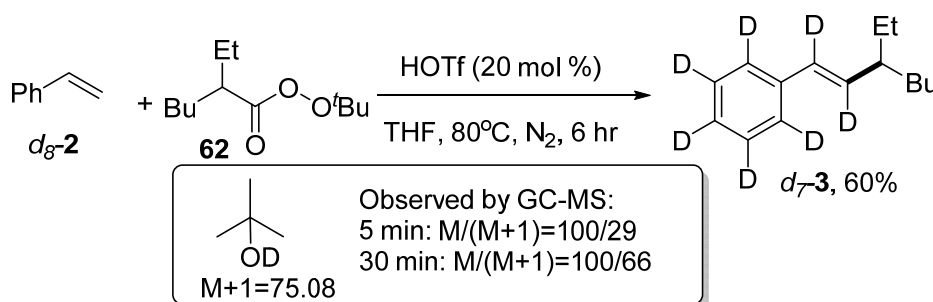


To a flame-dried Schlenk tube were added acid (1.5 mmol, 3.0 equiv), TBHP (1.5 mmol, 3.0 equiv) and TFAA (2.0 mmol, 4.0 equiv) at 0°C under the atmosphere of nitrogen. The mixture was then stirred at rt for 5 hr. After completion, THF (2 mL), styrene (0.5 mmol, 1.0 equiv) and HOTf (0.05 mmol, 10 mol %) were added into the Schlenk tube under the atmosphere of nitrogen. The mixture was then stirred at 50°C for 8 hr. After completion detected by TLC, the solvent was removed by rotary evaporation under vacuum, and the residue was chromatographed on silica gel to give the desired product **61**.

Deuterium labeling experiment

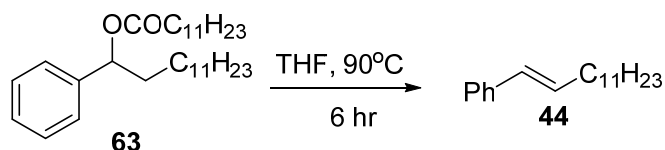


To a flame-dried Schlenk tube were added THF (1 mL), **2** (1.0 mmol, 1.0 equiv), d_8 -**2** (1.0 mmol, 1.0 equiv), LPO (0.5 mmol, 0.5 equiv) and HOTf (0.1 mmol, 20 mol %) under the atmosphere of nitrogen. The mixture was then stirred at 90°C for 6 hr. After completion detected by TLC, the solvent was removed by rotary evaporation under vacuum, and the residue was chromatographed on silica gel to give the desired product **44** and d_7 -**44**.



To a flame-dried Schlenk tube were added THF (2 mL), d_8 -**2** (0.50 mmol, 1.0 equiv), **62** (1.25 mmol, 2.5 equiv) and HOTf (0.1 mmol, 20 mol %) under the atmosphere of nitrogen. The mixture was then stirred at 80°C. The reaction mixture was tested by GC-MS after 5 minutes and 30 minutes. The deuterated side-products d (OD)-butanol was detected by GC-MS. The mixture was then stirred at 80°C for 6 hr. After the reaction mixture was cooled to ambient temperature. The solvent was removed by rotary evaporation under vacuum, and the residue was chromatographed on silica gel to give the desired d_7 -**3**.

Exclusion of possible intermediates



0%, **63** was recovered in 92% yield

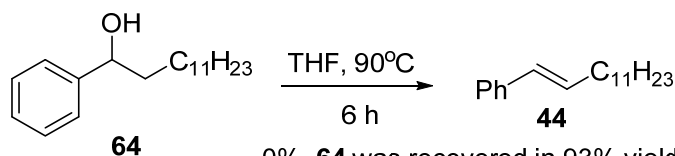
0%, C₁₁H₂₃COOH (1 equiv), **63** was recovered in 93% yield

91%, HOTf (20 mol %).

Ester **63** (Ge et al., 2017): (0.2 mmol) was charged in anhydrous THF (0.5 mL) at 90°C and then stirred for 6 hr. No reaction was observed and the ester **63** was recovered in 92% yield.

Ester **63** (0.2 mmol) and C₁₁H₂₃COOH (1 equiv) were charged in anhydrous THF (0.5 mL) at 90°C and then stirred for 6 hr. No reaction was observed and the ester **63** was recovered in 93% yield.

Ester **63** (0.2 mmol) and HOTf (20 mol %) were charged in anhydrous THF (0.5 mL) at 90°C and then stirred for 6hr. The reaction mixture was diluted with DCM (30 mL) and washed with saturated aq. NaHCO₃. The organic layer was dried (anhydrous Na₂SO₄), filtered, and concentrated in vacuo. The residue was chromatographed on silica gel affording product **44** in 91% yield.



0%, **64** was recovered in 93% yield

0%, C₁₁H₂₃COOH (1 equiv), **64** was recovered in 93% yield

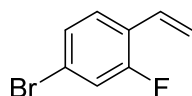
87%, HOTf(20 mol %, 6 hr)

Benzyl alcohol **64** (Jian et al., 2017) (0.2 mmol) was charged in anhydrous THF (0.5 mL) at 90°C and then stirred for 6 hr. No reaction was observed and the alcohol **64** was recovered in 93% yield.

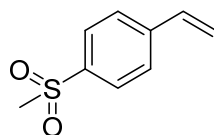
Benzyl alcohol **64** (0.2 mmol) and C₁₁H₂₃COOH (1 equiv) were charged in anhydrous THF (0.5 mL) at 90°C and then stirred for 6hr. No reaction was observed and the alcohol **64** was recovered in 93% yield.

Benzyl alcohol **64** (0.2 mmol) and HOTf (20 mol %) were charged in anhydrous THF (0.5 mL) at 90°C and then stirred for 6hr. The reaction mixture was diluted with DCM (30 mL) and washed with saturated aq. NaHCO₃. The organic layer was dried (anhydrous Na₂SO₄), filtered, and concentrated in vacuo. The residue was chromatographed on silica gel affording product **44** in 87% yield.

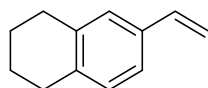
Characterization of all compounds



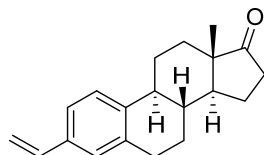
Following procedure A for the synthesis of alkenes, 4-bromo-2-fluoro-1-vinylbenzene (related to **Figure 1**) was obtained as a clear liquid. ^1H NMR (400 MHz, Chloroform-*d*) δ 7.34 (t, J = 8.3 Hz, 1H), 7.26 – 7.19 (m, 2H), 6.79 (dd, J = 17.7, 11.2 Hz, 1H), 5.81 (d, J = 17.7 Hz, 1H), 5.40 (d, J = 11.2 Hz, 1H). ^{13}C NMR (100 MHz, Chloroform-*d*) δ 159.92 (d, J = 254.0 Hz), 128.45 (d, J = 3.6 Hz), 128.11 (d, J = 4.4 Hz), 127.43 (d, J = 3.7 Hz), 124.49 (d, J = 12.4 Hz), 121.34 (d, J = 9.7 Hz), 119.34 (d, J = 25.5 Hz), 117.10 (d, J = 4.7 Hz). ^{19}F NMR (376 MHz, Chloroform-*d*) δ -115.94.



Following procedure A for synthesis of alkenes, 1-(methylsulfonyl)-4-vinylbenzene (related to **Figure 1**) was obtained as a white solid. ^1H NMR (400 MHz, Chloroform-*d*) δ 7.90 (d, J = 8.4 Hz, 2H), 7.58 (d, J = 8.3 Hz, 2H), 6.77 (dd, J = 17.6, 10.9 Hz, 1H), 5.91 (d, J = 17.6 Hz, 1H), 5.47 (d, J = 10.9 Hz, 1H), 3.05 (s, 3H). ^{13}C NMR (100 MHz, Chloroform-*d*) δ 142.88, 139.34, 135.21, 127.74, 126.95, 118.02, 44.57.

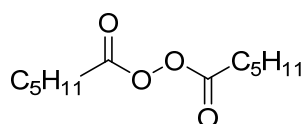


Following procedure B for synthesis of alkenes, 6-vinyl-1,2,3,4-tetrahydronaphthalene (related to **Figure 1**) was obtained as a clear liquid. ^1H NMR (400 MHz, Chloroform-*d*) δ 7.14 (d, J = 7.8 Hz, 1H), 7.09 (s, 1H), 7.01 (d, J = 7.9 Hz, 1H), 6.65 (dd, J = 17.6, 10.9 Hz, 1H), 5.67 (d, J = 17.6 Hz, 1H), 5.15 (d, J = 10.9 Hz, 1H), 2.79 – 2.70 (m, 4H), 1.84 – 1.74 (m, 4H). ^{13}C NMR (100 MHz, Chloroform-*d*) δ 137.19, 137.03, 136.91, 134.91, 129.32, 127.05, 123.27, 112.64, 29.46, 29.28, 23.26.

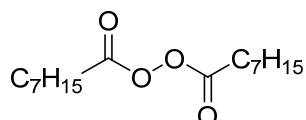


Following procedure B for synthesis of alkenes, (8*R*,9*S*,13*S*,14*S*)-13-Methyl-3-vinyl-6,7,8,9,11,12,13,14,15,16-decahydro-17*H*-cyclopenta[*a*]phenanthren-17-one (compound **57**, related to **scheme 2**) was obtained as a white solid. ^1H NMR (400 MHz, Chloroform-*d*) δ 7.28 – 7.20 (m, 2H), 7.14 (s, 1H), 6.66 (dd, J = 17.6, 10.9 Hz, 1H), 5.70 (dd, J = 17.6, 1.0 Hz, 1H), 5.19 (dd, J = 10.9, 0.9 Hz, 1H), 2.91 (dd, J = 9.0, 4.2 Hz, 2H), 2.50 (dd, J = 18.8, 8.7 Hz, 1H), 2.45 – 2.39 (m, 1H), 2.34 – 2.25 (m, 1H), 2.19 – 1.93 (m, 4H), 1.66 – 1.41 (m, 6H), 0.91 (s, 3H). ^{13}C NMR (100 MHz, Chloroform-*d*) δ 220.89, 139.55, 136.59, 135.22, 126.89, 125.56, 123.62, 113.20, 50.52, 48.00, 44.46, 38.18, 35.88, 31.61, 29.40, 26.52, 25.74, 21.61, 13.87. The spectrum data matches previously reported values

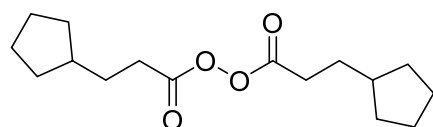
(Huang and Doyle, 2012)



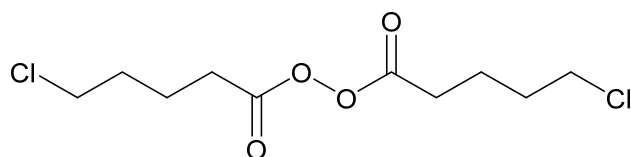
Following procedure C for synthesis of diacyl peroxides, hexanoic peroxyanhydride (related to **Figure 3**) was obtained as a clear liquid. 1H NMR (400 MHz, Chloroform-*d*) δ 2.42 (t, $J = 7.5$ Hz, 4H), 1.78 – 1.66 (m, 4H), 1.41 – 1.29 (m, 8H), 0.91 (t, $J = 7.1$ Hz, 6H). ^{13}C NMR (100 MHz, Chloroform-*d*) δ 169.25, 31.03, 29.95, 24.49, 22.15, 13.78.



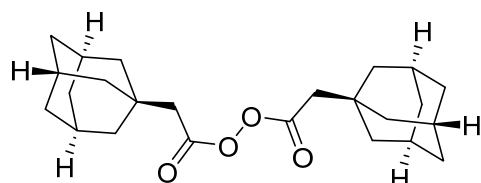
Following procedure C for synthesis of diacyl peroxides, octanoic peroxyanhydride (related to **Figure 3**) was obtained as a clear liquid. 1H NMR (400 MHz, Chloroform-*d*) δ 2.42 (t, $J = 7.5$ Hz, 4H), 1.71 (p, $J = 7.4$ Hz, 4H), 1.42 – 1.22 (m, 16H), 0.87 (t, 6H). ^{13}C NMR (100 MHz, Chloroform-*d*) δ 169.25, 31.54, 30.00, 28.87, 28.75, 24.81, 22.55, 14.00.



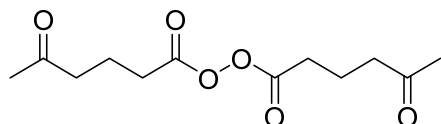
Following procedure C for synthesis of diacyl peroxides, 3-cyclopentylpropanoic peroxyanhydride (related to **Figure 3**) was obtained as a clear liquid. 1H NMR (400 MHz, Chloroform-*d*) δ 2.44 (t, $J = 7.8$ Hz, 4H), 1.86 – 1.69 (m, 10H), 1.68 – 1.49 (m, 8H), 1.17 – 1.03 (m, 4H). ^{13}C NMR (100 MHz, Chloroform-*d*) δ 169.39, 39.46, 32.29, 30.94, 29.35, 25.10.



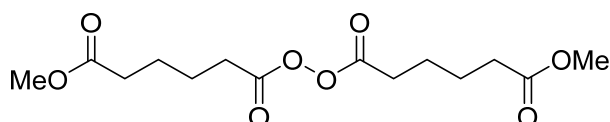
Following procedure C for synthesis of diacyl peroxides, 5-chloropentanoic peroxyanhydride (related to **Figure 3**) was obtained as a clear liquid. 1H NMR (400 MHz, Chloroform-*d*) δ 3.61 – 3.54 (m, 4H), 2.53 – 2.45 (m, 4H), 1.97 – 1.82 (m, 8H). ^{13}C NMR (100 MHz, Chloroform-*d*) δ 168.70, 44.17, 31.36, 29.14, 22.09.



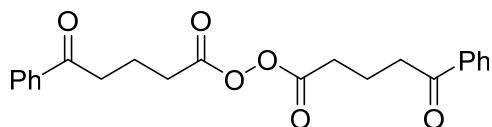
Following procedure C for synthesis of diacyl peroxides, 2-((3*r*,5*r*,7*r*)-adamantan-1-yl)acetic peroxyanhydride (related to **Figure 3**) was obtained as a white solid. 1H NMR (400 MHz, Chloroform-*d*) δ 2.19 (s, 4H), 2.00 (s, 6H), 1.74 – 1.62 (m, 24H). ^{13}C NMR (100 MHz, Chloroform-*d*) δ 166.72, 44.46, 42.11, 36.53, 32.99, 28.55.



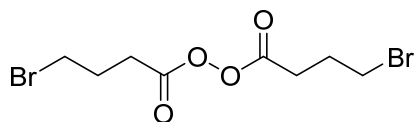
Following procedure C for synthesis of diacyl peroxides, 5-oxohexanoic peroxyanhydride (related to **Figure 3**) was obtained as a white solid. ^1H NMR (400 MHz, Chloroform-*d*) δ 2.60 (t, $J = 7.0$ Hz, 4H), 2.49 (t, $J = 7.1$ Hz, 4H), 2.16 (s, 6H), 1.97 (p, $J = 6.9$ Hz, 4H). ^{13}C NMR (100 MHz, Chloroform-*d*) δ 207.42, 168.74, 41.59, 29.94, 28.88, 18.63.



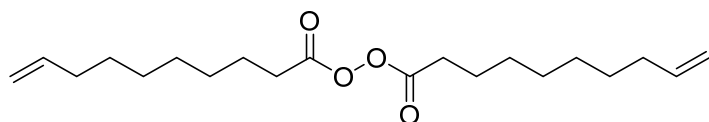
Following procedure C for synthesis of diacyl peroxides, 6-methoxy-6-oxohexanoic peroxyanhydride (related to **Figure 3**) was obtained as a white solid. ^1H NMR (400 MHz, Chloroform-*d*) δ 3.67 (s, 6H), 2.46 (t, $J = 7.0$ Hz, 4H), 2.35 (t, $J = 6.9$ Hz, 4H), 1.81 – 1.68 (m, 8H). ^{13}C NMR (100 MHz, Chloroform-*d*) δ 173.46, 168.75, 51.59, 33.42, 29.65, 24.21, 24.09.



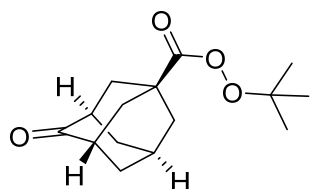
Following procedure C for synthesis of diacyl peroxides, 5-oxo-5-phenylpentanoic peroxyanhydride (related to **Figure 3**) was obtained as a white solid. ^1H NMR (400 MHz, Chloroform-*d*) δ 8.00 – 7.93 (m, 4H), 7.63 – 7.54 (m, 2H), 7.53 – 7.42 (m, 4H), 3.14 (t, $J = 7.0$ Hz, 4H), 2.60 (t, $J = 7.0$ Hz, 4H), 2.18 (p, $J = 7.0$ Hz, 4H). ^{13}C NMR (100 MHz, Chloroform-*d*) δ 198.85, 168.92, 136.68, 133.21, 128.64, 128.03, 36.85, 29.23, 19.20.



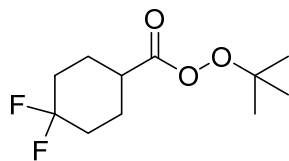
Following procedure C for synthesis of diacyl peroxides, 4-bromobutanoic peroxyanhydride (related to **Figure 3**) was obtained as a clear liquid. ^1H NMR (400 MHz, Chloroform-*d*) δ 3.55 – 3.40 (m, 4H), 2.69 – 2.56 (m, 4H), 2.31 – 2.14 (m, 4H). ^{13}C NMR (100 MHz, Chloroform-*d*) δ 168.19, 31.77, 28.39, 27.60.



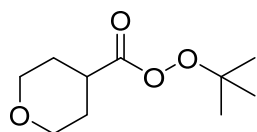
Following procedure C for synthesis of diacyl peroxides, dec-9-enoic peroxyanhydride (related to **Figure 3**) was obtained as a clear liquid. ^1H NMR (400 MHz, Chloroform-*d*) δ 5.88 – 5.72 (m, 2H), 5.17 – 4.77 (m, 4H), 2.42 (t, $J = 7.4$ Hz, 4H), 2.11 – 1.94 (m, 4H), 1.80 – 1.64 (m, 4H), 1.52 – 1.16 (m, 16H). ^{13}C NMR (100 MHz, Chloroform-*d*) δ 169.20, 138.99, 114.23, 33.71, 29.97, 28.92, 28.84, 28.80, 28.78, 24.78.



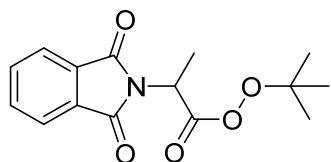
Following procedure D for synthesis of peresters, *tert*-butyl (1*s*,3*r*,5*s*,7*s*)-4-oxoadamantane-1-carboperoxoate (related to **Figure 2**) was obtained as a clear liquid. ^1H NMR (400 MHz, Chloroform-*d*) δ 2.62 (t, $J = 3.0$ Hz, 2H), 2.27 (d, $J = 2.9$ Hz, 4H), 2.22 (q, $J = 3.1$ Hz, 1H), 2.19 (d, $J = 3.2$ Hz, 2H), 2.11 – 1.99 (m, 4H), 1.32 (s, 9H). ^{13}C NMR (100 MHz, Chloroform-*d*) δ 215.64, 172.31, 83.74, 45.66, 40.59, 39.99, 38.12, 37.81, 27.15, 26.07.



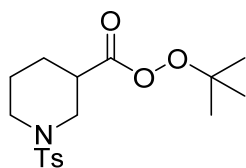
Following procedure D for synthesis of peresters, *tert*-butyl 4,4-difluorocyclohexane-1-carboperoxoate (related to **Figure 2**) was obtained as a white solid. ^1H NMR (400 MHz, Chloroform-*d*) δ 2.54 – 2.44 (m, 1H), 2.21 – 2.08 (m, 2H), 2.06 – 1.71 (m, 6H), 1.33 (s, 9H). ^{13}C NMR (100 MHz, Chloroform-*d*) δ 171.35, 122.25 (t, $J = 241.2$ Hz), 83.65, 38.63, 32.45 (t, $J = 24.7$ Hz), 26.11, 25.22 (dd, $J = 7.8$ Hz, $J = 2.5$ Hz). ^{19}F NMR (376 MHz, Chloroform-*d*) δ -94.22 (d, $J = 238.5$ Hz), -99.94 (d, $J = 237.9$ Hz).



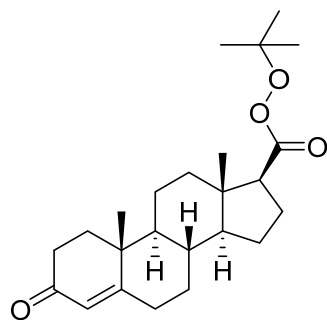
Following procedure D for synthesis of peresters, *tert*-butyl tetrahydro-2*H*-pyran-4-carboperoxoate (related to **Figure 2**) was obtained as a clear liquid. ^1H NMR (400 MHz, Chloroform-*d*) δ 4.00 (t, $J = 3.6$ Hz, 1H), 3.97 (t, $J = 3.6$ Hz, 1H), 3.48 – 3.41 (m, 2H), 2.68 – 2.59 (m, 1H), 1.93 – 1.82 (m, 4H), 1.33 (s, 9H). ^{13}C NMR (100 MHz, Chloroform-*d*) δ 171.51, 83.58, 66.87, 38.30, 28.58, 26.11.



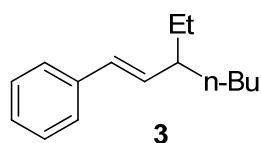
Following procedure D for synthesis of peresters, *tert*-butyl 2-(1,3-dioxoisindolin-2-yl)propaneperoxoate (related to **Figure 2**) was obtained as a clear liquid. ^1H NMR (400 MHz, Chloroform-*d*) δ 7.83 – 7.78 (m, 2H), 7.71 – 7.66 (m, 2H), 5.00 (q, J = 7.3 Hz, 1H), 1.68 (d, J = 7.3 Hz, 3H), 1.21 (s, 9H). ^{13}C NMR (100 MHz, Chloroform-*d*) δ 167.08, 166.96, 134.35, 131.73, 123.59, 84.49, 46.38, 26.04, 15.28.



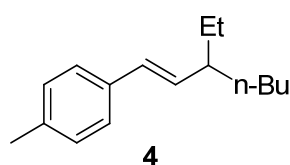
Following procedure D for synthesis of peresters, *tert*-butyl 1-tosylpiperidine-3-carboperoxoate (related to **Figure 2**) was obtained as a white solid. ^1H NMR (400 MHz, Chloroform-*d*) δ 7.64 (d, J = 8.1 Hz, 2H), 7.33 (d, J = 8.0 Hz, 2H), 3.80 (dd, J = 11.6, 3.7 Hz, 1H), 3.66 – 3.56 (m, 1H), 2.77 – 2.65 (m, 1H), 2.56 (t, J = 10.9 Hz, 1H), 2.44 (s, 3H), 2.40 – 2.29 (m, 1H), 2.03 – 1.88 (m, 1H), 1.83 – 1.76 (m, 1H), 1.73 – 1.61 (m, 1H), 1.56 – 1.42 (m, 1H), 1.33 (s, 9H). ^{13}C NMR (100 MHz, Chloroform-*d*) δ 170.12, 143.81, 132.89, 129.78, 127.66, 83.94, 47.55, 46.19, 39.23, 26.67, 26.12, 23.84, 21.54.



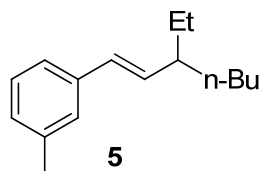
Following procedure D for synthesis of peresters, *tert*-butyl(8*S*,9*S*,10*R*,13*S*,14*S*,17*S*)-10,13-dimethyl-3-oxo-2,3,6,7,8,9,10,11,12,13,14,15,16,17-tetradecahydro-1*H*-cyclopenta[*a*]phenanthrene-17-carboperoxoate (compound **55**, related to **scheme 2**) was obtained as a white solid. ^1H NMR (400 MHz, Chloroform-*d*) δ 5.74 (s, 1H), 2.50 – 2.25 (m, 5H), 2.24 – 2.13 (m, 1H), 2.09 – 2.00 (m, 2H), 1.95 – 1.82 (m, 2H), 1.80 – 1.66 (m, 3H), 1.64 – 1.56 (m, 3H), 1.51 – 1.39 (m, 1H), 1.33 (s, 9H), 1.19 (s, 3H), 1.15 – 1.04 (m, 2H), 1.02 – 0.92 (m, 1H), 0.80 (s, 3H). ^{13}C NMR (100 MHz, Chloroform-*d*) δ 199.42, 170.94, 170.84, 123.96, 82.94, 55.30, 53.66, 52.67, 44.14, 38.59, 37.89, 35.72, 35.67, 33.95, 32.76, 31.88, 26.32, 24.45, 23.88, 20.90, 17.38, 13.46.



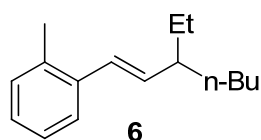
Following the procedure E, product **3** (related to **Figure 1**) was obtained as a clear liquid (75.8 mg, 75% yield). ¹H NMR (400 MHz, Chloroform-*d*) δ 7.36 (d, *J* = 7.5 Hz, 2H), 7.29 (t, *J* = 7.5 Hz, 2H), 7.18 (t, *J* = 7.2 Hz, 1H), 6.32 (d, *J* = 15.8 Hz, 1H), 5.95 (dd, *J* = 15.8, 9.0 Hz, 1H), 2.05 – 1.95 (m, 1H), 1.52 – 1.40 (m, 2H), 1.34 – 1.22 (m, 6H), 0.88 (t, *J* = 7.5 Hz, 6H). ¹³C NMR (100 MHz, Chloroform-*d*) δ 138.09, 135.64, 129.78, 128.55, 126.82, 126.08, 45.30, 35.02, 29.78, 28.36, 23.02, 14.24, 11.98. The spectrum data matches previously reported values (Xu et al., 2017).



Following the procedure E, product **4** (related to **Figure 1**) was obtained as a clear liquid (87.5 mg, 81% yield). ¹H NMR (400 MHz, Chloroform-*d*) δ 7.25 (d, *J* = 7.8 Hz, 2H), 7.09 (d, *J* = 7.7 Hz, 2H), 6.29 (d, *J* = 15.8 Hz, 1H), 5.89 (dd, *J* = 15.8, 9.0 Hz, 1H), 2.32 (s, 3H), 2.03 – 1.94 (m, 1H), 1.52 – 1.39 (m, 2H), 1.37 – 1.20 (m, 6H), 0.87 (t, *J* = 7.2 Hz, 6H). ¹³C NMR (100 MHz, Chloroform-*d*) δ 136.41, 135.24, 134.61, 129.44, 129.17, 125.87, 45.19, 34.97, 29.69, 28.31, 22.93, 21.16, 14.17, 11.91. HRMS (EI+) calcd for [C₁₆H₂₄]⁺ ([M]⁺): 216.1878, found: 216.1887.

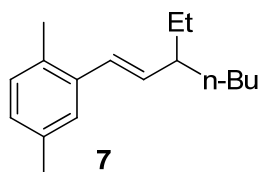


Following the procedure E, product **5** (related to **Figure 1**) was obtained as a clear liquid (78.8 mg, 73% yield). ¹H NMR (400 MHz, Chloroform-*d*) δ 7.21 – 7.13 (m, 3H), 7.00 (d, *J* = 7.2 Hz, 1H), 6.29 (d, *J* = 15.8 Hz, 1H), 5.94 (dd, *J* = 15.8, 9.0 Hz, 1H), 2.33 (s, 3H), 2.05 – 1.95 (m, 1H), 1.52 – 1.41 (m, 2H), 1.35 – 1.24 (m, 6H), 0.88 (t, *J* = 7.4 Hz, 6H). ¹³C NMR (100 MHz, Chloroform-*d*) δ 138.01, 135.40, 129.81, 128.45, 127.59, 126.74, 123.24, 45.31, 35.03, 29.76, 28.37, 22.99, 21.49, 14.21, 11.96. HRMS (EI+) calcd for [C₁₆H₂₄]⁺ ([M]⁺): 216.1878, found: 216.1880.

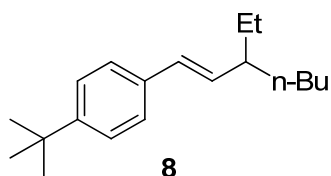


Following the procedure E, product **6** (related to **Figure 1**) was obtained as a clear liquid (79.9 mg, 74% yield). ¹H NMR (400 MHz, Chloroform-*d*) δ 7.41 (d, *J* = 7.0 Hz, 1H), 7.16 – 7.08 (m, 3H), 6.50 (d, *J* = 15.6 Hz, 1H), 5.79 (dd, *J* = 15.6, 9.0 Hz, 1H), 2.33 (s, 3H), 2.07 – 1.98 (m, 1H), 1.52 – 1.45 (m, 2H), 1.36 – 1.27 (m, 6H), 0.90 (t, *J* = 7.4 Hz, 6H). ¹³C NMR (100 MHz, Chloroform-*d*) δ 137.33, 137.09, 134.90, 130.12, 127.66, 126.72, 126.00, 125.61, 45.45, 34.91,

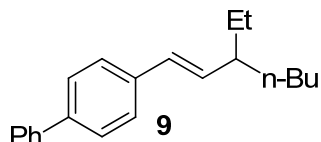
29.70, 28.29, 22.88, 19.91, 14.17, 11.93. HRMS (EI+) calcd for [C₁₆H₂₄]⁺ ([M]⁺): 216.1878, found: 216.1883.



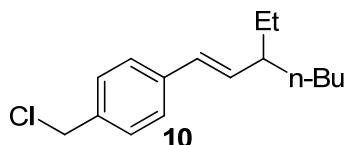
Following the procedure E, product **7** (related to **Figure 1**) was obtained as a clear liquid (90.7 mg, 79% yield). ¹H NMR (400 MHz, Chloroform-*d*) δ 7.24 (s, 1H), 7.01 (d, *J* = 7.7 Hz, 1H), 6.93 (dd, *J* = 7.8, 1.9 Hz, 1H), 6.48 (d, *J* = 15.6 Hz, 1H), 5.77 (dd, *J* = 15.7, 9.1 Hz, 1H), 2.31 (s, 3H), 2.29 (s, 3H), 2.07 – 1.98 (m, 1H), 1.54 – 1.42 (m, 2H), 1.37 – 1.25 (m, 6H), 0.93 – 0.86 (m, 6H). ¹³C NMR (100 MHz, Chloroform-*d*) δ 137.01, 136.75, 135.32, 131.84, 130.07, 127.70, 127.48, 126.16, 45.48, 34.95, 29.70, 28.32, 22.88, 21.07, 19.43, 14.17, 11.94. HRMS (EI+) calcd for [C₁₇H₂₆]⁺ ([M]⁺): 230.2035, found: 230.2028.



Following the procedure E, product **8** (related to **Figure 1**) was obtained as a clear liquid (108 mg, 84% yield). ¹H NMR (400 MHz, Chloroform-*d*) δ 7.43 – 7.26 (m, 4H), 6.30 (d, *J* = 15.8 Hz, 1H), 5.91 (dd, *J* = 15.8, 9.0 Hz, 1H), 2.06 – 1.95 (m, 1H), 1.53 – 1.41 (m, 2H), 1.35 – 1.24 (m, 15H), 0.87 (t, *J* = 7.3 Hz, 6H). ¹³C NMR (100 MHz, Chloroform-*d*) δ 149.75, 135.25, 134.86, 129.36, 125.68, 125.42, 45.27, 35.02, 34.52, 31.38, 29.71, 28.37, 22.92, 14.18, 11.93. HRMS (EI+) calcd for [C₁₉H₃₀]⁺ ([M]⁺): 258.2348, found: 258.2343.

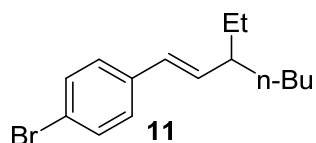


Following the procedure E, product **9** (related to **Figure 1**) was obtained as a white solid (94.5 mg, 68% yield). ¹H NMR (400 MHz, Chloroform-*d*) δ 7.59 – 7.55 (m, 2H), 7.54 – 7.50 (m, 2H), 7.43 – 7.38 (m, 4H), 7.33 – 7.26 (m, 1H), 6.36 (d, *J* = 15.8 Hz, 1H), 6.00 (dd, *J* = 15.8, 9.0 Hz, 1H), 2.08 – 1.97 (m, 1H), 1.55 – 1.44 (m, 2H), 1.37 – 1.24 (m, 6H), 0.92 – 0.85 (m, 6H). ¹³C NMR (100 MHz, Chloroform-*d*) δ 141.01, 139.61, 137.12, 135.90, 129.26, 128.82, 127.26, 127.19, 126.98, 126.45, 45.34, 34.99, 29.76, 28.34, 22.99, 14.23, 11.98. HRMS (EI+) calcd for [C₂₁H₂₆]⁺ ([M]⁺): 278.2035, found: 278.2040.

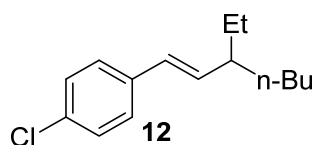


Following the procedure E, product **10** (related to **Figure 1**) was obtained as a clear liquid (87.6 mg, 70% yield). ¹H NMR (400 MHz, Chloroform-*d*) δ 7.36 – 7.28 (m, 4H), 6.32 (d, *J* = 15.8 Hz, 1H), 5.97 (dd, *J* = 15.8, 9.0 Hz, 1H), 4.57 (s, 2H), 2.07 – 1.96 (m, 1H), 1.53 – 1.41 (m, 2H), 1.35 – 1.23 (m, 6H), 0.87 (t, *J* = 7.3 Hz, 6H). ¹³C NMR (100 MHz, Chloroform-*d*) δ 138.25,

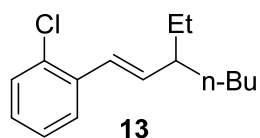
136.53, 135.80, 128.98, 128.83, 126.27, 46.26, 45.20, 34.81, 29.65, 28.17, 22.87, 14.12, 11.86. HRMS (EI+) calcd for $[C_{16}H_{24}Cl]^+$ ($[M]^+$): 250.1488, found: 250.1485.



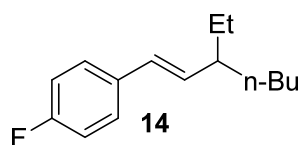
Following the procedure E product **11** (related to **Figure 1**) was obtained as a clear liquid (105.4 mg, 75% yield). 1H NMR (400 MHz, Chloroform-*d*) δ 7.40 (d, $J = 8.5$ Hz, 2H), 7.21 (d, $J = 8.5$ Hz, 2H), 6.26 (d, $J = 15.8$ Hz, 1H), 5.94 (dd, $J = 15.8, 9.0$ Hz, 1H), 2.05 – 1.95 (m, 1H), 1.51 – 1.42 (m, 2H), 1.35 – 1.22 (m, 6H), 0.87 (t, $J = 7.4$ Hz, 6H). ^{13}C NMR (100 MHz, Chloroform-*d*) δ 136.89, 136.53, 131.49, 128.46, 127.51, 120.30, 45.17, 34.74, 29.64, 28.10, 22.87, 14.12, 11.86. HRMS (EI+) calcd for $[C_{15}H_{21}Br]^+$ ($[M]^+$): 280.0827, found: 280.0829.



Following the procedure E, product **12** (related to **Figure 1**) was obtained as a clear liquid (93.9 mg, 80% yield). 1H NMR (400 MHz, Chloroform-*d*) δ 7.29 – 7.22 (m, 4H), 6.27 (d, $J = 15.8$ Hz, 1H), 5.93 (dd, $J = 15.8, 9.0$ Hz, 1H), 2.06 – 1.95 (m, 1H), 1.54 – 1.41 (m, 2H), 1.35 – 1.24 (m, 6H), 0.87 (t, $J = 7.4$ Hz, 6H). ^{13}C NMR (100 MHz, Chloroform-*d*) δ 136.48, 136.39, 132.25, 128.57, 128.44, 127.17, 45.16, 34.78, 29.65, 28.13, 22.88, 14.12, 11.85. The spectrum data matches previously reported values (Mai et al., 2016)

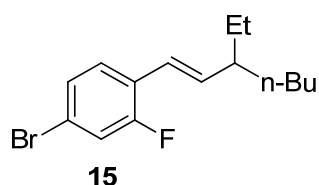


Following the procedure E, product **13** (related to **Figure 1**) was obtained as a clear liquid (81.3 mg, 69% yield). 1H NMR (400 MHz, Chloroform-*d*) δ 7.51 (dd, $J = 7.8, 1.8$ Hz, 1H), 7.32 (d, $J = 7.9$ Hz, 1H), 7.19 (t, $J = 7.4$ Hz, 1H), 7.15 – 7.09 (m, 1H), 6.70 (d, $J = 15.8$ Hz, 1H), 5.93 (dd, $J = 15.8, 9.0$ Hz, 1H), 2.13 – 2.04 (m, 1H), 1.52 – 1.43 (m, 2H), 1.35 – 1.27 (m, 6H), 0.90 (t, $J = 7.8$ Hz, 6H). ^{13}C NMR (100 MHz, Chloroform-*d*) δ 138.53, 136.11, 132.55, 129.57, 127.74, 126.68, 125.97, 45.21, 34.70, 29.59, 28.09, 22.86, 14.12, 11.84. HRMS (EI+) calcd for $[C_{15}H_{21}Cl]^+$ ($[M]^+$): 236.1332, found: 236.1329.

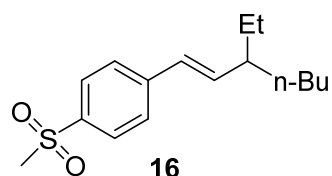


Following the procedure E, product **14** (related to **Figure 1**) was obtained as a clear liquid (76.8 mg, 70% yield). 1H NMR (400 MHz, Chloroform-*d*) δ 7.30 (dd, $J = 8.6, 5.4$ Hz, 2H), 6.97 (t, $J = 8.6$ Hz, 2H), 6.28 (d, $J = 15.8$ Hz, 1H), 5.86 (dd, $J = 15.8, 9.0$ Hz, 1H), 2.04 – 1.94 (m, 1H), 1.52 – 1.41 (m, 2H), 1.35 – 1.22 (m, 6H), 0.88 (t, $J = 7.4$ Hz, 6H). ^{13}C NMR (100 MHz, Chloroform-*d*) δ 161.85 (d, $J = 245.4$ Hz), 135.34 (d, $J = 2.2$ Hz), 134.13 (d, $J = 3.3$ Hz), 128.43, 127.33 (d, $J = 7.7$ Hz), 115.26 (d, $J = 21.5$ Hz), 45.13, 34.85, 29.66, 28.20, 22.89, 14.12, 11.86. ^{19}F NMR (376 MHz, Chloroform-*d*) δ -115.97. HRMS (EI+) calcd for $[C_{15}H_{21}F]^+$ ($[M]^+$):

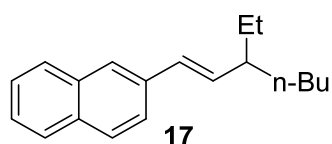
220.1627, found: 220.1621.



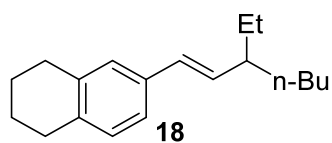
Following the procedure E, product **15** (related to **Figure 1**) was obtained as a clear liquid (80.5 mg, 54% yield). ^1H NMR (400 MHz, Chloroform-*d*) δ 7.31 (t, $J = 8.3$ Hz, 1H), 7.23 – 7.17 (m, 2H), 6.40 (d, $J = 16.0$ Hz, 1H), 6.03 (dd, $J = 16.0, 9.0$ Hz, 1H), 2.09 – 1.99 (m, 1H), 1.53 – 1.42 (m, 2H), 1.36 – 1.25 (m, 6H), 0.88 (t, $J = 7.4$ Hz, 6H). ^{13}C NMR (100 MHz, Chloroform-*d*) δ 159.57 (d, $J = 252.6$ Hz), 139.09 (d, $J = 4.3$ Hz), 128.01 (d, $J = 4.8$ Hz), 127.26 (d, $J = 3.6$ Hz), 124.87 (d, $J = 12.5$ Hz), 120.99 (d, $J = 3.3$ Hz), 119.90 (d, $J = 9.7$ Hz), 119.19 (d, $J = 25.7$ Hz), 45.57, 34.63, 29.60, 28.00, 22.84, 14.09, 11.81. ^{19}F NMR (376 MHz, Chloroform-*d*) δ -116.27. HRMS (EI+) calcd for $[\text{C}_{15}\text{H}_{20}\text{BrF}]^+$ ($[\text{M}]^+$): 298.0732, found: 298.0739.



Following the procedure E, product **16** (related to **Figure 1**) was obtained as a white solid (33.6 mg, 24% yield). ^1H NMR (400 MHz, Chloroform-*d*) δ 7.78 (d, $J = 8.4$ Hz, 2H), 7.44 (d, $J = 8.4$ Hz, 2H), 6.31 (d, $J = 15.8$ Hz, 1H), 6.08 (dd, $J = 15.8, 9.0$ Hz, 1H), 2.96 (s, 3H), 2.05 – 1.93 (m, 1H), 1.50 – 1.36 (m, 2H), 1.29 – 1.18 (m, 6H), 0.81 (t, $J = 7.5$ Hz, 6H). ^{13}C NMR (100 MHz, Chloroform-*d*) δ 143.44, 140.29, 138.16, 128.11, 127.69, 126.59, 45.32, 44.64, 34.57, 29.62, 27.96, 22.82, 14.08, 11.83. HRMS (EI+) calcd for $[\text{C}_{16}\text{H}_{24}\text{O}_2\text{S}]^+$ ($[\text{M}]^+$): 280.1497, found: 280.1501.

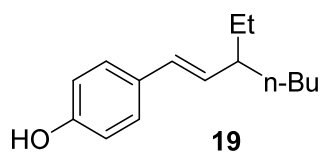


Following the procedure E, product **17** (related to **Figure 2**) was obtained as a clear liquid (91.9 mg, 73% yield). ^1H NMR (400 MHz, Chloroform-*d*) δ 7.84-7.78 (m, 3H), 7.72 (s, 1H), 7.63 (dd, $J = 8.6, 1.8$ Hz, 1H), 7.50 – 7.41 (m, 2H), 6.53 (d, $J = 15.8$ Hz, 1H), 6.13 (dd, $J = 15.8, 9.0$ Hz, 1H), 2.16 – 2.06 (m, 1H), 1.60 – 1.52 (m, 2H), 1.43 – 1.30 (m, 6H), 0.97 – 0.91 (m, 6H). ^{13}C NMR (100 MHz, Chloroform-*d*) δ 136.16, 135.44, 133.75, 132.64, 129.72, 128.00, 127.79, 127.62, 126.11, 125.39, 125.27, 123.68, 45.30, 34.91, 29.69, 28.26, 22.91, 14.14, 11.92. HRMS (EI+) calcd for $[\text{C}_{19}\text{H}_{24}]^+$ ($[\text{M}]^+$): 252.1878, found: 252.1873.

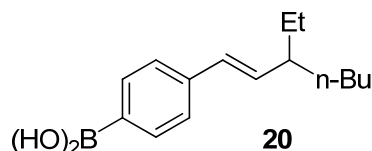


Following the procedure E, product **18** (related to **Figure 1**) was obtained as a clear liquid (79.8 mg, 63% yield). ^1H NMR (400 MHz, Chloroform-*d*) δ 7.10 (dd, $J = 7.9, 1.4$ Hz, 1H), 7.05 (s, 1H), 6.98 (d, $J = 7.9$ Hz, 1H), 6.25 (d, $J = 15.8$ Hz, 1H), 5.87 (dd, $J = 15.8, 9.0$ Hz, 1H), 2.74

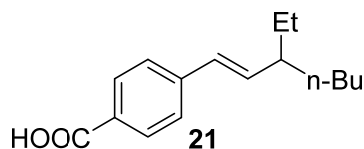
(d, $J = 6.1$ Hz, 4H), 2.04 – 1.93 (m, 1H), 1.82 – 1.74 (m, 4H), 1.52 – 1.40 (m, 2H), 1.33 – 1.23 (m, 6H), 0.87 (t, $J = 7.4$ Hz, 6H). ^{13}C NMR (100 MHz, Chloroform- d) δ 137.11, 135.86, 135.31, 134.47, 129.59, 129.27, 126.62, 123.16, 45.22, 35.00, 29.69, 29.49, 29.21, 28.35, 23.34, 23.32, 22.91, 14.16, 11.90. HRMS (EI+) calcd for $[\text{C}_{19}\text{H}_{28}]^+$ ($[\text{M}]^+$): 256.2191, found: 256.2197.



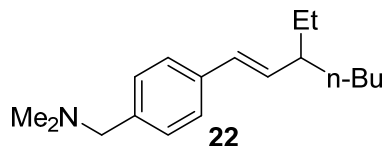
Following the procedure E, product **19** (related to **Figure 1**) was obtained as a clear liquid (89.3 mg, 82% yield). ^1H NMR (400 MHz, Chloroform- d) δ 7.24 (d, $J = 8.7$ Hz, 2H), 6.76 (d, $J = 8.5$ Hz, 2H), 6.25 (d, $J = 15.8$ Hz, 1H), 5.79 (dd, $J = 15.8, 9.0$ Hz, 1H), 4.88 (s, 1H), 2.02 – 1.94 (m, 1H), 1.52 – 1.38 (m, 2H), 1.32 – 1.25 (m, 6H), 0.87 (t, $J = 7.4$ Hz, 6H). ^{13}C NMR (100 MHz, Chloroform- d) δ 154.48, 133.55, 131.06, 128.82, 127.21, 115.33, 45.08, 34.94, 29.64, 28.28, 22.89, 14.12, 11.86. HRMS (EI+) calcd for $[\text{C}_{15}\text{H}_{22}\text{O}]^+$ ($[\text{M}]^+$): 218.1671, found: 218.1673.



Following the procedure E, product **20** (related to **Figure 1**) was obtained as a light yellow oil (43.9 mg, 36% yield). ^1H NMR (400 MHz, Chloroform- d) δ 8.17 (d, $J = 7.8$ Hz, 2H), 7.50 (d, $J = 7.9$ Hz, 2H), 6.43 (d, $J = 15.8$ Hz, 1H), 6.15 (dd, $J = 15.8, 8.9$ Hz, 1H), 2.10 (m, 1H), 1.61 – 1.47 (m, 2H), 1.44 – 1.30 (m, 6H), 0.96 – 0.90 (m, 6H). ^{13}C NMR (100 MHz, Chloroform- d) δ 142.23, 137.77, 136.14, 129.90, 125.73, 45.50, 34.99, 29.88, 28.35, 23.11, 14.34, 12.11. HRMS (DART-) calcd for $[\text{C}_{15}\text{H}_{22}\text{O}_2^{10}\text{B}]^-$ ($[\text{M}-\text{H}]^-$): 244.1755, found: 244.1757.

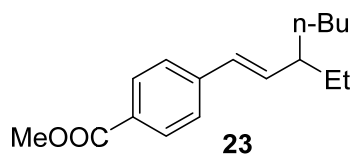


Following the procedure E, product **21** (related to **Figure 1**) was obtained as a clear liquid (64 mg, 52% yield). ^1H NMR (400 MHz, Chloroform- d) δ 8.04 (d, $J = 8.3$ Hz, 2H), 7.44 (d, $J = 8.3$ Hz, 2H), 6.38 (d, $J = 15.8$ Hz, 1H), 6.13 (dd, $J = 15.8, 9.0$ Hz, 1H), 2.13 – 2.00 (m, 1H), 1.56 – 1.44 (m, 2H), 1.32 – 1.25 (m, 6H), 0.91 – 0.86 (m, 6H). ^{13}C NMR (100 MHz, Chloroform- d) δ 171.83, 143.37, 139.21, 130.55, 128.87, 127.33, 125.91, 45.32, 34.67, 29.63, 28.04, 22.85, 14.09, 11.85. HRMS (EI+) calcd for $[\text{C}_{16}\text{H}_{22}\text{O}_2]^+$ ($[\text{M}]^+$): 246.1620, found: 246.1621.

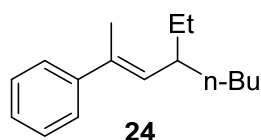


Following the procedure E, product **22** (related to **Figure 1**) was obtained as a clear liquid (65 mg, 50% yield). ^1H NMR (400 MHz, Chloroform- d) δ 7.32 (d, $J = 8.1$ Hz, 2H), 7.23 (d, $J = 7.9$ Hz, 2H), 6.32 (d, $J = 15.8$ Hz, 1H), 5.95 (dd, $J = 15.8, 9.0$ Hz, 1H), 3.40 (s, 2H), 2.24 (s, 6H), 2.07 – 1.95 (m, 1H), 1.54 – 1.43 (m, 2H), 1.31 – 1.26 (m, 6H), 0.92 – 0.85 (m, 6H). ^{13}C NMR (100 MHz, Chloroform- d) δ 137.27, 136.89, 135.33, 129.33, 129.28, 125.84, 64.11, 45.31, 45.16, 34.88, 29.64, 28.23, 22.88, 14.12, 11.87. HRMS (EI+) calcd for $[\text{C}_{18}\text{H}_{29}\text{N}]^+$ ($[\text{M}]^+$):

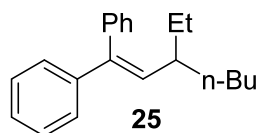
259.2300, found: 259.2305.



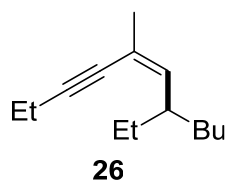
Following the procedure E, product **23** (related to **Figure 1**) was obtained as a clear liquid (66.3 mg, 51% yield). ^1H NMR (400 MHz, Chloroform-*d*) δ 7.88 (d, J = 8.4 Hz, 2H), 7.32 (d, J = 8.4 Hz, 2H), 6.28 (d, J = 15.8 Hz, 1H), 6.02 (dd, J = 15.8, 9.0 Hz, 1H), 3.82 (s, 3H), 2.01 – 1.92 (m, 1H), 1.50 – 1.33 (m, 2H), 1.32 – 1.14 (m, 6H), 0.81 (t, J = 7.5 Hz, 6H). ^{13}C NMR (100 MHz, Chloroform-*d*) δ 167.00, 142.49, 138.63, 129.87, 128.90, 128.19, 125.79, 51.97, 45.29, 34.68, 29.63, 28.05, 22.85, 14.09, 11.84. HRMS (EI+) calcd for $[\text{C}_{17}\text{H}_{24}\text{O}_2]^+$ ($[\text{M}]^+$): 260.1776, found: 260.1778.



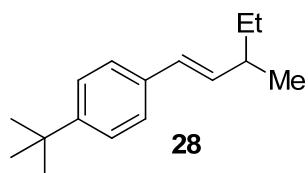
Following the procedure E, product **24** (related to **Figure 1**) was obtained as a clear liquid (88.5 mg, 82% yield). ^1H NMR (400 MHz, Chloroform-*d*) δ 7.42 – 7.36 (m, 2H), 7.30 (t, J = 7.7 Hz, 2H), 7.23 – 7.19 (m, 1H), 5.48 (d, J = 9.9 Hz, 1H), 2.36 – 2.27 (m, 1H), 2.03 (d, J = 1.4 Hz, 3H), 1.54 – 1.44 (m, 2H), 1.33 – 1.22 (m, 6H), 0.88 (t, J = 7.4 Hz, 6H). ^{13}C NMR (100 MHz, Chloroform-*d*) δ 144.52, 134.52, 134.42, 128.32, 126.60, 125.90, 40.63, 35.78, 29.98, 29.08, 23.21, 16.57, 14.37, 12.16. HRMS (EI+) calcd for $[\text{C}_{16}\text{H}_{24}]^+$ ($[\text{M}]^+$): 216.1878, found: 216.1875.



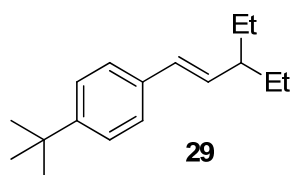
Following the procedure E, product **25** (related to **Figure 1**) was obtained as a clear liquid (129.7 mg, 93% yield). ^1H NMR (400 MHz, Chloroform-*d*) δ 7.37 – 7.32 (m, 2H), 7.30 – 7.21 (m, 5H), 7.21 – 7.13 (m, 3H), 5.82 (d, J = 10.5 Hz, 1H), 2.15 – 2.03 (m, 1H), 1.47 – 1.23 (m, 5H), 1.22 – 1.11 (m, 3H), 0.87 – 0.81 (m, 6H). ^{13}C NMR (100 MHz, Chloroform-*d*) δ 142.81, 141.37, 140.77, 135.25, 130.01, 128.08, 128.05, 127.01, 126.72, 126.63, 40.56, 35.47, 29.67, 28.82, 22.97, 14.11, 12.00. HRMS (EI+) calcd for $[\text{C}_{21}\text{H}_{26}]^+$ ($[\text{M}]^+$): 278.2035, found: 278.2038.



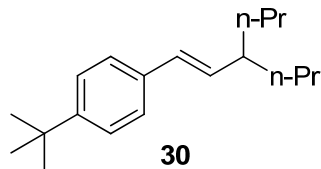
Following the procedure E, product **26** (related to **Figure 1**) was obtained as a clear liquid (68.2 mg, 71% yield). ^1H NMR (400 MHz, Chloroform-*d*) δ 5.27 (dd, J = 9.8, 1.6 Hz, 1H), 2.49 – 2.39 (m, 1H), 2.33 (q, J = 7.5 Hz, 2H), 1.82 (d, J = 1.4 Hz, 2H), 1.43 – 1.21 (m, 8H), 1.20 – 1.14 (m, 4H), 0.90 – 0.83 (m, 6H). ^{13}C NMR (100 MHz, Chloroform-*d*) δ 141.60, 117.98, 93.82, 79.91, 41.97, 34.89, 29.49, 28.32, 23.54, 22.90, 14.22, 14.13, 13.17, 11.77. HRMS (EI+) calcd for $[\text{C}_{14}\text{H}_{24}]^+$ ($[\text{M}]^+$): 192.1878, found: 192.1887.



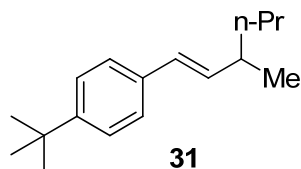
Following the procedure F, product **28** (related to **Figure 2**) was obtained as a clear liquid (97.2 mg, 90% yield). $^1\text{H NMR}$ (400 MHz, Chloroform-*d*) δ 7.34 – 7.27 (m, 4H), 6.32 (d, $J = 15.8$ Hz, 1H), 6.05 (dd, $J = 15.8, 7.9$ Hz, 1H), 2.24 – 2.14 (m, 1H), 1.45 – 1.35 (m, 2H), 1.31 (s, 9H), 1.06 (d, $J = 6.7$ Hz, 3H), 0.89 (t, $J = 7.4$ Hz, 3H). $^{13}\text{C NMR}$ (100 MHz, Chloroform-*d*) δ 149.76, 136.04, 135.22, 127.83, 125.65, 125.39, 38.96, 34.50, 31.35, 29.88, 20.33, 11.85. HRMS (EI+) calcd for $[\text{C}_{16}\text{H}_{24}]^+$ ($[\text{M}]^+$): 216.1878, found: 216.1877.



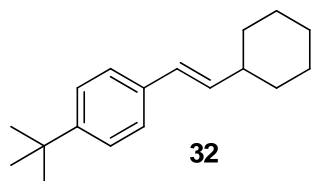
Following the procedure F, product **29** (related to **Figure 2**) was obtained as a clear liquid (93.4 mg, 81% yield). $^1\text{H NMR}$ (400 MHz, Chloroform-*d*) δ 7.36 – 7.27 (m, 4H), 6.31 (d, $J = 15.8$ Hz, 1H), 5.91 (dd, $J = 15.8, 8.9$ Hz, 1H), 1.97 – 1.87 (m, 1H), 1.52 – 1.44 (m, 2H), 1.33 – 1.28 (m, 11H), 0.87 (t, $J = 7.4$ Hz, 6H). $^{13}\text{C NMR}$ (100 MHz, Chloroform-*d*) δ 149.75, 135.23, 134.52, 129.54, 125.66, 125.38, 46.94, 34.50, 31.35, 27.91, 11.88. HRMS (EI+) calcd for $[\text{C}_{17}\text{H}_{26}]^+$ ($[\text{M}]^+$): 230.2035, found: 230.2030.



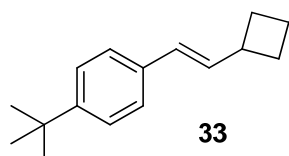
Following the procedure F, product **30** (related to **Figure 2**) was obtained as a clear liquid (105.8 mg, 82% yield). $^1\text{H NMR}$ (400 MHz, Chloroform-*d*) δ 7.35 – 7.27 (m, 4H), 6.29 (d, $J = 15.8$ Hz, 1H), 5.90 (dd, $J = 15.8, 9.1$ Hz, 1H), 2.18 – 2.08 (m, 1H), 1.37 – 1.25 (m, 17H), 0.87 (t, $J = 6.9$ Hz, 6H). $^{13}\text{C NMR}$ (100 MHz, Chloroform-*d*) δ 149.72, 135.18, 135.06, 129.06, 125.61, 125.38, 42.91, 37.84, 34.48, 31.33, 20.46, 14.19. HRMS (EI+) calcd for $[\text{C}_{19}\text{H}_{30}]^+$ ($[\text{M}]^+$): 258.2348, found: 258.2350.



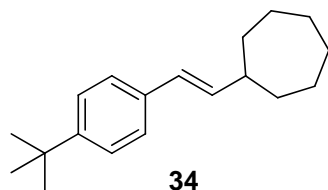
Following the procedure F, product **31** (related to **Figure 2**) was obtained as a clear liquid (90.9 mg, 79% yield). $^1\text{H NMR}$ (400 MHz, Chloroform-*d*) δ 7.33 – 7.26 (m, 4H), 6.31 (d, $J = 15.8$ Hz, 1H), 6.04 (dd, $J = 15.8, 8.0$ Hz, 1H), 2.33 – 2.23 (m, 1H), 1.36 – 1.31 (m, 4H), 1.30 (s, 9H), 1.05 (d, $J = 6.7$ Hz, 3H), 0.91 – 0.87 (m, 3H). $^{13}\text{C NMR}$ (100 MHz, Chloroform-*d*) δ 149.76, 136.32, 135.22, 127.64, 125.65, 125.39, 39.43, 37.05, 34.50, 31.36, 20.79, 20.52, 14.21. HRMS (EI+) calcd for $[\text{C}_{17}\text{H}_{26}]^+$ ($[\text{M}]^+$): 230.2035, found: 230.2038.



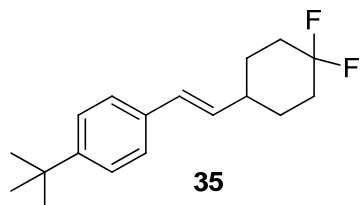
Following the procedure F, product **32** (related to **Figure 2**) was obtained as a clear liquid (115.0 mg, 95% yield). ^1H NMR (400 MHz, Chloroform-*d*) δ 7.33 – 7.25 (m, 4H), 6.32 (d, J = 16.0 Hz, 1H), 6.13 (dd, J = 15.9, 7.0 Hz, 1H), 2.17 – 2.06 (m, 1H), 1.91 – 1.62 (m, 6H), 1.30 (s, 9H), 1.27 – 1.13 (m, 4H). ^{13}C NMR (100 MHz, Chloroform-*d*) δ 149.74, 136.16, 135.30, 126.89, 125.61, 125.37, 41.18, 34.48, 33.04, 31.34, 26.21, 26.08. The spectrum data matches previously reported values (Zhu and Wei, 2014)



Following the procedure F, product **33** (related to **Figure 2**) was obtained as a clear liquid (80.1 mg, 75% yield). ^1H NMR (400 MHz, Chloroform-*d*) δ 7.33 – 7.27 (m, 4H), 6.31 – 6.26 (m, 2H), 3.14 – 3.03 (m, 1H), 2.21 – 2.13 (m, 2H), 2.00 – 1.78 (m, 4H), 1.31 (s, 9H). ^{13}C NMR (100 MHz, Chloroform-*d*) δ 149.82, 135.03, 134.58, 127.28, 125.67, 125.39, 38.79, 34.50, 31.34, 28.84, 18.59. HRMS (EI+) calcd for $[\text{C}_{16}\text{H}_{22}]^+$ ($[\text{M}]^+$): 214.1722, found: 214.1725.

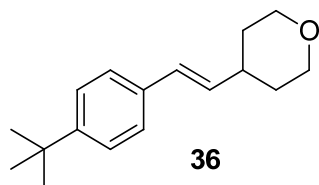


Following the procedure F, product **34** (related to **Figure 2**) was obtained as a clear liquid (117.8 mg, 92% yield). ^1H NMR (400 MHz, Chloroform-*d*) δ 7.34 – 7.27 (m, 4H), 6.31 (d, J = 15.9 Hz, 1H), 6.19 (dd, J = 15.9, 7.5 Hz, 1H), 2.38 – 2.26 (m, 1H), 1.87 – 1.78 (m, 2H), 1.74 – 1.67 (m, 2H), 1.66 – 1.61 (m, 1H), 1.58 – 1.51 (m, 4H), 1.50 – 1.38 (m, 3H), 1.32 (s, 9H). ^{13}C NMR (100 MHz, Chloroform-*d*) δ 148.88, 136.21, 134.57, 125.52, 124.82, 124.58, 42.46, 34.02, 33.68, 30.54, 27.62, 25.49. HRMS (EI+) calcd for $[\text{C}_{19}\text{H}_{28}]^+$ ($[\text{M}]^+$): 256.2191, found: 256.2190.

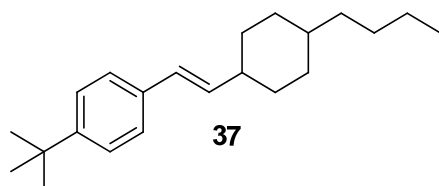


Following the procedure G for the reaction with perester, product **35** (related to **Figure 2**) was obtained as a white solid (73.7 mg, 53% yield). ^1H NMR (400 MHz, Chloroform-*d*) δ 7.35 – 7.26 (m, 4H), 6.39 (d, J = 16.0 Hz, 1H), 6.10 (dd, J = 16.0, 7.0 Hz, 1H), 2.29 – 2.19 (m, 1H), 2.18 – 2.07 (m, 2H), 1.92 – 1.70 (m, 4H), 1.63 – 1.54 (m, 2H), 1.31 (s, 9H). ^{13}C NMR (100 MHz, Chloroform-*d*) δ 150.29, 134.62, 132.88 (d, J = 2.5 Hz), 128.64, 125.74, 125.48, 122.14 (d, J = 240.2 Hz), 39.04, 34.54, 33.25 (dd, J = 25.2, 22.9 Hz), 31.32, 28.93 (d, J = 9.2 Hz). ^{19}F NMR

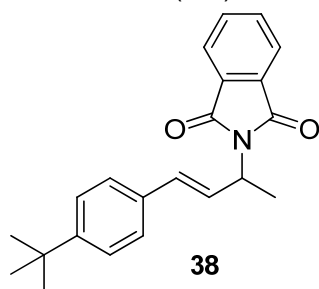
(376 MHz, Chloroform-*d*) δ -94.22 (d, J = 238.6 Hz), -99.94 (d, J = 238.3 Hz). HRMS (EI+) calcd for $[\text{C}_{18}\text{H}_{24}\text{F}_2]^+$ ($[\text{M}]^+$): 278.1846, found: 278.1848.



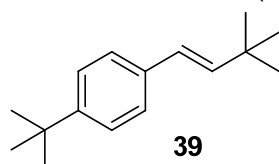
Following the procedure G for the reaction with perester, product **36** (related to **Figure 2**) was obtained as a white solid (90.3 mg, 74% yield). ^1H NMR (400 MHz, Chloroform-*d*) δ 7.34 – 7.27 (m, 4H), 6.36 (d, J = 16.0 Hz, 1H), 6.11 (dd, J = 15.9, 6.8 Hz, 1H), 4.02 – 3.96 (m, 2H), 3.48 – 3.37 (m, 2H), 2.40 – 2.30 (m, 1H), 1.71 – 1.65 (m, 2H), 1.61 – 1.49 (m, 2H), 1.30 (s, 9H). ^{13}C NMR (100 MHz, Chloroform-*d*) δ 150.30, 134.92, 134.02, 128.13, 125.90, 125.60, 67.90, 38.53, 34.67, 32.87, 31.48. HRMS (EI+) calcd for $[\text{C}_{17}\text{H}_{24}\text{O}]^+$ ($[\text{M}]^+$): 244.1827, found: 244.1835.



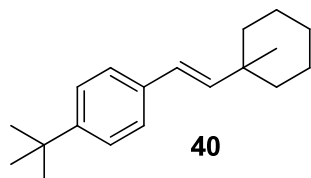
Following the procedure F, product **37** (related to **Figure 2**) was obtained as a clear liquid (104.5 mg, 70% yield, dr = 1:1). ^1H NMR (400 MHz, Chloroform-*d*) δ 7.33 – 7.26 (m, 4H), 6.38 – 6.29 (m, 1H), 6.25 (dd, J = 16.0, 6.4 Hz, 0.56H), 6.12 (dd, J = 15.9, 7.0 Hz, 0.41H), 2.39 – 2.32 (m, 0.54H), 2.09 – 1.99 (m, 0.49H), 1.85 – 1.76 (m, 2H), 1.63 – 1.54 (m, 3H), 1.42 – 1.32 (m, 3H), 1.31 – 1.30 (m, 9H), 1.27 – 1.14 (m, 7H), 0.89 (t, J = 6.9 Hz, 3H). ^{13}C NMR (100 MHz, Chloroform-*d*) δ 149.74, 136.12, 135.34, 135.29, 134.87, 127.80, 126.91, 125.60, 125.38, 125.37, 41.49, 37.31, 37.17, 34.48, 33.00, 31.34, 29.62, 29.41, 29.23, 29.05, 23.04, 23.01, 14.19. HRMS (EI+) calcd for $[\text{C}_{22}\text{H}_{34}]^+$ ($[\text{M}]^+$): 298.2661, found: 298.2668.



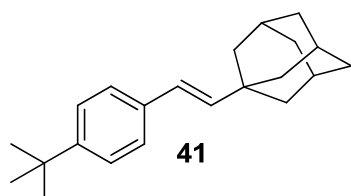
Following the procedure G for the reaction with perester, product **38** (related to **Figure 2**) was obtained as a clear liquid (95 mg, 57% yield). ^1H NMR (400 MHz, Chloroform-*d*) δ 7.82 (dd, J = 5.4, 3.1 Hz, 2H), 7.69 (dd, J = 5.5, 3.0 Hz, 2H), 7.33 – 7.30 (m, 4H), 6.64 – 6.55 (m, 2H), 5.13 – 5.04 (m, 1H), 1.66 (d, J = 7.1 Hz, 3H), 1.29 (s, 9H). ^{13}C NMR (100 MHz, Chloroform-*d*) δ 167.99, 150.97, 133.86, 133.61, 132.11, 131.80, 127.36, 126.29, 125.47, 123.13, 49.09, 34.58, 31.27, 19.06. HRMS (EI+) calcd for $[\text{C}_{22}\text{H}_{23}\text{NO}_2]^+$ ($[\text{M}]^+$): 333.1729, found: 333.1725.



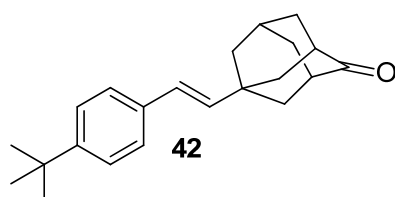
Following the procedure F, product **39** (related to **Figure 2**) was obtained as clear liquid (82.1 mg, 76 % yield). ^1H NMR (400 MHz, Chloroform-*d*) δ 7.36 – 7.26 (m, 4H), 6.28 (d, J = 16.2 Hz, 1H), 6.21 (d, J = 16.2, 1H), 1.31 (s, 9H), 1.11 (s, 9H). ^{13}C NMR (100 MHz, Chloroform-*d*) δ 149.76, 141.17, 135.27, 125.68, 125.39, 124.21, 34.49, 33.30, 31.35, 29.66. The spectrum data matches previously reported values (Aydin et al., 2009).



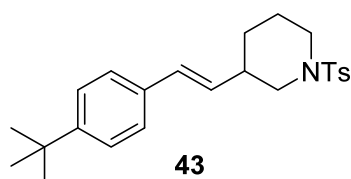
Following the procedure F, product **40** (related to **Figure 2**) was obtained as a clear liquid (102.4 mg, 80% yield). ^1H NMR (400 MHz, Chloroform-*d*) δ 7.35 – 7.28 (m, 4H), 6.30 (d, J = 16.4 Hz, 1H), 6.17 (d, J = 16.4 Hz, 1H), 1.64 – 1.56 (m, 2H), 1.52 – 1.46 (m, 4H), 1.42 – 1.32 (m, 4H), 1.31 (s, 9H), 1.05 (s, 3H). ^{13}C NMR (100 MHz, Chloroform-*d*) δ 149.74, 140.28, 135.49, 125.68, 125.61, 125.40, 38.06, 36.17, 34.49, 31.36, 27.84, 26.37, 22.51. HRMS (EI+) calcd for $[\text{C}_{19}\text{H}_{28}]^+$ ($[\text{M}]^+$): 256.2191, found: 256.2189.



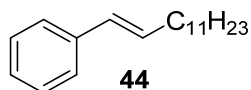
Following the procedure F, product **41** (related to **Figure 2**) was obtained as a white solid (128 mg, 87% yield). ^1H NMR (400 MHz, Chloroform-*d*) δ 7.34 – 7.27 (m, 4H), 6.22 (d, J = 16.2 Hz, 1H), 6.06 (d, J = 16.3, 1H), 2.05 – 1.99 (m, 3H), 1.77 – 1.67 (m, 12H), 1.32 – 1.29 (m, 9H). ^{13}C NMR (100 MHz, Chloroform-*d*) δ 149.71, 141.45, 135.43, 125.64, 125.37, 124.14, 42.31, 36.93, 35.11, 34.48, 31.34, 28.53. HRMS (EI+) calcd for $[\text{C}_{22}\text{H}_{30}]^+$ ($[\text{M}]^+$): 294.2348, found: 294.2352.



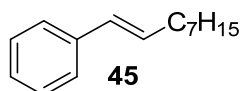
Following the procedure G for the reaction with perester, product **42** (related to **Figure 2**) was obtained as a white solid (127 mg, 82% yield). ^1H NMR (400 MHz, Chloroform-*d*) δ 7.28 – 7.20 (m, 4H), 6.21 (d, J = 16.2 Hz, 1H), 5.99 (d, J = 16.3 Hz, 1H), 2.56 – 2.52 (m, 2H), 2.17 – 2.11 (m, 1H), 1.98 – 1.84 (m, 10H), 1.23 (s, 9H). ^{13}C NMR (100 MHz, Chloroform-*d*) δ 217.99, 150.34, 137.54, 134.61, 125.95, 125.78, 125.49, 46.42, 43.44, 41.17, 38.66, 35.01, 34.54, 31.32, 27.78. HRMS (EI+) calcd for $[\text{C}_{22}\text{H}_{28}\text{O}]^+$ ($[\text{M}]^+$): 308.2140, found: 308.2134.



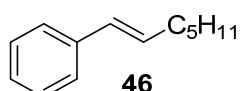
Following the procedure G for the reaction with perester, product **43** (related to **Figure 2**) was obtained as white solid (79 mg, 40% yield). ^1H NMR (400 MHz, Chloroform-*d*) δ 7.65 (d, J = 8.3 Hz, 2H), 7.34 – 7.29 (m, 4H), 7.26 (d, J = 5.2 Hz, 2H), 6.41 (d, J = 16.0 Hz, 1H), 5.96 (dd, J = 16.0, 7.2 Hz, 1H), 3.79 – 3.57 (m, 2H), 2.54 – 2.46 (m, 1H), 2.43 (s, 3H), 2.30 – 2.23 (m, 1H), 2.11 (t, J = 10.9 Hz, 1H), 1.86 – 1.65 (m, 3H), 1.30 (s, 9H), 1.13 (m, 1H). ^{13}C NMR (100 MHz, Chloroform-*d*) δ 150.53, 143.43, 134.30, 133.24, 130.25, 130.05, 129.64, 127.71, 125.82, 125.49, 51.38, 46.44, 39.08, 34.56, 31.32, 29.99, 24.43, 21.56. HRMS (EI+) calcd for $[\text{C}_{24}\text{H}_{31}\text{NO}_2\text{S}]^+$ ($[\text{M}]^+$): 397.2075, found: 397.2079.



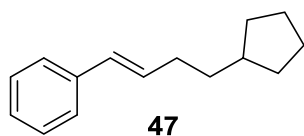
Following the procedure H for the reaction with diacyl peroxide, product **44** (related to **Figure 3**) was obtained as a clear liquid (94 mg, 73% yield). ^1H NMR (400 MHz, Chloroform-*d*) δ 7.34 (d, J = 7.7 Hz, 2H), 7.28 (t, J = 7.5 Hz, 2H), 7.18 (t, J = 7.2 Hz, 1H), 6.37 (d, J = 15.8 Hz, 1H), 6.27 – 6.18 (m, 1H), 2.24 – 2.16 (m, 2H), 1.49 – 1.40 (m, 2H), 1.34 – 1.22 (m, 16H), 0.88 (t, J = 6.6 Hz, 3H). ^{13}C NMR (100 MHz, Chloroform-*d*) δ 137.97, 131.28, 129.67, 128.46, 126.73, 125.90, 33.09, 31.96, 29.71, 29.68, 29.66, 29.57, 29.42, 29.39, 29.28, 22.73, 14.15. The spectrum data matches previously reported values (Habrant et al., 2007).



Following the procedure H for the reaction with diacyl peroxide, product **45** (related to **Figure 3**) was obtained as a clear liquid (61 mg, 60% yield). ^1H NMR (400 MHz, Chloroform-*d*) δ 7.33 (d, J = 7.6 Hz, 2H), 7.27 (t, J = 7.5 Hz, 2H), 7.17 (t, J = 7.2 Hz, 1H), 6.37 (d, J = 15.8 Hz, 1H), 6.27 – 6.15 (m, 1H), 2.25 – 2.14 (m, 2H), 1.52 – 1.41 (m, 2H), 1.36 – 1.25 (m, 8H), 0.88 (t, J = 6.5 Hz, 3H). ^{13}C NMR (100 MHz, Chloroform-*d*) δ 137.99, 131.27, 129.71, 128.48, 126.76, 125.93, 33.11, 31.91, 29.45, 29.27, 22.73, 14.16. The spectrum data matches previously reported values (Thiot et al., 2007).

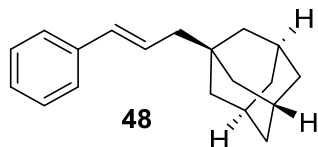


Following the procedure H for the reaction with diacyl peroxide, product **46** (related to **Figure 3**) was obtained as a clear liquid (59 mg, 68% yield). ^1H NMR (400 MHz, Chloroform-*d*) δ 7.34 (d, J = 7.1 Hz, 2H), 7.28 (t, J = 7.5 Hz, 2H), 7.22 – 7.15 (m, 1H), 6.37 (d, J = 15.8 Hz, 1H), 6.27 – 6.18 (m, 1H), 2.24 – 2.17 (m, 2H), 1.50 – 1.43 (m, 2H), 1.37 – 1.29 (m, 4H), 0.90 (t, J = 6.7 Hz, 3H). ^{13}C NMR (100 MHz, Chloroform-*d*) δ 137.97, 131.27, 129.68, 128.47, 126.74, 125.90, 33.05, 31.47, 29.09, 22.60, 14.10. The spectrum data matches previously reported values (Denmark and Wehrli, 2000).

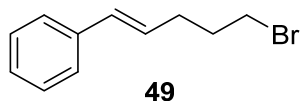


Following the procedure H for the reaction with diacyl peroxide, product **47** (related to **Figure 3**) was obtained as a clear liquid (77 mg, 77% yield). ^1H NMR (400 MHz, Chloroform-*d*) δ 7.33 (d,

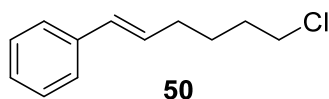
$J = 7.2$ Hz, 2H), 7.28 (t, $J = 7.6$ Hz, 2H), 7.17 (t, $J = 7.2$ Hz, 1H), 6.37 (d, $J = 15.9$ Hz, 1H), 6.27 – 6.18 (m, 1H), 2.25 – 2.18 (m, 2H), 1.84 – 1.73 (m, 3H), 1.66 – 1.57 (m, 2H), 1.54 – 1.44 (m, 4H), 1.17 – 1.04 (m, 2H). ^{13}C NMR (100 MHz, Chloroform-*d*) δ 138.00, 131.41, 129.54, 128.49, 126.75, 125.91, 39.73, 35.91, 32.70, 32.32, 25.25. The spectrum data matches previously reported values (Li et al., 2016).



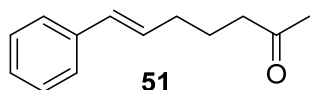
Following the procedure H for the reaction with diacyl peroxide, product **48** (related to **Figure 3**) was obtained as clear liquid (83 mg, 66% yield). ^1H NMR (400 MHz, Chloroform-*d*) δ 7.37 – 7.33 (m, 2H), 7.32 – 7.26 (m, 2H), 7.21 – 7.15 (m, 1H), 6.33 (d, $J = 15.9$ Hz, 1H), 6.29 – 6.22 (m, 1H), 1.98 – 1.93 (m, 5H), 1.73 – 1.67 (m, 3H), 1.66 – 1.59 (m, 3H), 1.55 – 1.52 (m, 6H). ^{13}C NMR (100 MHz, Chloroform-*d*) δ 137.96, 131.88, 128.48, 127.09, 126.76, 125.98, 48.12, 42.61, 37.14, 33.52, 28.81. The spectrum data matches previously reported values (Tanaka et al., 1987).



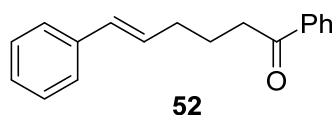
Following the procedure H for the reaction with diacyl peroxide, product **49** (related to **Figure 3**) was obtained as a clear liquid (62 mg, 55% yield). ^1H NMR (400 MHz, Chloroform-*d*) δ 7.36 – 7.32 (m, 2H), 7.32 – 7.27 (m, 2H), 7.23 – 7.18 (m, 1H), 6.44 (d, $J = 15.8$ Hz, 1H), 6.21 – 6.10 (m, 1H), 3.45 (t, $J = 6.7$ Hz, 2H), 2.42 – 2.34 (m, 2H), 2.07 – 1.99 (m, 2H). ^{13}C NMR (100 MHz, Chloroform-*d*) δ 137.43, 131.31, 128.54, 128.47, 127.14, 126.02, 33.19, 32.21, 31.30. The spectrum data matches previously reported values (Matsubara and Jamison, 2010)



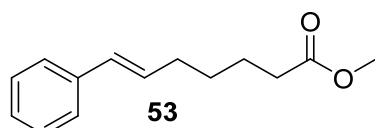
Following the procedure H for the reaction with diacyl peroxide, product **50** (related to **Figure 3**) was obtained as a clear liquid (53 mg, 55% yield). ^1H NMR (400 MHz, Chloroform-*d*) δ 7.38 – 7.26 (m, 4H), 7.23 – 7.17 (m, 1H), 6.40 (d, $J = 15.8$ Hz, 1H), 6.26 – 6.15 (m, 1H), 3.56 (t, $J = 6.7$ Hz, 2H), 2.29 – 2.22 (m, 2H), 1.90 – 1.77 (m, 2H), 1.69 – 1.57 (m, 2H). ^{13}C NMR (100 MHz, Chloroform-*d*) δ 137.63, 130.43, 130.06, 128.52, 126.98, 125.96, 44.98, 32.23, 32.0, 26.56. The spectrum data matches previously reported values (Hu et al., 1999).



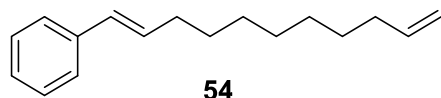
Following the procedure H for the reaction with diacyl peroxide, product **51** (related to **Figure 3**) was obtained as a white solid (50.7 mg, 54% yield). ^1H NMR (400 MHz, Chloroform-*d*) δ 7.36 – 7.26 (m, 4H), 7.24 – 7.17 (m, 1H), 6.39 (d, $J = 15.7$ Hz, 1H), 6.21 – 6.12 (m, 1H), 2.48 (t, $J = 7.4$ Hz, 2H), 2.26 – 2.19 (m, 1H), 2.14 (s, 3H), 1.82 – 1.72 (m, 1H). ^{13}C NMR (100 MHz, Chloroform-*d*) δ 208.85, 137.57, 130.68, 129.83, 128.52, 127.01, 125.97, 42.88, 32.30, 30.02, 23.25. The spectrum data matches previously reported values (Musacchio et al., 2014).



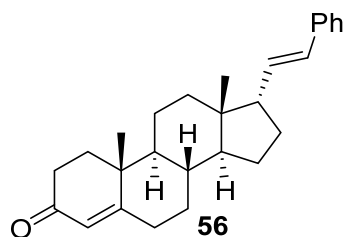
Following the procedure H for the reaction with diacyl peroxide, product **52** (related to **Figure 3**) was obtained as a white solid (70 mg, 56% yield). ^1H NMR (400 MHz, Chloroform-*d*) δ 7.98 – 7.93 (m, 2H), 7.58 – 7.53 (m, 1H), 7.48 – 7.42 (m, 2H), 7.36 – 7.27 (m, 4H), 7.23 – 7.17 (m, 1H), 6.41 (d, $J = 15.9$ Hz, 1H), 6.27 – 6.18 (m, 1H), 3.03 (t, $J = 7.3$ Hz, 2H), 2.36 – 2.29 (m, 2H), 1.99 – 1.91 (m, 2H). ^{13}C NMR (100 MHz, Chloroform-*d*) δ 200.22, 137.62, 137.02, 132.96, 130.73, 129.94, 128.58, 128.51, 128.05, 126.98, 125.99, 37.75, 32.47, 23.80. The spectrum data matches previously reported values (Hilt et al., 2016).



Following the procedure H for the reaction with diacyl peroxide, product **53** (related to **Figure 3**) was obtained as a white solid (61 mg, 56% yield). ^1H NMR (400 MHz, Chloroform-*d*) δ 7.35 – 7.25 (m, 4H), 7.21 – 7.15 (m, 1H), 6.38 (d, $J = 15.9$ Hz, 1H), 6.23 – 6.15 (m, 1H), 3.66 (s, 3H), 2.34 (t, $J = 7.5$ Hz, 2H), 2.26 – 2.19 (m, 2H), 1.74 – 1.65 (m, 2H), 1.55 – 1.46 (m, 2H). ^{13}C NMR (100 MHz, Chloroform-*d*) δ 174.11, 137.74, 130.32, 130.21, 128.49, 126.88, 125.95, 51.51, 33.96, 32.64, 28.84, 24.52. The spectrum data matches previously reported values (Ramón-Azcón et al., 2006).

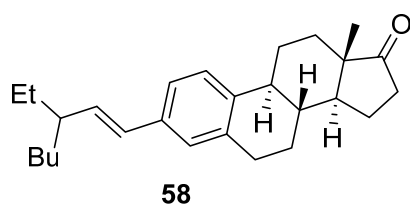


Following the procedure H for the reaction with diacyl peroxide, product **54** (related to **Figure 3**) was obtained as a clear liquid (70 mg, 61% yield). ^1H NMR (400 MHz, Chloroform-*d*) δ 7.36 – 7.32 (m, 2H), 7.30 – 7.25 (m, 2H), 7.21 – 7.15 (m, 1H), 6.37 (d, $J = 15.9$ Hz, 1H), 6.27 – 6.17 (m, 1H), 5.91 – 5.74 (m, 1H), 5.04 – 4.90 (m, 2H), 2.25 – 2.16 (m, 2H), 2.09 – 2.00 (m, 2H), 1.50 – 1.42 (m, 2H), 1.40 – 1.28 (m, 8H). ^{13}C NMR (100 MHz, Chloroform-*d*) δ 139.22, 137.96, 131.21, 129.73, 128.48, 126.76, 125.92, 114.17, 33.84, 33.07, 29.40, 29.21, 29.13, 28.96. The spectrum data matches previously reported values (Kulasegaram and Kulawiec, 1997).

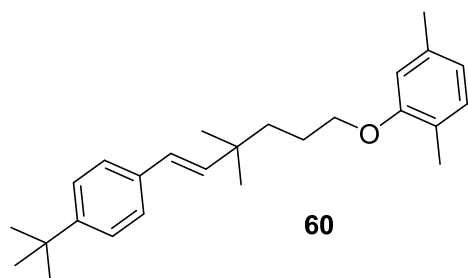


Following the procedure G, product **56** (related to **Scheme 2**) was obtained as a white solid (89.8 mg, 48% yield). ^1H NMR (400 MHz, Chloroform-*d*) δ 7.35 – 7.32 (m, 2H), 7.31 – 7.25 (m, 2H), 7.20 – 7.15 (m, 1H), 6.26 (d, $J = 15.7$ Hz, 1H), 6.13 (dd, $J = 15.7, 9.3$ Hz, 1H), 5.73 (s, 1H), 2.46 – 2.33 (m, 4H), 2.31–2.15 (m, 1H), 2.18 – 2.09 (m, 1H), 2.03 – 1.97 (m, 1H), 1.94 – 1.88 (m, 1H), 1.85 – 1.78 (m, 1H), 1.75 – 1.62 (m, 2H), 1.55 – 1.50 (m, 3H), 1.46 – 1.37 (m, 1H), 1.36 – 1.23 (m, 3H), 1.18 (s, 3H), 1.14 – 1.04 (m, 1H), 0.97 – 0.91 (m, 1H), 0.88 (s, 3H). ^{13}C NMR (100 MHz, Chloroform-*d*) δ 199.61, 171.46, 137.80, 133.85, 128.88, 128.50, 126.82,

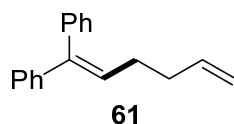
125.98, 123.80, 53.70, 52.59, 50.88, 44.66, 38.69, 36.15, 35.71, 34.75, 33.99, 32.97, 32.48, 28.49, 25.70, 20.93, 20.27, 17.48. HRMS (EI⁺) calcd for [C₂₇H₃₄O]⁺ ([M]⁺): 374.2610, found: 374.2613.



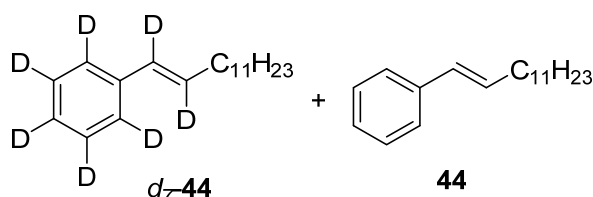
Following the procedure E, product **58** (related to **Scheme 2**) was obtained as a white solid (123 mg, 65% yield). ¹H NMR (400 MHz, Chloroform-*d*) δ 7.23 (d, *J* = 8.1 Hz, 1H), 7.16 (d, *J* = 8.3 Hz, 1H), 7.10 (s, 1H), 6.27 (d, *J* = 15.8 Hz, 1H), 5.90 (dd, *J* = 15.8, 9.0 Hz, 1H), 2.91 (dd, *J* = 8.8, 4.0 Hz, 2H), 2.50 (dd, *J* = 18.7, 8.6 Hz, 1H), 2.45 – 2.39 (m, 1H), 2.33 – 2.26 (m, 1H), 2.19 – 1.93 (m, 5H), 1.65 – 1.58 (m, 2H), 1.55 – 1.39 (m, 6H), 1.33 – 1.24 (m, 6H), 0.90 (s, 3H), 0.87 (t, *J* = 7.4 Hz, 6H). ¹³C NMR (100 MHz, Chloroform-*d*) δ 221.13, 138.58, 136.68, 135.81, 135.24, 129.44, 126.71, 126.68, 125.70, 123.65, 123.62, 50.69, 48.20, 45.39, 44.61, 38.44, 36.06, 35.13, 31.80, 29.84, 29.62, 28.48, 26.74, 25.97, 23.05, 21.79, 14.32, 14.04, 12.06. HRMS (EI⁺) calcd for [C₂₇H₃₈O]⁺ ([M]⁺): 378.2923, found: 378.2929.



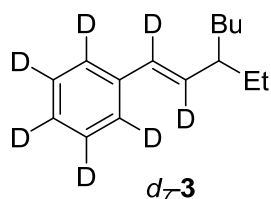
Following the procedure E, product **60** (related to **Scheme 2**) was obtained as a clear liquid (76 mg, 42% yield). ¹H NMR (400 MHz, Chloroform-*d*) δ 7.34 – 7.28 (m, 4H), 6.99 (d, *J* = 7.4 Hz, 1H), 6.64 (d, *J* = 8.1 Hz, 1H), 6.60 (s, 1H), 6.29 (d, *J* = 16.2 Hz, 1H), 6.16 (d, *J* = 16.2 Hz, 1H), 3.90 (t, *J* = 6.4 Hz, 2H), 2.28 (s, 3H), 2.18 (s, 3H), 1.80 – 1.71 (m, 2H), 1.59 – 1.52 (m, 2H), 1.31 (s, 9H), 1.13 (s, 6H). ¹³C NMR (100 MHz, Chloroform-*d*) δ 157.11, 149.90, 139.54, 136.45, 135.17, 130.28, 125.81, 125.74, 125.44, 123.62, 120.59, 112.01, 68.43, 39.44, 36.08, 34.52, 31.37, 27.37, 25.03, 21.44, 15.86. HRMS (EI⁺) calcd for [C₂₆H₃₆O]⁺ ([M]⁺): 364.2766, found: 364.2761.



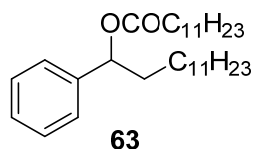
Following the procedure E, product **61** (related to **Scheme 3A**) was obtained as a clear liquid (72.3 mg, 62%). ¹H NMR (400 MHz, Chloroform-*d*) δ 7.38 – 7.33 (m, 2H), 7.32 – 7.28 (m, 1H), 7.27 – 7.24 (m, 1H), 7.24 – 7.19 (m, 4H), 7.19 – 7.16 (m, 2H), 6.10 – 6.05 (m, 1H), 5.86 – 5.73 (m, 1H), 5.08 – 4.80 (m, 2H), 2.25 – 2.17 (m, 4H). ¹³C NMR (100 MHz, Chloroform-*d*) δ 142.79, 141.95, 140.19, 138.13, 129.92, 129.20, 128.16, 128.08, 127.26, 126.91, 126.86, 114.94, 34.06, 29.15. The spectrum data matches previously reported values (Jiménez-Aquino et al., 2011).



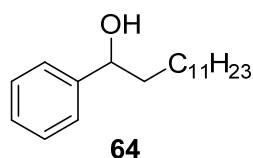
Following the procedure H, product **44** and *d*₇-**44** (related to **Scheme 3B**) were obtained as a clear liquid (60% total yield). ¹H NMR (400 MHz, Chloroform-*d*) δ 7.37 – 7.31 (m, 2H), 7.31 – 7.26 (m, 2H), 7.21 – 7.15 (m, 1H), 6.37 (d, *J* = 15.9 Hz, 1H), 6.27 – 6.17 (m, 1H), 2.23 – 2.16 (m, 4H), 1.50 – 1.41 (m, 4H), 1.34 – 1.24 (m, 32H), 0.88 (t, *J* = 6.8 Hz, 6H).



Following the procedure G, product *d*₇-**3** (related to **Scheme 3B**) was obtained as a clear liquid (62.2 mg, 60% yield). ¹H NMR (400 MHz, Chloroform-*d*) δ 2.05 – 1.97 (m, 1H), 1.54 – 1.41 (m, 2H), 1.35 – 1.24 (m, 6H), 0.88 (t, *J* = 7.5 Hz, 6H). ¹³C NMR (101 MHz, Chloroform-*d*) δ 137.80, 135.14 (t, *J* = 22.4 Hz), 129.14 (t, *J* = 22.9 Hz), 127.97 (t, *J* = 24.00 Hz), 126.20 (t, *J* = 23.8 Hz), 125.54 (t, *J* = 23.7 Hz), 45.02, 34.88, 29.68, 28.23, 22.92, 14.15, 11.89.



Compound **63** (related to **Scheme 3C**): ¹H NMR (400 MHz, Chloroform-*d*) δ 7.35-7.30 (m, 4H), 7.29-7.26 (m, 1H), 5.72 (dd, *J* = 7.8, 6.1 Hz, 1H), 2.34-2.28 (m, 2H), 1.94-1.83 (m, 1H), 1.80-1.69 (m, 1H), 1.65-1.58 (m, 2H), 1.31-1.21 (m, 36H), 0.88 (t, *J* = 6.7 Hz, 6H). ¹³C NMR (100 MHz, Chloroform-*d*) δ 173.23, 141.10, 128.37, 127.72, 126.49, 75.86, 36.42, 34.65, 31.94, 29.68, 29.66, 29.63, 29.58, 29.50, 29.38, 29.36, 29.30, 29.14, 25.55, 25.05, 22.72, 14.15. Synthesized according to reported method (Ge et al., 2017).



Compound **64** (related to **Scheme 3C**): ¹H NMR (400 MHz, Chloroform-*d*) δ 7.36 – 7.30 (m, 4H), 7.29 – 7.22 (m, 1H), 4.63 (dd, *J* = 7.5, 5.9 Hz, 1H), 2.06 (s, 1H), 1.83 – 1.73 (m, 1H), 1.72 – 1.62 (m, 1H), 1.45 – 1.35 (m, 1H), 1.31 – 1.18 (m, 19H), 0.88 (t, *J* = 6.9 Hz, 3H). ¹³C NMR (100 MHz, Chloroform-*d*) δ 144.96, 128.43, 127.47, 125.92, 74.72, 39.14, 31.97, 29.71, 29.69, 29.64, 29.60, 29.58, 29.41, 25.88, 22.74, 14.18. Synthesized according to reported method (Jian et al., 2017).

Supplemental References

- 1 Aydin, J., Larsson, J.M., Selander, N., and Szabó, K.J. (2009). Pincer complex-catalyzed redox coupling of alkenes with iodonium salts via presumed palladium(IV) intermediates. *Org. Lett.*, *11*, 2852–2854.
- 2 Becke, A.D. (1993). Density - functional thermochemistry. III. The role of exact exchange. *J. Chem. Phys.*, *98*, 5648–5652.
- 3 Denmark, S.E., and Wehrli, D. (2000). Highly stereospecific, palladium-catalyzed cross-coupling of alkenylsilanols. *Org. Lett.*, *2*, 565–568.
- 4 Frisch, M.J., Trucks, G.W., Schlegel, H.B., Scuseria, G.E., Robb, M.A., Cheeseman, J.R., Montgomery, J.A., Vreven, J., Kudin, T.K.N., Burant, J.C., Millam, J.M., Iyengar, S.S., Tomasi, J., Barone, V., Mennucci, B., Cossi, M., Scalmani, G., Rega, N., Petersson, G.A., Nakatsuji, H., Hada, M., Ehara, M., Toyota, K., Fukuda, R., Hasegawa, J., Ishida, M., Nakajima, T., Honda, Y., Kitao, O., Nakai, H., Klene, M., Li, X., Knox, J.E., Hratchian, H. P., Cross, J. B., Bakken, V., Adamo, C., Jaramillo, J., Gomperts, R., Stratmann, R.E., Yazyev, O., Austin, A.J., Cammi, R., Pomelli, C., Ochterski, J.W., Ayala, P.Y., Morokuma, K., Voth, G.A., Salvador, P., Dannenberg, J.J., Zakrzewski, V.G., Dapprich, S., Daniels, A.D., Strain, M.C., Farkas, O., Malick, D.K., Rabuck, A.D., Raghavachari, K., Foresman, J.B., Ortiz, J.V., Cui, Q., Baboul, A.G., Clifford, S., Cioslowski, J., Stefanov, B.B., Liu, G., Liashenko, A., Piskorz, P., Komaromi, I., Martin, R.L., Fox, D.J., Keith, T., Al-Laham, M.A., Peng, C.Y., Nanayakkara, A., Challacombe, M., Gill, P.M.W., Johnson, B., Chen, W., Wong, M.W., Gonzalez, C., and Pople, J.A., *Gaussian 09*, D01; Gaussian, Inc.: Wallingford CT, 2013.
- 5 Ge, L., Li, Y., Jian, W., and Bao, H. (2017). Alkyl esterification of vinylarenes enabled by visible-light-induced decarboxylation. *Chem. Eur. J.*, *23*, 11767–11770.
- 6 Habrant, D., Stengel, B., Meunier, S., and Mioskowski, C. (2007). Reactivity of aldehydes with semi-stabilised arsonium ylide anions: synthesis of terminal (*E*)-1,3-dienes. *Chem. Eur. J.*, *13*, 5433–5440.
- 7 Haubenreisser, S.T., Wöste, H., Martínez, C., Ishihara, K., and Muñoz, K. (2016). Structurally defined molecular hypervalent iodine catalysts for intermolecular enantioselective reactions. *Angew. Chem. Int. Ed.*, *55*, 413–417.
- 8 Hilt, G., Walter, C., and Bolze, P. (2006). Iron-salen complexes as efficient catalysts in ring expansion reactions of epoxyalkenes. *Adv. Synth. Catal.*, *348*, 1241–1247.
- 9 Hu, Y., Yu, J., Yang, S., Wang, J.-X., and Yin, Y. (1999). Substitution reaction of nitro group on α -nitrostyrene by organozinc halides under microwave irradiation. *Synthetic Commun.*, *29*, 1157–1164.
- 10 Huang, C.Y., and Doyle, A.G. (2012). Nickel-catalyzed Negishi alkylations of styrenyl aziridines. *J. Am. Chem. Soc.*, *134*, 9541–9544.
- 11 Jian, W., Ge, L., Jiao, Y., and Bao, H. (2017). Iron-catalyzed decarboxylative alkyl etherification of vinylarenes with aliphatic acids as the alkyl source. *Angew. Chem. Int. Ed.*, *56*, 3650–3654.
- 12 Jiménez-Aquino, A., Flegeau, E.F., Schneidera, U., and Kobayashi, S. (2011). Catalytic intermolecular allyl–allyl cross-couplings between alcohols and boronates. *Chem. Commun.*, *47*, 9456–9458.

- 13 Kulasegaram, S., and Kulawiec, R.J. (1997). Palladium-catalyzed isomerization of aryl-substituted epoxides: a selective synthesis of substituted benzylic aldehydes and ketones. *J. Org. Chem.*, *62*, 6547–6556.
- 14 Lee, C., Yang, W., Parr, R.G. (1998). Development of the colle-salvetti correlation-energy formula into a functional of the electron density. *Phys. Rev. B.*, *37*, 785–789.
- 15 Li, Y., Ge, L., Qian, B., Babu, K.R., and Bao, H. (2016). Hydroalkylation of terminal aryl alkynes with alkyl diacyl peroxides. *Tetrahedron Lett.*, *57*, 5677–5680.
- 16 Mai, W.-P., Song, G., Sun, G.-C., Yang, L.-R., Yuan, J.-W., Xiao, Y.-M., Mao, P., and Qu, L.-B. (2013). Cu/Ag-catalyzed double decarboxylative cross-coupling reaction between cinnamic acids and aliphatic acids in aqueous solution. *RSC Adv.*, *3*, 19264–19267.
- 17 Marenich, A.V., Cramer, C.J., and Truhlar, D.G. (2009). Universal solvation model based on solute electron density and on a continuum model of the solvent defined by the bulk dielectric constant and atomic surface tensions. *J. Phys. Chem. B.*, *113*, 6378–6396.
- 18 Matsubara, R., and Jamison, T.F. (2010). Nickel-catalyzed allylic substitution of simple alkenes. *J. Am. Chem. Soc.*, *132*, 6880–6881.
- 19 Musacchio, A.J., Nguyen, L.Q., Beard, H., and Knowles, R.R. (2014). Catalytic olefin hydroamination with aminium radical cations: a photoredox method for direct C–N bond formation. *J. Am. Chem. Soc.*, *136*, 12217–12220.
- 20 Ramón-Azcón, J., Galve, R., Sánchez-Baeza, F., and Marco, M.-P. (2006). Development of an enzyme-linked immunosorbent assay for the determination of the linear alkylbenzene sulfonates and long-chain sulfophenyl carboxylates using antibodies generated by pseudoheterologous immunization. *Anal. Chem.*, *78*, 71–81.
- 21 Thiot, C., Schmutz, M., Wagenr, A., and Mioskowski, C. (2007). A one-pot synthesis of (*E*)-disubstituted alkenes by a bimetallic [Rh–Pd]-catalyzed hydrosilylation/hiyama cross-coupling sequence. *Chem. Eur. J.*, *13*, 8971–8978.
- 22 Tanaka, J., Nojima, M., and Kusabayashi, S. (1987). Reaction of phenyl-substituted allyllithiums with tert-alkyl bromides. Remarkable difference in the alkylation regiochemistry between a polar process and the one involving single-electron transfer. *J. Am. Chem. Soc.*, *109*, 3391–3397.
- 23 Xu, K., Tan, Z., Zhang, H., Liu, J., Zhang, S., and Wang, Z. (2017). Photoredox catalysis enabled alkylation of alkenyl carboxylic acids with *N*-(acyloxy)phthalimide via dual decarboxylation. *Chem. Commun.*, *53*, 10719–10722.
- 24 Zhu, N., Zhao, J., and Bao, H. (2017). Iron catalyzed methylation and ethylation of vinyl arenes. *Chem. Sci.*, *8*, 2081–2085.
- 25 Zhu, Y., and Wei, Y. (2014). Copper catalyzed direct alkenylation of simple alkanes with styrenes. *Chem. Sci.*, *5*, 2379–2382.